

ISOLATION OF α -GLUCOSIDASE INHIBITORS AND CYTOTOXIC COMPOUNDS FROM
HEARTWOOD OF *Mansonia gagei* Drumm.



A Dissertation Submitted in Partial Fulfillment of the Requirements
for the Degree of Doctor of Philosophy in Chemistry

Department of Chemistry

FACULTY OF SCIENCE

Chulalongkorn University

Academic Year 2021

Copyright of Chulalongkorn University

การแยกตัวยับยั้งแอลฟาไกลูโคซิเดสและสารที่เป็นพิษต่อเซลล์จากเนื้อไม้จำนนชะมด *Mansonia gagei* Drumm.



วิทยานิพนธ์นี้เป็นส่วนหนึ่งของการศึกษาตามหลักสูตรปริญญาวิทยาศาสตรดุษฎีบัณฑิต
สาขาวิชาเคมี ภาควิชาเคมี
คณะวิทยาศาสตร์ จุฬาลงกรณ์มหาวิทยาลัย
ปีการศึกษา 2564
ลิขสิทธิ์ของจุฬาลงกรณ์มหาวิทยาลัย

Thesis Title ISOLATION OF α -GLUCOSIDASE INHIBITORS AND
CYTOTOXIC COMPOUNDS FROM HEARTWOOD OF
Mansonia gagei Drumm.
By Mrs. Le Thi Thu Huong
Field of Study Chemistry
Thesis Advisor Assistant Professor Dr. WARINTHORN CHAVASIRI

Accepted by the FACULTY OF SCIENCE, Chulalongkorn University in Partial
Fulfillment of the Requirement for the Doctor of Philosophy

..... Dean of the FACULTY OF SCIENCE
(Professor Dr. POLKIT SANGVANICH)

DISSERTATION COMMITTEE

..... Chairman
(Associate Professor Dr. Prasat Kittakoop)

..... Thesis Advisor
(Assistant Professor Dr. WARINTHORN CHAVASIRI)

..... Examiner
(Professor Dr. MONGKOL SUKWATTANASINITT)

..... Examiner
(Professor Dr. KHANITHA PUDHOM)

..... Examiner
(Associate Professor Dr. PIYANUCH WONGANAN)

..... External Examiner
(Associate Professor Dr. Prasat Kittakoop)

เล ธิ พู ฮวง : การแยกตัวยับยั้งแอลฟาไกลูโคซิเดสและสารที่เป็นพิษต่อเซลล์จากเนื้อไม้
 จันทน์ชะมด *Mansonia gagei* Drumm.. (ISOLATION OF α -GLUCOSIDASE
 INHIBITORS AND CYTOTOXIC COMPOUNDS FROM HEARTWOOD OF
Mansonia gagei Drumm.) อ.ที่ปรึกษาหลัก : วรินทร์ ชวศิริ

ได้ศึกษาพฤษเคมีและฤทธิ์ทางชีวภาพของเนื้อไม้จันทน์ชะมด สามารถแยกสารที่มี
 รายงานมาแล้วสิบสองตัว (1–11, 29) เซสควิเทอร์พินอยด์ชนิดใหม่สิบตัว (12–21) สารใหม่เจ็ดตัว
 (22–28) และนีโอลิกันแนใหม่หนึ่งตัว (30) ได้พิสูจน์ทราบโครงสร้างของสารโดยอาศัยการวิเคราะห์
 ทางสเปกโทรสโกปี (UV-Vis, FTIR, 1D, 2D NMR และ HRESIMS) และได้เสนอคอนฟิกรูเรชัน
 สัมบูรณ์โดยอาศัยการคำนวณของข้อมูล ECD ได้ประเมินฤทธิ์ต้านอนุมูลอิสระ ความเป็นพิษต่อ
 เซลล์และฤทธิ์ยับยั้งเอนไซม์แอลฟา-กลูโคซิเดส เป็นที่น่าสนใจว่า mansonialactam (21) แสดง
 ฤทธิ์ยับยั้งแอลฟา-กลูโคซิเดสจากยีสต์ด้วยค่า IC_{50} 0.2 ± 0.05 mM ซึ่งมีค่าต่ำกว่า acarbose 468
 เท่า (93.63 ± 0.49) การศึกษาทางจลนศาสตร์แสดงให้เห็นว่า 21 และ 24 เป็นตัวยับยั้งแบบไม่
 แข่งขัน ในส่วนฤทธิ์ต้านอนุมูลอิสระ 11, 25 และ 27 แสดงฤทธิ์ที่ตีมากด้วยค่า IC_{50} 13.66 ± 0.42 ,
 12.76 ± 0.15 และ 13.19 ± 0.72 μ M ตามลำดับ สำหรับฤทธิ์ความเป็นพิษต่อเซลล์ 18 แสดงฤทธิ์ที่
 สูงที่สุดต่อเซลล์ไลน์มะเร็งปอด A549 ด้วยค่า IC_{50} 15.59 ± 2.49 μ M



สาขาวิชา เคมี
 ปีการศึกษา 2564

ลายมือชื่อนิสิต

ลายมือชื่อ อ.ที่ปรึกษาหลัก

6172906223 : MAJOR CHEMISTRY

KEYWORD:

Le Thi Thu Huong : ISOLATION OF α -GLUCOSIDASE INHIBITORS AND
CYTOTOXIC COMPOUNDS FROM HEARTWOOD OF *Mansonia gagei* Drumm..

Advisor: Asst. Prof. Dr. WARINTHORN CHAVASIRI

Phytochemical and biological investigations were carried out on the heartwoods of *M. gagei*. Twelve known compounds (1–11, 29), ten new sesquiterpenoids (12–21), seven novel compounds (22–28) and one new neolignan (30) were isolated. Their structures were elucidated by spectroscopic data analysis (UV-Vis, FTIR, 1D, 2D NMR and HRESIMS), and their absolute configurations were established by calculation of ECD data. Isolated compounds were evaluated for antioxidant, cytotoxic activity and enzyme inhibitory activity against α -glucosidase. Interestingly, mansonialactam (21) showed significant inhibitory activity against α -glucosidase from the yeast with the IC_{50} value of 0.2 ± 0.05 mM which was 468 times lower than that of acarbose (93.63 ± 0.49). Kinetic study revealed that 21 and 24 were uncompetitive inhibitors. In terms of antioxidant activity, 11, 25 and 27 exhibited very good activities with the IC_{50} values of 13.66 ± 0.42 , 12.76 ± 0.15 and 13.19 ± 0.72 μ M, respectively. In regard to cytotoxic activity, 18 possessed the highest cytotoxicity on lung cancer cell line A549 with an IC_{50} value of 15.59 ± 2.49 μ M.

Field of Study: Chemistry

Student's Signature

Academic Year: 2021

Advisor's Signature

ACKNOWLEDGEMENTS

There are many individuals without whom my thesis might not be possible to complete, and to whom I am greatly indebted. First of all, I wish to direct my earnest thankfulness to my advisor, Assistant Professor Dr. Warinthorn Chavasiri, Department of Chemistry, Faculty of Science, Chulalongkorn University for his knowledge, suggestion, support, guidance and encouragement throughout this research. I also thank the Center of Excellence in Natural Products Chemistry and all members of WC-lab for their kind help in the research.

In addition, I would like to thank Associate Professor Dr. Piyanuch Wonganan, Professor Masaki Kita, Dr. Kieu Van Nguyen, Dr. Duong Thuc Huy, Mr. Ade Danova, Ms. Rita Hairani and Mr. Yusuke Hioki for their recommendation, testing bio-assays and encouragement throughout this research.

Moreover, I would also like to acknowledge Associate Professor Dr. Prasat Kittakoop, Professor Dr. Mongkol Sukwattanasinitt, Professor Dr. Khanitha Pudhom for serving as the chairman and committees of my thesis, for their help on comments, discussions, and suggestions.

I would like to thank the scholarship from the Graduate School, Chulalongkorn University to commemorate the 100th Anniversary Chulalongkorn University and the 90th Anniversary Chulalongkorn University Fund (Ratchadaphiseksomphot Endowment Fund). All kind support and opportunities supplied me to achieve my research goals.

Finally, I am grateful towards my family in Vietnam for loving, understanding motivating me how to achieve my aim, avoid cultural shock and homesick.

Le Thi Thu Huong

TABLE OF CONTENTS

	Page
.....	iii
ABSTRACT (THAI).....	iii
.....	iv
ABSTRACT (ENGLISH).....	iv
ACKNOWLEDGEMENTS.....	v
TABLE OF CONTENTS.....	vi
LIST OF FIGURES.....	ix
LIST OF TABLES.....	xvi
LIST OF SCHEMES.....	xviii
LIST OF ABBREVIATIONS.....	xix
Chapter 1.....	1
INTRODUCTION.....	1
1.1 The usage of Sterculiaceae.....	2
1.2 Sterculiaceae secondary metabolites.....	3
1.3 Biological activities of family Sterculiaceae.....	4
1.3.1 Cytotoxic activity.....	4
1.3.2 Anti-inflammatory activity.....	4
1.3.3 Antidiabetic activity.....	5
1.3.4 Antimicrobial activity.....	5
1.3.5 Antioxidant activity.....	6
1.4 Morphological characterization of <i>Mansonia gagei</i> Drumm.....	8

1.5 Chemical constituents of <i>Mansonia</i> genus and their biological activities	8
1.6 Mansonones in other genera.....	11
1.7 The aim of this research	14
Chapter 2.....	15
EXPERIMENTAL	15
2.1 Plant material.....	15
2.2 Instruments and chemicals.....	15
2.3 Computational Study.....	16
2.4 Extraction of plant material.....	16
2.5 Separation and purification of chemical constituents.....	16
2.6 Biological activities.....	28
2.6.1 α -glucosidase inhibitory.....	28
2.6.2 Antioxidant activity.....	29
2.6.3 Cytotoxic activity.....	29
Chapter 3.....	31
RESULTS AND DISCUSSION.....	31
3.1 Extraction of <i>M. gagei</i> heartwood.....	31
3.2 Separation of the EtOAc extract of <i>M. gagei</i> heartwood.....	31
3.3 Structural elucidation of compounds from the EtOAc extract.....	35
3.4 Biological activity study	74
3.4.1 α -Glucosidase inhibitory activity.....	74
3.4.2 Antioxidant activities.....	82
3.4.3 Cytotoxicity.....	85
Chapter 4.....	87

CONCLUSION	87
REFERENCES	89
APPENDIX.....	103
VITA.....	174



LIST OF FIGURES

Figure 1.1 Bioactive compounds of family Sterculiaceae	7
Figure 1.2 <i>Mansonia gagei</i> Drumm.	8
Figure 1.3 Chemical constituents of <i>Mansonia</i> genus	14
Figure 3.1 Isolated compounds from the EtOAc extract of <i>M. gagei</i> heartwoods.....	37
Figure 3.2 Key ^1H - ^1H COSY, HMBC correlations of 12	44
Figure 3.3 Experimental ECD spectra (200–400 nm) and calculated ECD spectra for 12	44
Figure 3.4 Key ^1H - ^1H COSY, HMBC correlations of 13–15	49
Figure 3.5 Experimental ECD spectra (200–400 nm) and calculated ECD spectra for 13–15	49
Figure 3.6 Key ^1H - ^1H COSY, HMBC correlations of 16	51
Figure 3.7 Key ^1H - ^1H COSY, HMBC correlations of 17–19	54
Figure 3.8 Experimental ECD spectra (200–400 nm) and calculated ECD spectra for 17–19	55
Figure 3.9 Key ^1H - ^1H COSY, HMBC correlations of 20 and 21	58
Figure 3.10 Key ^1H - ^1H COSY, HMBC correlations of 22–26	66
Figure 3.11 Key ^1H - ^1H COSY, HMBC correlations of 27–28	69
Figure 3.12 Key ^1H - ^1H COSY, HMBC correlations of 30	72
Figure 3.13 % Inhibition of the EtOAc extracts of <i>M. gagei</i> at various concentrations	75
Figure 3.14 α -Glucosidase inhibitory activities of 5–21	78
Figure 3.15 α -Glucosidase inhibitory activities of 1, 22–28	79

Figure 3.16 Lineweaver-Burk plot of the reaction of the yeast α -glucosidase in the presence of 21	80
Figure 3.17 Lineweaver-Burk plot of the reaction of the yeast α -glucosidase in the presence of 24	80
Figure 3.18 The antioxidant activity of sesquiterpenoids and ascorbic acid.....	83
Figure 3.19 The antioxidant activity of compounds (1, 3, 22-30) and ascorbic acid ..	84
Figure A1. ^1H NMR spectrum (500 MHz, methanol- d_4) of compound 12	104
Figure A2. ^{13}C NMR spectrum (125 MHz, methanol- d_4) of compound 12	104
Figure A3. ^1H - ^1H COSY spectrum of compound 12	105
Figure A4. HSQC spectrum of compound 12	105
Figure A5. HMBC spectrum of compound 12	106
Figure A6. NOESY spectrum of compound 12	106
Figure A7. HRESIMS spectrum of compound 12	107
Figure A8. ^1H NMR spectrum (500 MHz, methanol- d_4) of compound 13	108
Figure A9. ^{13}C NMR spectrum (125 MHz, methanol- d_4) of compound 13	108
Figure A10. ^1H - ^1H COSY spectrum of compound 13	109
Figure A11. HSQC spectrum of compound 13	109
Figure A12. HMBC spectrum of compound 13	110
Figure A13. NOESY spectrum of compound 13	110
Figure A14. HRESIMS spectrum of compound 13 in methanol	111
Figure A15. ^1H NMR spectrum (500 MHz, methanol- d_4) of compound 14	112
Figure A16. ^{13}C NMR spectrum (125 MHz, methanol- d_4) of compound 14	112
Figure A17. ^1H - ^1H COSY spectrum of compound 14	113

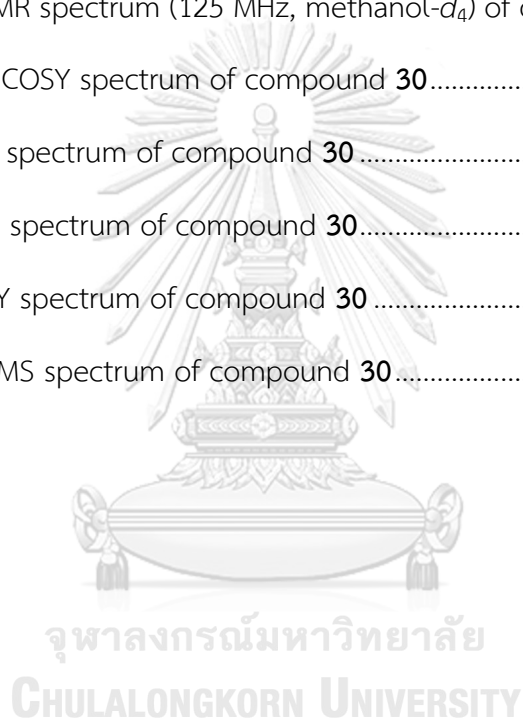
Figure A18. HSQC spectrum of compound 14	113
Figure A19. HMBC spectrum of compound 14	114
Figure A20. NOESY spectrum of compound 14	114
Figure A21. HRESIMS spectrum of compound 14	115
Figure A22. ^1H NMR spectrum (500 MHz, methanol- d_4) of compound 15	116
Figure A23. ^{13}C NMR spectrum (125 MHz, methanol- d_4) of compound 15	116
Figure A24. ^1H - ^1H COSY spectrum of compound 15	117
Figure A25. HSQC spectrum of compound 15	117
Figure A26. HMBC spectrum of compound 15	118
Figure A27. NOESY spectrum of compound 15	118
Figure A28. HRESIMS spectrum of compound 15	119
Figure A29. ^1H NMR spectrum (500 MHz, methanol- d_4) of compound 16	120
Figure A30. ^{13}C NMR spectrum (125 MHz, methanol- d_4) of compound 16	120
Figure A31. ^1H - ^1H COSY spectrum of compound 16	121
Figure A32. HSQC spectrum of compound 16	121
Figure A33. HMBC spectrum of compound 16	122
Figure A34. NOESY spectrum of compound 16	122
Figure A35. HRESIMS spectrum of compound 16 in methanol	123
Figure A36. Experimental ECD spectrum of compound 16	123
Figure A37. ^1H NMR spectrum (500 MHz, methanol- d_4) of compound 17	124
Figure A38. ^{13}C NMR spectrum (125 MHz, methanol- d_4) of compound 17	124
Figure A39. ^1H - ^1H COSY spectrum of compound 17	125
Figure A40. HSQC spectrum of compound 17	125
Figure A41. HMBC spectrum of compound 17	126

Figure A42. NOESY spectrum of compound 17	126
Figure A43. HRESIMS spectrum of compound 17 in methanol	127
Figure A44. ^1H NMR spectrum (500 MHz, methanol- d_4) of compound 18	128
Figure A45. ^{13}C NMR spectrum (125 MHz, methanol- d_4) of compound 18	128
Figure A46. ^1H - ^1H COSY spectrum of compound 18	129
Figure A47. HSQC spectrum of compound 18	129
Figure A48. HMBC spectrum of compound 18	130
Figure A49. NOESY spectrum of compound 18	130
Figure A50. HRESIMS spectrum of compound 18	131
Figure A51. ^1H NMR spectrum (500 MHz, methanol- d_4) of compound 19	132
Figure A52. ^{13}C NMR spectrum (125 MHz, methanol- d_4) of compound 19	132
Figure A53. ^1H - ^1H COSY spectrum of compound 19	133
Figure A54. HSQC spectrum of compound 19	133
Figure A55. HMBC spectrum of compound 19	134
Figure A56. NOESY spectrum of compound 19	134
Figure A57. HRESIMS spectrum of compound 19	135
Figure A58. ^1H NMR spectrum (500 MHz, acetone- d_6) of compound 20	136
Figure A59. ^{13}C NMR spectrum (125 MHz, acetone- d_6) of compound 20	136
Figure A60. ^1H - ^1H COSY spectrum of compound 20	137
Figure A61. HSQC spectrum of compound 20	137
Figure A62. HMBC spectrum of compound 20	138
Figure A63. HRESIMS spectrum of compound 20	138
Figure A64. ^1H NMR spectrum (500 MHz, DMSO- d_6) of compound 21	139
Figure A65. ^{13}C NMR spectrum (125 MHz, DMSO- d_6) of compound 21	139

Figure A66. ^1H - ^1H COSY spectrum of compound 21	140
Figure A67. HSQC spectrum of compound 21	140
Figure A68. HMBC spectrum of compound 21	141
Figure A69. HRESIMS spectrum of compound 21	141
Figure A70. ^1H NMR spectrum (500 MHz, methanol- d_4) of compound 22	142
Figure A71. ^{13}C NMR spectrum (125 MHz, methanol- d_4) of compound 22	142
Figure A72. ^1H - ^1H COSY spectrum of compound 22	143
Figure A73. HSQC spectrum of compound 22	143
Figure A74. HMBC spectrum of compound 22	144
Figure A75. NOESY spectrum of compound 22	144
Figure A76. HRESIMS spectrum of compound 22	145
Figure A77. ^1H NMR spectrum (500 MHz, methanol- d_4) of compound 23	146
Figure A78. ^{13}C NMR spectrum (125 MHz, methanol- d_4) of compound 23	146
Figure A79. ^1H - ^1H COSY spectrum of compound 23	147
Figure A80. HSQC spectrum of compound 23	147
Figure A81. HMBC spectrum of compound 23	148
Figure A82. NOESY spectrum of compound 23	148
Figure A83. HRESIMS spectrum of compound 23	149
Figure A84. ^1H NMR spectrum (500 MHz, methanol- d_4) of compound 24	150
Figure A 85. ^{13}C NMR spectrum (125 MHz, methanol- d_4) of compound 24	150
Figure A86. ^1H - ^1H COSY spectrum of compound 24	151
Figure A87. HSQC spectrum of compound 24	151
Figure A88. HMBC spectrum of compound 24	152
Figure A89. NOESY spectrum of compound 24	152

Figure A90. HRESIMS spectrum of compound 24	153
Figure A91. ^1H NMR spectrum (500 MHz, methanol- d_4) of compound 25	154
Figure A92. ^{13}C NMR spectrum (125 MHz, methanol- d_4) of compound 25	154
Figure A93. ^1H - ^1H COSY spectrum of compound 25	155
Figure A94. HSQC spectrum of compound 25	155
Figure A95. HMBC spectrum of compound 25	156
Figure A96. NOESY spectrum of compound 25	156
Figure A97. HRESIMS spectrum of compound 25	157
Figure A98. ^1H NMR spectrum (500 MHz, methanol- d_4) of compound 26	158
Figure A99. ^{13}C NMR spectrum (125 MHz, methanol- d_4) of compound 26	158
Figure A100. ^1H - ^1H COSY spectrum of compound 26	159
Figure A101. HSQC spectrum of compound 26	159
Figure A102. HMBC spectrum of compound 26	160
Figure A103. NOESY spectrum of compound 26	160
Figure A104. HRESIMS spectrum of compound 26	161
Figure A105. ^1H NMR spectrum (500 MHz, methanol- d_4) of compound 27	162
Figure A106. ^{13}C NMR spectrum (125 MHz, methanol- d_4) of compound 27	162
Figure A107. ^1H - ^1H COSY spectrum of compound 27	163
Figure A108. HSQC spectrum of compound 27	163
Figure A109. HMBC spectrum of compound 27	164
Figure A110. NOESY spectrum of compound 27	164
Figure A111. HRESIMS spectrum of compound 27	165
Figure A112. ^1H NMR spectrum (500 MHz, methanol- d_4) of compound 28	166
Figure A113. ^{13}C NMR spectrum (125 MHz, methanol- d_4) of compound 28	166

Figure A114. ^1H - ^1H COSY spectrum of compound 28	167
Figure A115. HSQC spectrum of compound 28	167
Figure A116. HMBC spectrum of compound 28	168
Figure A117. NOESY spectrum of compound 28	168
Figure A118. HRESIMS spectrum of compound 28	169
Figure A119. ^1H NMR spectrum (500 MHz, methanol- d_4) of compound 30	170
Figure A120. ^{13}C NMR spectrum (125 MHz, methanol- d_4) of compound 30	170
Figure A121. ^1H - ^1H COSY spectrum of compound 30	171
Figure A122. HSQC spectrum of compound 30	171
Figure A123. HMBC spectrum of compound 30	172
Figure A124. NOESY spectrum of compound 30	172
Figure A125. HRESIMS spectrum of compound 30	173



LIST OF TABLES

Table 3.1 The fractionation of the EtOAc extract of <i>M. gagei</i> heartwoods.....	32
Table 3.2 The ^1H (500 MHz) and ^{13}C (125 MHz) NMR spectroscopic data of 1 (acetone- d_6) 2, 3 (DMSO- d_6) (δ in ppm).....	38
Table 3.3 The ^1H (500 MHz) and ^{13}C (125 MHz) NMR spectroscopic data of 4 and 5 (acetone- d_6) (δ in ppm).....	39
Table 3.4 The ^1H (500 MHz) and ^{13}C (125 MHz) NMR spectroscopic data of 6 (acetone- d_6) and 7 (CD_3OD) (δ in ppm).....	40
Table 3.5 The ^1H (500 MHz) and ^{13}C (125 MHz) NMR spectroscopic data of 8 (CDCl_3), 9 and 10 (DMSO- d_6) (δ in ppm).....	41
Table 3.6 The ^1H (500 MHz) and ^{13}C (125 MHz) NMR spectroscopic data of 11 (DMSO- d_6), 12 , (CD_3OD) (δ in ppm).....	43
Table 3.7 The ^1H (500 MHz) and ^{13}C (125 MHz) NMR spectroscopic data of 13–15 , (CD_3OD) (δ in ppm).....	48
Table 3.8 The ^1H (500 MHz) and ^{13}C (125 MHz) NMR spectroscopic data of 16 , (CD_3OD) (δ in ppm).....	51
Table 3.9 The ^1H (500 MHz) and ^{13}C (125 MHz) NMR spectroscopic data of 17–19 , (CD_3OD) (δ in ppm).....	56
Table 3.10 The ^1H (500 MHz) and ^{13}C (125 MHz) NMR spectroscopic data of 20 (CD_3) $_2\text{CO}$ and 21 (DMSO- d_6) (δ in ppm).....	59
Table 3.11 The ^1H (500 MHz) NMR spectroscopic data of 22–26 (CD_3OD) (δ in ppm).....	64
Table 3.12 The ^{13}C (125 MHz) NMR spectroscopic data of 22–26 (CD_3OD) (δ in ppm)	65
Table 3.13 The ^1H (500 MHz) and ^{13}C (125 MHz) NMR spectroscopic data of 27 and 28 (CD_3OD).....	70

Table 3.14 The ^1H (500 MHz) and ^{13}C (125 MHz) NMR spectroscopic data of 29 (acetone- d_6) and 30 (CD_3OD)	73
Table 3.15 Inhibition of the EtOAc extract of <i>M. gagei</i> at various concentrations	74
Table 3.16 IC_{50} values of tested compounds for α -glucosidase inhibitory activities ..	76
Table 3.17 Kinetic effect of α -glucosidase inhibition on 21 and 24	81
Table 3.18 Antioxidant activity of tested compounds	82
Table 3.19 IC_{50} values of tested compounds against A549 cancer cell line	85



LIST OF SCHEMES

Scheme 2.1 The fractionation procedure of <i>M. gagei</i> heartwood	17
Scheme 3.1 Procedure for the separation of fraction HE3	34
Scheme 3.2 Procedure for the separation of fraction EA	34
Scheme 3.3 Procedure for the separation of fraction Ac	35



LIST OF ABBREVIATIONS

HR-ESI-MS	High Resolution Electrospray Ionization Mass Spectroscopy
FTIR	Fourier transform infrared spectroscopy
UV-Vis	Ultraviolet-visible
ECD	Electronic Circular Dichroism
^1H NMR	Proton Nuclear Magnetic Resonance
^{13}C NMR	Carbon-13 Nuclear Magnetic Resonance
1D-NMR	One-Dimensional Nuclear Magnetic Resonance
2D-NMR	Two-Dimensional Nuclear Magnetic Resonance
^1H - ^1H COSY	^1H - ^1H Correlation Spectroscopy
HSQC	Heteronuclear Single Quantum Correlation
HMBC	Heteronuclear Multiple Bond Correlation
NOESY	Nuclear Overhauser Effect Spectroscopy
m/z	Mass per charge number of ions (Mass Spectroscopy)
δ_{H}	Chemical shift of proton
δ_{C}	Chemical shift of carbon
J	Coupling constant
Hz	Hertz
s	singlet
d	doublet

t	triplet
q	quartet
m	multiplet
br s	broad singlet
dd	doublet of doublets
ddd	doublet of doublet of doublets
Acetone- d_6	deuterated acetone
$CDCl_3$	deuterated chloroform
CD_3OD	deuterated methanol
DMSO- d_6	deuterated dimethyl sulfoxide
Ac	Acetone
CH_2Cl_2	Dichloromethane
EtOAc	Ethyl acetate
Hexane	<i>n</i> -Hexane
MeOH	Methanol
calcd.	calculated
TLC	Thin Layer Chromatography
MTT	3-(4,5-dimethylthiazol-2-yl)-2,5-diphenyltetrazolium bromide
DPPH	2,2-diphenyl-1-picrylhydrazyl
IC ₅₀	the half-maximal inhibitory concentration

g	gram
mg	milligram (s)
min	minute (s)
mL	milliliter (s)
mM	millimolar
μg	micromolar
ppm	Part per million (chemical shift value)



Chapter 1

INTRODUCTION

Natural products and their derivatives have played a crucial role in drug discovery in modern society. They have got the attention of chemists and pharmacologists because of their diversity of chemical structures and interesting biological activities. Therefore, they have long been used particularly effective as anti-inflammatory, antifungal, anticancer and antidiabetic drugs.¹⁻⁴ There are two major classes of natural products: primary and secondary metabolites. The former are organic molecules that are directly involved in normal growth, development, and reproduction of an organism while the latter are those which are not directly involved in survival of plants but help to increase the competitiveness of the organism within its environment.⁵ From earlier decades, herbs were existent on the Earth. Thus, medicinal plants are helpful over the world. Each plant has possessed various therapeutic characteristics due to bioactive compounds. Natural drug substances have been found to be extremely useful because they offer bioactive molecules that are less toxic and more potent.⁶

In the past, humans used plants and their extracts to treat diseases and foster healing. Noticeably, Hippocrates in the fourth century BC knew how to use willow bark in the treatment of inflammatory pain.⁷ In the 18th century, the use of the bark of

cinchona tree in treatment of malaria and the potency of poppy extract in treating of dysenteries had been reported.⁸ Until the end of 19th century, natural products became principal sources of drugs. Many pure compounds namely quinine, morphine, codeine and effective compounds with significant benefits were isolated by chemists in that century. Up to now, natural products still are a source of half of all new drugs, including parent natural products and modified derivatives.⁹

Sterculiaceae is a large family of plants that comprises 70 genera, including around 1,500 species of tropical plants and shrubs, or lianas or herbs.¹⁰ *Mansonia gagei* Drumm. is a medium-sized tree belonging to this family, found in tropical countries, such as Myanmar and Thailand. This plant has been utilized as heart stimulant, onilivertigo, antiemetic, counteracts depression and refreshment agent.¹¹ Many papers reported about the phytochemical screening and bioactivities of the plant extracts and isolated compounds. Its chloroform fraction illustrated the most potent anti-estrogenic activity with 49 and 21% reduction of 17 β -estradiol activity in 100 and 10 μ g/mL concentrations, respectively.¹² In addition, the isolated mansonones and mansonins showed anticancer, larvicidal, antifungal, antioxidant activities.¹³⁻¹⁵

1.1 The usage of Sterculiaceae

The family Sterculiaceae is one of the primary families among flowering plants. Plants from family Sterculiaceae have been used as folk and traditional medicine in many countries. Indians utilized the roots of *Ambroma augusta* to treat dysmenorrhea,

amenorrhea sterility and other menstrual problems.¹⁰ *Guazuma ulmifolia* has been reported to be a traditional medicine as anti-diabetic, anti-hypertensive, vasorelaxing.¹⁶ The leaves of *Melochia corchorifolia* were used to decrease ulcers, abdominal swelling, headache and chest pain.¹⁷ *Cola gigantea* commonly known as giant Cola was reported treating whooping cough, asthma, malaria, and fever.¹⁸ The whole plants of *Waltheria dourandinha* were often used for treatment of respiratory diseases, stimulant, emetic, and diuretic, urinary diseases and healing agent.¹⁰ Some species from the genus *Helicteres* were found to possess interesting biological activities. Fernandes reported that *Helicteres sacarolha* was employed for treatment of hypertension and ulcers while *H. velutina* was also used effectively as an insect repellent.¹⁹

1.2 Sterculiaceae secondary metabolites

Family Sterculiaceae has illustrated a large number of secondary metabolites such as alkaloids,²⁰ flavonoids,^{21, 22} steroids, saponins and terpenoids.^{19, 23} A part from that, Sterculiaceae family also contained other substances namely phenylpropanoids and their derivatives, lignans and some phenolic acids.^{10, 23}

1.3 Biological activities of family Sterculiaceae

The biological activities of Sterculiaceae substances and their extracts have been exhibited effectively including cytotoxicity, anti-inflammatory, antidiabetic, antimicrobial, and antioxidant.

1.3.1 Cytotoxic activity

In 2006, Chen and coworkers revealed that cucurbitacin D and J showed significant antitumor activity against BEL-7402 and SK-MEL-28 cell lines.²⁴ Some isolated compounds from *Helicteres hirsuta* were tested for cytotoxicity on several cancer cell lines. The results showed that 3 β -O-acetylbetulinic acid and 4,4'-sulfinylbis(2-(tert-butyl)-5-methylphenol) possessed moderate activity on CCRF-CEM and HCT116 cancer cells with IC₅₀ values ranging from 14.6 to 31.5 μ M, respectively.²³ Another report, three cardenolides: strophanthojavoside, strophalloside and ascleposide have been found to be active against three tumor cell lines MCF-7, NCI-H460, and HepG2.²⁵

1.3.2 Anti-inflammatory activity

Jacob *et al.* indicated that the methanolic extract of *Pterospermum reticulatum* showed potent antiprotease activity (64.93%) and anti-LOX activity (56%), meanwhile that of *P. rubiginosum* only possessed an inhibition of 51.29% against trypsin enzyme.²⁶ Atolani *et al.* found that *Cola gigantea* seed oil illustrated higher

activity against ABTS radicals (IC_{50} 44.19 ± 6.27 mg/mL) than ascorbic acid or quercetin.¹⁸

1.3.3 Antidiabetic activity

Helicteres isora L. was evaluated for antidiabetic, antihyperglycemic and hypolipidemic activities, the ethanolic extracts experienced significant reduction in plasma glucose, triglycerides and insulin level in mice by Chakrabarti *et al.*²⁷ In 2014, Rathinavelusamy *et al.* reported that the bark ethyl acetate extracts of *Pterospermum acerifolium* possessed maximum α -amylase inhibition potential and maximum capacity in reducing hyperglycemia.²⁸ The root aqueous extracts of *Helicteres angustifolia* exhibited potent inhibition against rat intestinal maltase and sucrase activity with the same IC_{50} value of 1.44 ± 0.24 mg/mL, interestingly with low cytotoxic and acute toxicity.²⁹

1.3.4 Antimicrobial activity

Four species of *Cola* Schott & Endl had been tested for antimicrobial activities by Sonibare *et al.* in 2009. They found that the ethanolic extracts of *C. acuminata* had more impact on both bacteria and fungi, meanwhile that of *C. gigantea* also had effective effects on *Staphylococcus albus*, *Bacillus subtilis*, *Aspergillus niger* and *Candida albicans*. However, those of *C. nitida* and *C. millenii* showed weak inhibitory activities against the growth of all microorganisms.³⁰ The aqueous extracts of *Helicteres isora* had strong antibacterial activities against *Escherichia coli*, *Staphylococcus*

epidermidis, *Salmonella typhimurium*, *Proteus vulgaris*, and moderate activity against *Enterobacter aerogenes*, *Staphylococcus aureus*, and *Salmonella typhi*.³¹

1.3.5 Antioxidant activity

Polyphenols isolated from *Theobroma cacao* L. were investigated for antioxidant activities. It is noted that procyanidin B2 and procyanidin B5 displayed the highest activities on lipid peroxidation while (-)-epicatechin was the strongest inhibitory on the autoxidation of linoleic acid.³² The methanolic extracts from the barks of *Pterospermum rubiginosum* and *P. reticulatum* had potent activity against free radical scavenging property.²⁶ Another study, the extract of new regrown stem barks of *Sterculia quadrifida* inhibited strong antioxidant activity with an IC₅₀ value of 2.51±0.03 µg/ml.³³ The bioactive compounds from family Sterculiaceae are summarized in Figure 1.1.

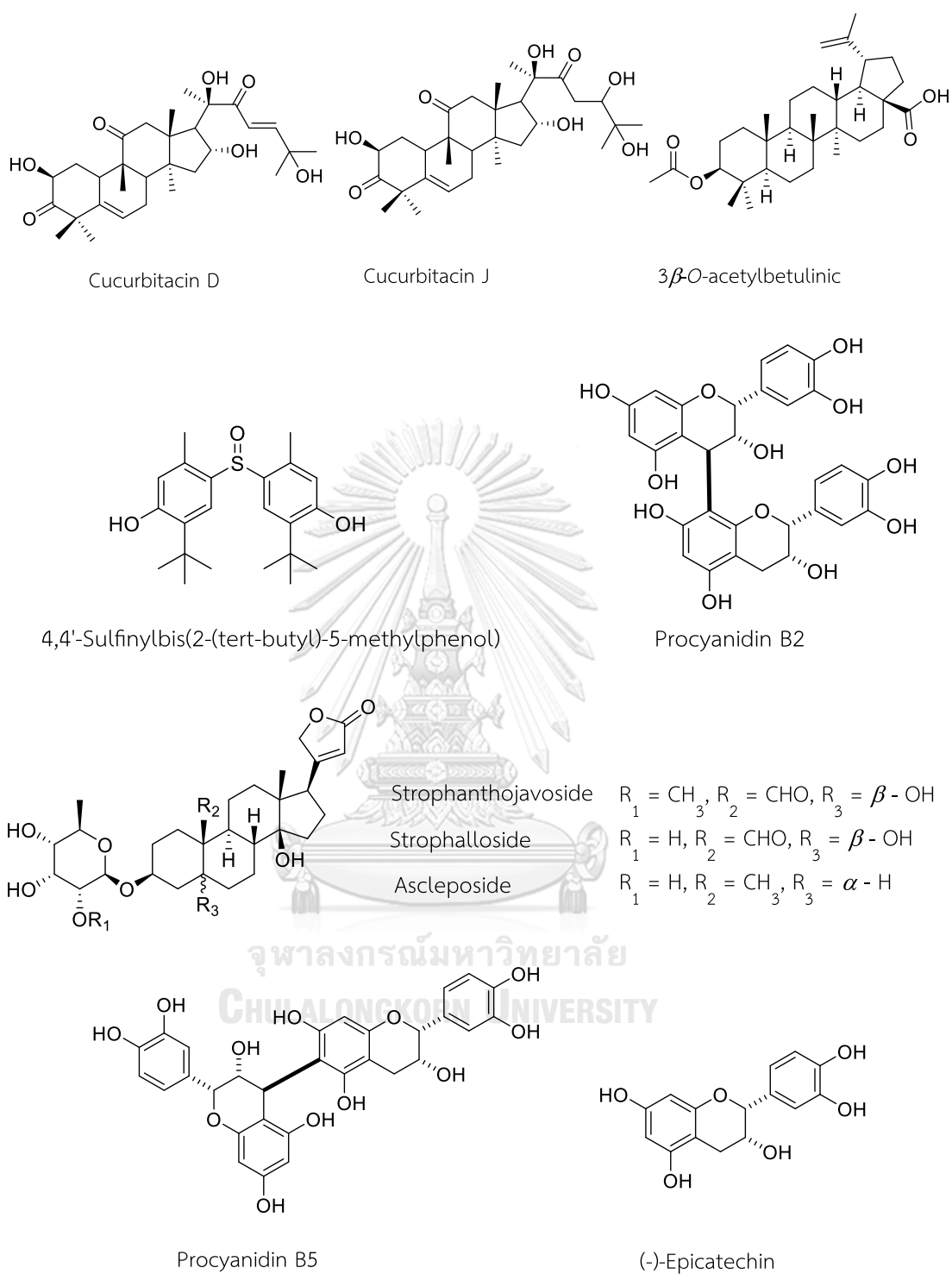


Figure 1.1 Bioactive compounds of family Sterculiaceae

1.4 Morphological characterization of *Mansonia gagei* Drumm

Mansonia gagei Drumm. (Figure 1.2) is widely known as chan-cha-mod, chan-hom, chan-khao or chan-pha-ma which is used as folk medicine in Thai traditional medicine. It is a medium-sized tree in evergreen forest. Its leaves are simple, and toothed. Their flowers are inflorescences. The color of mature heartwood is pale-brown.³⁴



Figure 1.2 *Mansonia gagei* Drumm.

1.5 Chemical constituents of *Mansonia* genus and their biological activities

Literature reviews concentrating on the chemical constituents of the genus *Mansonia* revealed the presence of a variety of natural compounds including coumarin, sesquiterpenoid and neolignan derivatives. Only two species, *M. gagei* Drumm. and *M. altissima* Chev. were investigated on their chemical compositions (Figure 1.3).

M. altissima Chev., from tropical West Africa, was studied for its chemical constituents in 1965 by Bettolo and coworkers.³⁵ Six compounds were separated from

the chloroform extract and identified as mansonones A (**a**), B, C, D, E and F, which possessed two main characteristics, the C₁₅ empirical formula with a cadinene sesquiterpenoid character and a quinonic skeleton.

Mansonones A (**b**), C, E, F and two additional mansonones, mansonones G and H were obtained from the acetone extract of *M. altissima* by Tanaka in 1966.³⁶ Interestingly, mansonone A was redressed as 1,2-naphthoquinone (**b**) instead of 1,4-naphthoquinone (**a**) because its absorption spectrum showed ν_{\max} (MeOH) at 432 nm which was the characteristic absorption of *ortho*-quinone structure. In addition, the dehydrogenation of mansonone A (**b**) with chloranil under mild conditions yielded mansonone C.

Further phytochemical investigation on the chemical constituents from the heartwood led to the isolation of mansonones I and L in 1967 by Shimada³⁷ and in 1969 by Galeffi³⁸, respectively.

For *M. gagei* chemical exploration, Tiew and coworkers¹¹ in 2002 isolated four mansonones C, E, G, H and three mansorins A-C from the heartwood. The cytotoxicity of isolated compounds was tested against brine shrimp *Artemia salina* Linn. Mansonone C and mansorin B illustrated very high cytotoxicity against brine shrimp with LC₅₀ values of 0.61 and 2.08 $\mu\text{g/mL}$, respectively, whereas mansonones E and G, mansorin A displayed medium activities. In the same year, four mansonones N-Q were

isolated from the dichloromethane extract.³⁹ Their structures were confirmed by the basis of spectroscopic data interpretation and the single crystal X-ray analysis.

In 2003, a novel neolignan, mansoxtane and two new sesquiterpenes, mansonones R and S, from the methanolic extract were reported.⁴⁰

Three new mansorins **I–III**, a new mansonone **I**, and eleven known compounds were separated by El-Halawany *et al.* in 2007.¹² The isolated compounds were evaluated on induction of β -galactosidase activity by 17 β -estradiol in yeast two hybrid assays (estrogen receptors α , and β , ER α , ER β). All examined compounds revealed lower binding affinities to ER α than to ER β . Interestingly, mansonones F and S demonstrated a good deal of potent estrogen binding and estrogen receptor antagonist effects.

Some isolated compounds from the heartwood were evaluated for antifungal activities. Mansonones C and E exhibited better activity against *Candida albicans* with a minimal amount of 0.15 and 2.5 μg , respectively. Surprisingly, mansonones B, C and E were active against *Cladosporium cucumerinum* with the same minimal inhibitory amount of 0.6 μg .⁴¹ Furthermore, mansonone E also revealed highly remarkable antibacterial activity against both *Xanthomonas oryzae pv. oryzae* and *X. oryzae pv. Oryzicola* with MIC and MBC as 7.8 and >500 $\mu\text{g/mL}$, respectively.¹⁴

Mansorins and mansonones were evaluated for cholinesterase (ChE) inhibitory activities by Changwong and coworkers in 2012.⁴² Mansonone E exhibited the highest

ChE inhibitory activities, with IC_{50} values towards AChE and BChE of 23.5 ± 6.4 and $62.4 \pm 5.9 \mu\text{M}$, respectively.

The isolated naphthoquinones and coumarins were tested for their potential anticancer activity against breast (MCF-7), cervix (HeLa), colorectal (HCT-116) and liver (HepG2) cancer cells using sulfarhodamine-B (SRB) assay in 2018 by Baghdadi. Among them, mansorin I and mansorin II possessed cytotoxic activities against all cancer cell lines with inhibitory concentrations (IC_{50}) in the range of 3.95 to 35.3 μM and 0.74 to 36 μM , respectively.¹³ Apart from that, five compounds (mansonone E, mansonone G, mansorin B, mansorin I, and populene F) were evaluated for their activity on melanogenesis. Mansonone E with low cytotoxicity displayed a considerably strong inhibition on melanogenesis compared to arbutin.⁴³

1.6 Mansonones in other genera

The presence of mansonones not only occurs in *Mansonia* genus but also in other genera. Mansonone M, a sesquiterpenoid quinone was isolated from the root barks of *Helicteres unguisjolia* by Chen *et al.* in 1990.⁴⁴ Mansonone M was also found in the heartwoods of *Thespesia populnea*.⁴⁵ (Figure 1.3).

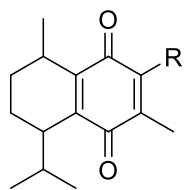
Mansonone D extracted from the heartwoods of *Thespesia populnea* had more potent cytotoxic effects on human breast cancer MCF-7 with LC_{50} value of 0.14 μM .⁴⁶ Mansonone D isolated from lignicolous freshwater fungus BCC 28210 also exhibited antimalarial activity against *Plasmodium falciparum* K1 with IC_{50} values of 0.55 $\mu\text{g/mL}$.⁴⁷

Mansonone E had a significant cytotoxic impact on four tumor cell lines, A375-S2, HeLa, MCF-7, and U937 with IC_{50} values of 2.2, 7.9, 3.1, and 0.9 μM , respectively.^{48, 49}

Mansonone F not only showed strong antioxidative activity with IC_{50} of 0.03 $\mu\text{g}/\text{mL}$ ¹⁵ but also active against MRSA with MIC value of 0.39-3.1 $\mu\text{g}/\text{mL}$, compared to vancomycin.⁵⁰

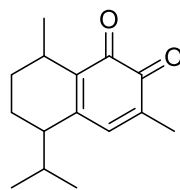
According to Wu and coworkers, mansonone H isolated from the stems of *Hibiscus taiwanensis* inhibited HIV replication in H9 lymphocyte cells with EC_{50} values of 16.58 $\mu\text{g}/\text{mL}$.⁵¹

In 2020, Sato addressed that mansonone I showed significant cytotoxicity against four human colon cancer cell lines (HCT116, DLD-1, RKO, and SW480) with IC_{50} values of 4.3–5.2 μM and low cytotoxicity against the 293 cells ($IC_{50} > 10 \mu\text{M}$).⁵²

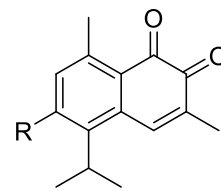


Mansonone A (a) R = H

Mansonone B R = OH

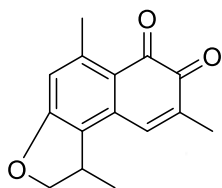


Mansonone A (b)

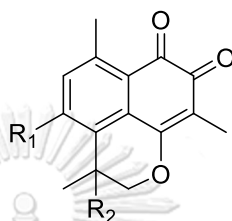


Mansonone C R = H

Mansonone G R = OH



Mansonone D

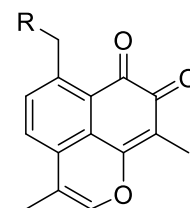


Mansonone E

Mansonone H

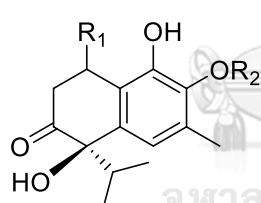
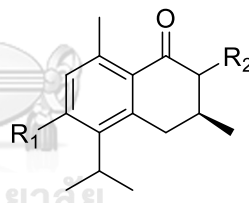
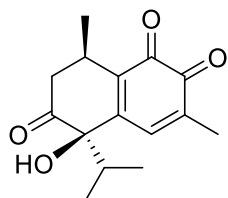
Mansonone I

Mansonone M

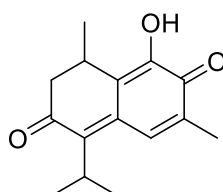
R₁ = H R₂ = HR₁ = OH R₂ = HR₁ = H, R₂ = OHR₁ = OCH₃ R₂ = H

Mansonone F R = H

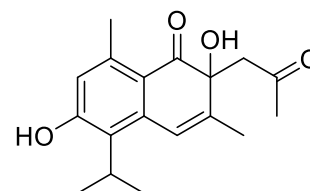
Mansonone L R = OH

Mansonone N R₁ = β-CH₃, R₂ = CH₃Mansonone Q R₁ = α-CH₃, R₂ = HMansonone P R₁ = OH, R₂ = α-OHMansonone R R₁ = H, R₂ = β-OH

Mansonone O



Mansonone S



Mansonone I

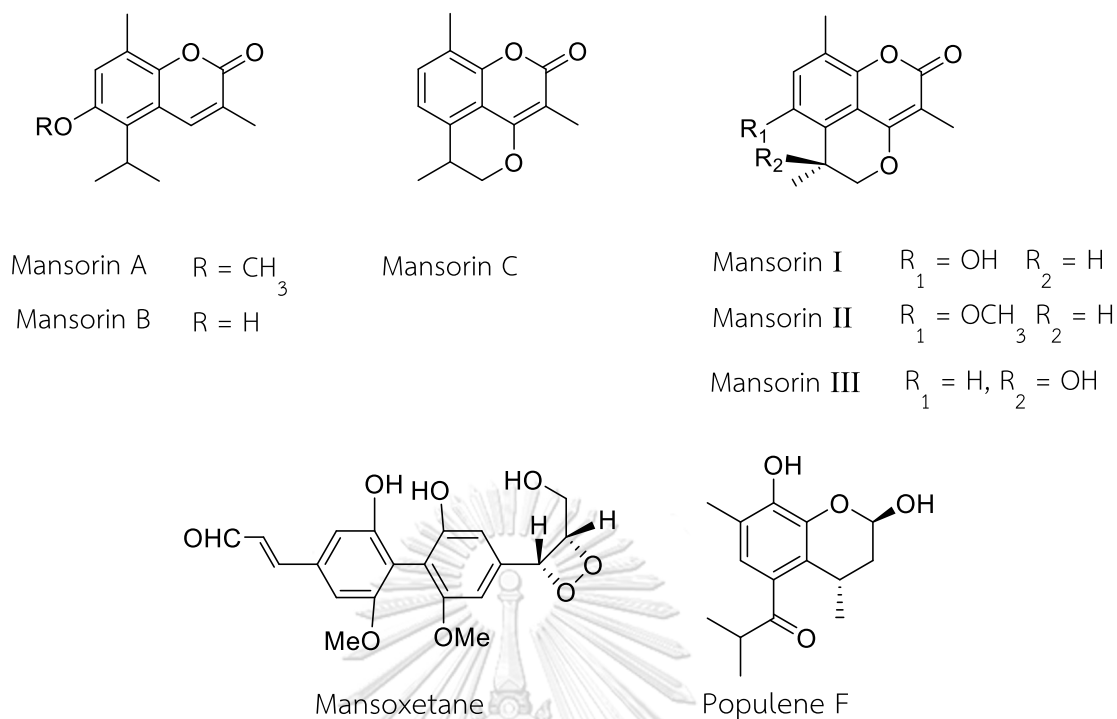


Figure 1.3 Chemical constituents of *Mansonia* genus

1.7 The aim of this research

In Thailand, the tropical and humid climate has facilitated the development of a variety of plants, and *Mansonia gagei* is a prevalent tree in this country. Due to a wide range of secondary metabolites as well as interesting bioactivities, the chemical constituents of *M. gagei* are worthwhile for further investigation in order to isolate new and/or biologically active compounds.

In this study, the isolation and purification process of the heartwoods of *M. gagei* will be investigated. Furthermore, their biological activities such as cytotoxicity, antioxidant, and α -glucosidase inhibitory activities will be conducted.

Chapter 2

EXPERIMENTAL

2.1 Plant material

The dried heartwoods of *Mansonia gagei* were collected from Saraburi province, Thailand in 2019. The identity of this plant was compared with a voucher specimen No. 43281 at the herbarium of the Royal Forestry Department of Thailand.

2.2 Instruments and chemicals

Optical rotations were measured on a JASCO P-1010 polarimeter (JASCO, Easton, MD, USA). The experimental ECD data were recorded on a JASCO J-815 spectropolarimeter. UV-Vis spectra were recorded with a PerkinElmer Lambda 950 UV-Vis-NIR spectrophotometer. IR spectra were recorded on a Bruker ALPHA FT-IR spectrometer. HR-ESIMS spectra were recorded on a Bruker micrOTOF mass spectrometer. The NMR spectra were measured using a JEOL 500 MHz spectrometer in methanol- d_4 , acetone- d_6 and DMSO- d_6 , with TMS as an internal standard. Silica gel 60G (Merck), silica gel 70-230 mesh (Merck), and Sephadex LH-20 (GE Chemical Corporation), reversed - phase silica gel C18 were used for column chromatography. TLC analyses were carried out on precoated silica gel 60 F254 and spots were visualized by spraying with 10% H₂SO₄ solution followed by heating.

2.3 Computational Study

Initial structures of new compounds were drawn in Chem3D based on their NMR data and subsequently subjected to a conformational search implemented in the MOE software⁵³ using the MMFF94S force field.⁵⁴ All conformers in the lowest 5 kcal/mol energy window were used for Density Functional Theory (DFT) optimizations. The DFT and ECD calculations were performed with the Gaussian 09 package.⁵⁵ The first optimization was performed by the B3LYP level of theory using the 6-31G basis set in gas phase. All of the optimized geometries in the lowest 2.5 kcal/mol energy window were further optimized at the CAM-B3LYP/6-311+G** level in MeOH (CPCM model). The frequency analysis and ECD calculation were performed at the same level of theory. The resultant theoretical ECD spectra for individual conformers were averaged according to their Boltzmann populations at 298.15 K and visualized with SpecDis software.⁵⁶

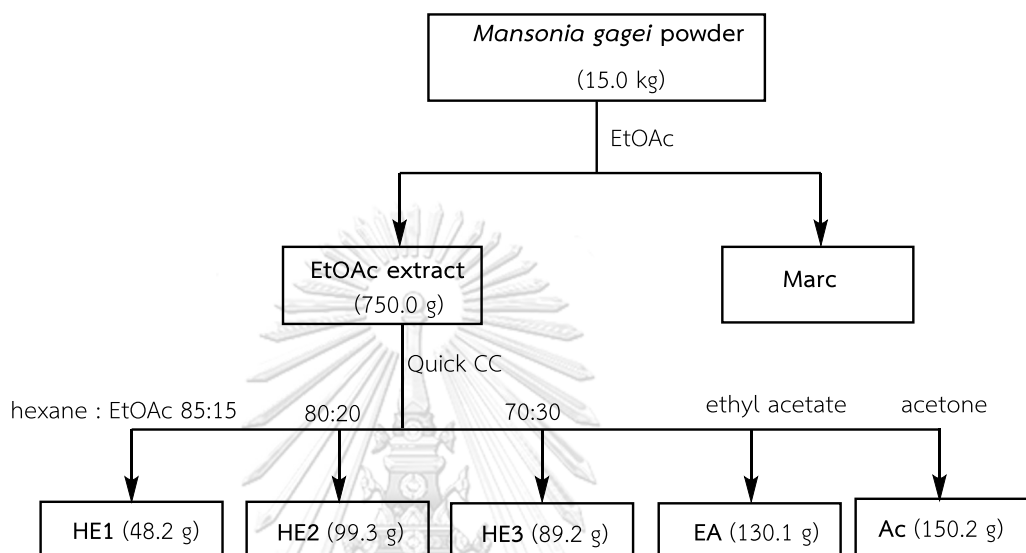
2.4 Extraction of plant material

The dried heartwoods of *M. gagei* (15.0 kg) were extracted three times with EtOAc (40 L x 3) at room temperature. The solvent was evaporated under reduced pressure to give a crude extract (750.0 g, 5.0 % yield of the dried heartwoods).

2.5 Separation and purification of chemical constituents

The EtOAc extract (750 g) was fractionated by silica gel quick column (No. 7729, Merck). A stepwise elution was conducted by a solvent system of hexane/EtOAc

(stepwise gradient, 85:15 to 0:100) and with acetone. The fractions were combined according to TLC profiles to give five fractions **HE1** (48.2 g), **HE2** (99.3 g), **HE3** (89.2 g), **EA** (130.1 g), **Ac** (150.2 g). The fractionation procedure is summarized in Schem 2.1.



Scheme 2.1 The fractionation procedure of *M. gagei* heartwood

HE3, **EA** and **Ac** fractions were further isolated on silica gel column [Silica gel 60G (Merck), silica gel 70–230 mesh (Merck), reversed-phase silica gel C18 and Sephadex LH-20 (GE Chemical Corporation)] using stepwise system of hexane/CH₂Cl₂/Ac, hexane/CH₂Cl₂/MeOH, CH₂Cl₂/MeOH, hexane/CH₂Cl₂/EtOAc/MeOH, MeOH/H₂O isocratic or gradient solvent systems. Further isolation of **HE3** furnished ten compounds, *i.e.* sinapaldehyde (**1**, 12.0 mg), vanillic acid (**2**, 10.0 mg), mansorin I (**5**, 8.0 mg), mansorin B (**6**, 30.0 mg), mansonone E (**8**, 20.0 mg), heliclactone (**11**, 9.0 mg), (10*S*)-7-*O*-methylheliclactone (**12**, 10.0 mg), (2*R*)-2,5-dihydroxy-4-isopropyl-2,7-dimethyl-1*H*-indene-1,3(2*H*)-dione (**16**, 12.0 mg), 5-acetyl-4,6-dihydroxy-3,8-

dimethylnaphthalene-1,2-dione (**20**, 10.0 mg) and **28** (20.0 mg). Whereas fourteen compounds were separated from **EA** fraction including syringic acid (**3**, 15.0 mg), phomoxydiene B (**4**, 20.0 mg), (11S)-6-hydroxy-5-(11-hydroxypropan-12-yl)-3,8-dimethyl-2*H*-chromen-2-one (**7**, 10.0 mg), mansonone H (**9**, 30.0 mg), dehydrooxoperezinone (**10**, 20.0 mg), mansoniafuranone A (**13**, 34.0 mg), mansoniafuranone B (**14**, 58.0 mg), mansoniafuranone C (**15**, 8.0 mg), mansonone T (**17**, 10.0 mg), mansonone U (**18**, 12.0 mg), mansonone V (**19**, 3.5 mg), mansonialactam (**21**, 21.0 mg), mansoxetane (**29**, 680.0 mg) and 9'-*O*-acetylmansoxetane (**30**, 60.0 mg). Additionally, further separation of **Ac** fraction yielded six compounds: **22** (30.0 mg), **23** (25.0 mg), **24** (41.0 mg), **25** (10.0 mg), **26** (6.0 mg) and **27** (8.0 mg). Their structures were determined by spectroscopic data analysis (1D, 2D NMR and HRESIMS), and the absolute configurations were established by calculation of ECD data as well as by comparison with previous reports.

Sinapaldehyde (**1**): yellow solid, ^1H NMR (500 MHz, acetone- d_6): δ_{H} (ppm) 9.63 (1H, d, $J = 7.5$ Hz), 7.56 (1H, d, $J = 16.0$ Hz), 7.08 (2H, s), 6.99 (1H, dd, $J = 16.0, 8.0$ Hz), 3.90 (6H, s). ^{13}C NMR (125 MHz, acetone- d_6): δ_{C} (ppm) 193.9, 154.5, 149.0, 140.2, 127.3, 126.1, 107.2, 56.7.

Vanillic acid (**2**): light yellow powder, ^1H NMR (500 MHz, DMSO- d_6): δ_{H} (ppm) 7.43 (1H, dd, $J = 8.0, 2.0$ Hz), 7.42 (1H, d, $J = 2.0$ Hz), 6.84 (1H, d, $J = 8.0$ Hz), 3.80 (3H,

s). ^{13}C NMR (125 MHz, $\text{DMSO-}d_6$): δ_{C} (ppm) 167.3, 151.2, 147.3, 123.6, 121.7, 115.1, 112.7, 55.6.

Syringic acid (**3**): colorless powder, ^1H NMR (500 MHz, $\text{DMSO-}d_6$): δ_{H} (ppm) 7.20 (2H, s), 3.79 (6H, s). ^{13}C NMR (125 MHz, $\text{DMSO-}d_6$): δ_{C} (ppm) 167.4, 147.4, 140.1, 120.8, 106.8, 56.0.

Phomoxydiene B (**4**): pale yellow solid, ^1H NMR (500 MHz, $\text{acetone-}d_6$): δ_{H} (ppm) 6.26 (1H, dd, $J = 10.5, 6.0$ Hz), 6.06 (1H, dd, $J = 11.5, 4.5$ Hz), 5.85 (1H, dd, $J = 11.5, 6.5$ Hz), 5.79 (1H, dd, $J = 10.5, 7.0$ Hz), 4.56 (1H, m), 4.36 (1H, t, $J = 6.0$ Hz), 4.17 (1H, d, $J = 4.5$ Hz), 3.62 (1H, t, $J = 8.0$ Hz), 2.81 (1H, m), 2.74 (1H, m), 2.45 (2H, m), 2.29 (2H, m), 1.10 (3H, d, $J = 7.0$ Hz). ^{13}C NMR (125 MHz, $\text{acetone-}d_6$): δ_{C} (ppm) 177.8, 140.0, 138.5, 126.0, 125.2, 87.1, 82.8, 77.8, 72.4, 54.7, 54.1, 28.9, 24.8, 14.4.

Mansorin I (**5**): white needles, ^1H NMR (500 MHz, $\text{acetone-}d_6$): δ_{H} (ppm) 6.99 (1H, s), 4.48 (1H, dd, $J = 11.0, 1.5$ Hz), 4.31 (1H, dd, $J = 11.0, 3.5$ Hz), 3.34 (1H, m), 2.29 (3H, s), 1.96 (3H, s), 1.29 (3H, d, $J = 7.0$ Hz). ^{13}C NMR (125 MHz, $\text{acetone-}d_6$): δ_{C} (ppm) 163.9, 159.8, 149.3, 144.5, 124.7, 120.9, 120.1, 111.8, 102.5, 73.5, 27.5, 17.9, 15.3, 9.2.

Mansorin B (**6**): pale yellow powder, ^1H NMR (500 MHz, $\text{acetone-}d_6$): δ_{H} (ppm) 8.11 (1H, d, $J = 1.5$ Hz), 6.93 (1H, d, $J = 0.5$ Hz), 3.62 (1H, m), 2.27 (3H, d, $J = 1$ Hz), 2.15 (3H, d, $J = 1$ Hz), 1.39 (6H, d, $J = 7$ Hz). ^{13}C NMR (125 MHz, $\text{acetone-}d_6$): δ_{C} (ppm) 162.0, 152.1, 146.8, 137.5, 127.6, 125.0, 124.0, 121.2, 118.7, 27.3, 21.3, 17.4, 15.2.

(11S)-6-hydroxy-5-(11-hydroxypropan-12-yl)-3,8-dimethyl-2H-chromen-2-one (**7**): white amorphous powder, ^1H NMR (500 MHz, $\text{methanol-}d_4$): δ_{H} (ppm) 8.08 (1H, s),

6.85 (1H, s), 3.97 (1H, dd, $J = 10.5, 6.5$ Hz), 3.90 (1H, dd, $J = 10.5, 6.0$ Hz), 3.52 (1H, m), 2.33 (3H, s), 2.17 (3H, s), 1.38 (3H, d, $J = 7.0$ Hz). ^{13}C NMR (125 MHz, methanol- d_4): δ_{C} (ppm) 164.2, 153.3, 147.1, 139.1, 125.4, 125.0, 124.6, 122.0, 120.1, 66.5, 36.6, 17.3, 16.0, 15.3.

Mansonone E (**8**): orange powder, ^1H NMR (500 MHz, CDCl_3): δ_{H} (ppm) 7.34 (1H, d, $J = 8.0$ Hz), 7.25 (1H, d, $J = 8.0$ Hz), 4.40 (1H, dd, $J = 10.5, 4.0$ Hz), 4.22 (1H, dd, $J = 11.0, 5.0$ Hz), 3.09 (1H, m), 2.64 (3H, s), 1.95 (3H, s), 1.36 (3H, d, $J = 7.0$ Hz). ^{13}C NMR (125 MHz, CDCl_3): δ_{C} (ppm) 182.4, 180.4, 162.7, 143.1, 137.0, 135.0, 132.8, 127.4, 127.0, 116.4, 71.5, 31.4, 22.7, 17.7, 7.9.

Mansonone H (**9**): red platelet, ^1H NMR (500 MHz, $\text{DMSO}-d_6$): δ_{H} (ppm) 6.75 (1H, s), 4.41 (1H, d, $J = 11.0$ Hz), 4.28 (1H, dd, $J = 11.0, 3.5$ Hz), 3.18 (1H, m), 2.48 (3H, s), 1.80 (3H, s), 1.21 (3H, d, $J = 7.0$ Hz). ^{13}C NMR (125 MHz, $\text{DMSO}-d_6$): δ_{C} (ppm) 180.1, 179.5, 161.7, 159.7, 144.6, 128.0, 125.4, 119.1, 118.9, 114.6, 71.7, 25.6, 22.7, 17.0, 7.9.

Dehydrooxoperezinone (**10**): yellow powder, ^1H NMR (500 MHz, $\text{DMSO}-d_6$): δ_{H} (ppm) 6.72 (1H, s), 2.51 (3H, s), 1.77 (3H, s), 1.70 (6H, s). ^{13}C NMR (125 MHz, $\text{DMSO}-d_6$): δ_{C} (ppm) 180.0, 176.9, 167.5, 157.4, 146.0, 135.7, 130.5, 120.1, 116.0, 107.2, 95.9, 25.5, 20.1, 8.0.

Heliclactone (**11**): pale yellow powder, ^1H NMR (500 MHz, $\text{DMSO}-d_6$): δ_{H} (ppm) 3.36 (1H, m), 2.80 (1H, m), 2.67 (1H, m), 2.16 (3H, s), 2.00 (3H, s), 1.86 (1H, m), 1.76 (1H, m), 1.12 (3H, d, $J = 7.0$ Hz). ^{13}C NMR (125 MHz, $\text{DMSO}-d_6$): δ_{C} (ppm) 161.9, 148.3, 147.3, 145.1, 138.4, 124.9, 114.1, 108.9, 108.1, 27.3, 25.4, 21.6, 18.6, 12.1, 8.5.

(10S)-7-O-methylheliclactone (**12**): yellowish amorphous powder; $[\alpha]_D^{25} +42$ (c 0.60 in MeOH); UV (MeOH) λ_{\max} (log ϵ) 210 (4.08), 296 (3.44); IR ν_{\max} 3485, 2938, 1674, 1599, 1576, 1393 cm^{-1} ; ^1H NMR (500 MHz, methanol- d_4): δ_{H} (ppm) 3.79 (3H, s), 3.45 (1H, m), 2.91 (1H, m), 2.79 (1H, m), 2.30 (3H, s), 2.10 (3H, d, $J = 1$ Hz), 1.96 (1H, m), 1.87 (1H, m), 1.23 (3H, d, $J = 7.5$ Hz), ^{13}C NMR (125 MHz, methanol- d_4): δ_{C} (ppm) 164.9, 150.4, 150.0, 145.6, 144.6, 126.6, 118.0, 117.2, 113.9, 61.2, 28.7, 27.2, 23.1, 18.8, 12.3, 8.8; HRESIMS m/z 273.1122, $[\text{M} - \text{H}]^-$ (calcd for $\text{C}_{16}\text{H}_{17}\text{O}_4$, 273.1127).

Mansoniafuranone A (**13**): pale yellow amorphous solid; $[\alpha]_D^{25} + 131$ (c 1.0 in MeOH); UV (MeOH) λ_{\max} (log ϵ) 215 (4.03), 264 (3.62); IR ν_{\max} 3451, 3226, 2964, 2926, 1721, 1711, 1589, 1281 cm^{-1} ; ^1H NMR (500 MHz, methanol- d_4): δ_{H} (ppm) 6.63 (1H, s), 5.52 (1H, d, $J = 2.5$ Hz), 3.15 (1H, m), 2.89 (1H, m), 2.44 (3H, s), 1.41 (3H, d, $J = 7.0$ Hz), 1.38 (3H, d, $J = 7.0$ Hz), 1.33 (3H, d, $J = 7.0$ Hz). ^{13}C NMR (125 MHz, methanol- d_4): δ_{C} (ppm) 175.0, 173.3, 163.1, 150.0, 139.3, 127.1, 120.1, 115.9, 82.4, 44.4, 30.7, 20.7, 20.2, 17.1, 15.3; HRESIMS m/z 301.1063 $[\text{M} + \text{Na}]^+$ (calcd for $\text{C}_{15}\text{H}_{18}\text{O}_5\text{Na}$, 301.1052).

Mansoniafuranone B (**14**): pale yellow needle; $[\alpha]_D^{25} + 172$ (c 1.0 in MeOH); UV (MeOH) λ_{\max} (log ϵ) 215 (4.06), 264 (3.64); IR ν_{\max} 3248, 2986, 2940, 1721, 1713, 1588, 1220 cm^{-1} ; ^1H NMR (500 MHz, methanol- d_4): δ_{H} (ppm) 6.70 (1H, s), 6.03 (1H, br. s), 3.12 (1H, m), 2.96 (1H, m), 2.48 (3H, s), 1.37 (3H, d, $J = 7.0$ Hz), 1.34 (3H, d, $J = 7.0$ Hz), 0.67 (3H, d, $J = 7.0$ Hz). ^{13}C NMR (125 MHz, methanol- d_4): δ_{C} (ppm) 176.1, 173.1, 163.4, 149.6, 139.8, 126.8, 120.3, 115.6, 81.5, 42.2, 30.3, 20.6, 20.3, 17.1, 8.1; HRESIMS m/z 301.1072 $[\text{M} + \text{Na}]^+$ (calcd for $\text{C}_{15}\text{H}_{18}\text{O}_5\text{Na}$, 301.1052).

Mansoniafuranone C (**15**): yellowish amorphous powder; $[\alpha]_D^{25}$ -131 (c 0.35 in MeOH); UV (MeOH) λ_{\max} (log ϵ) 214 (3.99), 265 (3.57); IR ν_{\max} 3342, 2963, 2928, 1725, 1711, 1582, 1284 cm^{-1} ; ^1H NMR (500 MHz, methanol- d_4): δ_{H} (ppm) 6.60 (1H, s), 5.52 (1H, d, $J = 2.5$ Hz), 2.98 (1H, m), 2.92 (1H, m), 2.44 (3H, s), 1.40 (3H, d, $J = 7.0$ Hz), 1.32 (3H, d, $J = 7.0$ Hz), ^{13}C NMR (125 MHz, methanol- d_4): δ_{C} (ppm) 180.7, 174.1, 163.0, 151.1, 139.0, 127.1, 119.8, 116.5, 83.8, 47.0, 30.7, 20.8, 20.5, 17.2, 16.2; HRESIMS m/z 301.1067 $[\text{M} + \text{Na}]^+$ (calcd for $\text{C}_{15}\text{H}_{18}\text{O}_5\text{Na}$, 301.1052).

(2*R*)-2,5-Dihydroxy-4-isopropyl-2,7-dimethyl-1*H*-indene-1,3(2*H*)-dione (**16**): yellow powder; $[\alpha]_D^{25}$ +72 (c 0.77 in MeOH); UV (MeOH) λ_{\max} (log ϵ) 204 (3.71), 246 (3.89), 294 (3.37), 334 (3.04); IR ν_{\max} 3280, 2962, 1716, 1678, 1601, 1565, 1386 cm^{-1} ; ^1H NMR (500 MHz, methanol- d_4): δ_{H} (ppm) 7.01 (1H, s), 4.39 (1H, m), 2.60 (3H, s), 1.35 (3H, s), 1.34 (3H, d, $J = 7.0$ Hz), 1.34 (3H, d, $J = 7.0$ Hz), ^{13}C NMR (125 MHz, methanol- d_4): δ_{C} (ppm) 204.7, 201.7, 165.2, 140.3, 139.9, 133.6, 130.6, 126.1, 76.4, 26.8, 21.9, 20.4, 20.2, 18.8; HRESIMS m/z 247.0964 $[\text{M} - \text{H}]^-$ (calcd for $\text{C}_{14}\text{H}_{15}\text{O}_4$, 247.0970).

Mansonone T (**17**): yellow amorphous solid; $[\alpha]_D^{25}$ +129 (c 0.40 in MeOH); UV (MeOH) λ_{\max} (log ϵ) 203 (3.71), 248 (3.88), 293 (3.37); IR ν_{\max} 3414, 2957, 2926, 1726, 1710, 1462, 1382, 1037 cm^{-1} ; ^1H NMR (500 MHz, methanol- d_4): δ_{H} (ppm) 6.74 (1H, d, $J = 1.5$ Hz), 4.13 (1H, m), 2.93 (1H, m), 2.48 (1H, t, $J = 4.0$ Hz), 2.31 (1H, m), 1.91 (3H, d, $J = 2.0$ Hz), 1.89 (1H, m), 1.51 (1H, m), 1.20 (3H, d, $J = 7.0$ Hz), 1.14 (3H, d, $J = 7.0$ Hz), 0.97 (3H, d, $J = 7.5$ Hz), ^{13}C NMR (125 MHz, methanol- d_4): δ_{C} (ppm) 182.4, 181.0, 151.1,

142.7, 139.4, 136.8, 66.9, 52.0, 34.6, 29.2, 28.0, 25.8, 22.0, 21.9, 15.0; HRESIMS m/z 271.1295 $[M + Na]^+$ (calcd for $C_{15}H_{20}O_3Na$, 271.1310).

Mansonone U (**18**): yellow amorphous solid; $[\alpha]_D^{25} +159$ (c 0.60 in MeOH); UV (MeOH) λ_{max} (log ϵ) 206 (4.08), 280 (2.88); IR ν_{max} 3438, 2959, 1427, 1292, 1026 cm^{-1} ; 1H NMR (500 MHz, methanol- d_4): δ_H (ppm) 6.32 (1H, s), 4.20 (1H, m), 3.23 (1H, m), 2.65 (1H, t, $J = 4.0$ Hz), 2.20 (1H, m), 2.16 (3H, s), 2.05 (1H, m), 1.54 (1H, m), 1.23 (3H, d, $J = 7.0$ Hz), 1.06 (3H, d, $J = 7.0$ Hz), 0.44 (3H, d, $J = 7.0$ Hz), ^{13}C NMR (125 MHz, methanol- d_4): δ_C (ppm) 144.2, 142.3, 130.3, 127.2, 123.7, 123.3, 68.4, 51.5, 35.4, 29.7, 27.2, 25.9, 22.9, 21.9, 16.2; HRESIMS m/z 273.1452 $[M + Na]^+$ (calcd for $C_{15}H_{22}O_3Na$, 273.1467).

Mansonone V (**19**): pale yellow amorphous; $[\alpha]_D^{25} -142$ (c 0.35 in MeOH); UV (MeOH) λ_{max} (log ϵ) 204 (3.97), 236 (3.75), 291 (3.51); IR ν_{max} 3410, 2959, 2934, 2873, 1654, 1567, 1454 cm^{-1} ; 1H NMR (500 MHz, methanol- d_4): δ_H (ppm) 10.36 (1H, s), 4.26 (1H, m), 3.64 (1H, t, $J = 4.0$ Hz), 3.32 (1H, m), 2.43 (3H, s), 2.17 (1H, m), 2.10 (1H, m), 1.60 (1H, dd, $J = 12.5, 3.5$ Hz), 1.25 (3H, d, $J = 7.0$ Hz), 1.05 (3H, d, $J = 6.5$ Hz), 0.31 (3H, d, $J = 7.5$ Hz), ^{13}C NMR (125 MHz, methanol- d_4): δ_C (ppm) 195.3, 150.7, 142.2, 137.9, 127.9, 127.7, 127.6, 68.3, 45.7, 33.8, 29.8, 28.9, 25.4, 23.2, 21.9, 13.3; HRESIMS m/z , 301.1420 $[M + Na]^+$ (calcd for $C_{16}H_{22}O_4Na$, 301.1416).

5-Acetyl-4,6-dihydroxy-3,8-dimethylnaphthalene-1,2-dione (**20**): yellow powder; UV (MeOH) λ_{max} (log ϵ) 204 (4.09), 270 (3.78), 297 (3.73); IR ν_{max} 3042, 1668, 1650, 1627, 1590, 1378 cm^{-1} ; 1H NMR (500 MHz, acetone- d_6): δ_H (ppm) 7.05 (1H, s), 2.63 (3H, s), 2.40 (3H, s), 1.91 (3H, s), ^{13}C NMR (125 MHz, acetone- d_6): δ_C (ppm) 201.5, 186.0,

181.3, 158.8, 156.1, 145.3, 134.2, 131.1, 123.0, 120.6, 117.8, 30.9, 22.9, 8.3; HRESIMS m/z 259.0604, $[M - H]^-$ (calcd for $C_{14}H_{11}O_5$, 259.0606)

Mansonialactam (**21**): yellow amorphous powder; UV (MeOH) λ_{max} (log ϵ) 223 (3.95), 253 (4.03), 304 (3.22); IR ν_{max} 3213, 2950, 1666, 1604, 1284 cm^{-1} ; 1H NMR (500 MHz, DMSO- d_6): δ_H (ppm) 9.62 (1H, s), 7.51 (1H, s), 7.44 (1H, s), 3.79 (1H, m), 2.35 (3H, s), 1.41 (6H, d, $J = 7.0$), ^{13}C NMR (125 MHz, DMSO- d_6): δ_C (ppm) 167.5, 153.8, 135.0, 132.1, 131.6, 123.9, 123.5, 121.4, 119.8, 118.3, 113.8, 26.5, 21.1, 18.1; HRESIMS m/z 280.0953, $[M + Na]^+$ (calcd for $C_{15}H_{15}NO_3Na$, 280.0950).

Compound **22**: pale yellow powder, $[\alpha]_D^{25} +177$ (c 1.0 in MeOH); UV (MeOH) λ_{max} (log ϵ) 207 (4.36), 241 (3.89), 302 (3.82); IR ν_{max} 3331, 2960, 2922, 1733, 1648, 1588, 1520, 1449, 1358, 1178 cm^{-1} ; 1H NMR (500 MHz, methanol- d_4): δ_H (ppm) 6.65 (2H, br. s), 6.46 (1H, s), 5.57 (1H, s), 3.82 (3H, s), 3.68 (1H, d, $J = 4.5$ Hz), 3.37 (1H, m), 2.90 (1H, dd, $J = 12.0, 4.5$ Hz), 2.37 (3H, s), 2.24 (1H, m), 2.10 (1H, d, $J = 12.0$ Hz), 1.36 (3H, d, $J = 7.0$ Hz), 1.35 (3H, d, $J = 8.0$ Hz), 1.32 (3H, d, $J = 7.5$ Hz), ^{13}C NMR (125 MHz, methanol- d_4): δ_C (ppm) 215.4, 193.0, 162.1, 151.5, 148.8, 145.7, 143.9, 134.3, 134.2, 129.0, 123.1, 119.4, 109.8, 104.7, 77.1, 71.4, 56.6, 49.5, 41.0, 33.8, 28.9, 23.6, 21.1, 15.9; HRESIMS m/z 463.1740, $[M + Na]^+$ (calcd. for $C_{25}H_{28}O_7Na$, 463.1733).

Compound **23**: pale yellow powder, $[\alpha]_D^{25} +278$ (c 0.7 in MeOH); UV (MeOH) λ_{max} (log ϵ) 207 (4.25), 241 (3.86), 302 (3.80); IR ν_{max} 3378, 2927, 1732, 1588, 1517, 1450 cm^{-1} ; 1H NMR (500 MHz, methanol- d_4): δ_H (ppm) 6.53 (1H, s), 6.53 (1H, d, $J = 2.0$ Hz), 6.49 (1H, d, $J = 1.5$ Hz), 5.69 (1H, s), 3.81 (3H, s), 3.58 (1H, d, $J = 4.5$ Hz), 3.31 (1H,

m), 2.59 (1H, dd, $J = 12.5, 5.0$ Hz), 2.52 (3H, s), 2.45 (1H, d, $J = 13.0$ Hz), 2.10 (1H, m), 1.34 (3H, d, $J = 7.0$ Hz), 1.32 (3H, d, $J = 7.0$ Hz), 0.71 (3H, d, $J = 7.5$ Hz), ^{13}C NMR (125 MHz, methanol- d_4): δ_{C} (ppm) 215.2, 193.2, 162.4, 151.6, 149.0, 146.0, 144.4, 134.5, 132.4, 129.1, 123.0, 119.6, 109.8, 104.8, 76.7, 72.4, 56.6, 50.0, 41.2, 33.2, 28.8, 23.9, 21.0, 15.1; HRESIMS m/z 463.1735, $[\text{M} + \text{Na}]^+$ (calcd. for $\text{C}_{25}\text{H}_{28}\text{O}_7\text{Na}$, 463.1733).

Compound **24**: yellowish amorphous powder; $[\alpha]_{\text{D}}^{25} +255$ (c 0.2 in MeOH); UV (MeOH) λ_{max} (log ϵ) 207 (4.19), 239 (3.12); IR ν_{max} 3358, 2932, 1735, 1588, 1518, 1449, 1090 cm^{-1} ; ^1H NMR (500 MHz, methanol- d_4): δ_{H} (ppm) 6.63 (1H, s), 6.63 (1H, s), 6.44 (1H, s), 5.01 (1H, s), 3.83 (3H, s), 3.68 (1H, d, $J = 5.0$ Hz), 3.34 (1H, m), 3.18 (3H, s), 2.92 (1H, dd, $J = 12.0, 4.5$ Hz), 2.35 (3H, s), 2.24 (1H, m), 2.10 (1H, d, $J = 12.0$ Hz), 1.36 (3H, d, $J = 7.0$ Hz), 1.34 (3H, d, $J = 7.0$ Hz), 1.32 (3H, d, $J = 7.5$ Hz), ^{13}C NMR (125 MHz, methanol- d_4): δ_{C} (ppm) 215.0, 192.0, 162.1, 151.0, 149.0, 145.9, 143.9, 134.2, 130.6, 129.0, 122.9, 119.4, 110.3, 105.4, 81.1, 76.8, 57.8, 56.6, 49.6, 42.7, 35.0, 29.0, 23.6, 21.1, 15.9; HRESIMS m/z 477.1921, $[\text{M} + \text{Na}]^+$ (calcd. for $\text{C}_{26}\text{H}_{30}\text{O}_7\text{Na}$, 477.1889).

Compound **25**: pale yellow powder, $[\alpha]_{\text{D}}^{25} +291$ (c 1.0 in MeOH); UV (MeOH) λ_{max} (log ϵ) 207 (4.18), 240 (3.02); IR ν_{max} 3389, 2967, 1737, 1588, 1450, 1361 cm^{-1} ; ^1H NMR (500 MHz, methanol- d_4): δ_{H} (ppm) δ_{H} (ppm) 6.51 (1H, s), 6.48 (1H, d, $J = 2.0$ Hz), 6.43 (1H, d, $J = 1.5$ Hz), 5.15 (1H, s), 3.80 (3H, s), 3.57 (1H, d, $J = 4.5$ Hz), 3.30 (1H, m), 3.26 (3H, s), 2.63 (1H, dd, $J = 12.0, 4.5$ Hz), 2.50 (3H, s), 2.39 (1H, d, $J = 12.5$ Hz), 2.06 (1H, m), 1.33 (3H, d, $J = 7.0$ Hz), 1.30 (3H, d, $J = 7.0$ Hz), 0.68 (3H, d, $J = 7.5$ Hz), ^{13}C NMR (125 MHz, methanol- d_4): δ_{C} (ppm) 214.4, 192.0, 162.3, 151.9, 149.2, 146.3, 144.2, 134.8,

129.1, 129.1, 123.0, 119.6, 110.3, 105.5, 81.7, 76.1, 57.6, 56.6, 49.6, 41.4, 33.2, 28.6, 23.8, 21.0, 15.0; HRESIMS m/z 477.1918, $[M + Na]^+$ (calcd. for $C_{26}H_{30}O_7Na$, 477.1889).

Compound **26**: pale yellow powder, $[\alpha]_D^{25} +290$ (c 0.7 in MeOH); UV (MeOH) λ_{max} (log ϵ) 207 (4.20), 240 (3.36); IR ν_{max} 3357, 2969, 2935, 1739, 1660, 1588, 1449, 1359, 1088 cm^{-1} ; 1H NMR (500 MHz, methanol- d_4): δ_H (ppm) δ_H (ppm) 6.64 (1H, s), 6.64 (1H, s), 6.44 (1H, s), 5.12 (1H, s), 3.82 (3H, s), 3.67 (1H, d, $J = 4.5$ Hz), 3.35 (1H, m), 3.34 (2H, q, $J = 7.0$ Hz), 2.95 (1H, dd, $J = 12.0, 5.0$ Hz), 2.35 (3H, s), 2.23 (1H, m), 2.06 (1H, d, $J = 12.0$ Hz), 1.35 (3H, d, $J = 7.0$ Hz), 1.34 (3H, d, $J = 7.0$ Hz), 1.33 (3H, d, $J = 7.5$ Hz), 1.08 (3H, t, $J = 7.0$ Hz), ^{13}C NMR (125 MHz, methanol- d_4): δ_C (ppm) 215.2, 192.1, 162.1, 151.1, 149.0, 145.9, 143.9, 134.6, 131.4, 129.1, 123.0, 119.5, 110.1, 105.3, 79.1, 76.9, 65.5, 56.6, 49.6, 41.2, 34.1, 29.0, 23.6, 21.1, 15.8, 15.6; HRESIMS m/z 491.2049, $[M + Na]^+$ (calcd. for $C_{27}H_{32}O_7Na$, 491.2046).

Compound **27**: yellow powder, $[\alpha]_D^{25} +98$ (c 0.4 in MeOH); UV (MeOH) λ_{max} (log ϵ) 209 (4.36), 298 (2.56); IR ν_{max} 3268, 2926, 1684, 1587, 1514, 1449, 1089 cm^{-1} ; 1H NMR (500 MHz, methanol- d_4): δ_H (ppm) δ_H (ppm) 7.68 (1H, d, $J = 2.5$ Hz), 6.66 (1H, d, $J = 2.0$ Hz), 6.64 (1H, d, $J = 2.0$ Hz), 6.60 (1H, s), 3.86 (3H, s), 3.70 (1H, ddd, $J = 7.5, 7.5, 3.5$ Hz), 3.43 (1H, m), 3.37 (1H, m), 2.78 (1H, m), 2.46 (3H, s), 2.39 (1H, m), 1.45 (3H, d, $J = 7.0$ Hz), 1.35 (3H, d, $J = 7.0$ Hz), 0.96 (3H, d, $J = 7.0$ Hz), ^{13}C NMR (125 MHz, methanol- d_4): δ_C (ppm) 191.3, 180.2, 161.4, 149.4, 146.4, 145.7, 141.7, 138.8, 136.7, 133.1, 130.8, 128.0, 125.9, 119.4, 112.0, 107.1, 56.7, 46.6, 37.7, 32.5, 29.5, 22.6, 21.2, 20.3, 17.2; HRESIMS m/z 441.1910, $[M + H]^+$ (calcd. for $C_{25}H_{29}O_7$, 441.1913).

Compound **28**: yellow powder, $[\alpha]_D^{25} +29$ (c 0.9 in MeOH); UV (MeOH) λ_{\max} (log ϵ) 212 (4.20), 289 (3.74); IR ν_{\max} 3399, 2917, 1651, 1587, 1515, 1448, 1362, 1111 cm^{-1} ; ^1H NMR (500 MHz, methanol- d_4): δ_{H} (ppm) 6.59 (2H, s), 6.53 (1H, s), 6.48 (1H, s), 3.79 (6H, s), 3.72 (1H, d, $J = 7.0$ Hz), 3.52 (1H, m), 3.35 (1H, m), 2.53 (3H, s), 2.34 (1H, m), 2.16 (1H, m), 1.40 (3H, d, $J = 7.0$ Hz), 1.38 (3H, d, $J = 7.5$ Hz), 1.10 (3H, d, $J = 7.0$ Hz), ^{13}C NMR (125 MHz, methanol- d_4): δ_{C} (ppm) 199.0, 162.1, 153.5, 149.0, 144.2, 137.1, 136.0, 130.0, 128.5, 127.6, 120.3, 119.1, 106.7, 89.4, 56.6, 48.8, 42.7, 35.4, 23.6, 21.2, 14.2; HRESIMS m/z 437.1956, $[\text{M} - \text{H}]^-$ (calcd for $\text{C}_{26}\text{H}_{29}\text{O}_6$, 437.1964).

Mansoxetane (**29**): pale brown solid, ^1H NMR (500 MHz, acetone- d_6): δ_{H} (ppm) 9.64 (1H, d, $J = 7.5$ Hz), 7.54 (1H, d, $J = 15.5$ Hz), 7.02 (1H, d, $J = 2.0$ Hz), 6.93 (1H, d, $J = 2.0$ Hz), 6.68 (1H, dd, $J = 16.0, 7.5$ Hz), 6.68 (1H, s), 6.67 (1H, s), 4.93 (1H, d, $J = 7.5$ Hz), 4.12 (1H, m), 3.91 (3H, s), 3.83 (3H, s), 3.80 (1H, d, $J = 12.5$ Hz), 3.57 (1H, d, $J = 12.5$ Hz). ^{13}C NMR (125 MHz, acetone- d_6): δ_{C} (ppm) 194.1, 153.9, 150.3, 149.1, 146.4, 145.5, 137.3, 135.3, 128.2, 128.0, 127.5, 111.9, 109.3, 105.3, 103.9, 79.8, 77.1, 61.6, 56.5, 56.5.

9'-O-acetylmansoxetane (**30**): colorless oil, $[\alpha]_D^{25} + 99$ (c 0.67 in MeOH); UV (MeOH) λ_{\max} (log ϵ) 210 (4.15), 234 (3.74), 330 (3.06); IR ν_{\max} 3379, 2918, 1738, 1660, 1587, 1505, 1451, 1432, 1320, 1088 cm^{-1} ; ^1H NMR (500 MHz, methanol- d_4): δ_{H} (ppm) 9.58 (1H, d, $J = 7.5$ Hz), 7.54 (1H, d, $J = 16.0$ Hz), 6.95 (1H, d, $J = 2.0$ Hz), 6.93 (1H, d, $J = 1.5$ Hz), 6.66 (1H, dd, $J = 16.0, 8.0$ Hz), 6.55 (1H, d, $J = 2.0$ Hz), 6.53 (1H, d, $J = 2.0$ Hz), 4.81 (1H, d, $J = 8.0$ Hz), 4.30 (1H, m), 4.27 (1H, d, $J = 12.0$ Hz), 3.98 (1H, dd, $J = 12.0, 4.5$ Hz), 3.89 (3H, s), 3.83 (3H, s), 2.04 (3H, s). ^{13}C NMR (125 MHz, methanol- d_4): δ_{C} (ppm)

196.1, 172.3, 155.5, 150.8, 149.9, 146.9, 146.0, 137.4, 136.2, 128.3, 128.2, 127.6, 112.3, 109.3, 106.0, 103.9, 77.9, 77.4, 64.0, 56.8, 56.7, 20.5; HRESIMS m/z 453.1164 $[M+Na]^+$ (calcd for $C_{22}H_{22}O_9Na$, 453.1162).

2.6 Biological activities

2.6.1 α -glucosidase inhibitory

This activity was performed by the method described by Ramadhan and coworkers.⁵⁷ Briefly, α -glucosidase (0.1 U/mL) and substrate (1 mM *p*-nitrophenyl- α -D-glucopyranoside) were dissolved in 0.1 M phosphate buffer (pH 6.9). A 10 μ L test sample was pre-incubated with α -glucosidase (40 μ L) at 37° C for 10 minutes. A substrate solution (50 μ L) was then added to the reaction mixture and incubated at 37° C for an additional 20 minutes, and terminated by adding 1 M Na_2CO_3 solution (100 μ L). Enzymatic activity was quantified by measuring the absorbance at 405 nm (ALLSHENG AMR-100 microplate reader). The percentage inhibition of activity was calculated as follows:

$$\% \text{ Inhibition} = [(A_0 - A_1) / A_0] \times 100$$

where: A_0 is the absorbance without the sample; A_1 is the absorbance with the sample.

The IC_{50} value was deduced from the plot of % inhibition versus concentration of test sample. Acarbose was used as standard control and the experiment was performed in triplicate.

2.6.2 Antioxidant activity

The antioxidant activity was followed the method described by Rankovic⁵⁸ with slightly modification. The sample was prepared with various concentrations in methanol. DPPH solution was prepared with concentration of 0.05 mg/mL. 50 μ L of samples were placed on 96 multiple wells channel and 100 μ L of DPPH solution then added. Mixed the solution well and incubate the plate at dark room for 30 minutes. The absorbance of DPPH inhibition was read by using microplate reader (ALLSHENG AMR-100 microplate reader) at 520 nm. Ascorbic acid was used as the positive control. The DPPH radical concentration was calculated using the following equation:

$$\text{DPPH scavenging effect (\%)} = [(A_0 - A_1)/A_0] \times 100$$

where A_0 is the absorbance of the negative control and A_1 is the absorbance of reaction mixture or standard. The inhibition concentration at 50% inhibition (IC_{50}) was the parameter used to compare the radical scavenging activity.

2.6.3 Cytotoxic activity

This experiment was conducted under the collaboration with Department of Pharmacology, Faculty of Medicine, Chulalongkorn University. Cell viability assay: Cell A549 was seeded into 96-well plates at 5×10^3 cells/well. After overnight incubation, cell was treated with isolated compounds and cisplatin at concentrations of 1, 3, 10, 30 μ M and 0.2% DMSO (vehicle control) for 48 h. MTT solution was added and incubated for additional 4 h. The medium was removed and 200 μ L of DMSO was

added to each well. The absorbance of the converted dye was measured at 570 nm using a microplate reading spectrophotometer. IC_{50} values were calculated using GraphPad Prism 7 software.



Chapter 3

RESULTS AND DISCUSSION

3.1 Extraction of *M. gagei* heartwood

Dried powder of *M. gagei* heartwoods (15 kg) was extracted by maceration with EtOAc at room temperature, shaking occasionally during three days, filtering and evaporating. This stage was repeated three times with pure solvent. The crude EtOAc extract was obtained as dark-brown (750 g, 5.0 % yield of dried-powdered heartwoods).

3.2 Separation of the EtOAc extract of *M. gagei* heartwood

The crude EtOAc extract (750 g) was fractionated by silica gel quick column using hexane/EtOAc (85:15 – 0:100) mixtures and acetone as the eluent. The fractions were collected and combined based on TLC results, and five fractions were obtained. The results of fractionation of the EtOAc extract are shown in Table 3.1.

Table 3.1 The fractionation of the EtOAc extract of *M. gagei* heartwoods

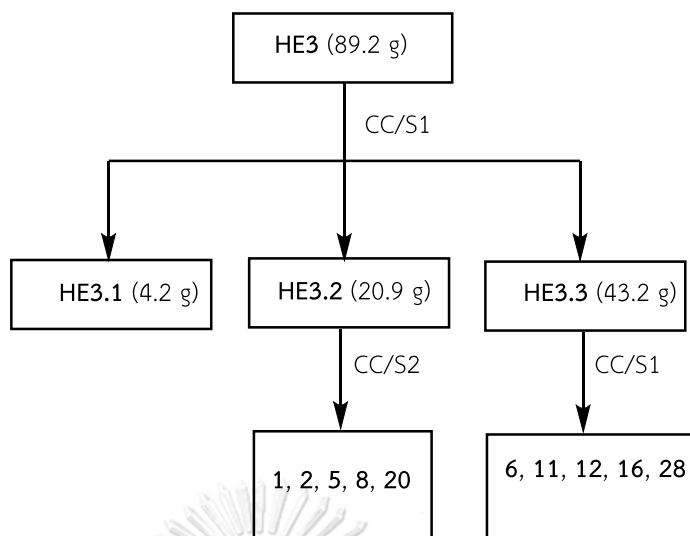
Eluent (% V/V)	Fractions	Remarks	Weight (g)
15% EtOAc/hexane	HE1	Yellow oil	48.2
20% EtOAc/hexane	HE2	Yellow-brown solid	99.3
30% EtOAc/hexane	HE3	Red-brown solid	89.2
EtOAc	EA	Brown solid	130.1
Ac	Ac	Brown solid	150.2

Fraction **HE3** (89.2 g) was re-separated by column chromatography using an isocratic elution solvent system consisting of hexane/CH₂Cl₂/Ac (3:5:0.5) to afford three subfractions **HE3.1-3**. Further fractionation of **HE3.2** (20.9 g) by silica gel column using hexane/CH₂Cl₂/MeOH (1:7:0.1) solvent system furnishing compounds **1** (12.0 mg), **2** (10.0 mg), **5** (8.0 mg), **8** (20.0 mg), and **20** (10.0 mg). Further fractionation of **HE3.3** (43.2 g) by silica gel column using hexane/CH₂Cl₂/Ac (5:3:0.5) solvent system yielding compounds **6** (30.0 mg), **11** (9.0 mg), **12** (10.0 mg), **16** (12.0 mg) and **28** (20.0 mg).

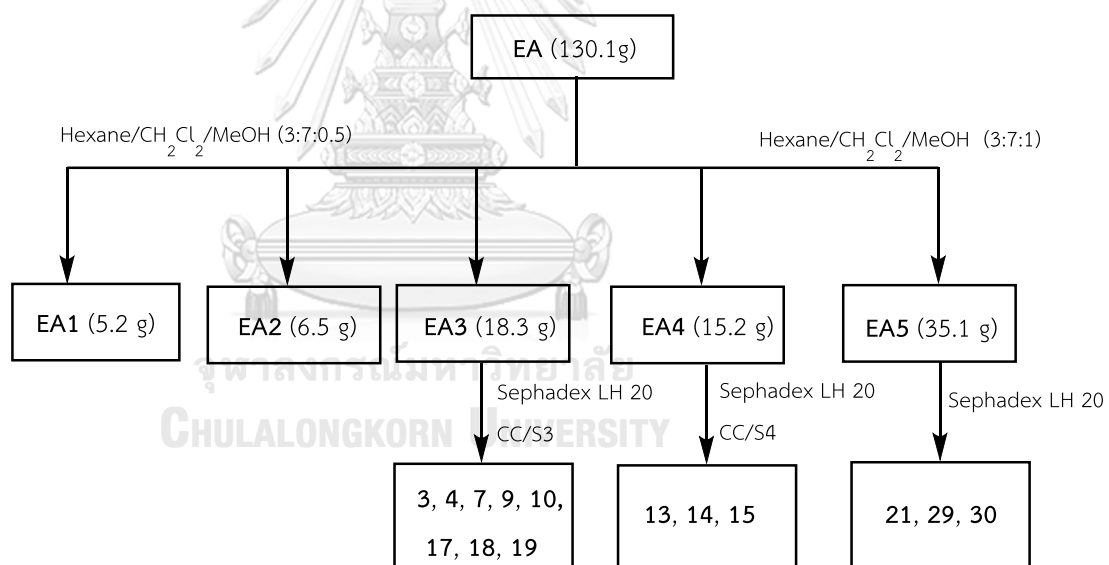
EA fraction (130.1 g) was subjected to silica gel column using mixtures of hexane/CH₂Cl₂/MeOH of increasing polarity to obtain five fractions (**EA1-EA5**). Fraction **EA3** (18.3 g) was chromatographed on a Sephadex LH-20 column with CH₂Cl₂/MeOH (1:1) to obtain three subfractions **EA3.1-EA3.3**. Subfraction **EA3.2** (651 mg) was separated by silica gel column and eluted with hexane/CH₂Cl₂/Ac (5:3:1) to attain **3**

(15.0 mg), **4** (20.0 mg), **17** (10.0 mg), **18** (12.0 mg), and **19** (3.5 mg) while subfraction **EA3.3** (1.3 g) using the same isocratic elution solvent resulted in the isolation of **7** (10.0 mg), **9** (30.0 mg), and **10** (20.0 mg). Fractions **EA4** (15.2 g) and **EA5** (35.1 g) were fractionated over Sephadex LH-20 column with CH₂Cl₂/MeOH (1:1) to afford subfractions **EA4.1-EA4.4** and **EA5.1-EA5.4**, respectively. Subfraction **EA4.2** (1.3 g) was separated by silica gel column eluting with CH₂Cl₂/MeOH (3:0.1) to obtain **13** (34.0 mg), **14** (58.0 mg) and **15** (8.0 mg). Subfraction **EA5.1** (601.1 mg) was purified on Sephadex LH-20 column using MeOH to yield **21** (21.0 mg), **29** (680.0 mg), and **30** (60.0 mg).

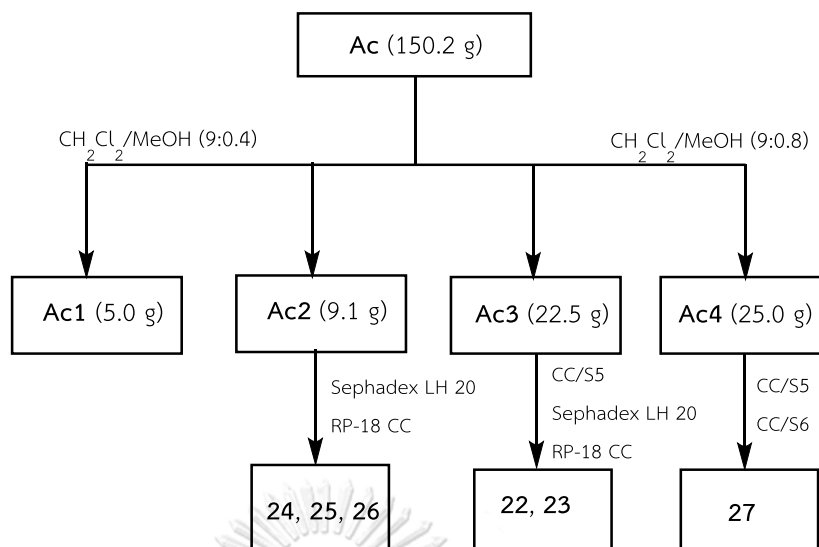
Fraction **Ac** (150.2 g) was fractionated using silica gel column with CH₂Cl₂/MeOH of increasing polarity to give four fractions **Ac1-Ac4**. Fraction **Ac2** (9.1 g) was chromatographed on a Sephadex LH-20 column with CH₂Cl₂/MeOH (1:1) to obtain three subfractions **Ac2.1-Ac2.3**. Subfraction **Ac2.2** was further purified by RP-18 column and eluted with MeOH/H₂O (2:1) to get **24** (41.0 mg), **25** (10.0 mg) and **26** (6.0 mg). Fraction **Ac3** (22.5 g) and **Ac4** (25.0 g) were separated on silica gel column with hexane/CH₂Cl₂/Ac (5:3:2) to get six subfractions **Ac3.1-Ac3.3**, **Ac4.1-Ac4.3**, respectively. Subfraction **Ac3.3** was subjected to a Sephadex LH-20 column with CH₂Cl₂/MeOH (1:1), and then a RP-18 column, eluted with MeOH-H₂O (2:1) to give **22** (30.0 mg) and **23** (25.0 mg). Subfraction **Ac4.2** was subjected to silica gel column eluting with a solvent system hexane/CH₂Cl₂/EtOAc/MeOH (1:2:1:0.2) to yield **27** (8.0 mg). The procedure for the isolation of the EtOAc extract of *M. gagei* is summarized in Schemes 3.1- 3.3.



Scheme 3.1 Procedure for the separation of fraction HE3



Scheme 3.2 Procedure for the separation of fraction EA



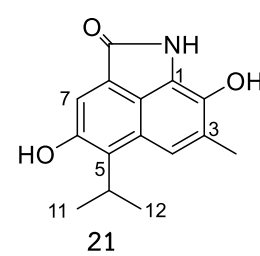
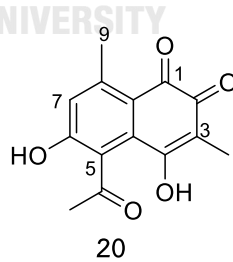
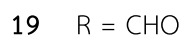
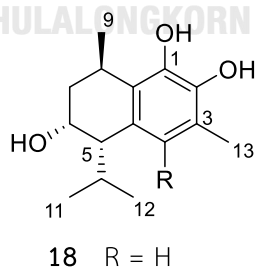
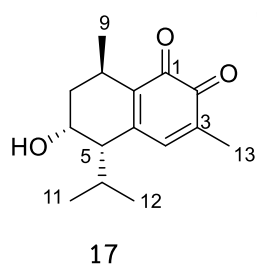
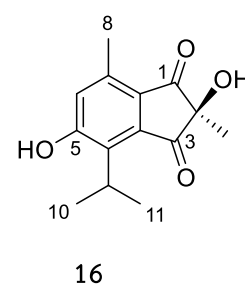
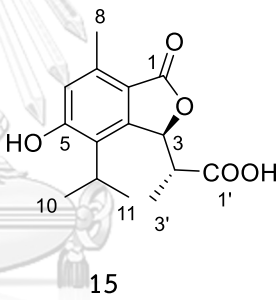
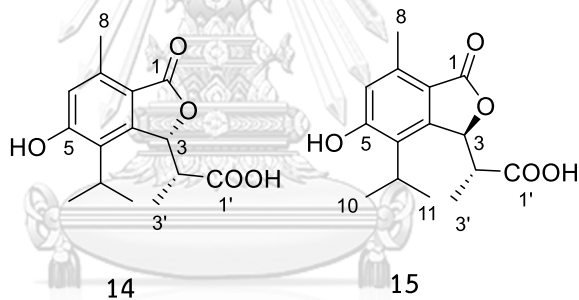
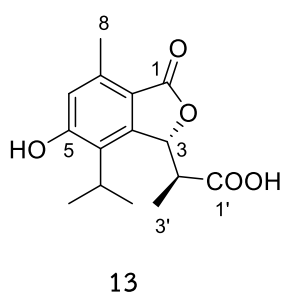
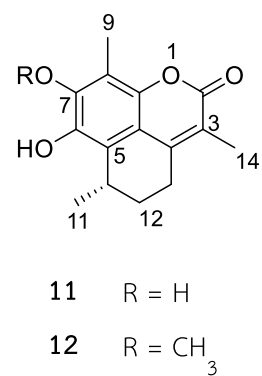
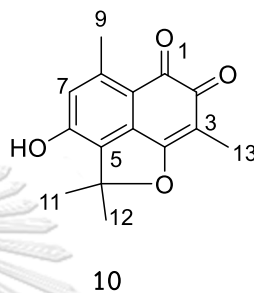
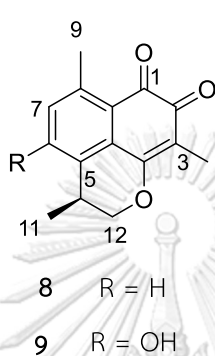
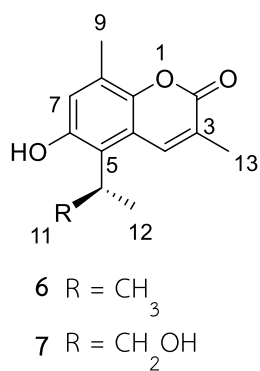
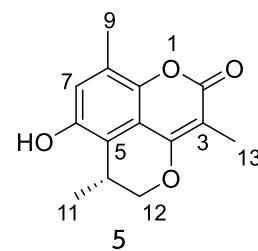
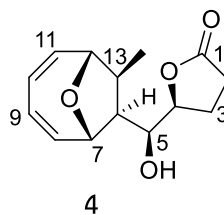
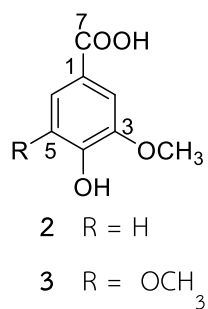
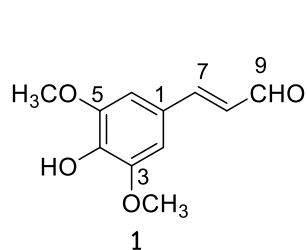
Solvent system:

S1: hexane/ CH_2Cl_2 /Ac (3:5:0.5), S2: hexane/ CH_2Cl_2 /MeOH (1:7:0.1), S3: hexane/ CH_2Cl_2 /Ac (5:3:1)
 S4: CH_2Cl_2 /MeOH (3:0.1), S5: hexane/ CH_2Cl_2 /Ac (5:3:2), S6: hexane/ CH_2Cl_2 /EtOAc/MeOH (1:2:1:0.2)
 CC: chromatography column

Scheme 3.3 Procedure for the separation of fraction Ac

3.3 Structural elucidation of compounds from the EtOAc extract

The structural identification of isolated compounds was determined by spectroscopic data analysis (1D, 2D NMR and HRESIMS), and the absolute configurations were established by calculation of ECD data. The structures of all isolated compounds are presented in Figure 3.1.



จุฬาลงกรณ์มหาวิทยาลัย

CHULALONGKORN UNIVERSITY

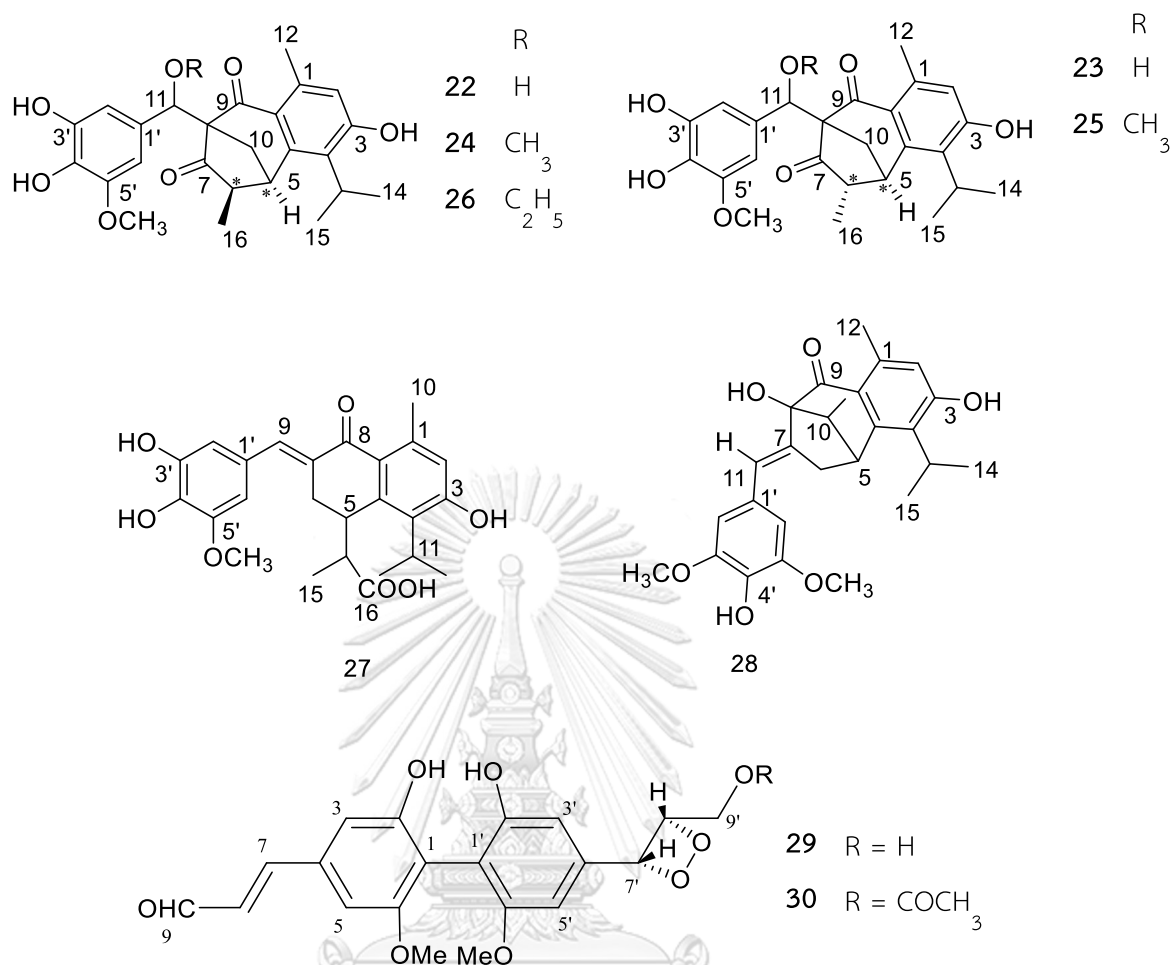


Figure 3.1 Isolated compounds from the EtOAc extract of *M. gagei* heartwoods

The structures of the known compounds were identified as sinapaldehyde (**1**),⁵⁹ vanillic acid (**2**),⁶⁰ syringic acid (**3**),⁶¹ phomoxydiene B (**4**),⁶² mansorin I (**5**),¹² mansorin B (**6**),¹¹ (11*S*)-6-hydroxy-5-(11-hydroxypropan-12-yl)-3,8-dimethyl-2*H*-chromen-2-one (**7**),⁶³ mansonone E (**8**),¹⁵ mansonone H (**9**),¹⁵ dehydrooxoperezinone (**10**),⁶⁴ heliclactone (**11**),⁶⁵ and mansoxetan (**29**)⁴⁰ by analysis of their spectroscopic data and comparison with literature. The NMR spectral data of **1–11** and **29** are presented in Tables 3.2-3.6, and Table 3.14.

Table 3.2 The ^1H (500 MHz) and ^{13}C (125 MHz) NMR spectroscopic data of **1**
(acetone- d_6) **2**, **3** (DMSO- d_6) (δ in ppm)

No.	(1)		(2)		(3)	
	δ_{H} (J in Hz)	δ_{C}	δ_{H} (J in Hz)	δ_{C}	δ_{H} (J in Hz)	δ_{C}
1		126.1		121.7		120.8
2	7.08, s	107.2	7.42, d (2.0)	112.7	7.20, s	106.8
3		149.0		147.3		147.4
4		140.2		151.2		140.1
5		149.0	6.84, d (8.0)	115.1		147.4
6	7.08, s	107.2	7.43, dd (8.0, 2.0)	123.6	7.20, s	106.8
7	7.56, d (16.0)	154.5		167.3		167.4
8	6.69, dd (15.0, 8.0)	127.3				
9	9.63, d (7.5)	193.9				
OCH ₃	3.90, s	56.7	3.80, s	55.6	3.79, s	56.0

Table 3.3 The ^1H (500 MHz) and ^{13}C (125 MHz) NMR spectroscopic data of **4** and **5**(acetone- d_6) (δ in ppm)

No.	(4)		(5)	
	δ_{H} (J in Hz)	δ_{C}	δ_{H} (J in Hz)	δ_{C}
1		177.8		
2	2.45, m	28.9		163.9
3	2.29, m	24.8		102.5
4	4.56, m	82.8		159.8
4a				111.8
5	3.62, t (8.0)	72.4		120.1
6	2.74, m	54.7		149.3
7	4.36, t (6.0)	77.8	6.99, s	120.9
8	6.26, dd (10.5, 6.0)	140.0		124.7
8a				144.5
9	5.79, dd (10.5, 7.0)	126.0	2.29, s	15.3
10	5.85, dd (11.5, 6.5)	125.2	3.34, m	27.5
11	6.06, dd (11.5, 4.5)	138.5	1.29, d (7.0)	17.9
12	4.17, d (4.5)	87.1	4.48, dd (11.0, 1.5)	73.5
			4.31, dd (11.0, 3.5)	
13	2.81, m	54.1	1.96, s	9.2
14	1.10, d (7.0)	14.4		

Table 3.4 The ^1H (500 MHz) and ^{13}C (125 MHz) NMR spectroscopic data of **6** (acetone- d_6) and **7** (CD_3OD) (δ in ppm)

No.	(6)		(7)	
	δ_{H} (ν in Hz)	δ_{C}	δ_{H} (ν in Hz)	δ_{C}
2		162.0		164.2
3		125.0		125.0
4	8.11, d (1.5)	137.5	8.08, s	139.1
4a		118.7		147.1
5		127.6		124.6
6		152.1		153.3
7	6.93, d (0.5)	121.2	6.85, s	122.0
8		124.0		125.4
8a		146.8		120.1
9	2.27, d (1.0)	15.2	2.33, s	15.3
10	3.62, m	27.3	3.52, m	36.6
11	1.39, d (7.0)	21.3	3.97, dd (10.5, 6.5) 3.90, dd (10.5, 6)	66.5
12	1.39, d (7.0)	21.3	1.38, d (7.0)	16.0
13	2.15, d (1.0)	17.4	2.17, s	17.3

Table 3.5 The ^1H (500 MHz) and ^{13}C (125 MHz) NMR spectroscopic data of **8** (CDCl_3),
9 and **10** ($\text{DMSO}-d_6$) (δ in ppm)

No.	(8)		(9)		(10)	
	δ_{H} (J in Hz)	δ_{C}	δ_{H} (J in Hz)	δ_{C}	δ_{H} (J in Hz)	δ_{C}
1		182.4		180.1		180.0
2		180.4		179.5		176.9
3		116.4		114.6		107.2
4		162.7		161.7		167.5
4a		127.0		125.4		135.7
5		137.0		118.9		130.5
6	7.34, d (8.0)	132.8		159.7		157.4
7	7.25, d (8.0)	135.0	6.75, s	119.1	6.72, s	120.1
8		143.1		144.6		146.0
8a		127.4		128.0		116.0
9	2.64, s	22.7	2.48, s	22.7	2.51, s	20.1
10	3.09, m	31.4	3.18, m	25.6		95.9
11	1.36, d (7.0)	17.7	1.21, d (7.0)	17.0	1.70, s	25.5
12	4.40, dd (10.5, 4.0)	71.5	4.41, d (11.0)	71.7	1.70, s	25.5
	4.22, dd (11.0, 5.0)		4.28, dd (11.0, 3.5)			
13	1.95, s	7.9	1.80, s	7.9	1.77, s	8.0

(10S)-7-O-Methylheliclactone (**12**) was obtained as yellowish amorphous powder. Its molecular formula was deduced as C₁₆H₁₈O₄ by HRESIMS with *m/z* 273.1122 ([M - H]⁻, calcd 273.1127). The ¹³C NMR and HSQC revealed the resonances of 16 carbons, including nine quaternary carbons, one methine, two methylene groups and four methyl groups. The ¹H NMR data (Table 3.6) displayed characteristic resonances for one methoxy group at δ_{H} 3.79 (3H, s), one methine proton at δ_{H} 3.45 (1H, m), two methylene groups at δ_{H} [2.91 (1H, m), 2.79 (1H, m), 1.96 (1H, m) and 1.87 (1H, m)], and three methyl groups at δ_{H} 2.30 (3H, s), 2.10 (3H, d, *J* = 1.0 Hz), 1.23 (3H, d, *J* = 7.5 Hz). 1D NMR (Table 3.6) indicated that **12** possessed a coumarin skeleton, containing a carbonyl lactone carbon at δ_{C} 164.9 and eight olefinic and aromatic carbons (δ_{C} 150.4, 150.0, 145.6, 144.6, 126.6, 118.0, 117.2 and 113.9). The ¹H-¹H COSY correlation of H₃-11/H-10/H₂-12/H₂-13 and HMBC cross-peaks from H-10 to C-4a, C-5, C-6, C-11, C-12, and C-13; from H₃-13 to C-3, C-4, C-4a, C-10, and C-11 confirmed the connections of butane-1,3-diyl moiety in **12** with the coumarin ring at carbons C-4 and C-5. The 1D NMR data (Table 3.6) was close to those of heliclactone (**11**),⁶⁵ indicating **12** also a sesquiterpenoid coumarin, except that the hydroxy group at C-7 in heliclactone was substituted by the methoxy group in **12**. This was confirmed by the HMBC correlation from methoxy group (δ_{H} 3.79) to C-7 (δ_{C} 150.0). The key ¹H-¹H COSY, HMBC correlations of **12** are summarized in Figure 3.2. The absolute configuration of **12** was defined to be (10S) through comparison of the experimental and calculated ECD spectral data

(Figure 3.3). Thus, **12** was designated as (10*S*)-7-*O*-methylheliclactone as a new sesquiterpenoid coumarin.

Table 3.6 The ^1H (500 MHz) and ^{13}C (125 MHz) NMR spectroscopic data of **11** (DMSO- d_6), **12**, (CD_3OD) (δ in ppm)

No.	(11)		(12)	
	δ_{H} (J in Hz)	δ_{C}	δ_{H} (J in Hz)	δ_{C}
1				
2		161.9		164.9
3		114.1		118.0
4		148.3		150.4
4a		108.1		113.9
5		124.9		126.6
6		138.4		144.6
7		147.3		150.0
8		108.9		117.2
8a		145.1		145.6
9	2.16, s	8.5	2.30, s	8.8
10	3.36, m	25.4	3.45, m	27.2
11	1.12, d (7.0)	18.6	1.23, d (7.5)	18.8
12	1.86, m	27.3	1.96, m	28.7
	1.76, m		1.87, m	
13	2.80, m	21.6	2.91, m	23.1
	2.67, m		2.79, m	
14	2.00, s	12.1	2.10, d (1.0)	12.3
OCH_3			3.79, s	61.2

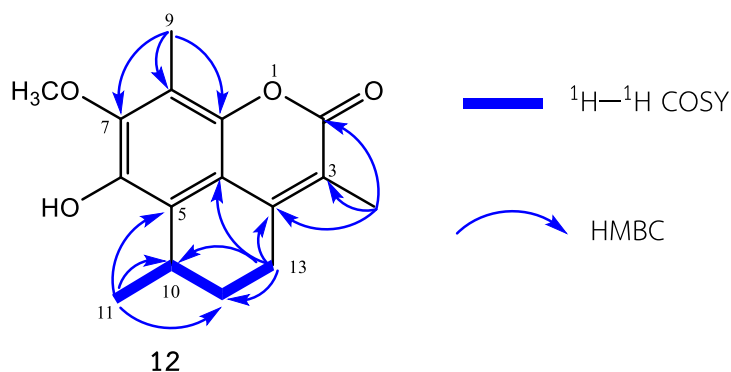


Figure 3.2 Key ^1H - ^1H COSY, HMBC correlations of **12**

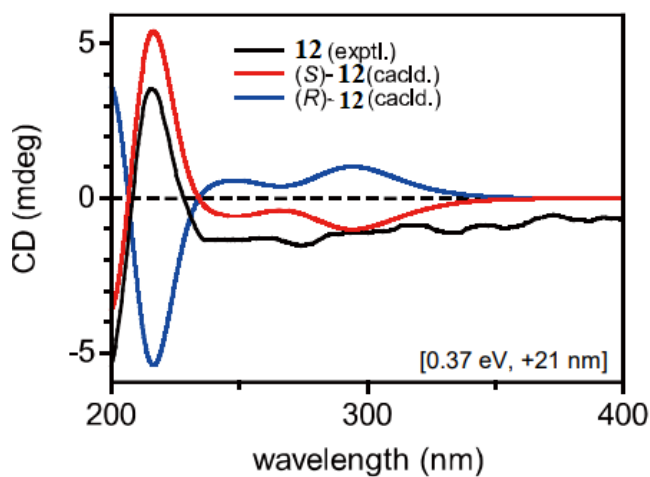


Figure 3.3 Experimental ECD spectra (200-400 nm) and calculated ECD spectra for **12**

Mansoniafuranone A (**13**) was isolated as pale yellow amorphous solid with $[\alpha]_D^{20} + 131$ (c 1.0 in MeOH). Its molecular formula was assigned as $\text{C}_{15}\text{H}_{18}\text{O}_5$ by HRESIMS m/z 301.1063 $[\text{M} + \text{Na}]^+$ (calcd for $\text{C}_{15}\text{H}_{18}\text{O}_5\text{Na}$, 301.1052), indicating 7 indices of hydrogen deficiency. The ^1H NMR spectrum of **13** (Table 3.7) revealed the presence of one aromatic proton at δ_{H} 6.63 (1H, s), an oxygenated methine proton at δ_{H} 5.52 (1H, d, $J = 2.5$ Hz), one methine proton at δ_{H} 2.89 (1H, m), and four methyl groups at δ_{H} 2.44 (3H, s), 1.41 (3H, d, $J = 7.0$ Hz), 1.38 (3H, d, $J = 7.0$ Hz) and 1.33 (3H, d, $J = 7.0$ Hz).

The ^{13}C NMR and HSQC spectra showed the presence of fifteen carbon resonances, including two carbonyl carbons (δ_{C} 175.0 and 173.3), four methyls (δ_{C} 20.7, 20.2, 17.1, and 15.3), four methines (δ_{C} 120.1, 82.4, 44.4, and 30.7), and five quaternary carbons (δ_{C} 163.1, 150.0, 139.3, and 115.9).

The ^1H - ^1H COSY spectrum of **13** identified the spin systems through H-3/H-2'/H₃-3' and H₃-10/H-9/H₃-11 that were supported by the HMBC correlation of both H-3 (δ_{H} 5.52) and H₃-3' (δ_{H} 1.41) to C-2' (δ_{C} 44.4); of H₃-3' to C-1' (δ_{C} 175.0); and both H₃-10 (δ_{H} 1.33) and H₃-11 (δ_{H} 1.38) to C-9 (δ_{C} 30.7), respectively. That further suggested the occurrence of 2-carboxy-1-hydroxypropyl and isopropyl moieties in **13**. Two methine protons H-6 (δ_{H} 6.63) and H-9 (δ_{H} 2.89) also showed the correlations with the same oxygenated aromatic carbon C-5 (δ_{C} 163.1). Additionally, the HMBC correlations of methyl protons H₃-8 (δ_{H} 2.44) to C-6 (δ_{C} 120.1), C-7 (δ_{C} 139.3), and C-7a (δ_{C} 115.9); and methine proton H-3 (δ_{H} 5.52) to C-3a (δ_{C} 150.0), C-4 (δ_{C} 127.1), and C-7a (δ_{C} 115.9) determined the occurrence of 1,2,3,4,5-pentasubstituted benzene ring moiety accommodated these five substituents in the following order: hydroxy, isopropyl, 2-carboxy-1-hydroxypropyl, carbonyl, and methyl group. Furthermore, the five-membered ring lactone linked between 3-OH and C-1 was indicated by the key HMBC correlation of methine proton H-3 to C-1 (δ_{C} 173.3) as same as that of emerfuranone B.⁶⁶ Thus, the structure of **13**, named mansoniafuranone A was elucidated as a new sesquiterpenoid in nature.

Compound **14**, named mansoniafuranone B, isolated as a pale yellow needle, with a molecular formula of $C_{15}H_{18}O_5$ was established by the HRESIMS ion at m/z 301.1072 $[M + Na]^+$ (calcd for $C_{15}H_{18}O_5Na$, 301.1052), suggesting 7 double bond equivalents. The 1H NMR of **14** displayed proton signals corresponding to one aromatic proton at δ_H 6.70 (1H, s), an oxygenated methine proton at δ_H 6.03 (1H, br. s), one methine proton at δ_H 2.96 (1H, m), and four methyl groups at δ_H 2.48 (3H, s), 1.37 (3H, d, $J = 7.0$ Hz), 1.34 (3H, d, $J = 7.0$ Hz) and 0.67 (3H, d, $J = 7.0$ Hz). The ^{13}C NMR and HSQC spectra gave information about 15 carbons, including two carbonyl carbons (δ_C 176.1 and 173.1), four methyls (δ_C 20.6, 20.3, 17.1, and 8.1), four methines (δ_C 120.3, 81.5, 42.2, and 30.3), and five quaternary carbons (δ_C 163.4, 149.6, 139.8, and 115.6). The spectroscopic data indicated that **14** is a stereoisomer of **13**, with the only difference being the resonances of methyl protons at δ_H 0.67 (3H, d, $J = 7.0$ Hz, H-3') and carbon at δ_C 8.1 (C-3'), which were more upfield than those of **13**. This would be explained by the fact that the methyl protons in **14** were shielded by anisotropic effect of the carbonyl group. Thus, **14** is a diastereomer of **13**.

Compound **15**, mansoniafuranone C was isolated as yellowish amorphous powder. The molecular formula was deduced as $C_{15}H_{18}O_5$ by HRESIMS m/z 301.1067 $[M + Na]^+$ (calcd for $C_{15}H_{18}O_5Na$, 301.1052). The 1H NMR of **15** revealed the resonances of one aromatic proton, an oxygenated methine proton, one methine proton, and four methyl groups. The ^{13}C NMR and HSQC spectra depicted fifteen carbons, including two

carbonyl carbons, four methylys, four methines, and five quaternary carbons. The NMR characteristics of **15** were the same as those of **13** with the only difference in the opposite of optical rotation $[\alpha]_D^{20}$ - 131 (c 0.35 in MeOH) and ECD spectrum. Therefore, **15** is an enantiomer of **13**. The key ^1H - ^1H COSY, HMBC, NOESY correlations of **13**-**15** are summarized in Figure 3.4.

The relative configurations of **13**-**15** were assigned by NOESY data. Correlations between H-3 and H₃-3' in NOESY spectra of **13** and **15** indicated a *cis* relative configuration between H-3 and methyl group at C-2' position, whereas enhancement was not observed for H₃-3' in the spectrum of **14**, suggesting a *trans* relationship between H-3 and H₃-3'.⁶⁷ The ECD spectra were used to define the absolute configuration of **13**-**15**. The calculated ECD spectra of the (2'S,3R), (2'R,3R) and (2'R,3S) stereoisomers were consistent with the experimental ECD spectra (Fig. 3.5) of **13**-**15**, respectively.

Table 3.7 The ^1H (500 MHz) and ^{13}C (125 MHz) NMR spectroscopic data of **13–15**,
(CD_3OD) (δ in ppm)

No.	(13)		(14)		(15)	
	δ_{H} (J in Hz)	δ_{C}	δ_{H} (J in Hz)	δ_{C}	δ_{H} (J in Hz)	δ_{C}
1		173.3		173.1		174.1
2						
3	5.52, d (2.5)	82.4	6.03, br. s	81.5	5.52, d (2.5)	83.8
3a		150.0		149.6		151.1
4		127.1		126.8		127.1
5		163.1		163.4		163.0
6	6.63, s	120.1	6.70, s	120.3	6.60, s	119.8
7		139.3		139.8		139.0
7a		115.9		115.6		116.5
8	2.44, s	17.1	2.48, s	17.1	2.44, s	17.2
9	2.89, m	30.7	2.96, m	30.3	2.92, m	30.7
10	1.33, d (7.0)	20.7	1.37, d (7.0)	20.6	1.32, d (7.0)	20.8
11	1.38, d (7.0)	20.2	1.34, d (7.0)	20.3	1.40, d (7.0)	20.5
1'		175.0		176.1		180.7
2'	3.15, m	44.4	3.12, m	42.2	2.98, m	47.0
3'	1.41, d (7.0)	15.3	0.67, d (7.0)	8.1	1.33, d (8.0)	16.2

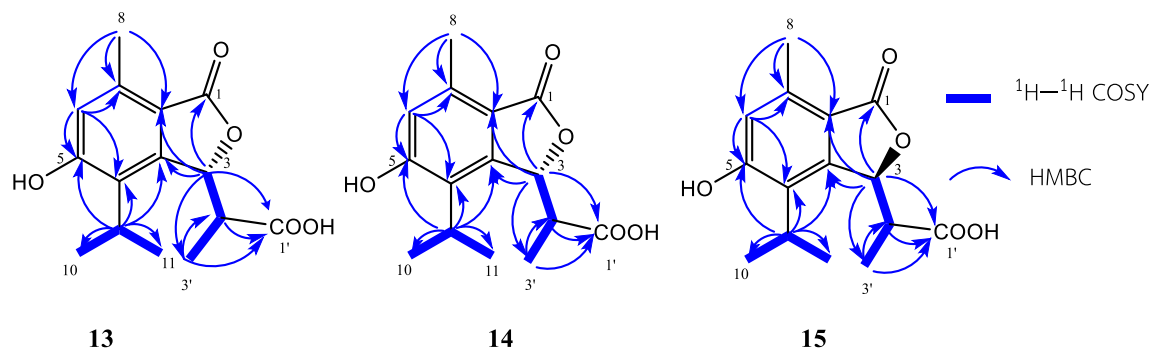


Figure 3.4 Key ^1H - ^1H COSY, HMBC correlations of 13–15

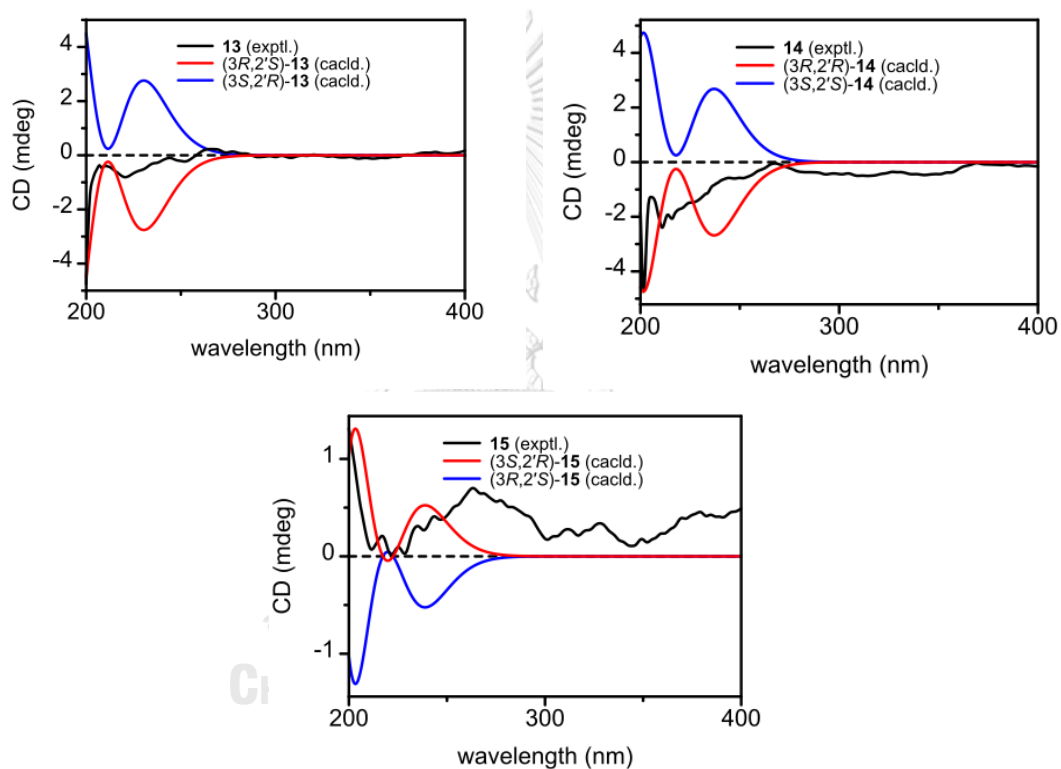


Figure 3.5 Experimental ECD spectra (200–400 nm) and calculated ECD spectra for

13–15

Compound **16** was isolated as yellow powder. The HRESIMS data suggested a molecular formula of $\text{C}_{14}\text{H}_{16}\text{O}_4$ based on the $[\text{M} - \text{H}]^-$ ion signal at m/z 247.0964 (calcd 247.0970). The NMR data (Table 3.8) showed the presence of an aromatic proton at δ_{H} 7.01 (1H, s), a methine proton at δ_{H} 4.39 (1H, m), four methyls at δ_{H} 2.60 (3H, s), 1.35

(3H, s) and two signals at 1.34 (3H, d, $J = 7.0$ Hz), a pentasubstituted benzene moiety, and two carbonyl groups (δ_C 204.7, 201.7) suggesting that **16** was a primnatriene-type nor-sesquiterpenoid.^{68, 69} NMR data of **16** was similar to those of 6-methoxyprimnatriene-1,3-dione⁶⁸ with the differences being the loss of methyl and methoxy group at C-2 and C-6, and the presence of two hydroxy groups at C-2 and C-5. The location of 2-Me was confirmed by the HMBC correlations of H₃-12 with two carbonyl carbons at δ_C 204.7 (C-1) and 201.7 (C-3) and the oxygenated tertiary carbon at δ_C 76.4 (C-2). In addition, the hydroxy group substituted at C-5 was established from the HMBC cross-peaks of H-6 (δ_H 7.01) to C-4 (δ_C 133.6), C-5 (δ_C 165.2), C-7a (δ_C 130.6) and C-8 (δ_C 18.8). Thus, the planar structure of **16** was deduced as 2,5-dihydroxy-4-isopropyl-2,7-dimethyl-1*H*-indene-1,3(2*H*)-dione. The key ¹H-¹H COSY, HMBC, correlations of **16** are summarized in Figure 3.6. The absolute configuration of **16** was determined by ECD experiment and comparison with the previous research.⁷⁰ The ECD spectrum of **16** showed a negative cotton effect at 211 nm ($\Delta\epsilon = -4.1$), defined a 2*R* configuration.⁷⁰

Table 3.8 The ^1H (500 MHz) and ^{13}C (125 MHz) NMR spectroscopic data of **16**,
(CD_3OD) (δ in ppm)

No.	(16)		No.	(16)	
	δ_{H} (ν in Hz)	δ_{C}		δ_{H} (ν in Hz)	δ_{C}
1		204.7	7		140.3
2		76.4	7a		130.6
3		201.7	8	2.60, s	18.8
3a		139.9	9	4.39, m	26.8
4		133.6	10	1.34, d (7.0)	20.4
5		165.2	11	1.34, d (7.0)	20.2
6	7.01, s	126.1	12	1.35, s	21.9

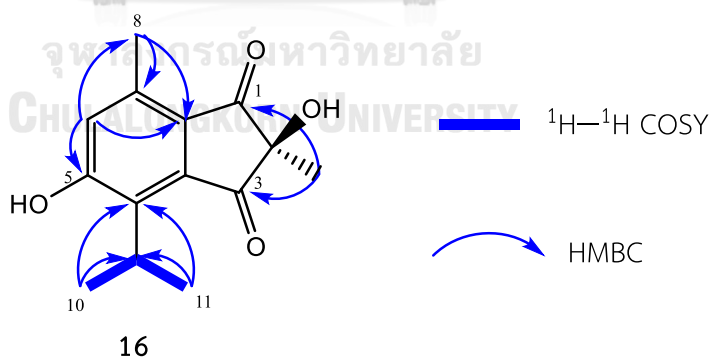


Figure 3.6 Key ^1H - ^1H COSY, HMBC correlations of **16**

Compound **17**, named mansonone T, was obtained as yellow amorphous solid with a molecular formula of $\text{C}_{15}\text{H}_{20}\text{O}_3$, established by the HRESIMS m/z 271.1295 [$\text{M} +$

$\text{Na}]^+$ (calcd for $\text{C}_{15}\text{H}_{20}\text{O}_3\text{Na}$, 271.1310). Analysis of its ^1H NMR (Table 3.9) exhibited the presence of one olefinic proton δ_{H} 6.74 (1H, d, $J = 1.5$ Hz), one oxygenated methine δ_{H} 4.13 (1H, m), three methines δ_{H} 2.93 (1H, m), 2.48 (1H, t, $J = 4.0$ Hz), 2.31 (1H, m), one methylene group δ_{H} 1.89 (1H, m) and 1.51 (1H, m), and four methyls δ_{H} 1.91 (3H, d, $J = 2.0$ Hz), 1.20 (3H, d, $J = 7.0$ Hz), 1.14 (3H, d, $J = 7.0$ Hz), and 0.97 (3H, d, $J = 7.5$ Hz) (Table 3.9). In the ^{13}C NMR and HSQC spectra, the characteristic signals for fifteen carbons were observed, including two carbonyls (δ_{C} 182.4 and 181.0), four methyls (δ_{C} 25.8, 22.0, 21.9, and 15.0), one methylene (δ_{C} 34.6), five methines (one oxygenated and one olefinic) and three quaternary carbons (δ_{C} 151.1, 139.4 and 136.8). These data, suggesting that **17** has a sesquiterpenoid skeleton and being close to a known compound, mansonone A.³⁶ The obvious difference was the presence of oxymethine proton δ_{H} (4.13, m, H-6) in **17** instead of methylene protons in mansonone A. The HMBC correlations of H-5 (δ_{H} 2.48), H₂-7 (δ_{H} 1.51, 1.89), H-8 (δ_{H} 2.93) with C-6 (δ_{C} 66.9) and the ^1H - ^1H COSY correlations of H-5/H-6/H₂-7 confirmed that hydroxy group was assigned at C-6 in **17**.

Compound **18**, named mansonone U, was obtained as yellow amorphous solid, with the molecular formula $\text{C}_{15}\text{H}_{22}\text{O}_3$ assigned from its HRESIMS data (m/z 273.1452, calcd for $\text{C}_{15}\text{H}_{22}\text{O}_3\text{Na}$, 273.1467). The proton signals in the ^1H NMR spectrum showed the presence of one aromatic proton δ_{H} 6.32 (1H, s), one oxygenated methine δ_{H} 4.20 (1H, m), three methines δ_{H} 3.23 (1H, m), 2.65 (1H, t, $J = 4.0$ Hz), 2.20 (1H, m), one

methylene group δ_{H} [2.05 (1H, m) and 1.54 (1H, m)], and four methyls 2.16 (3H, s), 1.23 (3H, d, $J = 7.0$ Hz), 1.06 (3H, d, $J = 7.0$ Hz), and 0.44 (3H, d, $J = 7.0$ Hz) (Table 3.9). The ^{13}C NMR spectrum illustrated the presence of 15 carbons, including an aromatic ring (δ_{C} 144.2, 142.3, 130.3, 127.2, 123.7 and 123.3), one oxygenated carbon (δ_{C} 68.4), one methylene (δ_{C} 35.4), three methines (δ_{C} 51.5, 29.7 and 27.2) and four methyl carbons (δ_{C} 25.9, 22.9, 21.9 and 16.2). The 1D NMR data of **18** were similar to those of **17** with the significant differences being the absence of two carbonyl groups in **17**, and the presence of two hydroxy groups at C-1 (δ_{C} 144.2) and C-2 (δ_{C} 142.3) which were confirmed by the HMBC cross-peaks from H-4 and H₃-13 to C-2 (δ_{C} 142.3).

Compound **19** was obtained as pale yellow amorphous. Its molecular formula was deduced to be $\text{C}_{16}\text{H}_{22}\text{O}_4$ on the basis of the HRESIMS (m/z 301.1420, calcd for $\text{C}_{16}\text{H}_{22}\text{O}_4\text{Na}$, 301.1416) and its ^{13}C NMR spectroscopic data (Table 3.9), indicating 6 degrees of unsaturation. The ^1H NMR spectrum (Table 3.9) of **19** depicted one aldehyde group at δ_{H} 10.36 (1H, s) and four methyl signals at δ_{H} 2.43 (3H, s), 1.25 (3H, d, $J = 7.0$ Hz), 1.05 (3H, d, $J = 6.5$ Hz) and 0.31 (3H, d, $J = 7.5$ Hz). Sixteen carbons including a carbonyl at δ_{C} 195.3, an aromatic ring (δ_{C} 150.7, 142.2, 138.0, 127.9, 127.7 and 127.6), an oxygenated carbon (δ_{C} 68.3), three methines and four methyls were observed in the ^{13}C NMR spectrum. The NMR data (Table 3.9) indicated that **19** was a sesquiterpenoid, and its structure was close to that of **18**. The only difference was the occurrence of an aldehyde group at C-4 position which was confirmed by the HMBC

correlations between aldehyde proton H-14 (δ_{H} 10.36) and carbon C-3 (δ_{C} 127.7), C-4 (δ_{C} 127.9) and C-4a (δ_{C} 138.0). **19** was thus identified as a new natural product and named mansonone V. The key ^1H - ^1H COSY, HMBC, correlations of **17**–**19** are summarized in Figure 3.7.

The relative configurations of **17**–**19** were determined through analysis of NOESY and ^1H - ^1H coupling constant data. NOESY correlations between H-5/H-6 and H-6/H₃-9 implied that these protons were on the same side of cyclohexene ring. The small ^1H - ^1H coupling constant between H-5/H-6 ($J = 4.0$ Hz) suggested the *cis* orientation of these protons.⁷¹ The calculated ECD spectra of (5*S*,6*R*,8*R*)-stereoisomers were close to the experimental ECD of **17**–**19** (Fig. 3.8), indicating the (5*S*,6*R*,8*R*) absolute configurations of **17**–**19**.

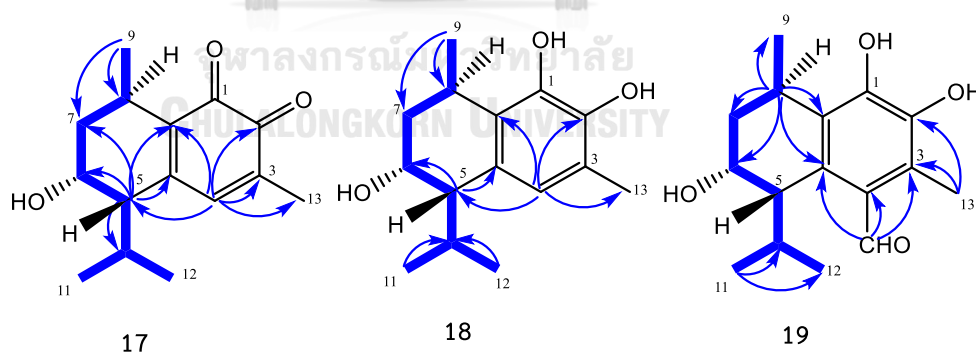


Figure 3.7 Key ^1H - ^1H COSY, HMBC correlations of **17**–**19**

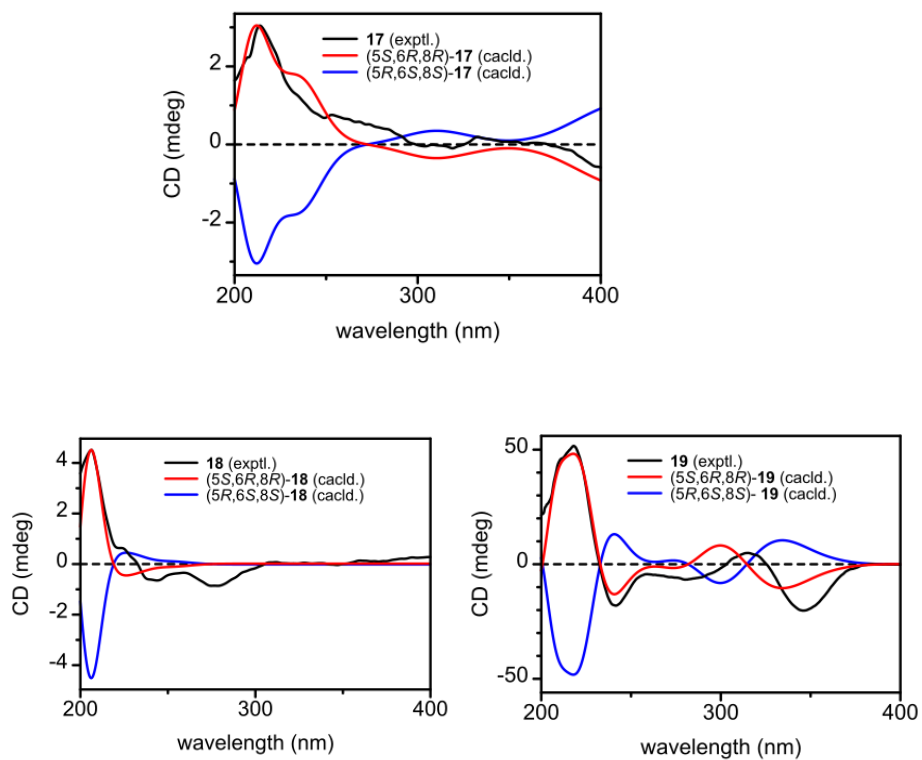


Figure 3.8 Experimental ECD spectra (200–400 nm) and calculated ECD spectra for 17–19

Table 3.9 The ^1H (500 MHz) and ^{13}C (125 MHz) NMR spectroscopic data of **17–19**,
(CD_3OD) (δ in ppm)

No.	(17)		(18)		(19)	
	δ_{H} (ν in Hz)	δ_{C}	δ_{H} (ν in Hz)	δ_{C}	δ_{H} (ν in Hz)	δ_{C}
1		181.0		144.2		150.7
2		182.4		142.3		142.2
3		136.8		123.3		127.7
4	6.74, d (1.5)	142.7	6.32, s	123.7		127.9
4a		151.1		130.3		138.0
5	2.48, t (4.0)	52.0	2.65, t (4.0)	51.5	3.64, t (4.0)	45.7
6	4.13, m	66.9	4.20, m	68.4	4.26, m	68.3
7	1.89, m	34.6	2.05, m	35.4	2.10, m	33.8
	1.51, m		1.54, m		1.60, dd (12.5, 3.5)	
8	2.93, m	29.2	3.23, m	29.7	3.32, m	29.8
8a		139.4		127.2		127.6
9	1.14, d (7.0)	21.9	1.23, d (7.0)	22.9	1.25, d (7.0)	23.2
10	2.31, m	28.0	2.20, m	27.2	2.17, m	28.9
11	0.97, d (7.5)	22.0	0.44, d (7.0)	21.9	1.05, d (6.5)	25.4
12	1.20, d (7.0)	25.8	1.06, d (7.0)	25.9	0.31, d (7.5)	21.9
13	1.91, d (2.0)	15.0	2.16, s	16.2	2.43, s	13.3
14					10.36, s	195.3

Compound **20** as yellow powder had the molecular formula $\text{C}_{14}\text{H}_{12}\text{O}_5$ deducing from its HRESIMS data (m/z 259.0604, calcd for $[\text{M} - \text{H}]^-$, 259.0606). The ^1H NMR data (Table 3.10) revealed the presence of one aromatic proton at δ_{H} 7.05 (1H, s), three

methyl protons at δ_{H} 2.63 (3H, s), 2.40 (3H, s) and 1.91 (3H, s). The ^{13}C NMR data along with the HSQC experiment showed 14 carbon signals, including a carbonyl carbon (δ_{C} 201.5), a 1,2-naphthoquinone moiety (δ_{C} 186.0, 181.3, 158.8, 156.1, 145.3, 134.2, 131.1, 123.0, 120.6, and 117.8), and three methyls (δ_{C} 30.9, 22.9 and 8.3). Comparison of the 1D NMR data with those of mansonone G¹¹ indicated their structural similarity. The obvious differences were the presence of a hydroxy group at C-4 which was confirmed by HMBC cross-peaks from H₃-12 (δ_{H} 1.91) to C-2 (δ_{C} 186.0), C-3 (δ_{C} 117.8) and C-4 (δ_{C} 156.1); and the appearance of an acetyl group located at C-5 instead of isopropyl group in mansonone G which was corroborated by HMBC correlations from H₃-11 (δ_{H} 2.40) to C-5 (δ_{C} 131.1) and C-10 (δ_{C} 201.5). According to these data, the structure of **20** was established to be a 5-acetyl-4,6-dihydroxy-3,8-dimethylnaphthalene-1,2-dione as a new nor-sesquiterpenoid.

Compound **21** was obtained as yellow amorphous powder. Its molecular formula was determined to be $\text{C}_{15}\text{H}_{15}\text{NO}_3$ by HRESIMS (m/z 280.0953, calcd for $\text{C}_{15}\text{H}_{15}\text{NO}_3\text{Na}$, 280.0950). The ^1H NMR spectrum of **21** (Table 3.10) displayed an amide proton δ_{H} 9.62 (1H, s), two aromatic protons δ_{H} [7.51 (1H, s), 7.44 (1H, s) each], an isopropyl group at δ_{H} [3.79 (1H, m) and 1.41 (6H, d, $J = 7.0$ Hz)], a quaternary methyl proton signal at δ_{H} 2.35 (3H, s). The ^{13}C NMR spectrum showed a characteristic amide carbon signal δ_{C} 167.5, ten aromatic carbons and four saturated carbons. In addition, IR absorption band at

1666 cm^{-1} also indicated the presence of an amide group. The ^1H and ^{13}C NMR data of **21** were similar to those of thespesilactam,⁷² except for that of the resonance at C-6 (**21**: δ_{C} 153.8, thespesilactam: δ_{C} 117.4) which was also corroborated by the observed HMBC data from H-10 (δ_{H} 3.79) to C-6 (δ_{C} 153.8). These facts suggested that hydroxy group in **21** locate at C-6 instead of C-7 in thespesilactam. The complete structure of **21**, a new natural product named mansonialactam, was fully confirmed by ^1H - ^1H COSY, HSQC and HMBC experiments (Fig. 3.9).

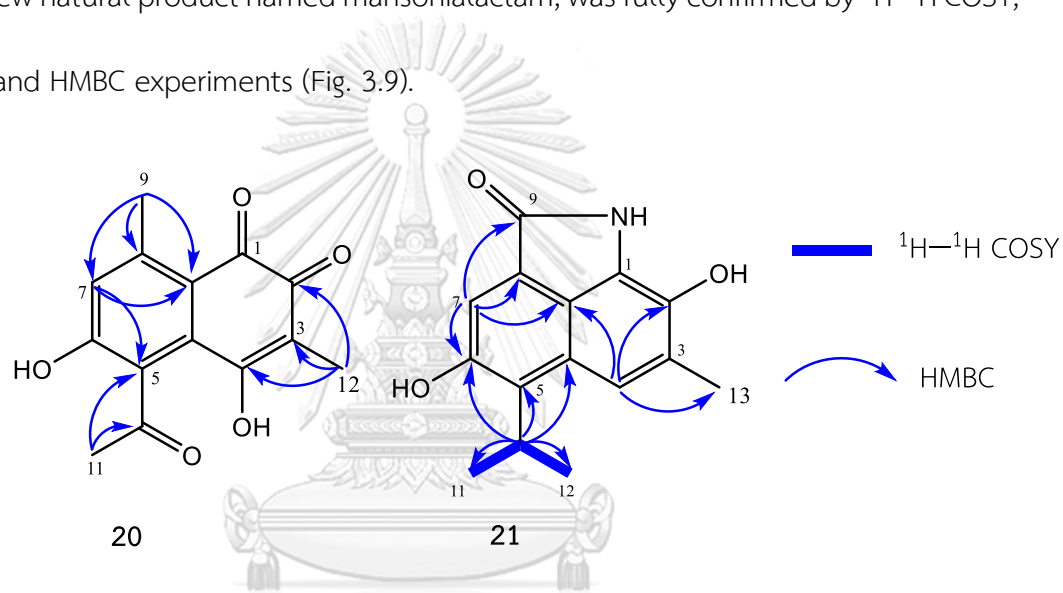


Figure 3.9 Key ^1H - ^1H COSY, HMBC correlations of **20** and **21**

Table 3.10 The ^1H (500 MHz) and ^{13}C (125 MHz) NMR spectroscopic data of **20** $(\text{CD}_3)_2\text{CO}$ and **21** ($\text{DMSO}-d_6$) (δ in ppm)

No.	(20)		(21)	
	δ_{H} (J in Hz)	δ_{C}	δ_{H} (J in Hz)	δ_{C}
1		181.3		119.8
2		186.0		135.0
3		117.8		131.6
4		156.1	7.51, s	118.3
4a		134.2		123.9
5		131.1		132.1
6		158.8		153.8
7	7.05, s	123.0	7.44, s	113.8
8		145.3		123.5
8a		120.6		121.4
9	2.63, s	22.9		167.5
10		201.5	3.79, m	26.5
11	2.40, s	30.9	1.41, d (7.0)	21.1
12	1.91, s	8.3	1.41, d (7.0)	21.1
13			2.35, s	18.1
NH			9.62, s	

Compound **22**, obtained as pale yellow powder, had the molecular formula $C_{25}H_{28}O_7$, deduced from the $[M + Na]^+$ ion peak at m/z 463.1740 (calcd. for $C_{25}H_{28}O_7Na$, 463.1733) in the HRESIMS spectrum, indicating twelve double bond equivalents. The 1H NMR spectrum of **22** illustrated a pair of *meta*-coupled aromatic protons at [δ_H 6.65 (1H, br s, H-2'), δ_H 6.65 (1H, br s, H-6')], one aromatic proton at δ_H 6.46 (1H, s, H-2), an oxygenated methine proton at δ_H 5.57 (1H, s, H-11), one methoxy group at δ_H 3.82 (3H, s), three methine protons, one methylene, and four methyl groups at δ_H 2.37 (3H, s, H-12), 1.36 (3H, d, $J = 7.0$ Hz, H-14), 1.35 (3H, d, $J = 8.0$ Hz, H-15) and 1.32 (3H, d, $J = 7.5$ Hz, H-16) (Table 3.11). The ^{13}C NMR and HSQC spectra revealed the presence of twenty-five carbon resonances, including two carbonyl carbons (δ_C 215.4 and 193.0), one methoxy (δ_C 56.6), four methyls (δ_C 23.6, 21.1, 21.1, and 15.9), seven methines (δ_C 119.4, 109.8, 104.7, 71.4, 49.5, 41.0, 28.9), ten quaternary carbons (δ_C 162.1, 151.5, 148.8, 145.7, 143.9, 134.3, 134.2, 129.0, 123.1, 77.1), and one methylene carbon (δ_C 33.8) (Table 3.12).

The planar structure of **22** was determined by a detailed analysis of its 2D NMR spectra including correlation spectroscopy (1H - 1H COSY) and HMBC data (Figure 3.10). The appearance of one 1,3,4,5-substituted aromatic ring (ring A) was identified by HMBC correlations from H-2' (δ_H 6.65) to C-11 (δ_C 71.4), C-1' (δ_C 134.2), C-3' (δ_C 145.7), C-4' (δ_C 134.3), and C-6' (δ_C 104.7), and from H-6' (δ_H 6.65) to C-11 (δ_C 71.4), C-1' (δ_C 134.2), C-2' (δ_C 109.8), C-4' (δ_C 134.3), and C-5' (δ_C 148.8) which accommodated these four

substituents in the following order: oxygenated methine, two hydroxy groups and methoxy group. Moreover, the HMBC correlations of methyl protons H₃-12 (δ_{H} 2.37) to C-1 (δ_{C} 143.9), C-2 (δ_{C} 119.4), and C-9a (δ_{C} 123.1), and methine proton H-2 to C-3 (δ_{C} 162.1), C-4 (δ_{C} 129.0), C-9a (δ_{C} 123.1), and C-12 (δ_{C} 23.6) determined the occurrence of 1,2,3,4,5-pentasubstituted benzene ring moiety (ring B). The HMBC cross peaks from H₃-14 and H₃-15 to C-4 and the ¹H-¹H COSY correlations of H₃-14/H-13 and H₃-15/H-13 suggested the isopropyl group be assigned at C-4.

The HMBC correlations of H-11 (δ_{H} 5.57) to C-8 (δ_{C} 77.1), C-9 (δ_{C} 193.0), C-10 (δ_{C} 33.8) and H₃-16 (δ_{H} 1.32) to C-5 (δ_{C} 41.0), C-6 (δ_{C} 49.5), C-7 (δ_{C} 215.4) indicated the presence of two fragments (a) CH-11—C-8(CO-9)—CH₂-10 and (b) CH₃-16—CH-6(CO-7)—CH-5 respectively. The connections of C-7, C-9, C-10, C-11 with quaternary C-8 were established by HMBC correlations from H-11 to C-7, C-8, C-9, C-10 and H₂-10 to C-7, C-8, C-9, C-11. Furthermore, the HMBC correlations of H-5 to C-4, C-4a, C-6, C-9a, C-10, and the key ¹H-¹H COSY correlation of H-5/H₂-10 confirmed the connections of C-6, C-10, C-4a through tertiary carbon C-5. In addition, a smaller chemical shift of a carbonyl group at C-9 (δ_{C} 193.0), which contained a conjugated carbonyl system and the remaining one degree of unsaturation in **22** indicated C-C bond formation at C-9 and C-9a. Thus, the planar structure of **22** was elucidated as a novel compound that contained bicyclo[3.2.1]octane unit occurring in both natural and synthetic compounds.⁷³⁻⁷⁶

Compound **23** as pale yellow solid, had the same molecular formula as that of **22** by positive HRESIMS (m/z 463.1735 $[M+Na]^+$, calcd. for $C_{25}H_{28}O_7Na$, 463.1733). Analysis of 1H NMR spectroscopic data gave information about characteristic resonances of three aromatic protons at δ_H 6.53 (1H, d, $J = 2.0$ Hz, H-2'), δ_H 6.49 (1H, d, $J = 1.5$ Hz, H-6'), δ_H 6.53 (1H, s, H-2), an oxygenated methine proton, one methoxy group and four methyl groups. The ^{13}C NMR data along with the HSQC experiment illustrated 25 carbon signals, including one methoxy, four methyls, one methylene, seven methines, and twelve quaternary carbons. The spectroscopic data (Tables 3.11 and 3.12) suggested that **23** consist of 1,3,4,5-substituted aromatic ring (ring A), 1,2,3,4,5-pentasubstituted benzene ring (ring B) and a bicyclo[3.2.1]octane unit which were confirmed by HMBC cross-peaks from H-5 (δ_H 3.58) to C-4a (δ_C 151.6), C-6 (δ_C 50.0), C-7 (δ_C 215.2), C-8 (δ_C 76.7), C-9a (δ_C 123.0) and C-10 (δ_C 33.2); from H₂-10 (δ_H 2.59 and 2.45) to C-7 (δ_C 215.2), C-8 (δ_C 76.7), and C-9 (δ_C 193.2); and from H₃-16 (δ_H 0.71) to C-5 (δ_C 41.2), C-6 (δ_C 50.0), C-7 (δ_C 215.2). Comparison of the 1D NMR data with those of **22** showed their structural similarity. The obvious differences were due to the resonances at δ_H 0.71 (3H, d, $J = 7.5$ Hz, H-16), δ_C 15.1 (C-16) in **23** replacing those at δ_H 1.32 (3H, d, $J = 7.5$ Hz, H-16) and δ_C 15.9 (C-16) in **22**. This implied that **23** was a diastereomer of **22**.

The positive-ion HRESIMS, with the ions $[M + Na]^+$ at m/z 477.1921 (calcd. for $C_{26}H_{30}O_7Na$, 477.1889, **24**), at m/z 477.1918 (calcd. for $C_{26}H_{30}O_7Na$, 477.1889, **25**), and

at m/z 491.2049 (calcd. for $C_{27}H_{32}O_7Na$, 491.2046, **26**) showed that these isolates can be considered as a pair of isomers: **24** and **25** ($C_{26}H_{30}O_7$), on one hand, as a homologous series **24** and **26** ($C_{26}H_{30}O_7$, $C_{27}H_{30}O_7$), on the other hand. The 1H and ^{13}C NMR spectra (Tables 3.11 and 3.12) of **24** and **26** are also close to those of **22**, with the significant differences being the appearances of a methoxy resonance at δ_H 3.18 (3H, s, 11-OCH₃) and δ_C 57.8 (11-OCH₃) in **24** and an ethoxy resonance at δ_H 1.08 (3H, t, $J = 7.0$ Hz), δ_H 3.34 (2H, q, $J = 7.0$ Hz), δ_C 15.6 and 65.5 in **25**, respectively. Likewise, **25** had similar 1H and ^{13}C NMR spectroscopic data to those of **23** with the only difference was an added methoxy resonance at [δ_H 3.26 (3H, s, 11-OCH₃) and δ_C 57.6 (11-OCH₃)] in **25**. The position of the methoxy or ethoxy moiety at C-11 was further confirmed by the HMBC correlation of OCH₃/C-11 and H-11/OCH₂CH₃ (Fig. 3.10). This implied that **24**, **26** were methoxylated and ethoxylated of **22**, whereas **25** was methoxylated of **23**.

Relative configurations of **23** and **25** were defined based on NOESY connection (Figure A82 and A96, Appendix) between H-5 and H-16 indicating that these protons were on the same side of the ring. However, the correlations between H-5 and H-16 in **22**, **24** and **26** were not observed suggesting that these protons had different orientation in space. The key 1H - 1H COSY, HMBC, correlations of **22** - **26** are summarized in Figure 3.10.

Table 3.11 The ^1H (500 MHz) NMR spectroscopic data of **22–26** (CD_3OD) (δ in ppm)

No.	(22)	(23)	(24)	(25)	(26)
2	6.46, s	6.53, s	6.44, s	6.51, s	6.44, s
5	3.68, d (4.5)	3.58, d (4.5)	3.68, d (5.0)	3.57, d (4.5)	3.67, d (4.5)
6	2.24, m	2.10, m	2.24, m	2.06, m	2.23, m
10	2.90, dd (12.0, 4.5)	2.59, dd (12.5, 5.0)	2.92, dd (12.0, 4.5)	2.63, dd (12.0, 4.5)	2.95, dd (12.0, 5.0)
	2.10, d (12.0)	2.45, d (13.0)	2.10, d (12.0)	2.39, d (12.5)	2.06, d (12.0)
11	5.57, s	5.69, s	5.01, s	5.15, s	5.12, s
12	2.37, s	2.52, s	2.35, s	2.50, s	2.35, s
13	3.37, m	3.31, m	3.34, m	3.30, m	3.35, m
14	1.36, d (7.0)	1.34, d (7.0)	1.36, d (7.0)	1.33, d (7.0)	1.35, d (7.0)
15	1.35, d (8.0)	1.32, d (7.0)	1.34, d (7.0)	1.30, d (7.0)	1.34, d (7.0)
16	1.32, d (7.5)	0.71, d (7.5)	1.32, d (7.5)	0.68, d (7.5)	1.33, d (7.5)
2'	6.65, br s	6.53, d (2.0)	6.63, s	6.48, d (2.0)	6.64, s
6'	6.65, br s	6.49, d (1.5)	6.63, s	6.43, d (1.5)	6.64, s
5'-OCH ₃	3.82, s	3.81, s	3.83, s	3.80, s	3.82, s
11-O-R			3.18, s	3.26, s	3.34, q (7.0)
					1.08, t (7.0)

Table 3.12 The ^{13}C (125 MHz) NMR spectroscopic data of **22–26** (CD_3OD) (δ in ppm)

No.	(22)	(23)	(24)	(25)	(26)
1	143.9	144.4	143.9	144.2	143.9
2	119.4	119.6	119.4	119.6	119.5
3	162.1	162.4	162.1	162.3	162.1
4	129.0	129.1	129.0	129.1	129.1
4a	151.5	151.6	151.0	151.9	151.1
5	41.0	41.2	42.7	41.4	41.2
6	49.5	50.0	49.6	49.6	49.6
7	215.4	215.2	215.0	214.4	215.2
8	77.1	76.7	76.8	76.1	76.9
9	193.0	193.2	192.0	192.0	192.1
9a	123.1	123.0	122.9	123.1	123.0
10	33.8	33.2	35.0	33.2	34.1
11	71.4	72.4	81.1	81.8	79.1
12	23.6	23.9	23.6	23.8	23.6
13	28.9	28.8	29.0	28.6	29.0
14	21.1	21.0	21.1	21.0	21.1
15	21.1	21.0	21.1	21.0	21.1
16	15.9	15.1	15.9	15.0	15.8

No.	(22)	(23)	(24)	(25)	(26)
1'	134.2	132.4	130.6	129.1	131.4
2'	109.8	109.8	110.3	110.3	110.1
3'	145.7	146.0	145.9	146.3	145.9
4'	134.3	134.5	134.2	134.8	134.6
5'	148.8	149.0	149.0	149.2	149.0
6'	104.7	104.8	105.4	105.5	105.3
5'-OCH ₃	56.6	56.6	56.6	56.6	56.6
11-O-R			57.8	57.6	65.5
					15.6

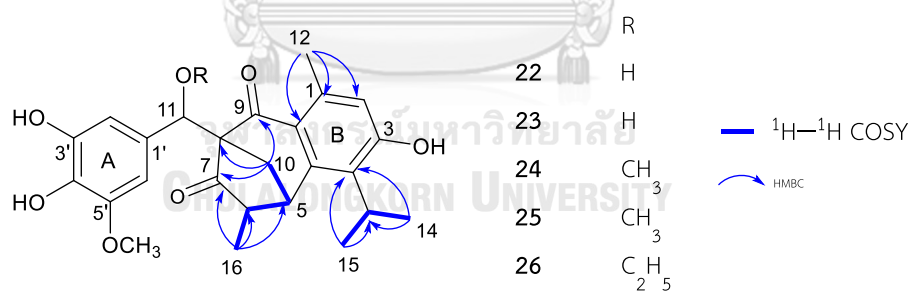


Figure 3.10 Key ^1H - ^1H COSY, HMBC correlations of **22–26**

Compound **27** was isolated as yellow powder. The (+)-HRESIMS spectrum depicted a protonated molecular ion $[\text{M} + \text{H}]^+$ at m/z 441.1910 (calcd. for $\text{C}_{25}\text{H}_{29}\text{O}_7$, 441.1913, assigned to a molecular formula of $\text{C}_{25}\text{H}_{28}\text{O}_7$ with 12 double-bond equivalents. The ^1H NMR spectrum (Table 3.13) showed the signals for an olefinic

proton δ_{H} 7.68 (1H, d, $J = 2.5$ Hz, H-9), three aromatic protons 6.66 (1H, d, $J = 2.0$ Hz, H-2'), 6.64 (1H, d, $J = 2.0$ Hz, H-6'), and 6.60 (1H, s, H-2), a methoxy group δ_{H} 3.86 (3H, s), three methine protons, one methylene, and four methyl groups. The combined ^{13}C NMR and HSQC data (Table 3.13) revealed the presence of 25 carbons including two carbonyls (δ_{C} 191.3 and 180.2), one methoxy (δ_{C} 56.7), four methyls (δ_{C} , 22.6, 21.2, 20.3, and 17.2), seven methines (δ_{C} 138.8, 119.4, 112.0, 107.1, 46.6, 37.7, 29.5), ten quaternary carbons (δ_{C} 161.4, 149.4, 146.4, 145.7, 141.7, 136.7, 133.1, 130.8, 128.1, 125.9), and one methylene carbon (δ_{C} 32.5). Analysis of the NMR spectra of **27** and comparison with those of **22** allowed the identification of two aromatic rings: 1,3,4,5-tetrasubstituted aromatic ring (ring A) and 1,2,3,4,5-pentasubstituted benzene ring (ring B) which were also confirmed by the observed HMBC data (Fig. 3.11)

The shielded resonance of a carbonyl group at C-8 (δ_{C} 191.3) indicated a conjugated ketone, and HMBC correlations of H-5 to C-4, C-4a, C-6, C-7, C-8a; H-6 to C-4a, C-5, C-7, C-8; H₃-15 to C-5, C-14, C-16; and H-14 to C-5, C-6, C-15, C-16 contributed to establish a cyclohexenone ring that was substituted with a 1-carboxyethyl group at C-5. In addition, the HMBC correlations of H-9 to C-1', C-2', C-6', and C-7 confirmed the connection of C-1' and C-7 through C-9. Ring B linked to the cyclohexenone unit which was established by HMBC correlations from H-2 and H₃-10 to C-8a and H-5 to C-4, C-4a and C-8a. Thus, the planar structure of **27** bearing an unprecedented 2-

benzylidene-1-tetralone motif was identified which was similar to some synthetic compounds.⁷⁷⁻⁷⁹

Compound **28**, was obtained as yellow amorphous solid with a molecular formula of C₂₆H₃₀O₆, established by the HRESIMS m/z 437.1956 [M - H]⁻ (calcd for C₂₆H₂₉O₆, 437.1964). The ¹H NMR spectrum of **28** (Table 3.13) revealed the presence of three aromatic protons at δ_{H} 6.59 (2H, s), 6.53 (1H, s), an olefinic proton at δ_{H} 6.48 (1H, s), two methoxy group at δ_{H} 3.79 (6H, s), a methylene proton at δ_{H} 3.35 (1H, m) and 2.34 (1H, m), and four methyl groups at δ_{H} 2.53 (3H, s), 1.40 (3H, d, $J = 7.0$ Hz), 1.38 (3H, d, $J = 7.5$ Hz) and 1.10 (3H, d, $J = 7.0$ Hz). In the ¹³C NMR and HSQC spectra, the characteristic signals for twenty-six carbons were observed, including one carbonyl (δ_{C} 199.0), two methoxy (δ_{C} 56.6, 56.6), four methyls (δ_{C} 23.6, 21.2, 21.2, and 14.2), one methylene (δ_{C} 35.4), seven methines (δ_{C} 127.6, 119.1, 106.7, 106.7, 48.8, 42.7, and 28.6), and eleven quaternary carbons (δ_{C} 162.1, 153.5, 149.0, 149.0, 144.2, 137.1, 136.0, 130.0, 128.5, 120.3, and 89.4). These data, suggesting that **28** have a 1,3,4,5-substituted aromatic ring (ring A) and 1,2,3,4,5-pentasubstituted benzene ring moiety (ring B) which were similar to those of **22**. The obvious difference was the presence of one methoxy group at C-3' in **28** which was confirmed by HMBC correlation from methoxy group (δ_{H} 3.79) to C-3' (δ_{C} 106.7).

The planar structure of **28** was also determined by an analysis of its 2D NMR spectra. The presence of a bicyclo[3.2.1]octane unit was confirmed by ¹H-¹H COSY

correlations of H-5/H-6 and H-10/H-16, together with HMBC correlations from H-5 to C-4, C-4a, C-6, C-7, C-8, C-9a, C-10 and C-16; from H₂-6 to C-4a, C-5, C-7, C-8 and C-10; from H-10 to C-6, C-7, C-8, C-9 and C-16. In addition, the HMBC correlations from H-11 to C-1', C-2', C-6', C-6, C-7, C-8 suggested that ring A link with bicyclo[3.2.1]octane moiety through C-11. Furthermore, ring B connected to the bicyclo[3.2.1]octane moiety through C-4a and C-9a which was collaborated by HMBC cross-peaks from H-2 and H₃-12 to C-9a and from H-5 to C-4, C-4a and C-9a. Thus, the planar structure of **28** was fully defined as a novel compound bearing a bicyclo[3.2.1]octane unit. The geometric double bonds at Δ^7 in **27** and **28** were determined to be *E* by the key NOESY correlations from H-6 to H-6' (Figure A110 and A117, Appendix). The key ¹H-¹H COSY, HMBC, correlations of **27**-**28** are summarized in Figure 3.11.

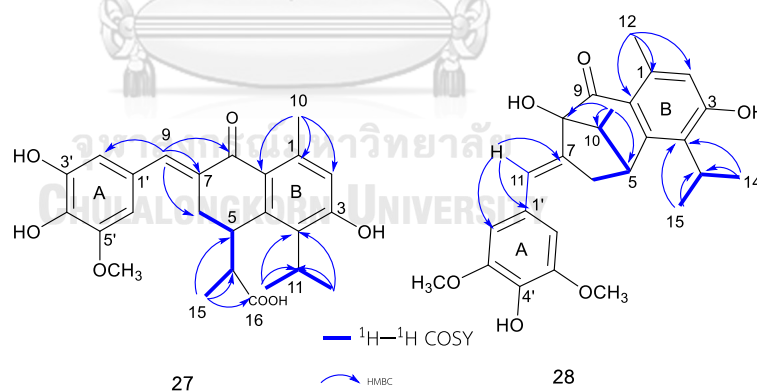


Figure 3.11 Key ¹H-¹H COSY, HMBC correlations of **27**-**28**

Table 3.13 The ^1H (500 MHz) and ^{13}C (125 MHz) NMR spectroscopic data of **27** and **28** (CD_3OD)

No.	(27)		(28)	
	δ_{H} (J in Hz)	δ_{C}	δ_{H} (J in Hz)	δ_{C}
1		141.7		144.2
2	6.60, s	119.4	6.53, s	119.1
3		161.4		162.1
4		130.8		128.5
4a		145.7		153.5
5	3.70, ddd (7.5, 7.5, 3.5)	37.7	3.72, d (7.0)	42.7
6	3.37, m	32.5	3.35, m	35.4
	2.78, m		2.34, m	
7		133.1		137.1
8		191.3		89.4
8a		125.9		
9	7.68, d (2.5)	138.8		199.0
9a				120.3
10	2.46, s	22.6	2.16, m	48.8
11	3.43, m	29.5	6.48, s	127.6
12	1.45, d (7.0)	20.3	2.53, s	23.6

No.	(27)		(28)	
	δ_{H} (J in Hz)	δ_{C}	δ_{H} (J in Hz)	δ_{C}
13	1.35, d (7.0)	21.2	3.52, m	28.6
14	2.39, m	46.6	1.40, d (7.0)	21.2
15	0.96, d (7.0)	17.2	1.38, d (7.5)	21.2
16		180.2	1.10, d (7.0)	14.2
1'		128.1		130.0
2'	6.66, d (2.0)	112.0	6.59, s	106.7
3'		146.4		149.0
4'		136.7		136.0
5'		149.4		149.0
6'	6.64, d (2.0)	107.1	6.59, s	106.7
3'-OCH ₃			3.79, s	56.6
5'-OCH ₃	3.86, s	56.7	3.79, s	56.6

Compound **30** as colorless oil, had the molecular formula C₂₂H₂₂O₉ deducing from its HRESIMS data (m/z 453.1164 [M+Na]⁺, calcd for C₂₂H₂₂O₉Na, 453.1162). The ¹H NMR data (Table 3.14) revealed an aldehyde proton at δ_{H} 9.58 (1H, d, $J = 7.5$ Hz), two sets of 1,3,4,5-tetrasubstituted aromatic rings at δ_{H} 6.95 (1H, d, $J = 2.0$ Hz), 6.93 (1H, d, $J = 1.5$ Hz), 6.55 (1H, d, $J = 2.0$ Hz), and 6.53 (1H, d, $J = 2.0$ Hz), two olefinic protons at

δ_{H} 7.54 (1H, d, $J = 16.0$ Hz) and 6.66 (1H, dd, $J = 16.0, 8.0$ Hz), two oxygenated protons at δ_{H} 4.81 (1H, d, $J = 8.0$ Hz), and 4.30 (1H, m), two methoxy groups at δ_{H} 3.83 (3H, s) and 3.89 (3H, s), one oxygenated methylene and one methyl group at δ_{H} 2.04 (3H, s). The ^{13}C NMR and HSQC data of **30** (Table 3.14) showed 22 carbon signals comprising an aldehyde group, two olefinic carbons, two benzene rings, two methoxy groups, one oxygenated methylene, two oxygenated methines, and an acetyl group. The NMR data similarities between **30** and mansoxetane **29**,⁴⁰ indicated that **30** was also a neolignan. The only difference was the presence of an acetyl group at C-9' which was supported by the HMBC cross peaks from H₂-9' (δ_{H} 4.27, 3.98) and methyl (δ_{H} 2.04) to the carbonyl carbon at δ_{C} 172.3. This suggested that **30** with trial name 9'-O-acetylmansoxetane be an acetylated derivative of **29**. The key ^1H - ^1H COSY, HMBC, correlations of **30** are summarized in Figure 3.12.

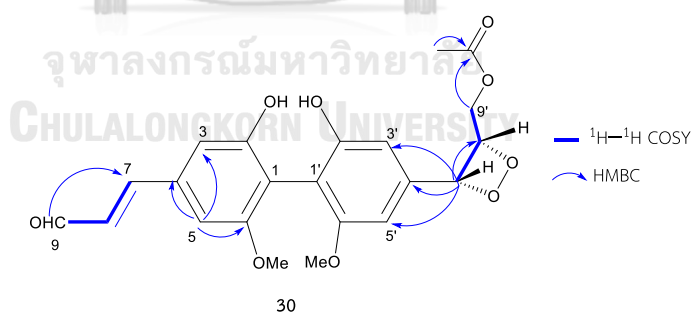


Figure 3.12 Key ^1H - ^1H COSY, HMBC correlations of **30**

Table 3.14 The ^1H (500 MHz) and ^{13}C (125 MHz) NMR spectroscopic data of **29** (acetone- d_6) and **30** (CD_3OD)

No.	(29)		(30)	
	δ_{H} (ν in Hz)	δ_{C}	δ_{H} (ν in Hz)	δ_{C}
1		137.3		137.4
2		145.5		146.0
3	6.93, d (2.0)	111.9	6.93, d (1.5)	112.3
4		127.5		128.3
5	7.02, d (2.0)	105.3	6.95, d (2.0)	106.0
6		150.3		150.8
7	7.54, d (15.5)	153.9	7.54, d (16.0)	155.5
8	6.68, dd (16.0, 8.0)	127.9	6.66, dd (16.0, 8.0)	128.2
9	9.64, d (7.5)	194.1	9.58, d (7.5)	196.1
1'		135.3		136.2
2'		146.4		146.9
3'	6.67, d (1.5)	109.3	6.53, d (2.0)	109.3
4'		128.2		127.5
5'	6.68, d (2.0)	103.9	6.55, d (2.0)	103.9
6'		149.1		149.9
7'	4.93, d (7.5)	77.1	4.81, d (8.0)	77.9
8'	4.12, m	79.9	4.30, m	77.4
9'	3.57, d (12.5)	61.6	4.27, d (12.0)	64.0
	3.80, d (12.5)		3.98, dd (12.0, 4.5)	
6-OMe	3.91, s	56.5	3.89, s	56.8
6'-OMe	3.83, s	56.5	3.83, s	56.7
9'- COCH_3				172.3
9'- COCH_3			2.04, s	20.5

3.4 Biological activity study

3.4.1 α -Glucosidase inhibitory activity

The inhibitory activity of the EtOAc extract of *M. gagei* heartwoods on yeast α -glucosidase was carried out and the results are presented in Table 3.15 and Figure 3.13.

Table 3.15 Inhibition of the EtOAc extract of *M. gagei* at various concentrations

Concentration ($\mu\text{g/mL}$)	% Inhibition					
	HE1	HE2	HE3	EA	Ac	acarbose
125	93.1	83.3	97.0	98.4	97.3	50.0
62.5	48.2	68.1	95.2	60.5	95.9	29.1
31.25	32.4	63.2	94.3	41.3	95.4	15.9
15.62	16.2	57.9	94.1	34.1	95.1	10.3
7.81	7.3	56.6	93.5	27.3	93.1	5.7

Fractions **HE2**, **HE3** and **Ac** exhibited the excellent activities against α -glucosidase inhibitory activity with % inhibition of 56.6, 93.5 and 93.1 % at 7.81 $\mu\text{g/mL}$ respectively, meanwhile **EA** and **HE1** showed good activity in comparison with acarbose as a positive control.

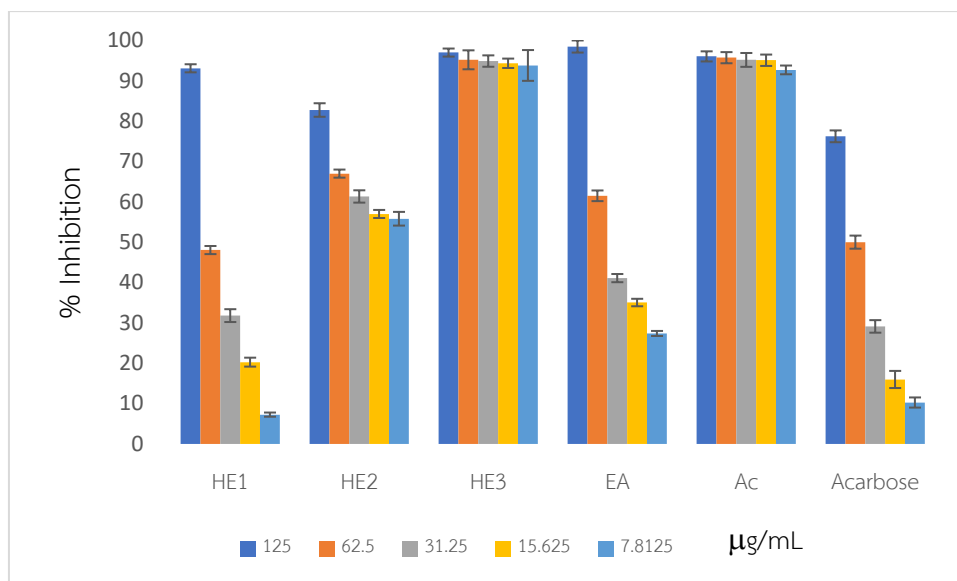


Figure 3.13 % Inhibition of the EtOAc extracts of *M. gagei* at various concentrations



Twenty-seven isolated compounds were evaluated for inhibitory effect against α -glucosidase and the IC_{50} values are displayed in Table 3.16.

Table 3.16 IC_{50} values of tested compounds for α -glucosidase inhibitory activities

Compounds	IC_{50} (μ M)	Compounds	IC_{50} (μ M)
1	108.43 \pm 11.18	16	51.08 \pm 0.56
3	> 200	17	25.81 \pm 3.48
4	> 200	18	12.38 \pm 0.71
5	108.21 \pm 10.98	20	> 200
6	102.41 \pm 10.15	21	0.20 \pm 0.05
7	46.86 \pm 1.58	22	17.54 \pm 0.80
8	116.77 \pm 7.20	23	27.38 \pm 1.58
9	46.09 \pm 1.73	24	3.57 \pm 0.37
10	169.58 \pm 15.08	25	4.33 \pm 0.04
11	13.12 \pm 2.85	27	33.43 \pm 3.67
12	112.14 \pm 9.44	28	3.45 \pm 0.33
13	> 200	29	145.87 \pm 10.08
14	> 200	30	84.74 \pm 2.78
15	> 200	acarbose	93.63 \pm 0.49

Values are presented as mean \pm SD of triplicate experiments.

Note: excellent ($IC_{50} < 10$), very good ($10 \leq IC_{50} \leq 50$), good ($50 < IC_{50} \leq 100$), moderate ($100 < IC_{50} \leq 150$), weak ($150 < IC_{50} \leq 200$), no activity ($IC_{50} > 200 \mu M$).

Several sesquiterpenoids carrying cadinane backbones exhibited strong α -glucosidase inhibitory activities. Among them, **21** was found to be the highest inhibitory activity with an IC_{50} value of $0.20 \pm 0.05 \mu M$. **7**, **9**, **11**, **17** and **18** demonstrated very good activity compared to the standard acarbose ($IC_{50} = 93.63 \pm 0.49 \mu M$), meanwhile **5**, **6**, **8**, and **12** illustrated moderate activity against yeast α -glucosidase (Figure 3.14). According to α -glucosidase inhibition results, those showed a correlation between the number of hydroxy groups with inhibitory activity of sesquiterpenoid derivatives. For example, one of the most potent sesquiterpenoid coumarins was **11** bearing two hydroxy groups at C-6 and C-7 with IC_{50} value of $13.12 \pm 2.85 \mu M$. The presence of methoxy group at C-7 in **12** reduced its inhibitory activity (IC_{50} value of $112.14 \pm 9.44 \mu M$). Furthermore, the addition of a hydroxy group at C-11 in compound **7** increased its activity compared to that of **6**.

The role of the position of hydroxy group was also important. When **9**, a cadinane sesquiterpenoid with $-OH$ group at 6-position was examined, it displayed more than twice as strong as **8** without $-OH$ at C-6 in reference to α -glucosidase activity. Similarly, **18** with two hydroxy groups at C-1 and C-2 was more potential than **17**. Particularly, **21** bearing a pyrrole alkaloid experienced a significant increase in the

inhibitory activity. The number of hydroxy groups enhanced the interaction between molecules and enzymes by H-bonding resulting an increase inhibition.^{80,81}

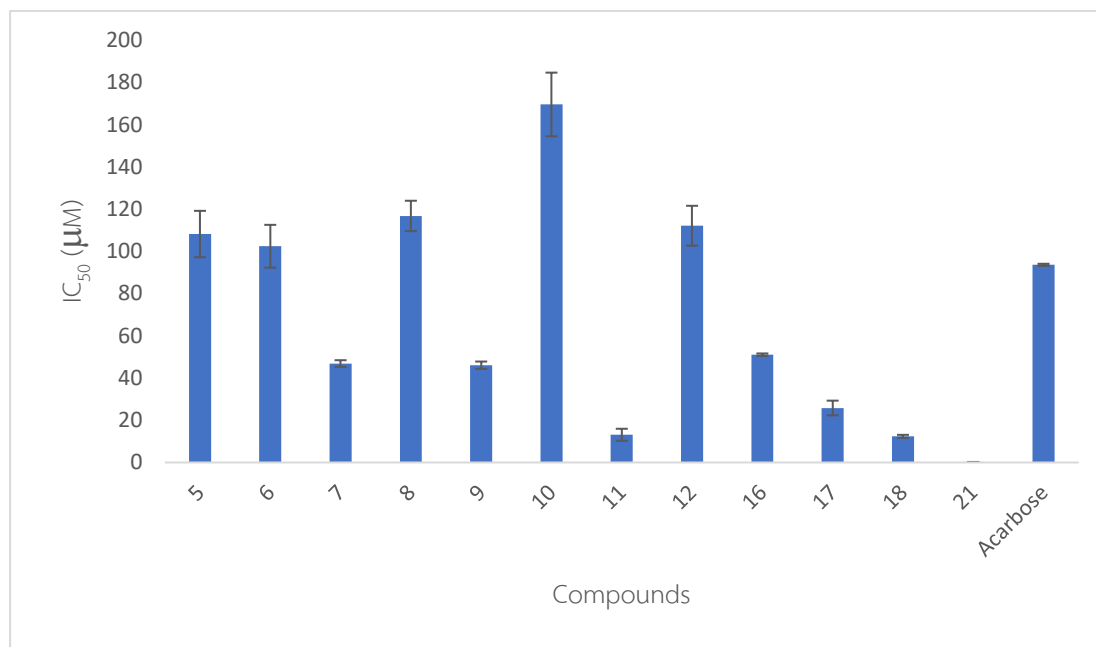


Figure 3.14 α -Glucosidase inhibitory activities of 5–21

Moreover, **22–28** possessed higher inhibitory activity than acarbose (Figure 3.15). It is noticeable that **24** and **28** showed the strongest inhibitions with IC₅₀ values of 3.57 ± 0.37 and 3.45 ± 0.33 μM , respectively. From the bar graph, it can be seen that when the cyclohexane moiety in **27** was replaced by bicyclo[3.2.1]octane in **22–25** and **28**, the activities against α -glucosidase increased significantly. Similarly, the addition of a methoxy group at C-11 in **24** and **25** witnessed an excellent increase in their activity. In addition, **1** bearing 1,3,4,5-substituted aromatic ring exhibited a moderate activity with IC₅₀ value of 108.43 ± 11.18 μM . Thus, bicyclo[3.2.1]octane skeleton plays an vital role in α -glucosidase inhibition.

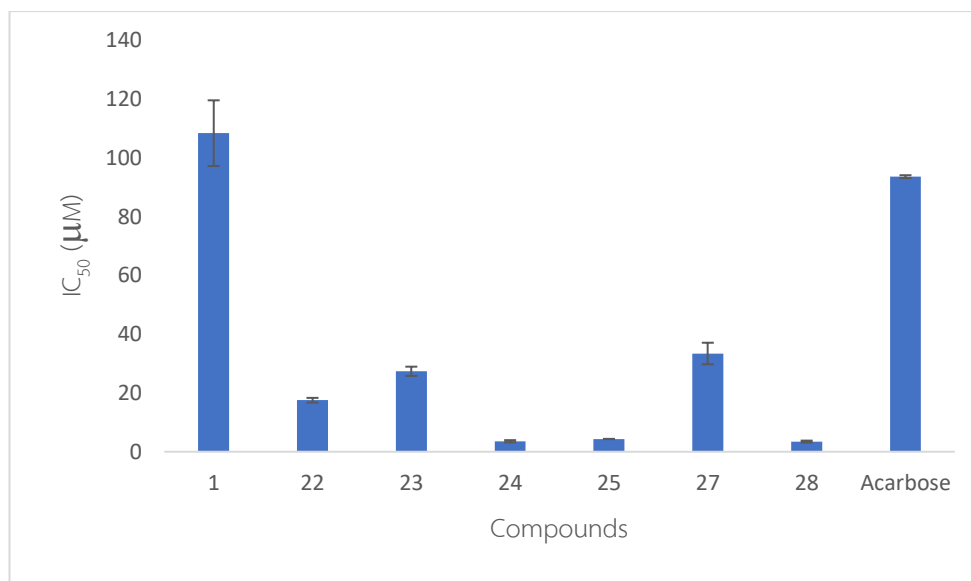


Figure 3.15 α -Glucosidase inhibitory activities of **1**, **22–28**

With the aim of studying the mode of action of **21** and **24**, kinetic evaluations were conducted using Lineweaver-Burk plot analysis (Figs. 3.16 and 3.17) to identify the kinetic parameters: maximum enzyme velocity (V_{max}) and Michaelis-Menten constant (K_m) (Table 3.17).

The inhibitory mechanisms of **21**, **24** against α -glucosidase were also examined using the above methodology. The apparent V_{max} and K_m values were changed significantly, suggesting that the enzyme inhibition of **21** and **24** fitted with uncompetitive types. The uncompetitive inhibitor bound to the enzyme-substrate complex, lowering the K_m and the maximum enzyme activity.⁸²

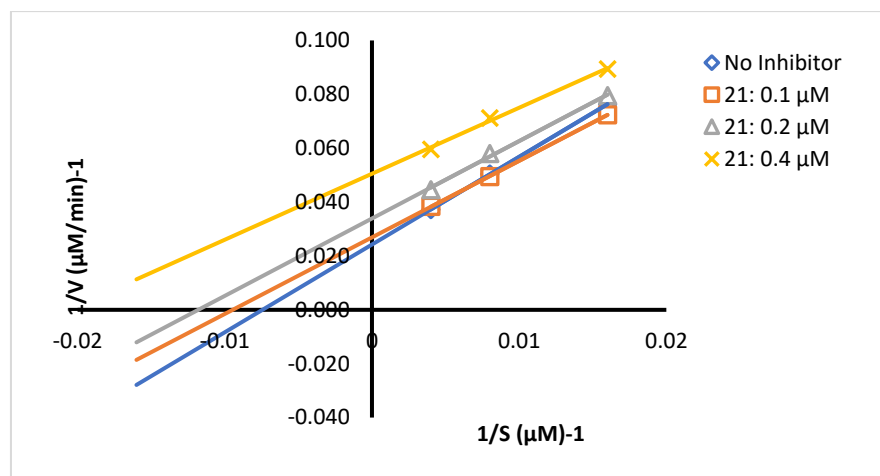


Figure 3.16 Lineweaver-Burk plot of the reaction of the yeast α -glucosidase in the presence of **21**

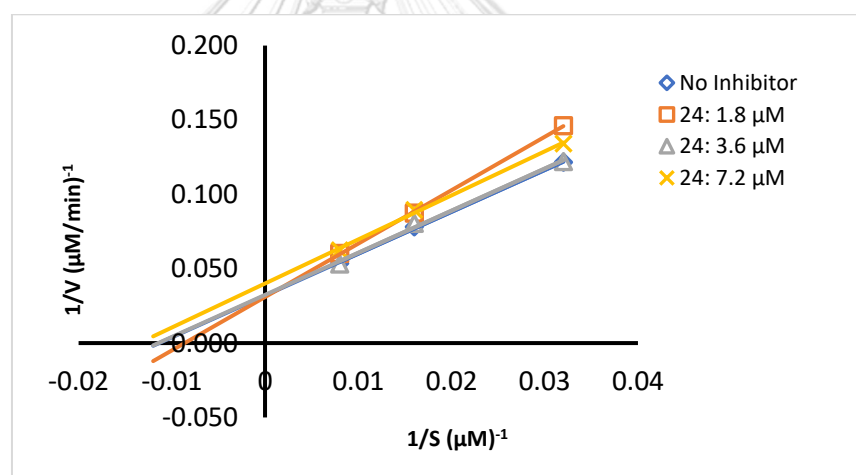


Figure 3.17 Lineweaver-Burk plot of the reaction of the yeast α -glucosidase in the presence of **24**.

Table 3.17 Kinetic effect of α -glucosidase inhibition on **21** and **24**

Concentration of 21 (μM)	K_m (μM)	V_{max} ($\mu\text{M}/\text{min}$)
0	134.591	41.322
0.1	105.658	37.175
0.2	84.755	29.499
0.4	48.519	19.802
Concentration of 24 (μM)	K_m (μM)	V_{max} ($\mu\text{M}/\text{min}$)
0	88.166	31.348
1.8	115.806	32.258
3.6	87.355	30.864
7.2	74.030	25.000

3.4.2 Antioxidant activities

The antioxidant activities of twenty-seven compounds were conducted using the DPPH radical scavenging assay with ascorbic acid as a positive control. The results are presented in Table 3.18.

Table 3.18 Antioxidant activity of tested compounds

Compounds	IC ₅₀ (μM)	Compounds	IC ₅₀ (μM)
1	20.62 ± 2.93	16	229.73 ± 20.08
3	21.69 ± 0.43	17	72.27 ± 0.17
4	> 1000	18	88.24 ± 0.94
5	506.21 ± 38.97	20	> 1000
6	> 1000	21	18.99 ± 1.41
7	456.00 ± 32.59	22	20.06 ± 0.35
8	> 1000	23	19.28 ± 0.49
9	823.28 ± 4.38	25	12.76 ± 0.15
10	> 1000	26	57.60 ± 6.85
11	13.66 ± 0.42	27	13.19 ± 0.72
12	538.20 ± 7.40	28	50.09 ± 2.53
13	> 1000	29	17.46 ± 0.16
14	> 1000	30	14.91 ± 1.10
15	> 1000	ascorbic acid	30.20 ± 0.47

In this activity, five levels of inhibition were classified based on the IC_{50} values, *i.e.*, excellent ($IC_{50} < 10$), very good ($10 \leq IC_{50} \leq 15$), good ($15 < IC_{50} \leq 30$), moderate ($30 < IC_{50} \leq 100$), weak ($100 < IC_{50} \leq 1000$), no activity ($IC_{50} > 1000 \mu\text{M}$).

More than half of isolated sesquiterpenoids (**5–21**) showed antioxidant activity (Figure 3.18). Interestingly, **11** exhibited the highest free-radical scavenging effect which was more than twice as strong as that of ascorbic acid. **21** has been found to be one of the most active compounds and its antioxidant activity was 1.6 times higher than ascorbic acid. The added methoxy group at C-7 in **12** decreased significantly its activity compared to that of **11**. The structure of **12** is close to **11** with the only difference of the methoxy substituent at C-7. Similarly, the addition of a hydroxy group in **7**, **9** increased slightly activity compared to those of **6** and **8**. However, the sesquiterpenoids bearing five-membered ring lactone (**13–15**) did not show antioxidant activity.

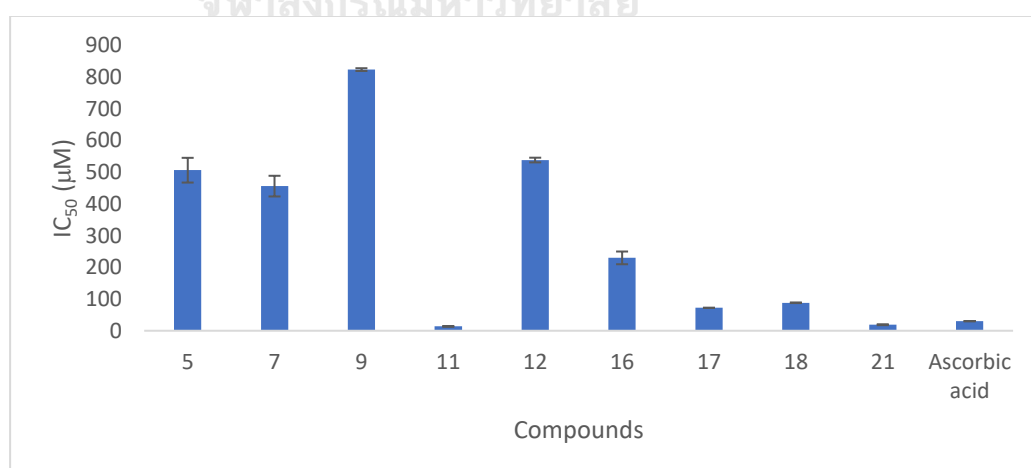


Figure 3.18 The antioxidant activity of sesquiterpenoids and ascorbic acid

The rest of isolated compounds possessed potent antioxidant activity (Figure 3.19). Phenolic compounds **1** and **3** were more active than ascorbic acid with the IC_{50} values of 20.62 ± 2.93 and $21.69 \pm 0.43 \mu\text{M}$ respectively. In addition, both neolignans showed good antioxidant activity and the acetyl group substituted at C-9' in **30** increasing slightly activity in comparison with **29**. Relating to compounds containing bicyclo[3.2.1]octane moiety, the most potential compound was **25**. The replacement of the hydroxy group in **23** at C-11 by methoxy group in **25** increased the antioxidant activity while the addition of ethoxy group at this position in **26** reduced significantly radical scavenging activity.

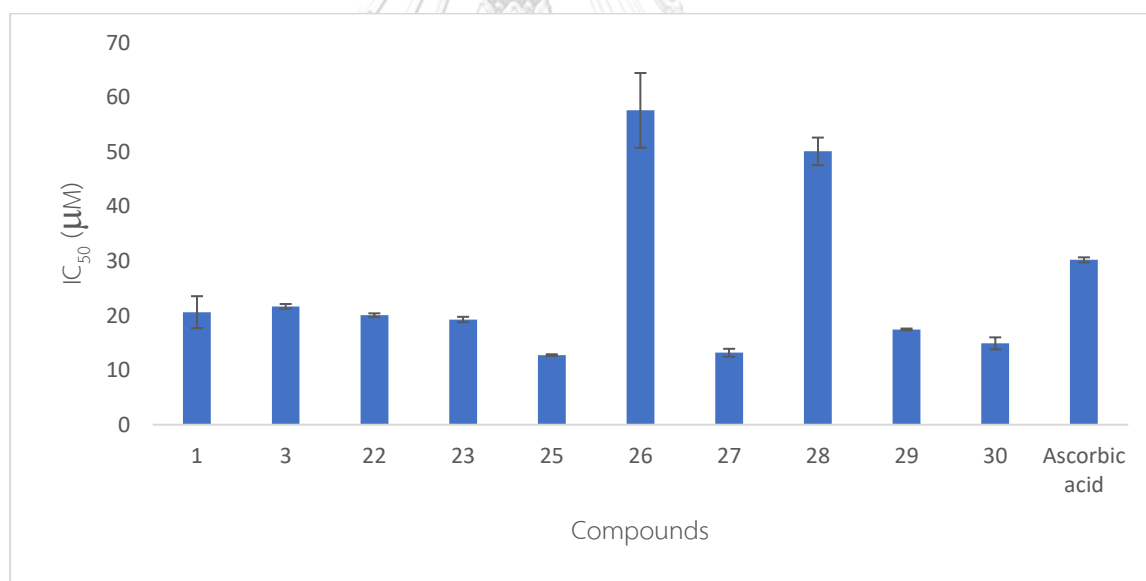


Figure 3.19 The antioxidant activity of compounds (**1**, **3**, **22-30**) and ascorbic acid

3.4.3 Cytotoxicity

Cancer is a serious disease and has become the leading cause of the death nowadays. Lung cancer is the most common type of cancer in the worldwide.⁸³ With the collaboration with Department of Pharmacology, Faculty of Medicine, Chulalongkorn University, isolated compounds were tested for cytotoxic activity against A549 (human lung adenocarcinoma) by MTT method.⁸⁴ The results are presented in Table 3.19.

Table 3.19 IC₅₀ values of tested compounds against A549 cancer cell line

Compounds	IC ₅₀ (μM)	Compounds	IC ₅₀ (μM)
3	> 100	18	15.59 ± 2.49
4	> 100	21	53.84 ± 6.00
7	> 100	22	> 100
9	> 100	23	> 100
10	59.66 ± 0.99	24	> 100
13	> 100	26	insoluble
14	> 100	29	26.04 ± 2.95
15	> 100	cisplatin	19.78 ± 2.14
17	60.15 ± 6.89		

Among these isolates, sesquiterpenoid (**18**) displayed the best activity against lung cancer cell line A549 with an IC_{50} value of $15.59 \pm 2.49 \mu\text{M}$, followed by neolignan (**29**) with an IC_{50} of $26.04 \pm 2.95 \mu\text{M}$. Three sesquiterpenoids (**10**, **17**, **21**) exhibited moderate inhibitory activity against A459 cell line. Other compounds revealed no cytotoxicity against lung cancer cell line.



Chapter 4

CONCLUSION

Thirty secondary metabolites were successfully isolated from the heartwoods of *Mansonia gagei*, including 10 new sesquiterpenoids (**12–21**), 7 novel structures (**22–28**), 1 new neolignan (**30**), and 12 known derivatives (**1–11, 29**). Their structures were determined by spectroscopic data analysis (UV-Vis, FTIR, 1D, 2D NMR and HRESIMS), and their absolute configurations were established by calculation of ECD data. In addition, isolated compounds were also investigated for antioxidant, cytotoxic activity and enzyme inhibitory effect against α -glucosidase. Interestingly, most cadinane sesquiterpenoids and novel skeletons bearing bicyclo[3.2.1]octane were significant active against yeast α -glucosidase with the IC_{50} values lower than 51.08 μ M. The kinetic study against α -glucosidase enzyme on **21** and **24** showed uncompetitive inhibition. The majority of novel compounds displayed stronger antioxidant activity than ascorbic acid. Only a few compounds (**18, 29**) had potent cytotoxicity on lung cancer cell line A549.

The outcome of this study provided information about diversity of chemical constituents of *M. gagei* heartwood and an attractive source of bioactive compounds. Thus, it could be concluded that some of these α -glucosidase inhibitors from *M. gagei* might lead to the development of anti-diabetic drugs in the future. Besides, *M. gagei* may be a reliable source of powerful antioxidants.

Suggestion for future work

A phytochemical study would be continued to the remaining EtOAc fraction. Furthermore, the absolute configurations of novel skeletons should be determined by ECD and DP4 calculations or by single-crystal X-ray diffraction. Computational calculation study is crucial to predict the binding of a compound with a protein, or the relationship between chemical structures and biological activities



REFERENCES



จุฬาลงกรณ์มหาวิทยาลัย
CHULALONGKORN UNIVERSITY

1. Wright, G. D., Unlocking the potential of natural products in drug discovery. *Microb. Biotechnol.* **2019**, *12*, 55-57.
2. Osadebe, P. O.; Odoh, E. U.; Uzor, P. F., Natural products as potential sources of antidiabetic drugs. *J. Pharm. Res. Int.* **2014**, *4*, 2075-2095.
3. Gautam, R.; Jachak, S. M., Recent developments in anti-inflammatory natural products. *Med. Res. Rev.* **2009**, *29*, 767-820.
4. Dutta, S.; Mahalanobish, S.; Saha, S.; Ghosh, S.; Sil, P. C., Natural products: An upcoming therapeutic approach to cancer. *Food Chem. Toxicol.* **2019**, *128*, 240-255.
5. Raghuv eer, I.; Anurag, K.; Anumalik, Y.; Nitika, G.; Swadesh, K.; Nikhil, G.; Santosh, K.; Vinay, Y.; Anuj, P.; Himanshu, G., Metabolites in plants and its classification. *World J. Pharm. Pharm. Sci.* **2015**, *4*, 287-305.
6. Koparde, A. A.; Doijad, R. C.; Magdum, C. S., *Natural products in drug discovery*. 2019; p 1-20.
7. Wood, J. N., From plant extract to molecular panacea: a commentary on Stone (1763)'An account of the success of the bark of the willow in the cure of the agues'. *Philos. Trans. R. Soc. Lond., B, Biol. Sci.* **2015**, *370*, 20140317.
8. Kulka, M., *Using Old Solutions to New Problems: Natural Drug Discovery in the 21st Century*. BoD–Books on Demand: 2013.
9. Christensen, S. B., Natural products that changed society. *Biomedicines* **2021**, *9*, 472.

10. Al Muqarrabun, L.; Ahmat, N., Medicinal uses, phytochemistry and pharmacology of family Sterculiaceae: A review. *Eur. J. Med. Chem.* **2015**, *92*, 514-530.
11. Tiew, P.; Puntumchai, A.; Kokpol, U.; Chavasiri, W., Coumarins from the heartwoods of *Mansonia gagei* Drumm. *Phytochemistry* **2002**, *60*, 773-776.
12. El-Halawany, A. M.; Chung, M. H.; Ma, C.-M.; Komatsu, K.; Nishihara, T.; Hattori, M., Anti-estrogenic activity of mansorins and mansonones from the heartwood of *Mansonia gagei* Drumm. *Chem. Pharm. Bull.* **2007**, *55*, 1332-1337.
13. Baghdadi, M. A.; Al-Abbasi, F. A.; El-Halawany, A. M.; Aseeri, A. H.; Al-Abd, A. M., Anticancer profiling for coumarins and related *O*-naphthoquinones from *Mansonia gagei* against solid tumor cells in vitro. *Molecules* **2018**, *23*, 1020.
14. Mongkol, R.; Chavasiri, W., Antimicrobial, herbicidal and antifeedant activities of mansonone E from the heartwoods of *Mansonia gagei* Drumm. *J. Integr. Agric.* **2016**, *15*, 2795-2802.
15. Kim, J.-P.; Kim, W.-G.; Koshino, H.; Jung, J.; Yoo, I.-D., Sesquiterpene *O*-naphthoquinones from the root bark of *Ulmus davidiana*. *Phytochemistry* **1996**, *43*, 425-430.
16. Singanan, M.; Duraiswamy, B.; Varadarajan, V., Physicochemical, phytochemicals and antioxidant evaluation of *Guazuma ulmifolia* fruit. *Int. J. Pharm. Pharm. Sci.* **2018**, *10*, 87-91.
17. Mamatha, B.; Palaksha, M.; Gnanasekaran, D.; Senthilkumar, G.; Tamizmani, T., *Melochia corchorifolia* L: A review. *World J. Pharm. Res.* **2018**, *7*, 482-491.

18. Atolani, O.; Oguntoye, H.; Areh, E.; Adeyemi, O.; Kambizi, L., Chemical composition, anti-toxoplasma, cytotoxicity, antioxidant, and anti-inflammatory potentials of *Cola gigantea* seed oil. *Pharm. Biol.* **2019**, *57*, 154-160.
19. Fernandes, D. A.; Souza, M. S.; Teles, Y. C.; Oliveira, L. H.; Lima, J. B.; Conceição, A. S.; Nunes, F. C.; Silva, T.; Souza, M. d. F. V. d., New sulphated flavonoids and larvicidal activity of *Helicteres velutina* K. Schum (Sterculiaceae). *Molecules* **2018**, *23*, 2784.
20. Damor, B.; Gaur, K.; Dashora, A.; Parra, S. A., Evaluation of analgesic and anti-inflammatory activity of methanolic extract of *Guazuma ulmifolia*. *J. Appl. Pharm. Sci.* **2018**, *1*, 23-29.
21. Taparia, S. S.; Khanna, A., Procyanidin-rich extract of natural cocoa powder causes ROS-mediated caspase-3 dependent apoptosis and reduction of pro-MMP-2 in epithelial ovarian carcinoma cell lines. *Biomed. Pharmacother.* **2016**, *83*, 130-140.
22. Povi, L.; Batomayena, B.; Hodé, T.; Kwashie, E.; Kodjo, A.; Messanvi, G., Phytochemical screening, antioxidant and hypoglycemic activity of *Coccoloba uvifera* leaves and *Waltheria indica* roots extracts. *Int. J. Pharm. Pharm. Sci.* **2015**, *7*, 279-283.
23. Nguyen, T. T.; Kretschmer, N.; Pferschy-Wenzig, E.-M.; Kunert, O.; Bauer, R., Triterpenoidal and phenolic compounds Isolated from the aerial parts of *Helicteres hirsuta* and their cytotoxicity on several cancer cell lines. *Nat. Prod. Commun.* **2019**, *14*, 7-10.

24. Chen, W.; Tang, W.; Lou, L.; Zhao, W., Pregnane, coumarin and lupane derivatives and cytotoxic constituents from *Helicteres angustifolia*. *Phytochemistry* **2006**, *67*, 1041-1047.
25. Chang, H.-S.; Lin, C.-H.; Hsiao, P.-Y.; Peng, H.-T.; Lee, S.-J.; Cheng, M.-J.; Chen, I.-S., Bioactive composition of *Reevesia formosana* root and stem with cytotoxic activity potential. *RSC advances* **2017**, *7*, 27040-27047.
26. Jacob, J.; Sreejith, K., Antioxidant and anti-inflammatory properties of *Pterospermum rubiginosum* Heyne ex Wight and Arn and *Pterospermum reticulatum* Wight and Arn (Sterculiaceae): An in vitro comparative study. *Asian J. Pharm. Clin. Res.* **2019**, *12*, 272-275.
27. Chakrabarti, R.; Vikramadithyan, R. K.; Mullangi, R.; Sharma, V.; Jagadheshan, H.; Rao, Y.; Sairam, P.; Rajagopalan, R., Antidiabetic and hypolipidemic activity of *Helicteres isora* in animal models. *J. Ethnopharmacol.* **2002**, *81*, 343-349.
28. Rathinavelusamy, P.; Mazumder, P. M.; Sasmal, D.; Jayaprakash, V., Evaluation of in silico, in vitro α -amylase inhibition potential and antidiabetic activity of *Pterospermum acerifolium* bark. *Pharm. Biol.* **2014**, *52*, 199-207.
29. Hu, X.; Cheng, D.; Li, K.; Wang, L.; Yang, X.; Sun, S.; Wang, Y.; Li, S.; Lei, Z.; Zhang, Z., Glucose consumption and alpha-glucosidase inhibitory activities of aqueous root extract of *Helicteres angustifolia*. *Eur. Rev. Med. Pharmacol. Sci.* **2016**, *20*, 1423-1429.

30. Sonibare, M.; Soladoye, M.; Esan, O.; Sonibare, O., Phytochemical and antimicrobial studies of four species of *Cola* Schott & Endl. (Sterculiaceae). *Afr. J. Tradit. Complement. Altern. Med.* **2009**, *6*, 518-525.
31. Gaikwad, M. S.; Dhasade, V. V., Review on Phytochemicals and Pharmacological Profile of *Helicteres isora* Linn. *J. Curr. Pharm. Res.* **2019**, *9*, 2955-2969.
32. Hatano, T.; Miyatake, H.; Natsume, M.; Osakabe, N.; Takizawa, T.; Ito, H.; Yoshida, T., Proanthocyanidin glycosides and related polyphenols from cacao liquor and their antioxidant effects. *Phytochemistry* **2002**, *59*, 749-758.
33. Saragih, G. S.; Siswadi, S., Antioxidant activity of plant parts extracts from *Sterculia quadrifida* R. Br. *Asian J. Pharm. Clin. Res.* **2019**, *12*, 143-148.
34. Tiew, P. Bioactive compounds from *Mansonia gagei* Drumm. Chulalongkorn University, **2002**.
35. Bettòlo, G. M.; Casinovi, C.; Galeffi, C., A new class of quinones: sesquiterpenoid quinones of *Mansonia altissima* Chev. *Tetrahedron Lett.* **1965**, *6*, 4857-4864.
36. Tanaka, N.; Yasue, M.; Imamura, H., The quinonoid pigments of *Mansonia altissima* wood. *Tetrahedron Lett.* **1966**, *7*, 2767-2773.
37. Shimada, K. Y., M.; Imamura, H., Structure of mansonone I, a new pigment from *Mansonia altissima* wood. *Nippon Mokuzai Gakkaishi* **1967**, *13*, 126.
38. Galeffi, C.; delle Monache, E. M.; Casinovi, C.; Bettolo, G. M., A new quinone from the heartwood of *Mansonia altissima* Chev: Mansonone L. *Tetrahedron Lett.* **1969**, *10*, 3583-3584.

39. Tiew, P.; Loset, J.-R.; Kokpol, U.; Schenk, K.; Jaiboon, N.; Chaichit, N.; Chavasiri, W.; Hostettmann, K., Four new sesquiterpenoid derivatives from the heartwood of *Mansonia gagei*. *J. Nat. Prod.* **2002**, *65*, 1332-1335.
40. Tiew, P.; Takayama, H.; Kitajima, M.; Aimi, N.; Kokpol, U.; Chavasiri, W., A novel neolignan, mansoxetane, and two new sesquiterpenes, mansonones R and S, from *Mansonia gagei*. *Tetrahedron Lett.* **2003**, *44*, 6759-6761.
41. Tiew, P.; Loset, J. R.; Kokpol, U.; Chavasiri, W.; Hostettmann, K., Antifungal, antioxidant and larvicidal activities of compounds isolated from the heartwood of *Mansonia gagei*. *Phytother. Res.* **2003**, *17*, 190-193.
42. Changwong, N.; Sabphon, C.; Ingkaninan, K.; Sawasdee, P., Acetyl- and butyryl- cholinesterase inhibitory activities of mansorins and mansonones. *Phytother. Res.* **2012**, *26*, 392-396.
43. Nishina, A.; Miura, A.; Goto, M.; Terakado, K.; Sato, D.; Kimura, H.; Hirai, Y.; Sato, H.; Phay, N., Mansonone E from *Mansonia gagei* inhibited α -MSH-induced melanogenesis in B16 cells by inhibiting CREB expression and phosphorylation in the PI3K/Akt pathway. *Biol. Pharm. Bull.* **2018**, *41*, 770-776.
44. Chen, C.-M.; Chen, Z.-T.; Hong, Y.-L., A mansonone from *Helicteres angustifolia*. *Phytochemistry* **1990**, *29*, 980-982.
45. Puckhaber, L. S.; Stipanovic, R. D., Thespesenone and dehydrooxoperezinone-6-methyl ether, new sesquiterpene quinones from *Thespesia populnea*. *J. Nat. Prod.* **2004**, *67*, 1571-1573.

46. Johnson, J.; Gandhidasan, I.; Murugesan, R., Cytotoxicity and superoxide anion generation by some naturally occurring quinones. *Free Radic. Biol. Med.* **1999**, *26*, 1072-1078.
47. Yoiprommarat, S.; Kongthong, S.; Choowong, W.; Boonyuen, N.; Isaka, M.; Bunyapaiboonsri, T., Xanthonenes from a lignicolous freshwater fungus (BCC 28210). *Nat. Prod. Res.* **2020**, *34*, 1233-1237.
48. Wang, D.; Xia, M.; Cui, Z.; Tashiro, S.-i.; Onodera, S.; Ikejima, T., Cytotoxic effects of mansonone E and F isolated from *Ulmus pumila*. *Biol. Pharm. Bull.* **2004**, *27*, 1025-1030.
49. Boonsri, S.; Karalai, C.; Ponglimanont, C.; Chantrapromma, S.; Kanjana-Opas, A., Cytotoxic and antibacterial sesquiterpenes from *Thespesia populnea*. *J. Nat. Prod.* **2008**, *71*, 1173-1177.
50. Shin, D.-Y.; Kim, H.-S.; Min, K.-H.; Hyun, S.-S.; Kim, S.-A.; Huh, H.; Choi, E.-C.; Choi, Y. H.; Kim, J.; Choi, S.-H., Isolation of a potent anti-MRSA sesquiterpenoid quinone from *Ulmus davidiana* var. *japonica*. *Chem. Pharm. Bull.* **2000**, *48*, 1805-1806.
51. Wu, P.-L.; Wu, T.-S.; He, C.-X.; Su, C.-H.; Lee, K.-H., Constituents from the stems of *Hibiscus taiwanensis*. *Chem. Pharm. Bull.* **2005**, *53*, 56-59.
52. Sato, T.; Arai, M. A.; Hara, Y.; Koyano, T.; Kowithayakorn, T.; Ishibashi, M., Cadinane sesquiterpenoids isolated from *Santalum album* using a screening program for Wnt signal inhibitory activity. *J. Nat. Med.* **2020**, *74*, 476-481.

53. Molecular Operating Environment (MOE), 2019.01; Chemical Computing Group ULC, 1010 Sherbooke St. West, Suite #910, Montreal, QC, Canada, H3A 2R7. **2021**.
54. Halgren, T. A., Merck molecular force field. I. Basis, form, scope, parameterization, and performance of MMFF94. *J. Comput. Chem.* **1996**, *17*, 490-519.
55. Frisch, M. J.; Trucks, G. W.; Schlegel, H. B.; Scuseria, G. E.; Robb, M. A.; Cheeseman, J. R.; Scalmani, G.; Barone, V.; Petersson, G. A.; Nakatsuji, H.; Li, X.; Caricato, M.; Marenich, A.; Bloino, J.; Janesko, B. G.; Gomperts, R.; Mennucci, B.; Hratchian, H. P.; Ortiz, J. V.; Izmaylov, A. F.; Sonnenberg, J. L.; Williams-Young, D.; Ding, F.; Lipparini, F.; Egidi, F.; Goings, J.; Peng, B.; Petrone, A.; Henderson, T.; Ranasinghe, D.; Zakrzewski, V. G.; Gao, J.; Rega, N.; Zheng, G.; Liang, W.; Hada, M.; Ehara, M.; Toyota, K.; Fukuda, R.; Hasegawa, J.; Ishida, M.; Nakajima, T.; Honda, Y.; Kitao, O.; Nakai, H.; Vreven, T.; Throssell, K.; Montgomery, J. A., Jr.; Peralta, J. E.; Ogliaro, F.; Bearpark, M.; Heyd, J. J.; Brothers, E.; Kudin, K. N.; Staroverov, V. N.; Keith, T.; Kobayashi, R.; Normand, J.; Raghavachari, K.; Rendell, A.; Burant, J. C.; Iyengar, S. S.; Tomasi, J.; Cossi, M.; Millam, J. M.; Klene, M.; Adamo, C.; Cammi, R.; Ochterski, J. W.; Martin, R. L.; Morokuma, K.; Farkas, O.; Foresman, J. B.; and Fox, D. J., Gaussian 09, Revision B. 01, Wallingford, CT. **2016**.
56. Bruhn, T.; Schaumlöffel, A.; Hemberger, Y.; Pescitelli, G., SpecDis version 1.71. Berlin, Germany. **2017**.

57. Ramadhan, R.; Phuwapraisirisan, P., New arylalkanones from *Horsfieldia macrobotrys*, effective antidiabetic agents concomitantly inhibiting α -glucosidase and free radicals. *Bioorg. Med. Chem. Lett.* **2015**, *25*, 4529-4533.
58. Ranković, B.; Kosanić, M.; Stanojković, T.; Vasiljević, P.; Manojlović, N., Biological activities of *Toninia candida* and *Usnea barbata* together with their norstictic acid and usnic acid constituents. *Int. J. Mol. Sci.* **2012**, *13*, 14707-14722.
59. Panyo, J.; Matsunami, K.; Panichayupakaranant, P., Bioassay-guided isolation and evaluation of antimicrobial compounds from *Ixora megalophylla* against some oral pathogens. *Pharm. Biol.* **2016**, *54*, 1522-1527.
60. González-Baró, A. C.; Parajón-Costa, B. S.; Franca, C. A.; Pis-Diez, R., Theoretical and spectroscopic study of vanillic acid. *J. Mol. Struct.* **2008**, *889*, 204-210.
61. Öksüz, S.; Ulubelen, A.; Barla, A.; Voelter, W., Terpenoids and aromatic compounds from *Euphorbia heteradena*. *Turk. J. Chem.* **2002**, *26*, 457-464.
62. Kornsakulkarn, J.; Somyong, W.; Supothina, S.; Boonyuen, N.; Thongpanchang, C., Bioactive oxygen-bridged cyclooctadienes from endophytic fungus *Phomopsis* sp. BCC 45011. *Tetrahedron* **2015**, *71*, 9112-9116.
63. Zhang, Y.; Liu, Y.-B.; Li, Y.; Li, L.; Ma, S.-G.; Qu, J.; Jiang, J.-D.; Chen, X.-G.; Zhang, D.; Yu, S.-S., Terpenoids from the roots of *Alangium chinense*. *J. Asian Nat. Prod. Res.* **2015**, *17*, 1025-1038.
64. Wu, P.-L.; Su, G.-C.; Wu, T.-S., Constituents from the stems of *Aristolochia manshuriensis*. *J. Nat. Prod.* **2003**, *66*, 996-998.

65. Wang, M.; Liu, W.; Li, J.; Shen, F.; Lin, X.; Zheng, Q., Structure elucidation of heliclactone. *Acta Chim. Sinica* **1988**, *46*, 768-771.
66. Saito, T.; Itabashi, T.; Wakana, D.; Takeda, H.; Yaguchi, T.; Kawai, K.-i.; Hosoe, T., Isolation and structure elucidation of new phthalide and phthalane derivatives, isolated as antimicrobial agents from *Emericella* sp. IFM57991. *J. Antibiot.* **2016**, *69*, 89-96.
67. Ding, G.; Liu, S.; Guo, L.; Zhou, Y.; Che, Y., Antifungal metabolites from the plant endophytic fungus *Pestalotiopsis foedan.* *J. Nat. Prod.* **2008**, *71*, 615-618.
68. Cambie, R. C.; Craw, P.; Buckleton, J.; Clark, G.; Rickard, C., A new series of sesquiterpenoids from a Gorgonian. *Aust. J. Chem.* **1988**, *41*, 365-372.
69. Lewis, M. L.; de Meijere, A., Total synthesis of marine sesquiterpenoids containing a primnatriene skeleton. *Synlett* **1997**, *1997*, 261-262.
70. Luo, X.; Li, C.; Luo, P.; Lin, X.; Ma, H.; Seeram, N. P.; Song, C.; Xu, J.; Gu, Q., Pterisin sesquiterpenoids from *Pteris cretica* as hypolipidemic agents via activating liver X receptors. *J. Nat. Prod.* **2016**, *79*, 3014-3021.
71. Barnes, E. C.; Kavanagh, A. M.; Ramu, S.; Blaskovich, M. A.; Cooper, M. A.; Davis, R. A., Antibacterial serrulatane diterpenes from the Australian native plant *Eremophila microtheca.* *Phytochemistry* **2013**, *93*, 162-169.
72. Li, M.-Y.; Tian, Y.; Shen, L.; Buettner, R.; Li, H.-Z.; Liu, L.; Yuan, Y.-C.; Xiao, Q.; Wu, J.; Jove, R., 3-O-methylthespesilactam, a new small-molecule anticancer pan-

JAK inhibitor against A2058 human melanoma cells. *Biochem. Pharmacol.* **2013**, *86*, 1411-1418.

73. Kaysser, L.; Bernhardt, P.; Nam, S.-J.; Loesgen, S.; Ruby, J. G.; Skewes-Cox, P.; Jensen, P. R.; Fenical, W.; Moore, B. S., Merochlorins A–D, cyclic meroterpenoid antibiotics biosynthesized in divergent pathways with vanadium-dependent chloroperoxidases. *J. Am. Chem. Soc.* **2012**, *134*, 11988-11991.

74. Ramachary, D. B.; Anif Pasha, M.; Thirupathi, G., Organocatalytic asymmetric formal [3 + 2] cycloaddition as a versatile platform to access methanobenzo [7] annulenes. *Angew. Chem. Int. Ed.* **2017**, *56*, 12930-12934.

75. Sakoulas, G.; Nam, S.-J.; Loesgen, S.; Fenical, W.; Jensen, P. R.; Nizet, V.; Hensler, M., Novel bacterial metabolite merochlorin A demonstrates in vitro activity against multi-drug resistant methicillin-resistant *Staphylococcus aureus*. *PLoS One* **2012**, *7*, e29439.

76. Winkelmann, K.; Heilmann, J.; Zerbe, O.; Rali, T.; Sticher, O., Further prenylated bi- and tricyclic phloroglucinol derivatives from *Hypericum papuanum*. *Helv. Chim. Acta* **2001**, *84*, 3380-3392.

77. Liu, J.; Zheng, C.-H.; Ren, X.-H.; Zhou, F.; Li, W.; Zhu, J.; Lv, J.-G.; Zhou, Y.-J., Synthesis and biological evaluation of 1-benzylidene-3, 4-dihydronaphthalen-2-one as a new class of microtubule-targeting agents. *J. Med. Chem.* **2012**, *55*, 5720-5733.

78. Maguire, C. J.; Carlson, G. J.; Ford, J. W.; Strecker, T. E.; Hamel, E.; Trawick, M. L.; Pinney, K. G., Synthesis and biological evaluation of structurally diverse α -

conformationally restricted chalcones and related analogues. *Med. Chem. Comm.* **2019**, *10*, 1445-1456.

79. Shih, H.; Deng, L.; Carrera, C. J.; Adachi, S.; Cottam, H. B.; Carson, D. A., Rational design, synthesis and structure–activity relationships of antitumor (*E*)-2-benzylidene-1-tetralones and (*E*)-2-benzylidene-1-indanones. *Bioorg. Med. Chem. Lett.* **2000**, *10*, 487-490.

80. Rengasamy, K. R.; Slavětinská, L. P.; Kulkarni, M. G.; Stirk, W. A.; Van Staden, J., Cuparane sesquiterpenes from *Laurencia natalensis* Kylin as inhibitors of alpha-glucosidase, dipeptidyl peptidase IV and xanthine oxidase. *Algal Res.* **2017**, *25*, 178-183.

81. Moon, H. E.; Islam, M. N.; Ahn, B. R.; Chowdhury, S. S.; Sohn, H. S.; Jung, H. A.; Choi, J. S., Protein tyrosine phosphatase 1B and α -glucosidase inhibitory phlorotannins from edible brown algae, *Ecklonia stolonifera* and *Eisenia bicyclis*. *Biosci. Biotechnol. Biochem.* **2011**, *75*, 1472-1480.

82. Yang, L.; Yang, Y.-L.; Dong, W.-H.; Li, W.; Wang, P.; Cao, X.; Yuan, J.-Z.; Chen, H.-Q.; Mei, W.-L.; Dai, H.-F., Sesquiterpenoids and 2-(2-phenylethyl) chromones respectively acting as α -glucosidase and tyrosinase inhibitors from agarwood of an *Aquilaria* plant. *Journal of enzyme inhibition and medicinal chemistry* **2019**, *34*, 853-862.

83. Gurunathan, S.; Qasim, M.; Kang, M.-H.; Kim, J.-H., Role and therapeutic potential of melatonin in various type of cancers. *Onco Targets Ther.* **2021**, *14*, 2019.

84. Riss, T. L.; Moravec, R. A.; Niles, A. L.; Duellman, S.; Benink, H. A.; Worzella, T. J.; Minor, L., Cell viability assays. *Assay Guidance Manual [Internet]* 2016.



APPENDIX



จุฬาลงกรณ์มหาวิทยาลัย
CHULALONGKORN UNIVERSITY

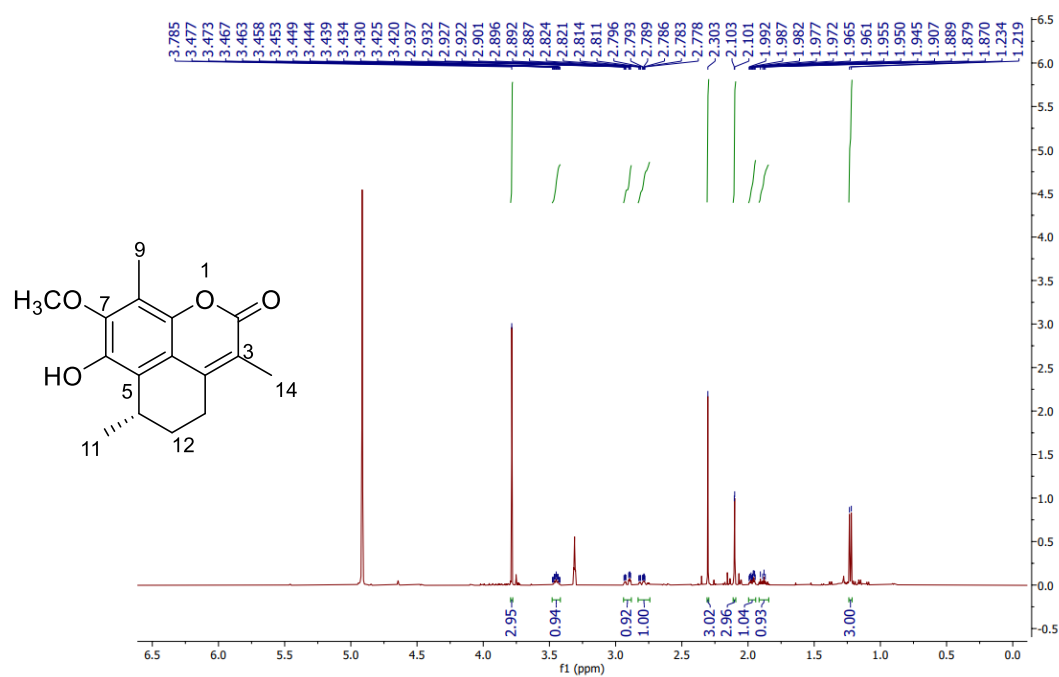


Figure A1. ^1H NMR spectrum (500 MHz, $\text{methanol-}d_4$) of compound **12**

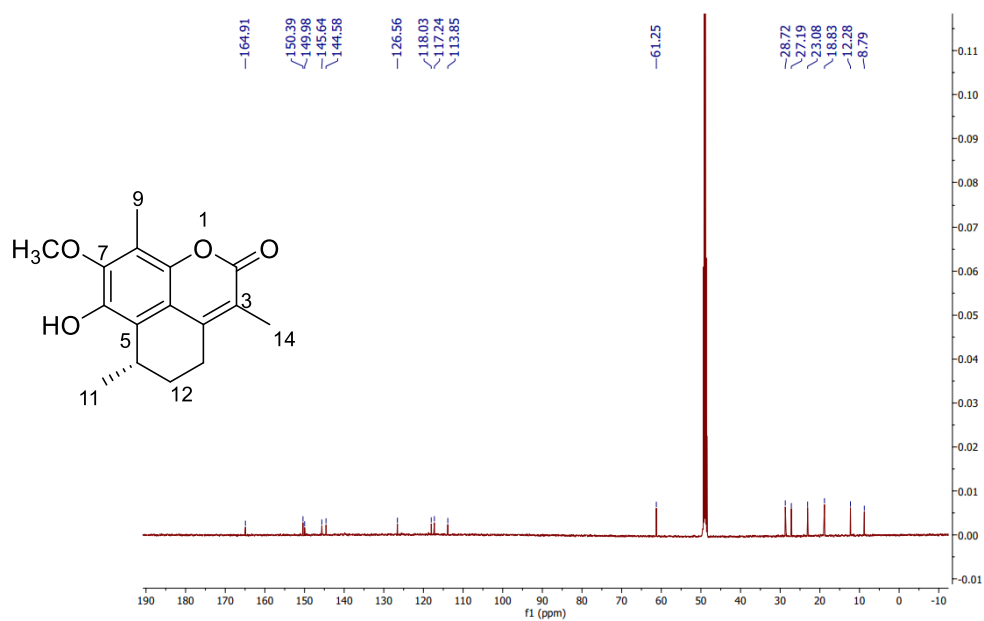


Figure A2. ^{13}C NMR spectrum (125 MHz, $\text{methanol-}d_4$) of compound **12**

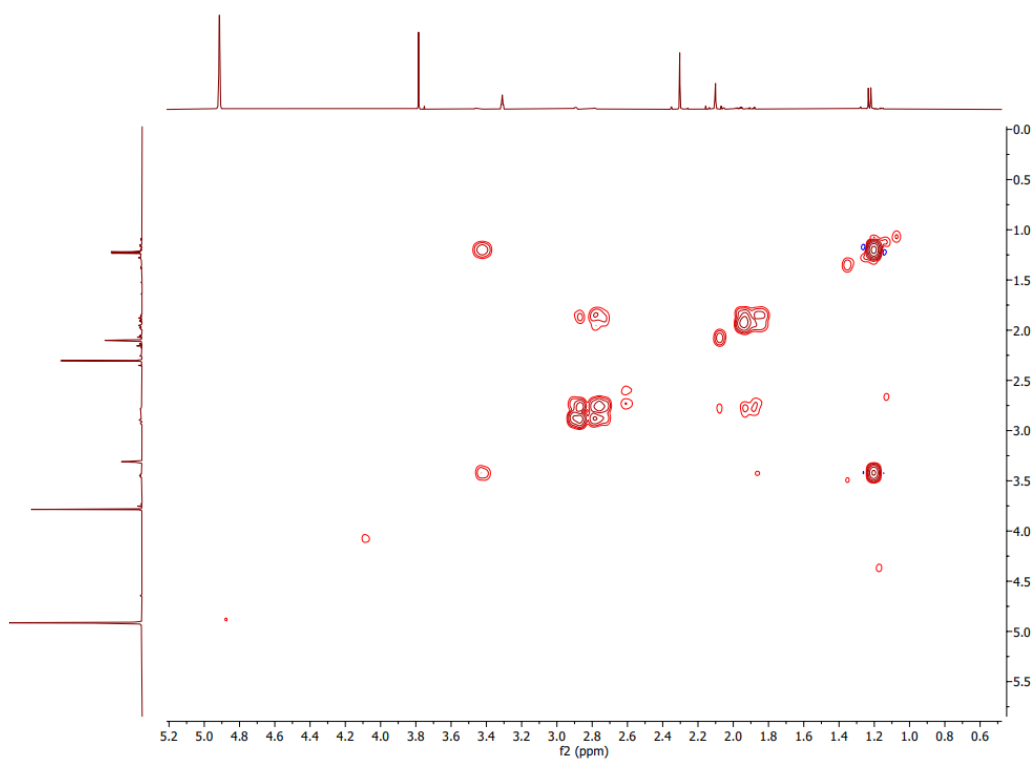
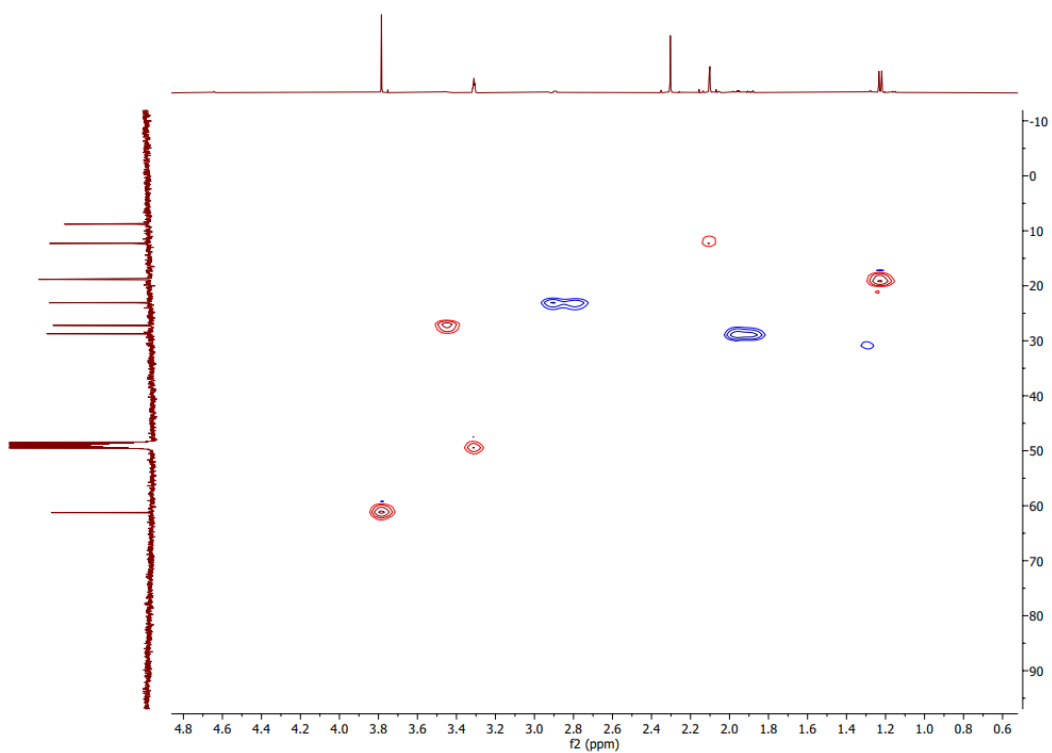
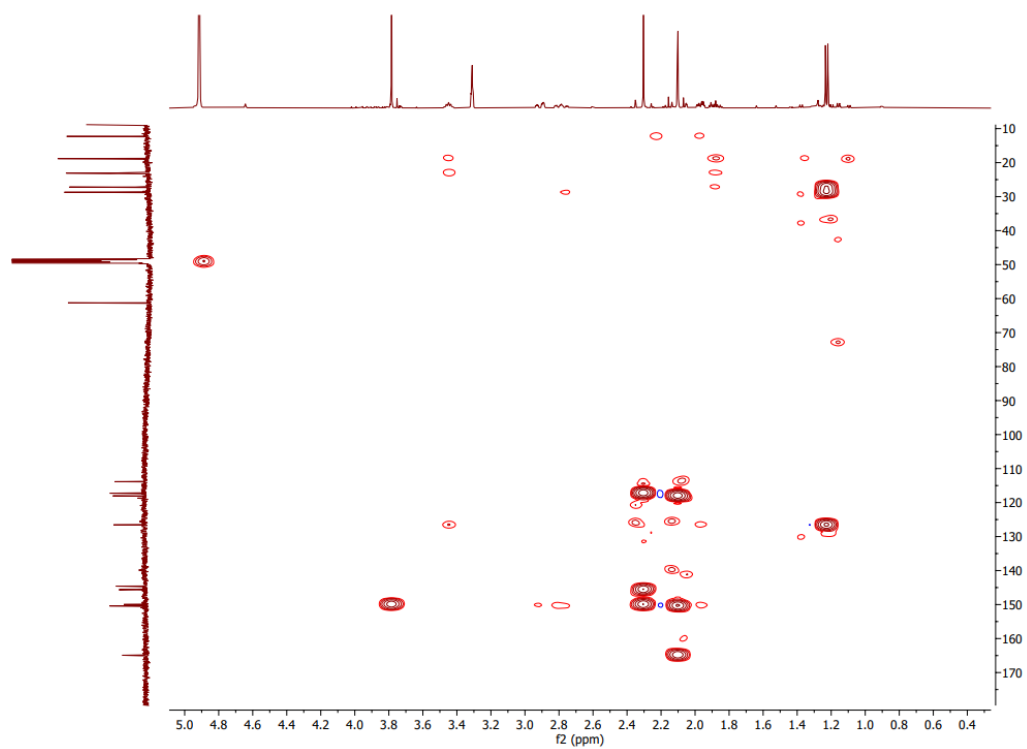
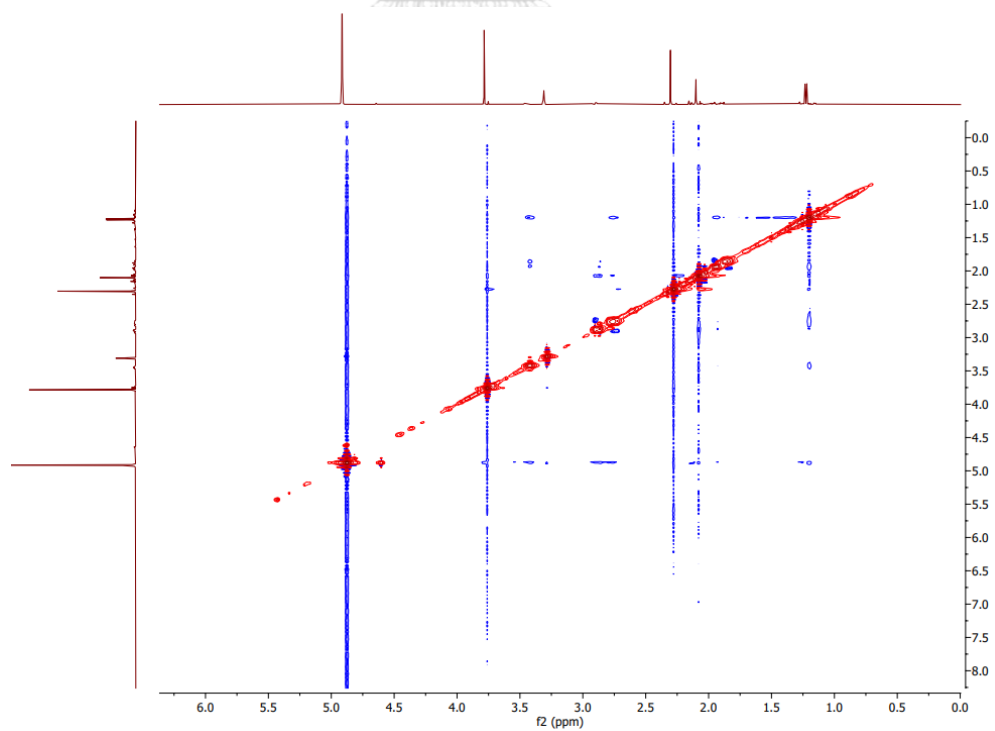
Figure A3. ^1H - ^1H COSY spectrum of compound 12

Figure A4. HSQC spectrum of compound 12

Figure A5. HMBC spectrum of compound **12**Figure A6. NOESY spectrum of compound **12**

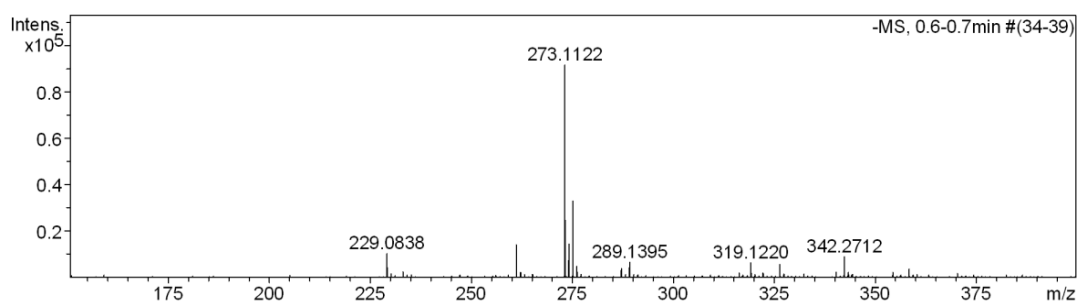
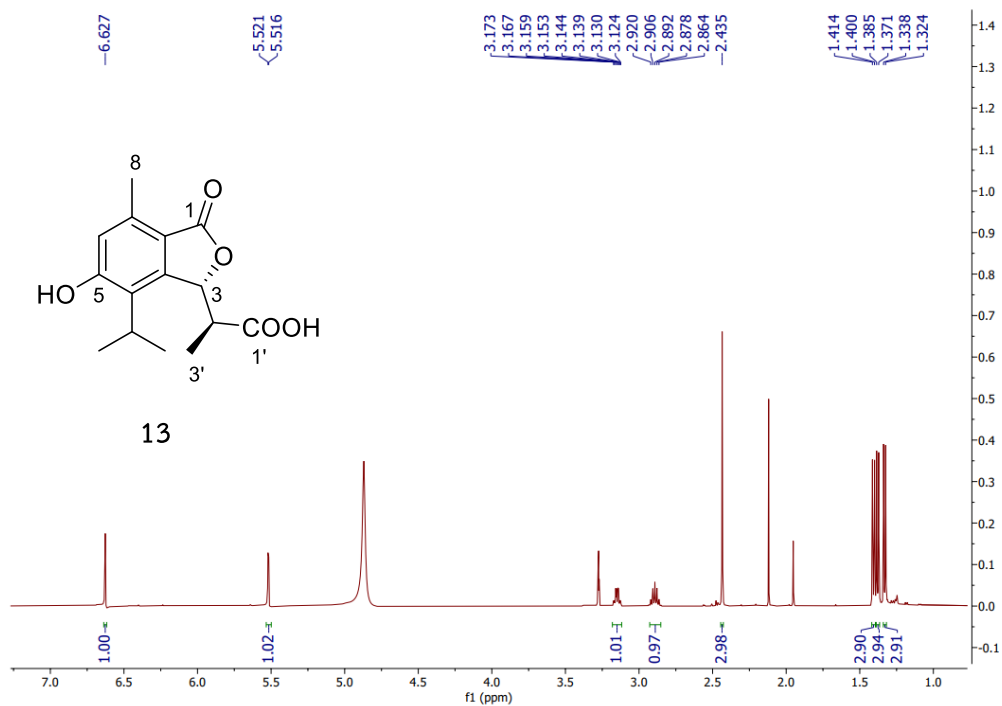
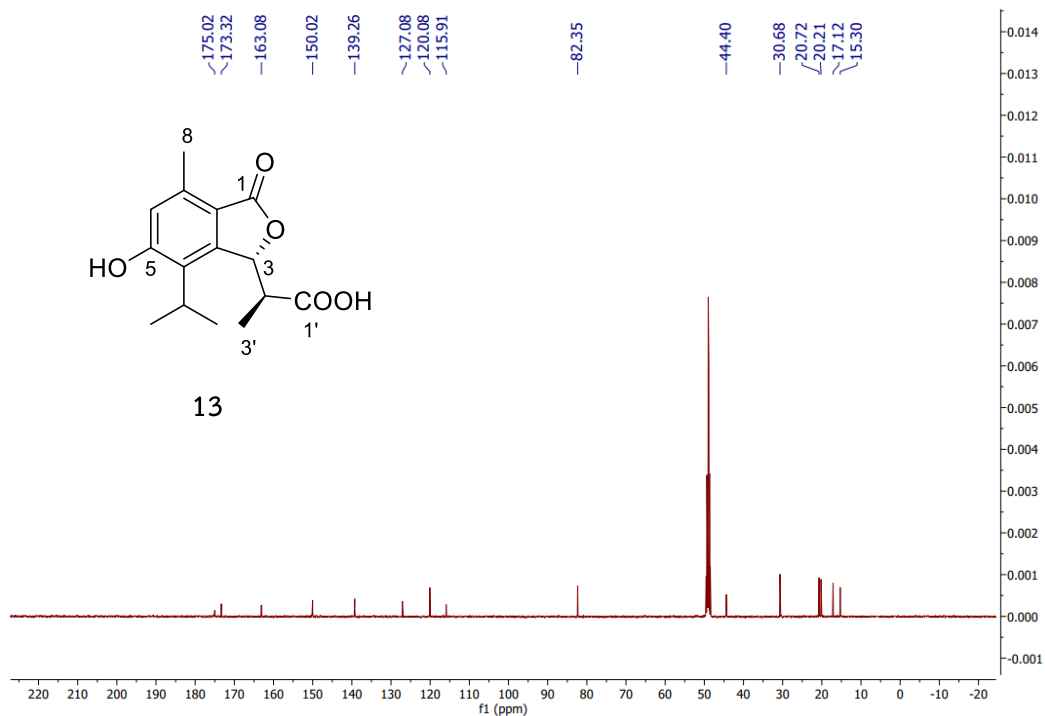
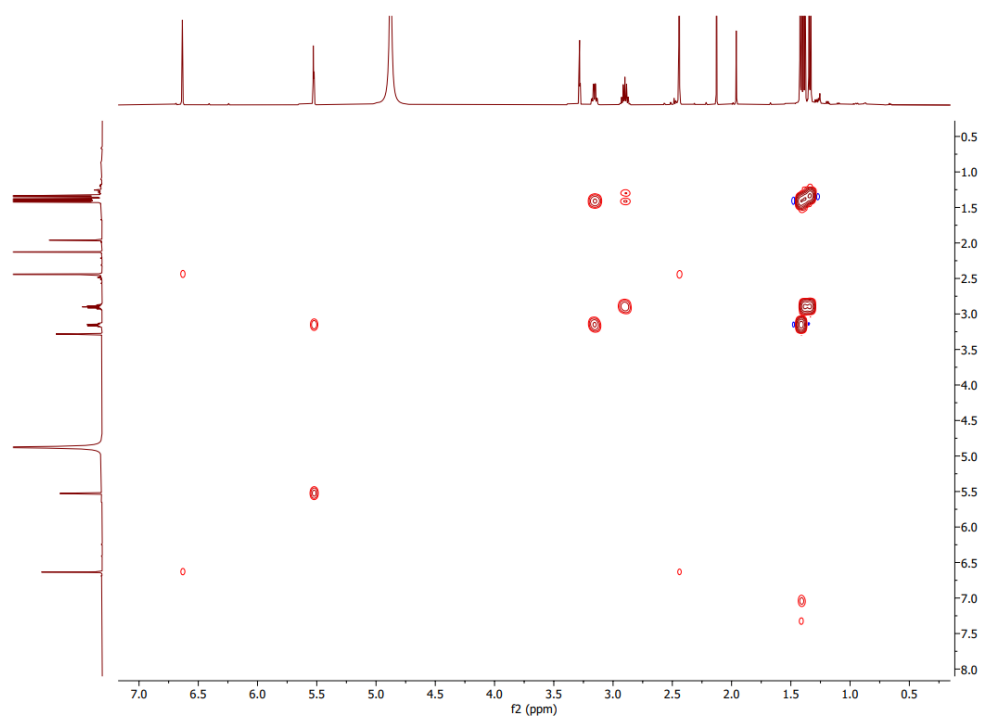
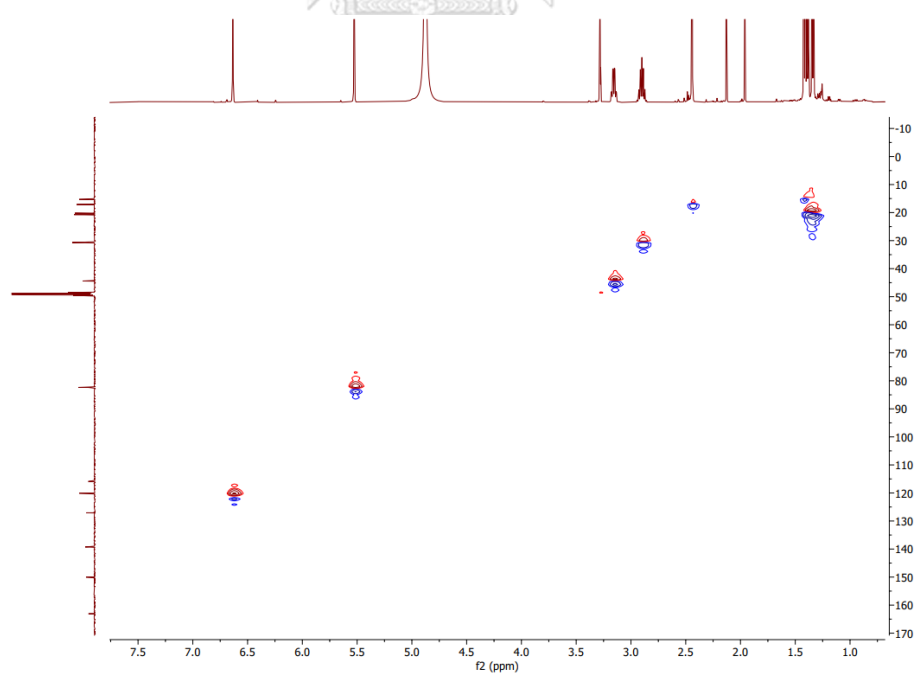
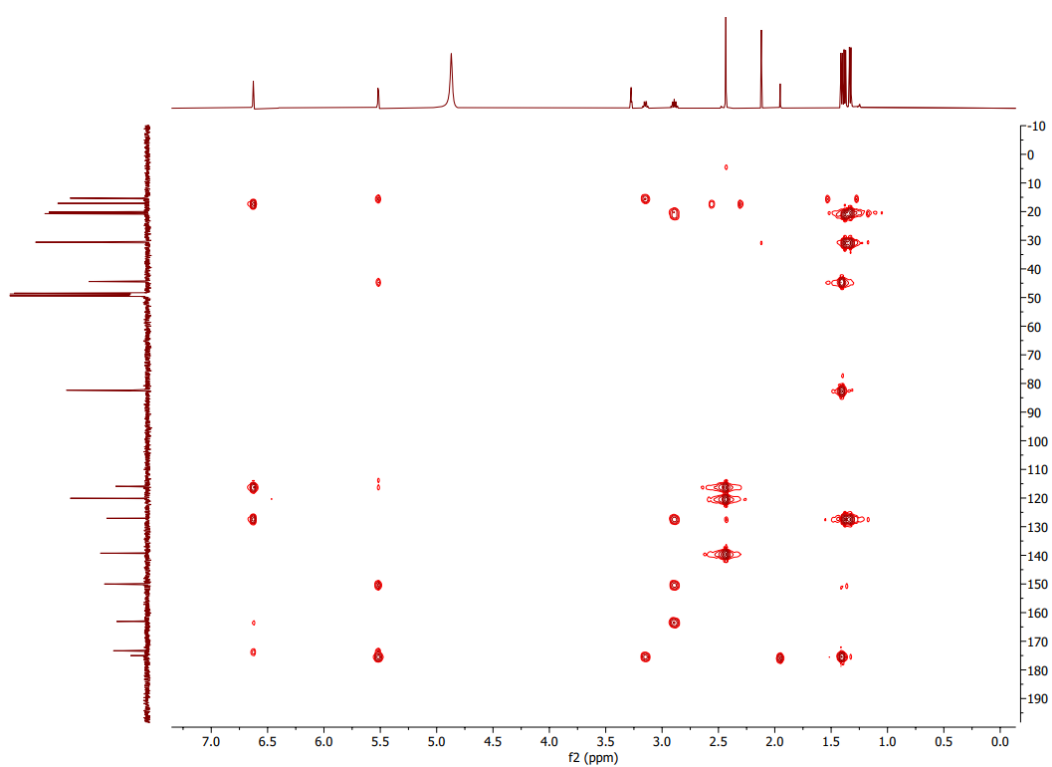
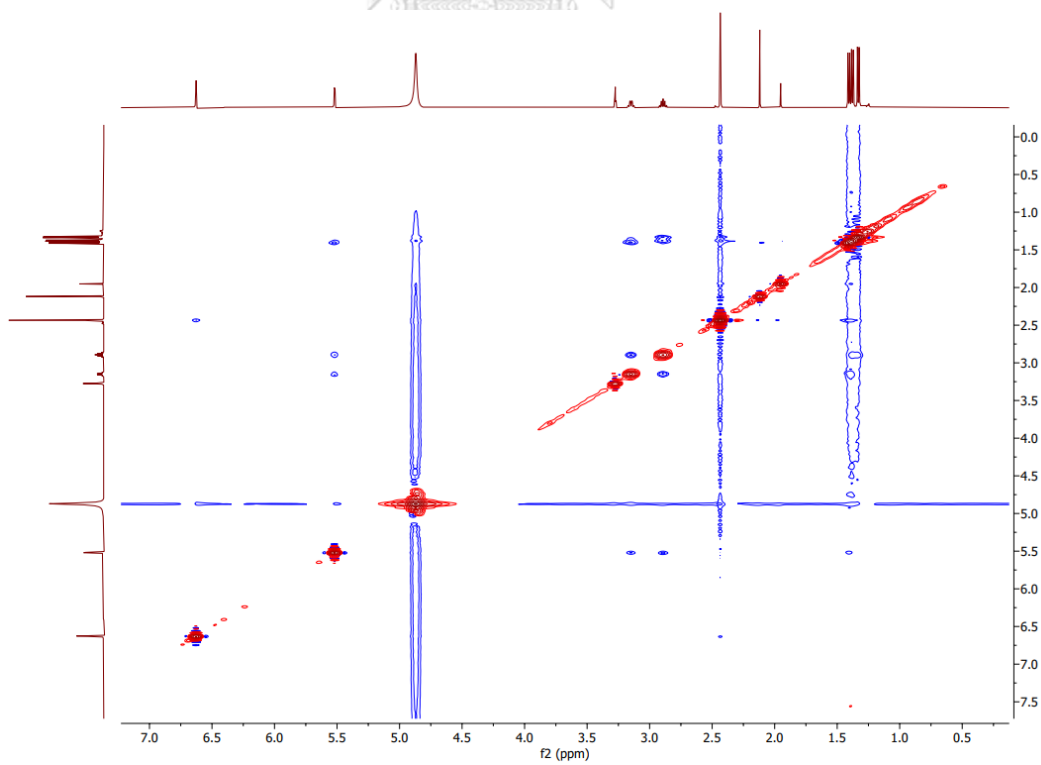


Figure A7. HRESIMS spectrum of compound **12**



Figure A8. ¹H NMR spectrum (500 MHz, methanol-*d*₄) of compound **13**Figure A9. ¹³C NMR spectrum (125 MHz, methanol-*d*₄) of compound **13**

Figure A10. ^1H - ^1H COSY spectrum of compound **13**Figure A11. HSQC spectrum of compound **13**

Figure A12. HMBC spectrum of compound **13**Figure A13. NOESY spectrum of compound **13**

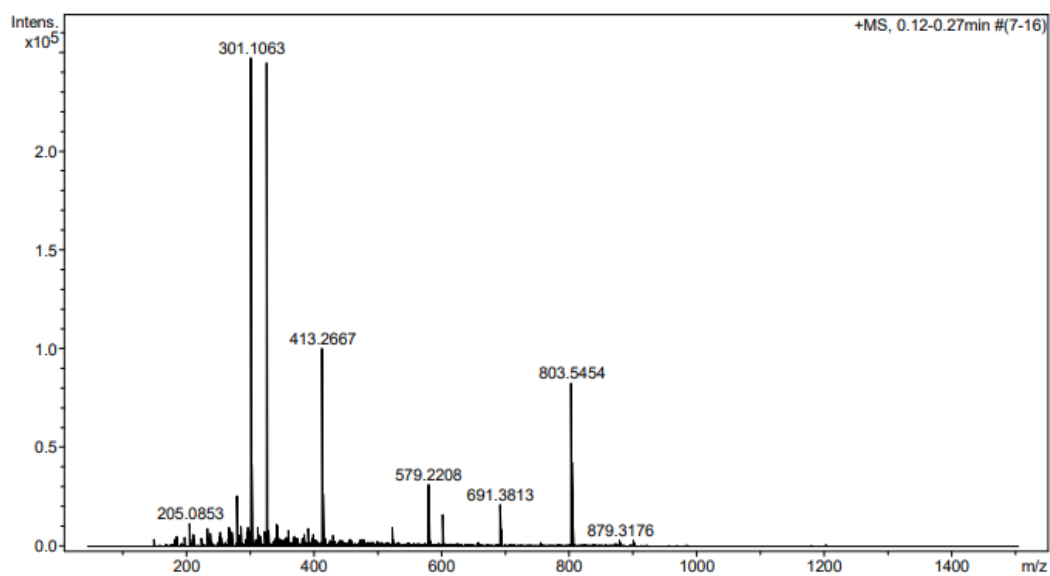
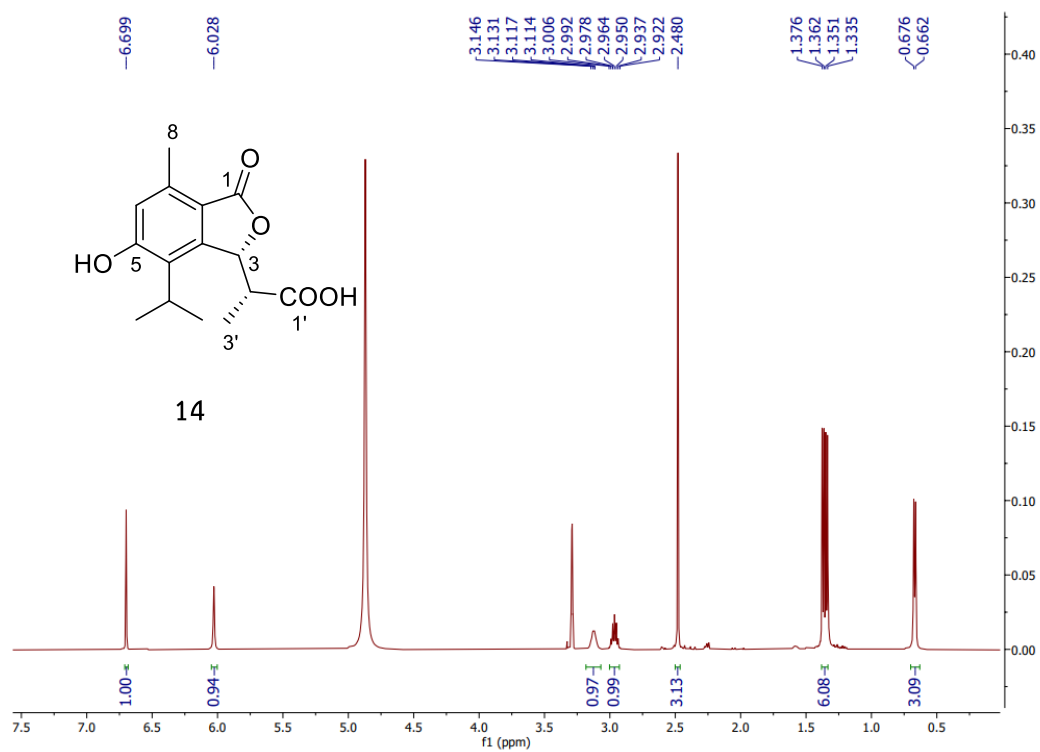
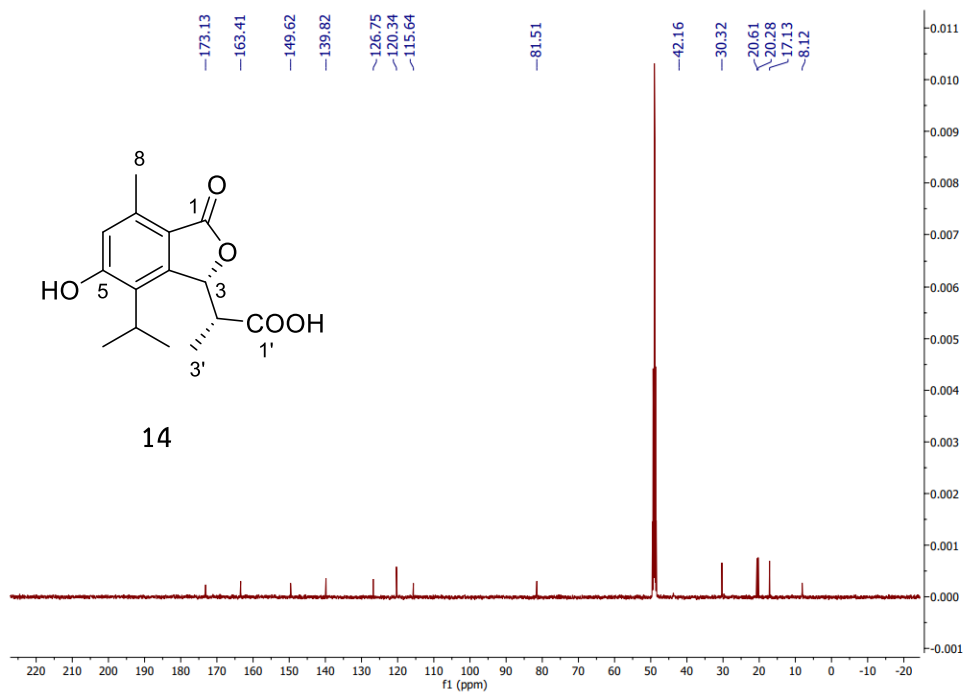
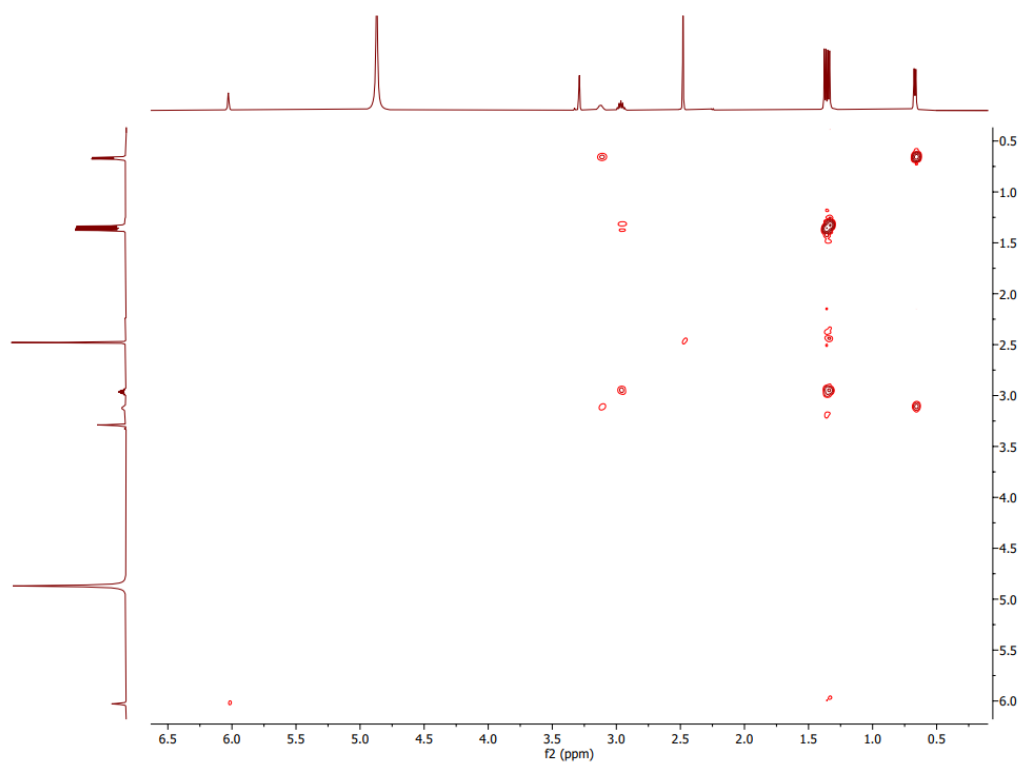
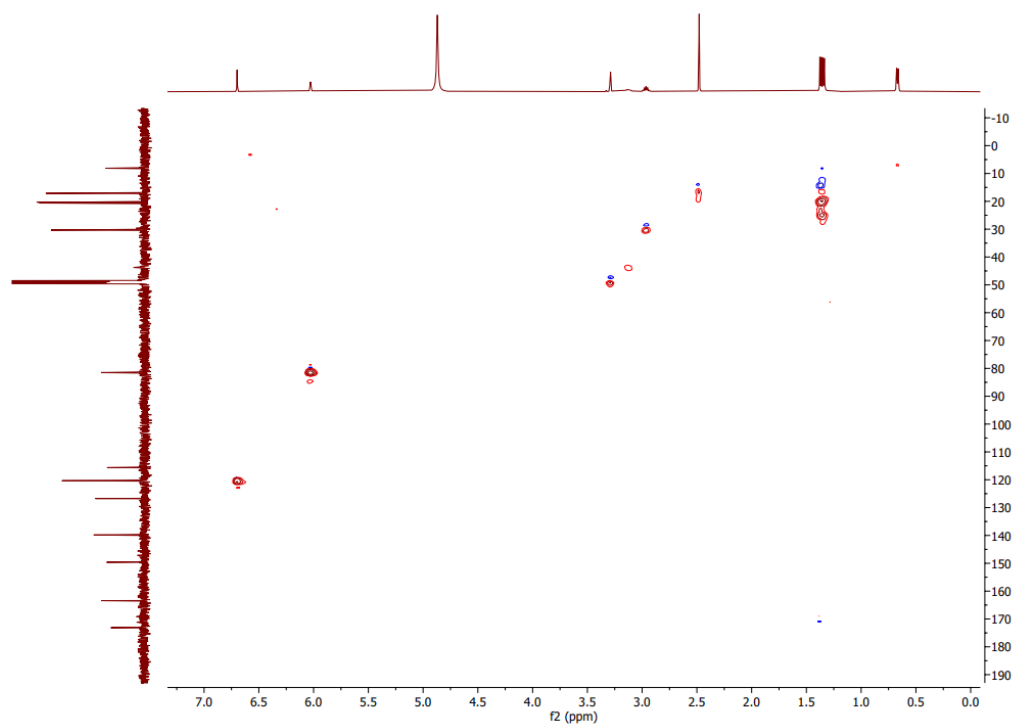
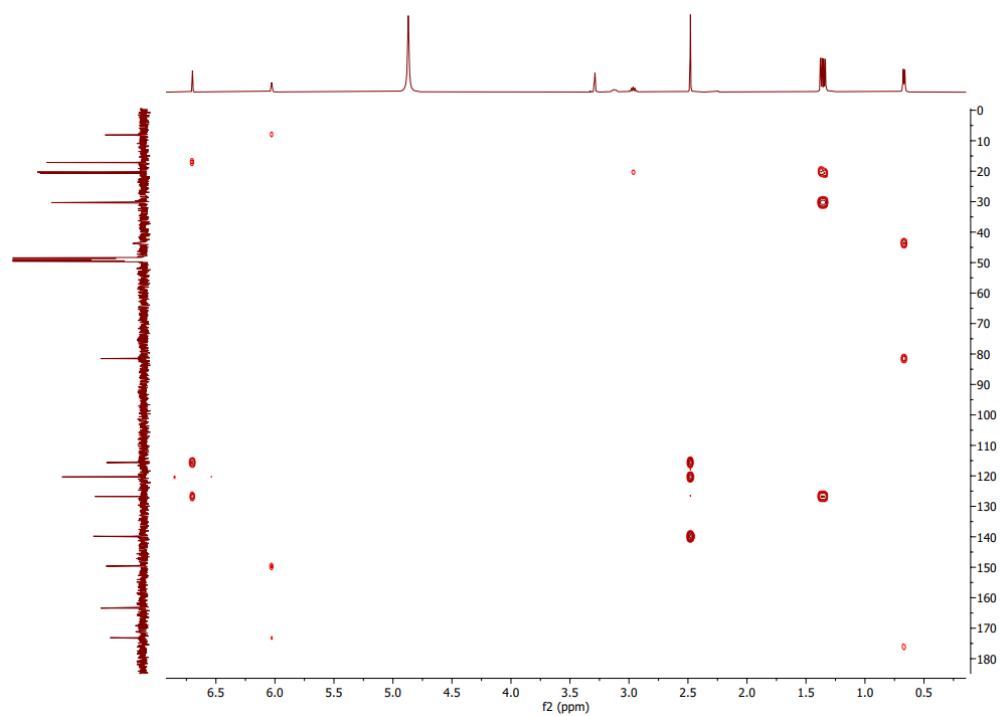
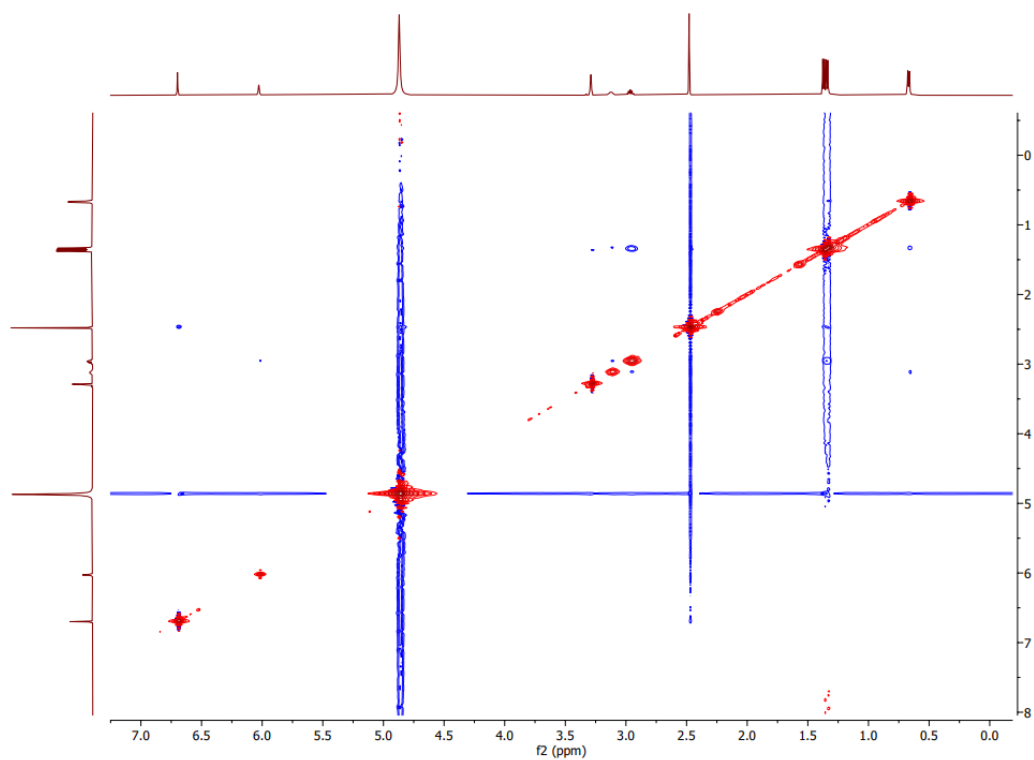


Figure A14. HRESIMS spectrum of compound **13** in methanol



Figure A15. ^1H NMR spectrum (500 MHz, methanol- d_4) of compound **14**Figure A16. ^{13}C NMR spectrum (125 MHz, methanol- d_4) of compound **14**

Figure A17. ^1H - ^1H COSY spectrum of compound **14**Figure A18. HSQC spectrum of compound **14**

Figure A19. HMBC spectrum of compound **14**Figure A20. NOESY spectrum of compound **14**

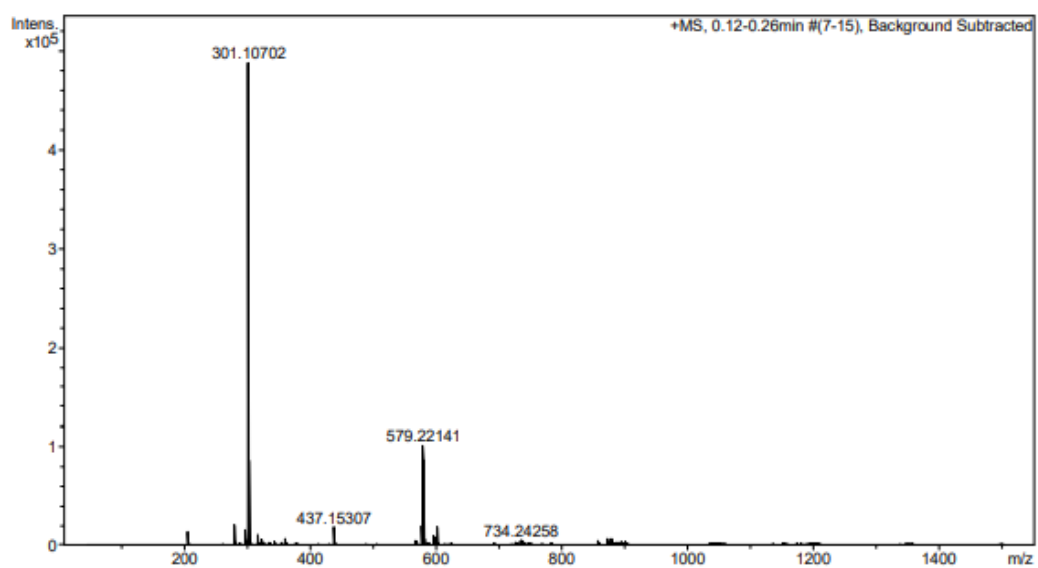
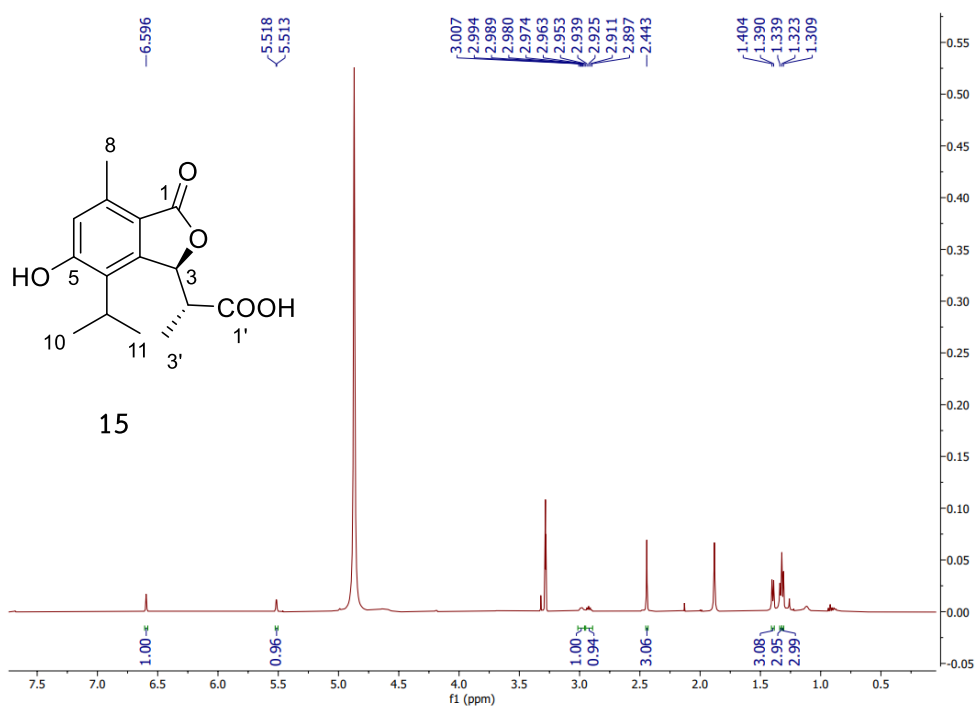
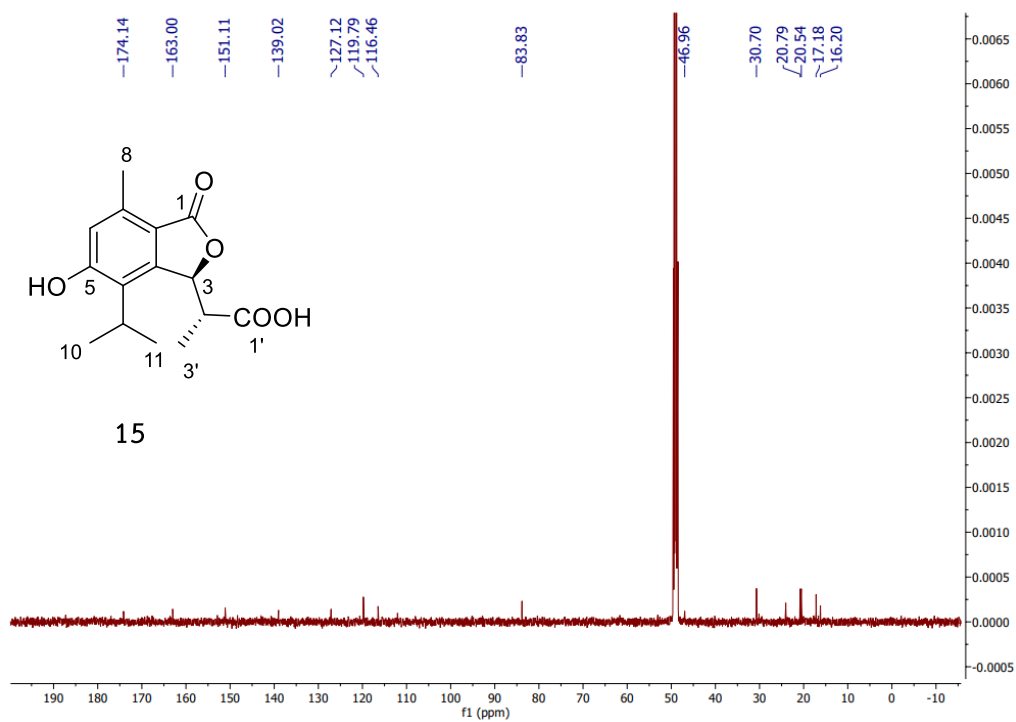
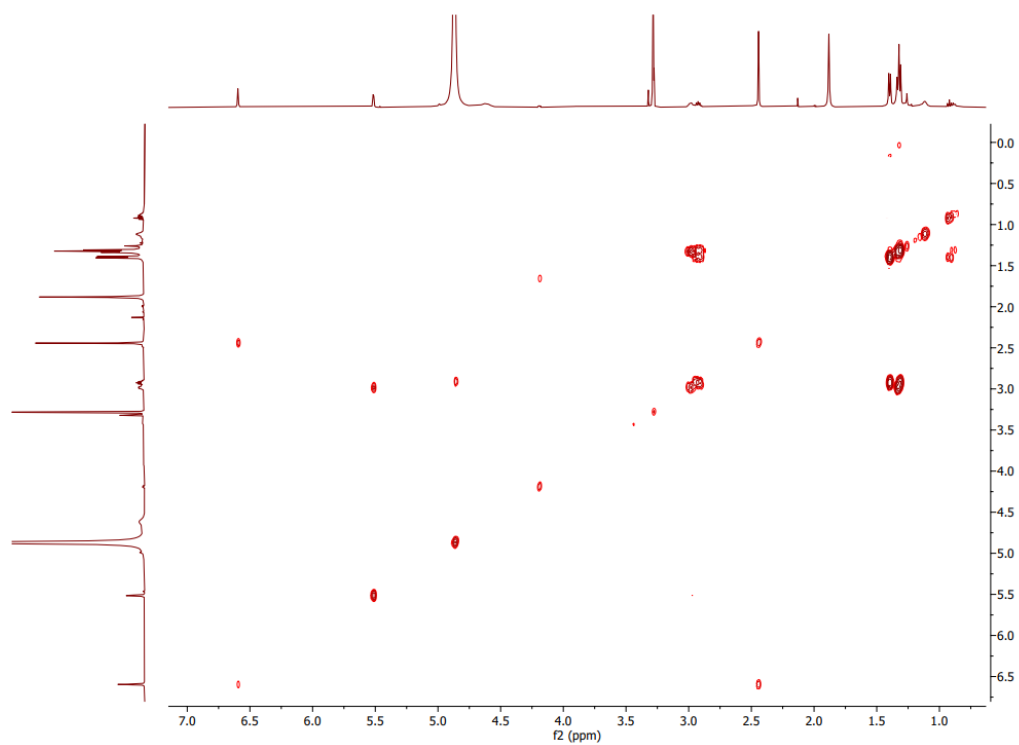
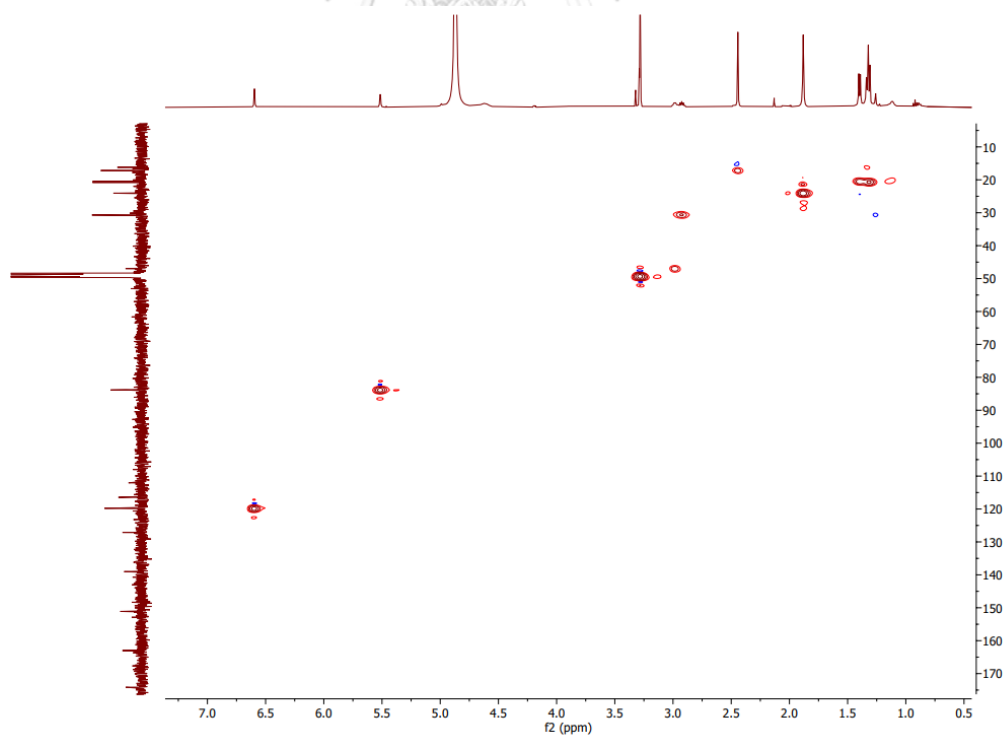
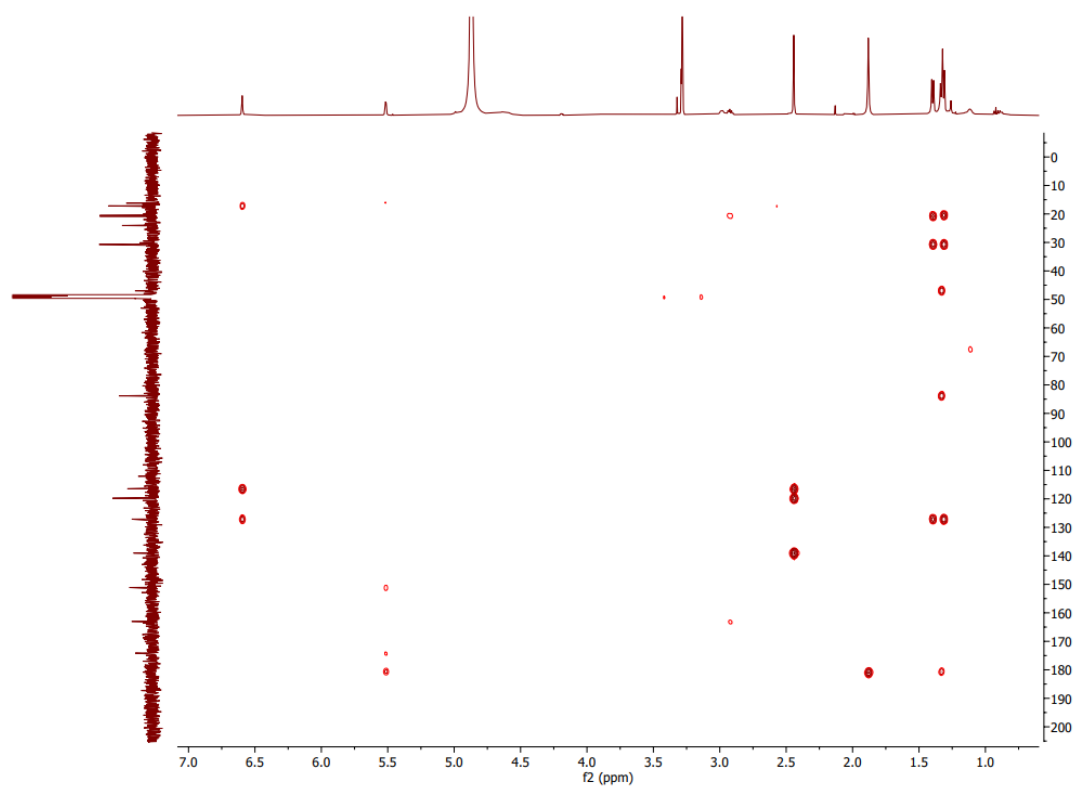
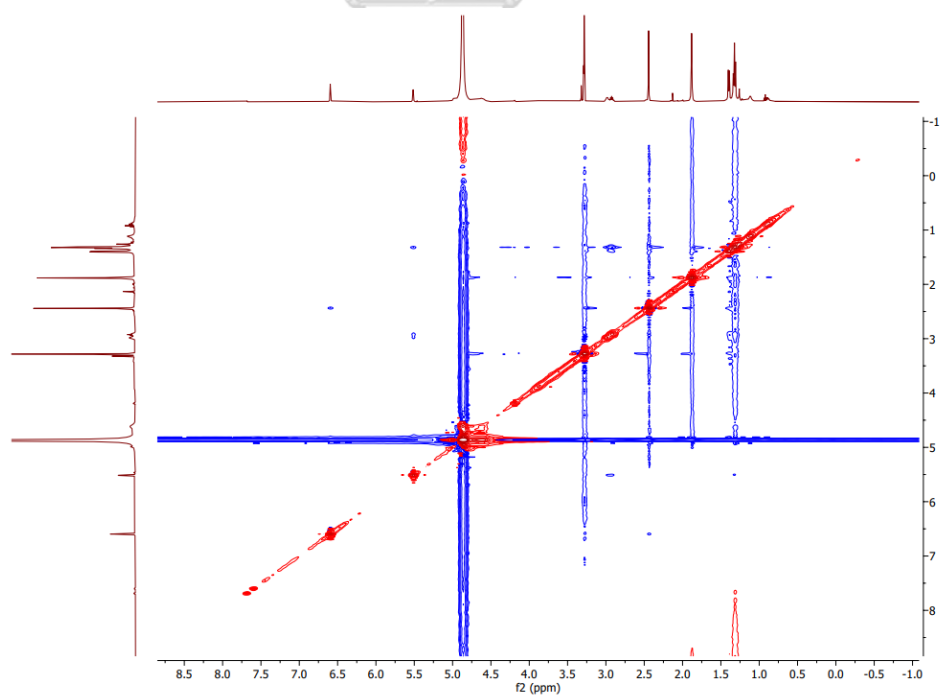


Figure A21. HRESIMS spectrum of compound 14



Figure A22. ^1H NMR spectrum (500 MHz, methanol- d_4) of compound **15**Figure A23. ^{13}C NMR spectrum (125 MHz, methanol- d_4) of compound **15**

Figure A24. ^1H - ^1H COSY spectrum of compound **15**Figure A25. HSQC spectrum of compound **15**

Figure A26. HMBC spectrum of compound **15**Figure A27. NOESY spectrum of compound **15**

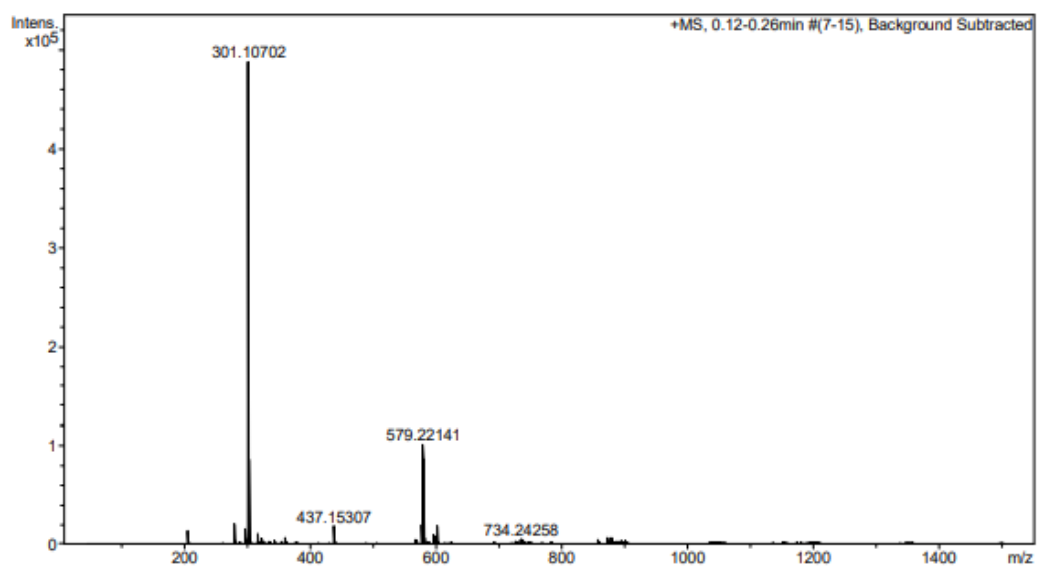
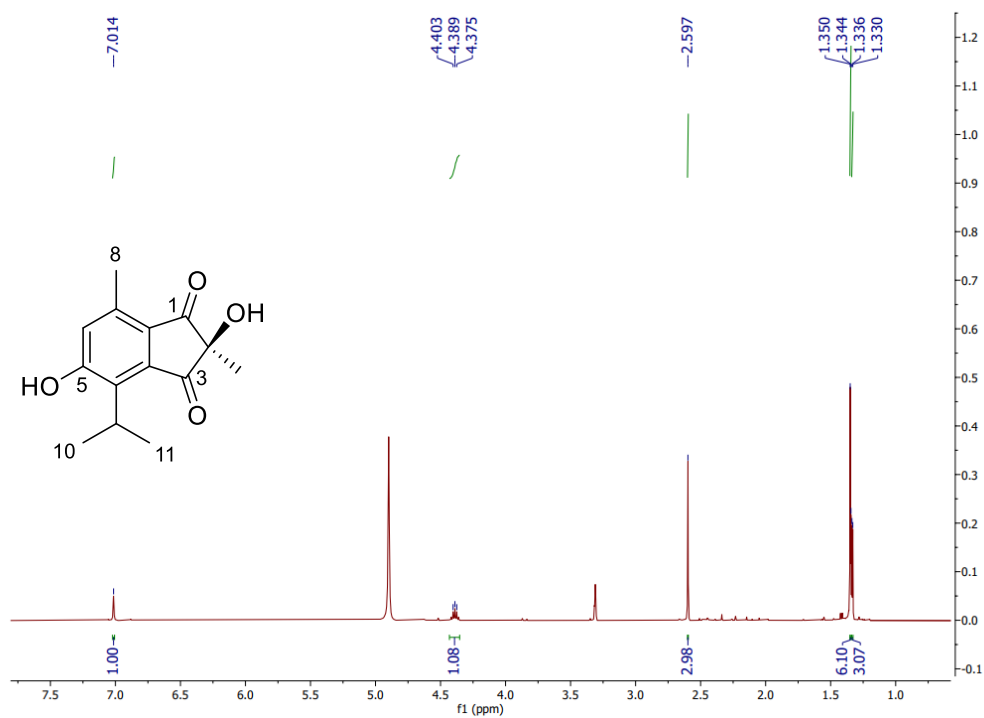
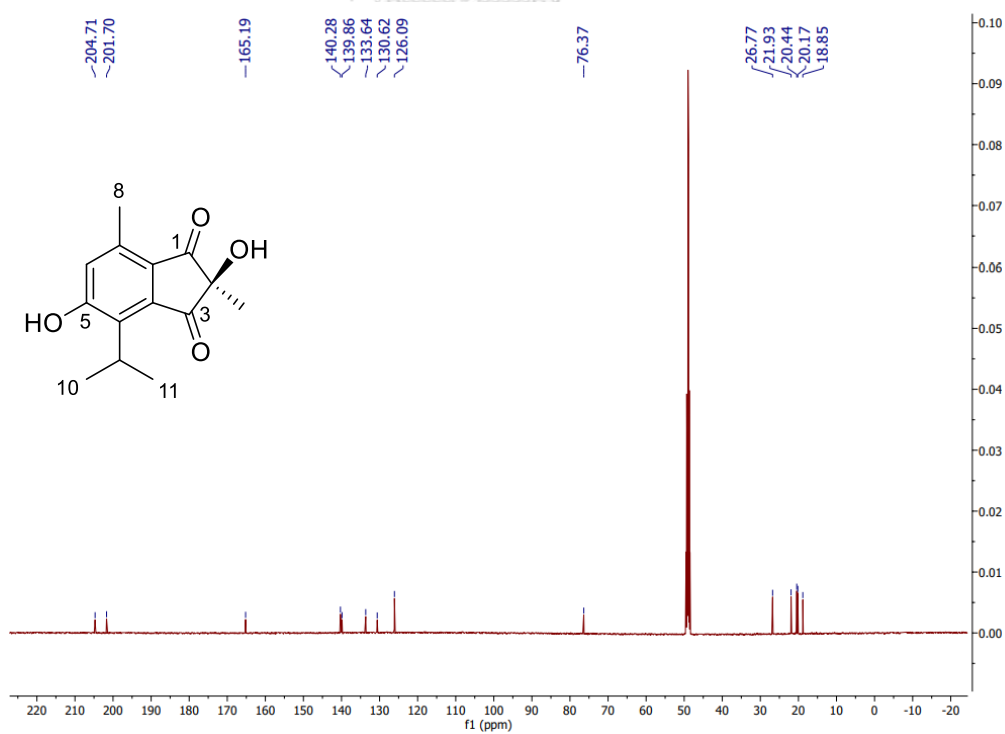
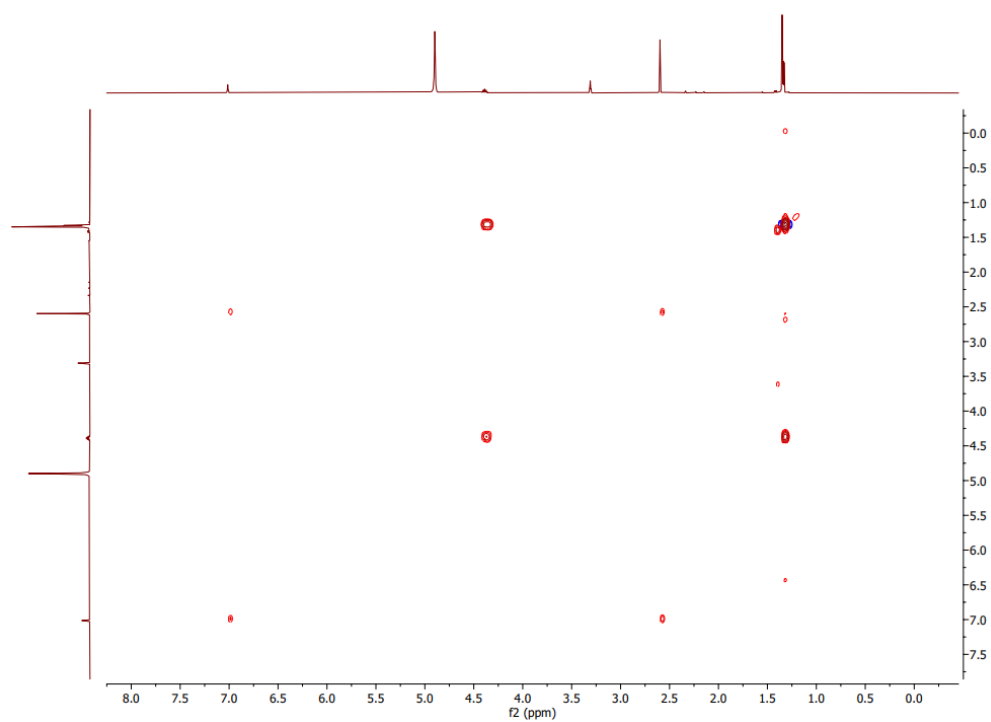
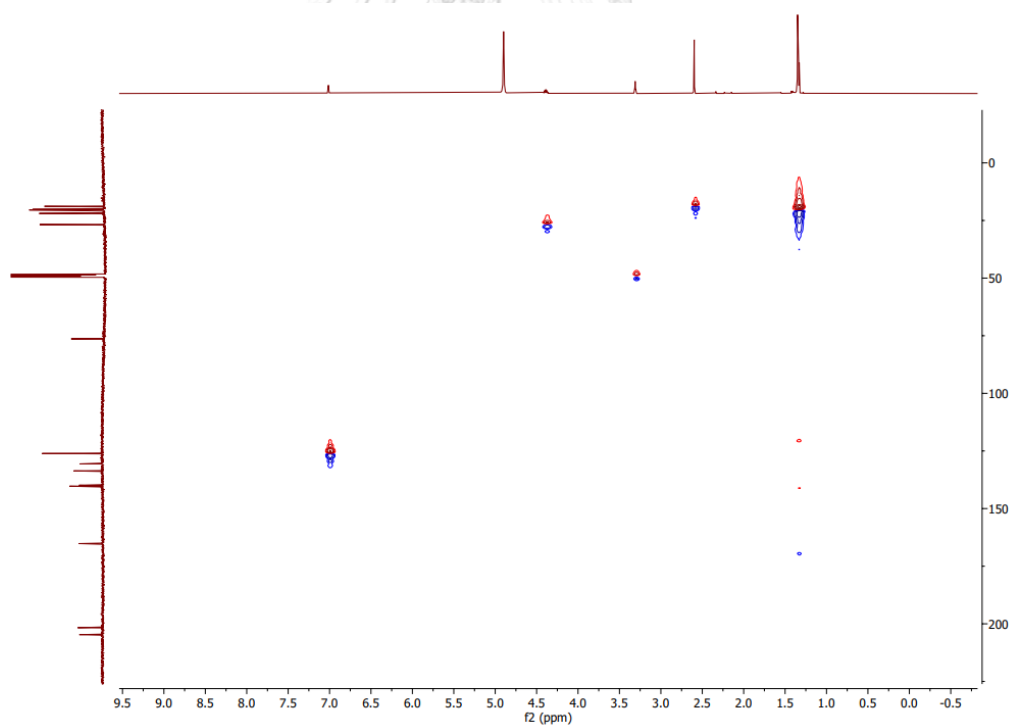
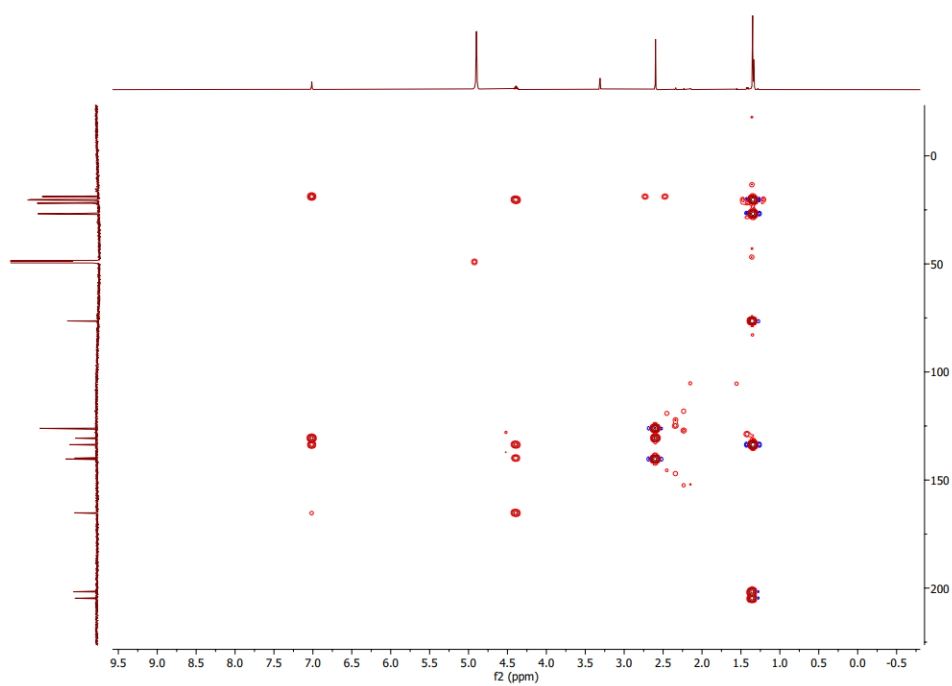
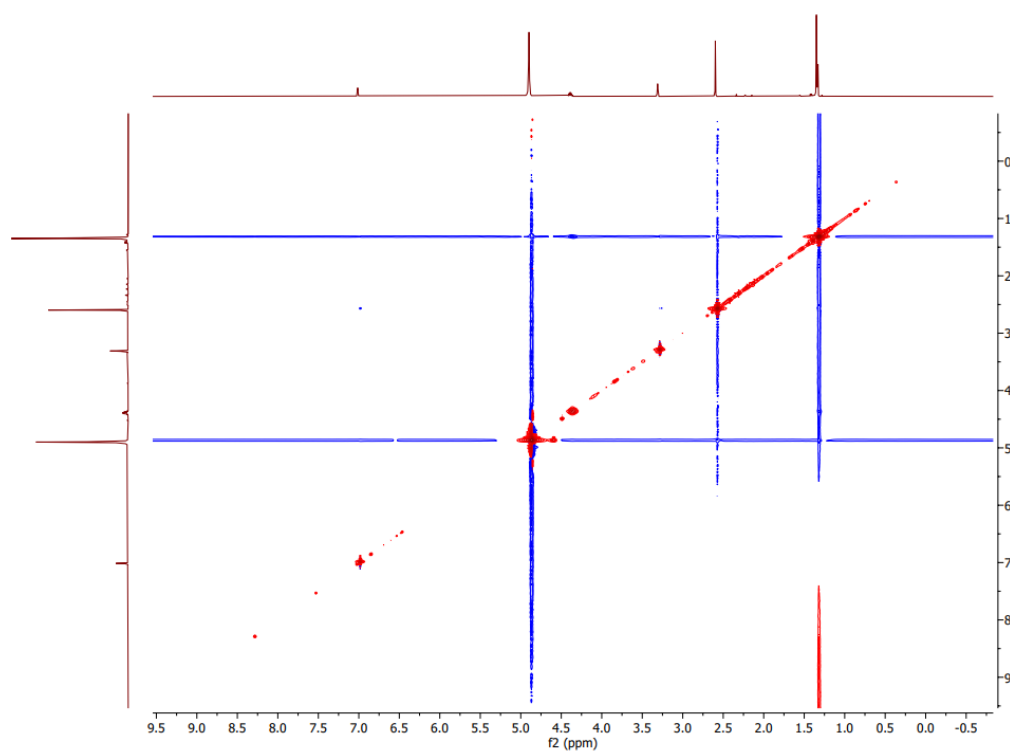


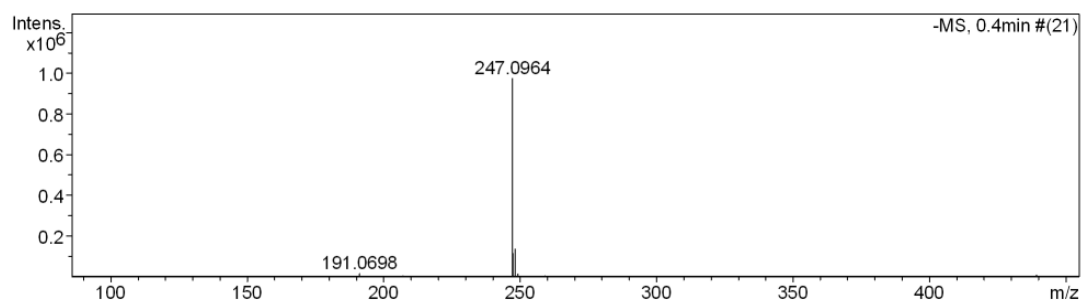
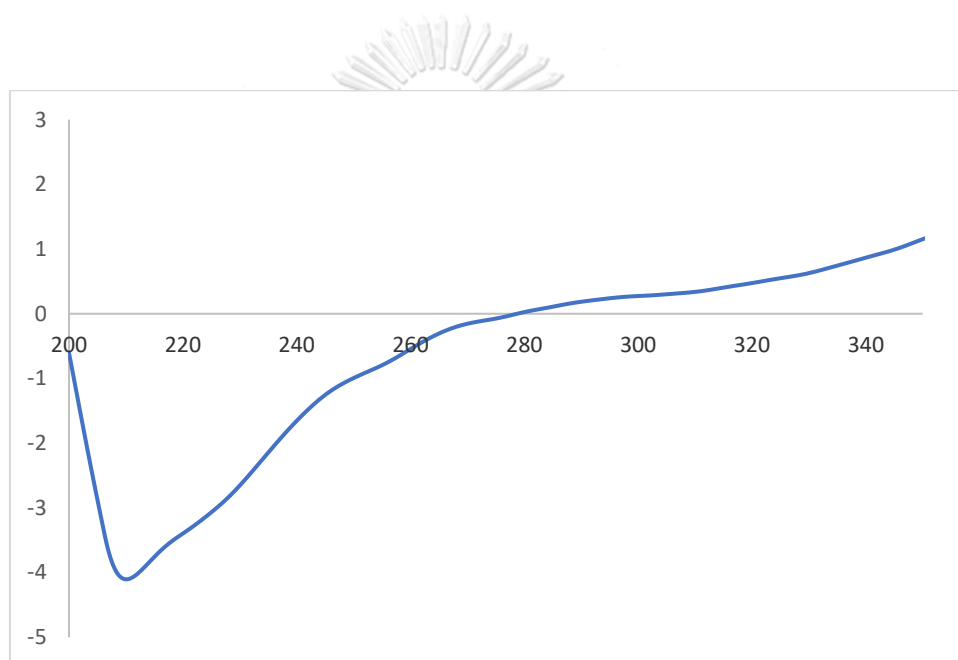
Figure A28. HRESIMS spectrum of compound **15**



Figure A29. ¹H NMR spectrum (500 MHz, methanol-*d*₄) of compound **16**Figure A30. ¹³C NMR spectrum (125 MHz, methanol-*d*₄) of compound **16**

Figure A31. ^1H - ^1H COSY spectrum of compound **16**Figure A32. HSQC spectrum of compound **16**

Figure A33. HMBC spectrum of compound **16**Figure A34. NOESY spectrum of compound **16**

Figure A35. HRESIMS spectrum of compound **16** in methanolFigure A36. Experimental ECD spectrum of compound **16**

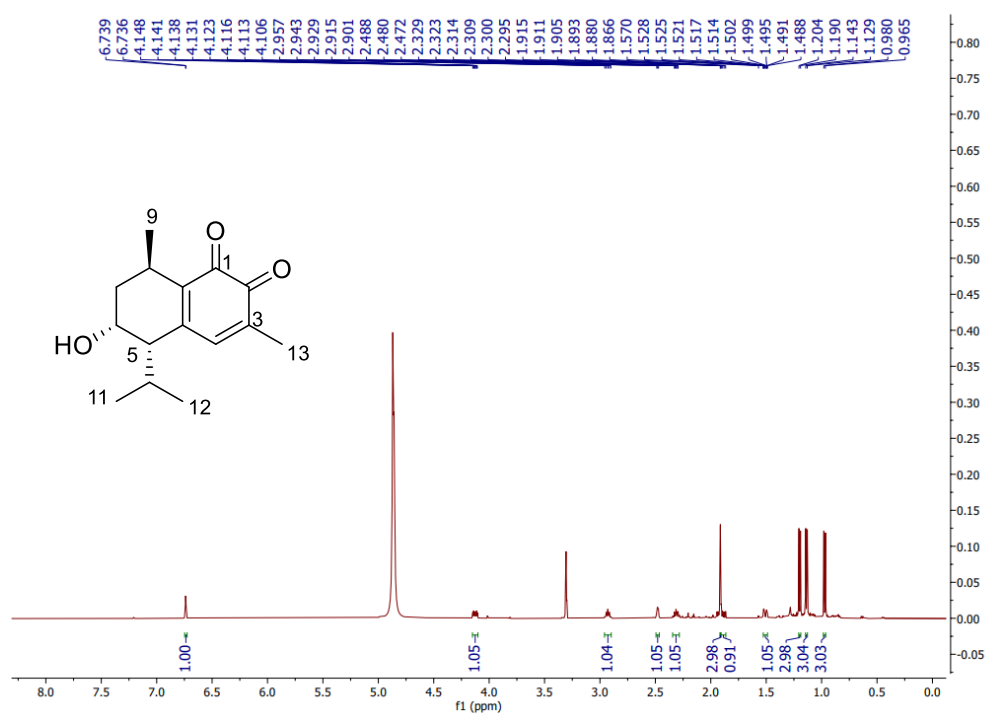


Figure A37. ^1H NMR spectrum (500 MHz, methanol- d_4) of compound 17

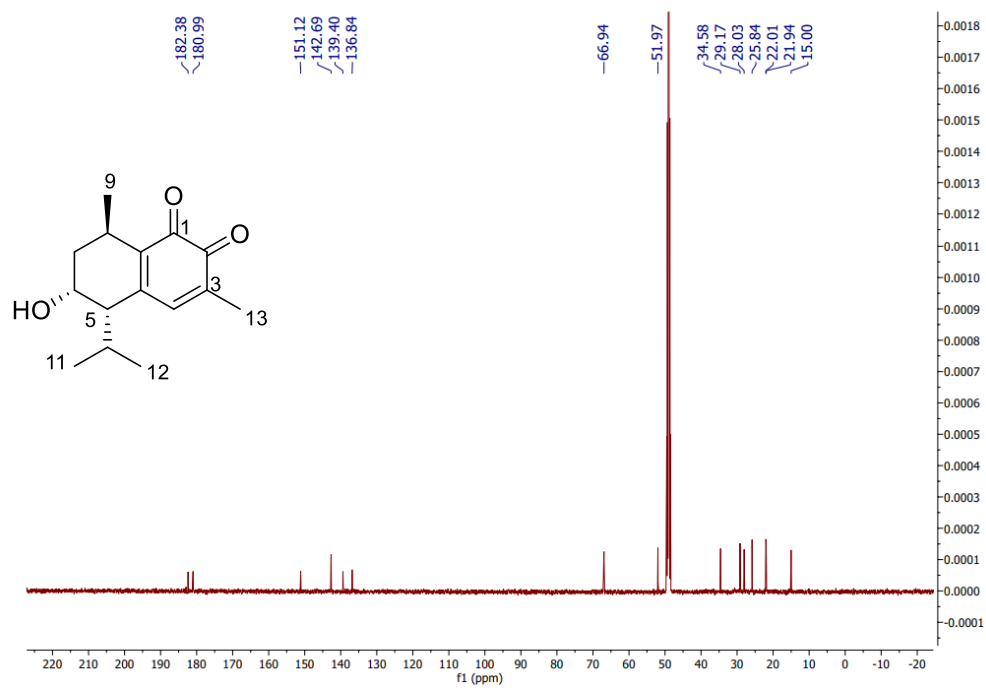
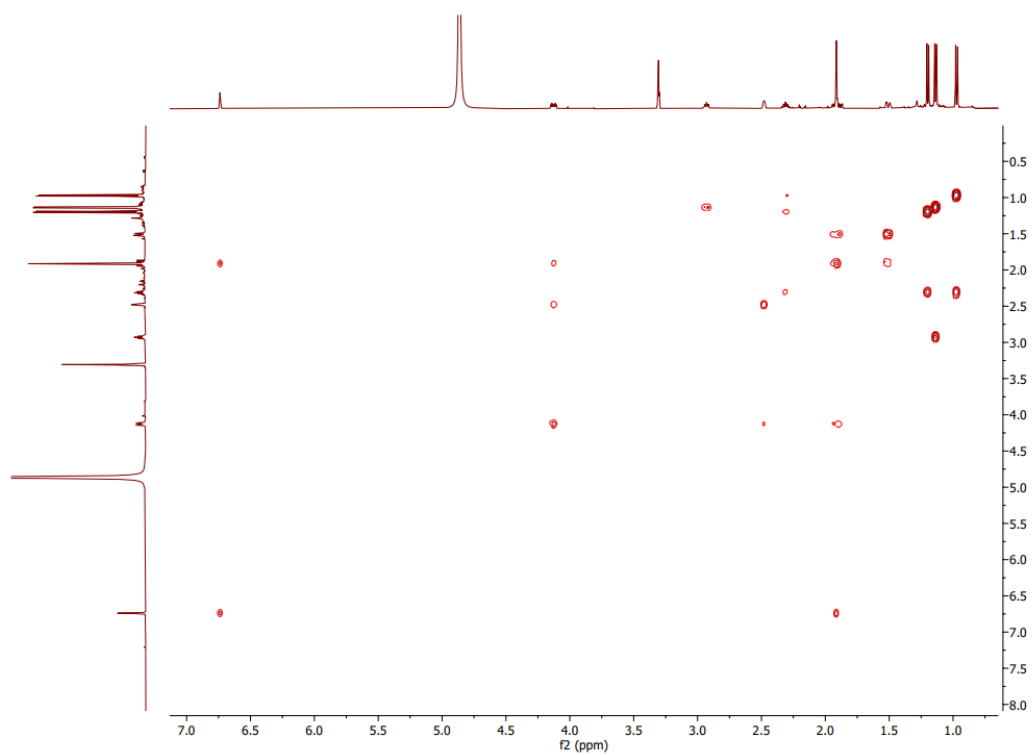
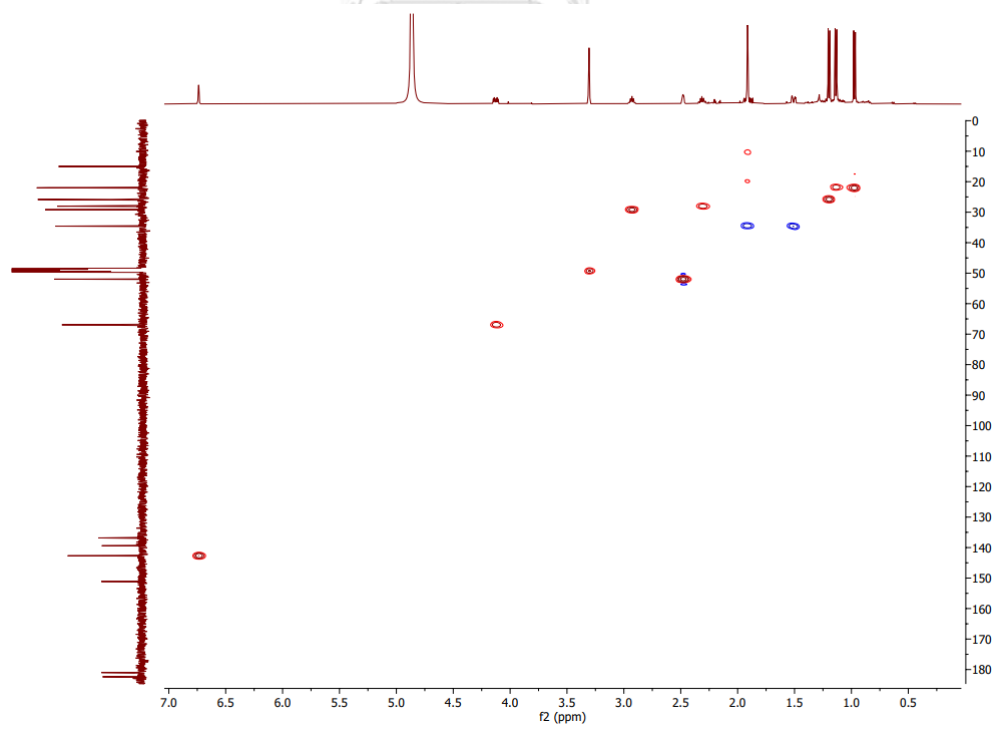
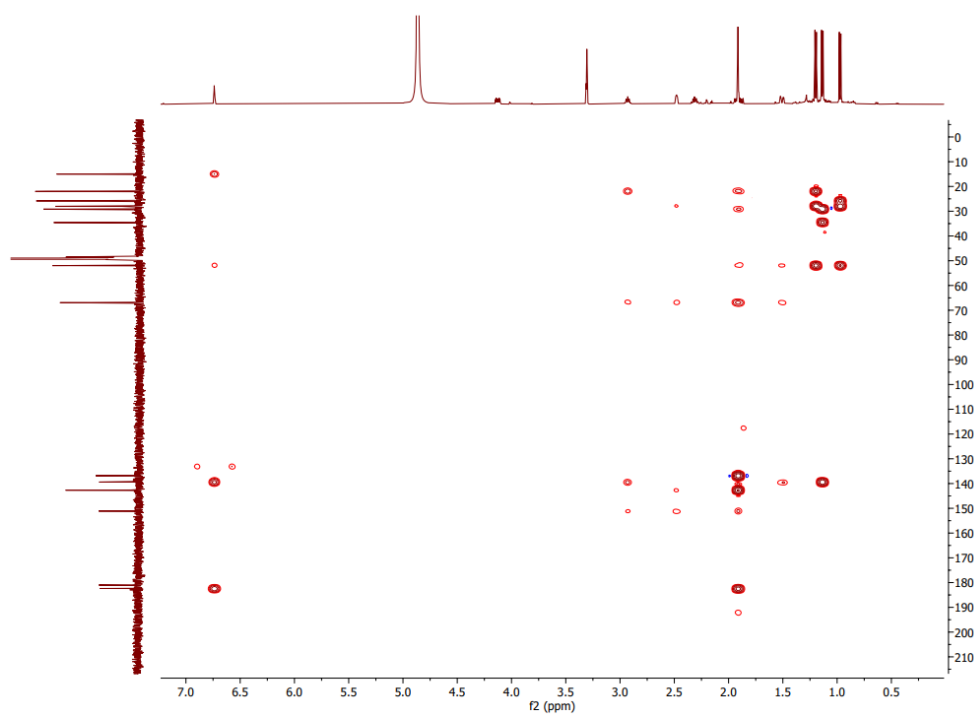
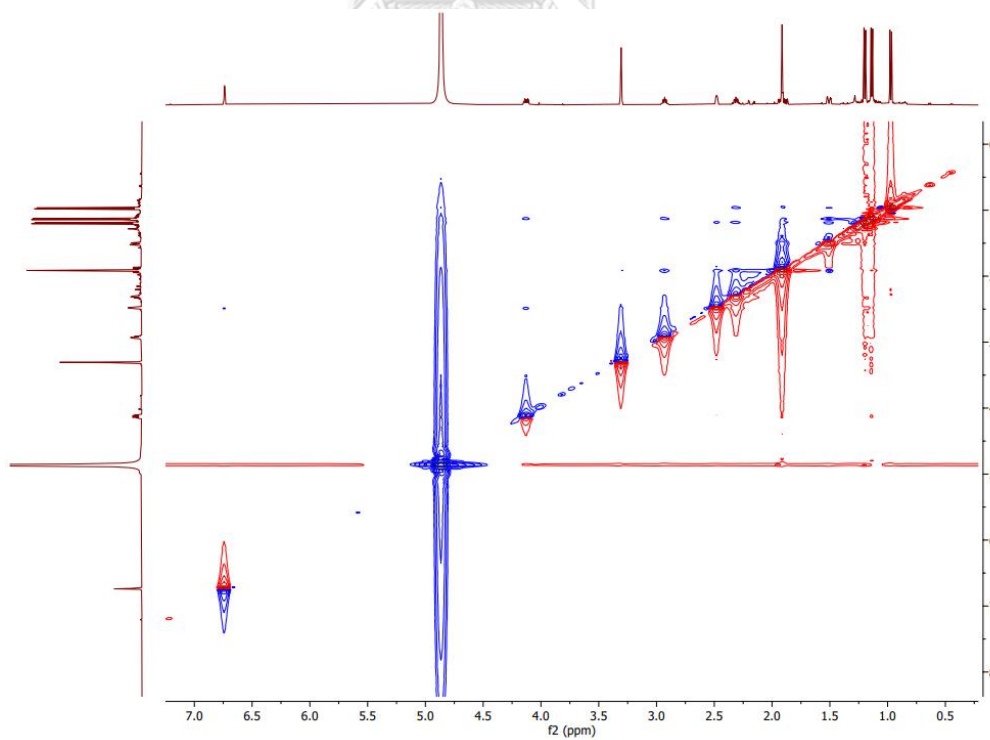


Figure A38. ^{13}C NMR spectrum (125 MHz, methanol- d_4) of compound 17

Figure A39. ^1H - ^1H COSY spectrum of compound **17**Figure A40. HSQC spectrum of compound **17**

Figure A41. HMBC spectrum of compound **17**Figure A42. NOESY spectrum of compound **17**

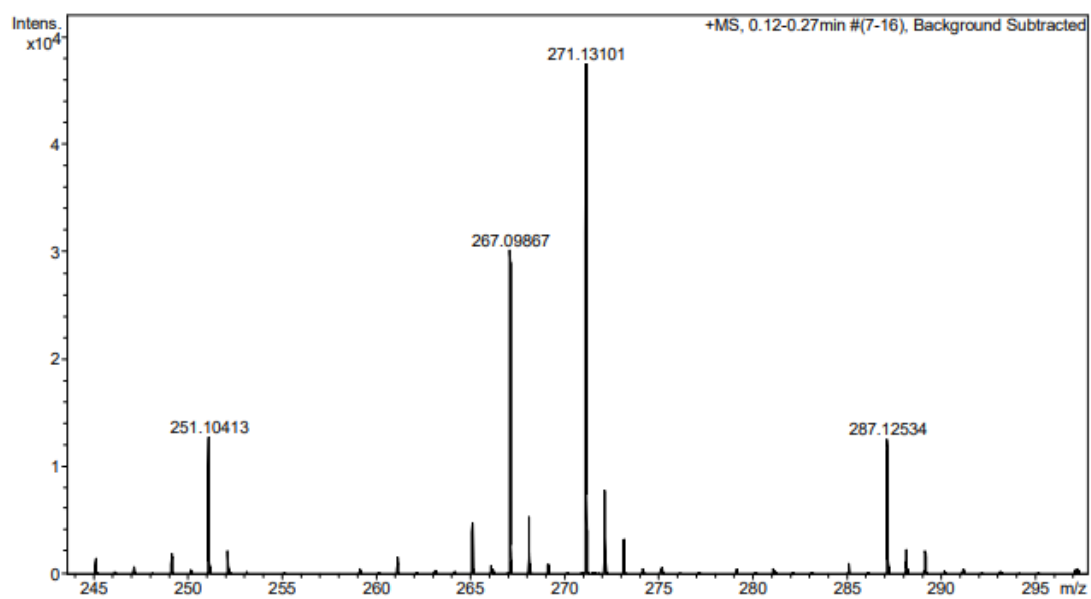


Figure A43. HRESIMS spectrum of compound **17** in methanol



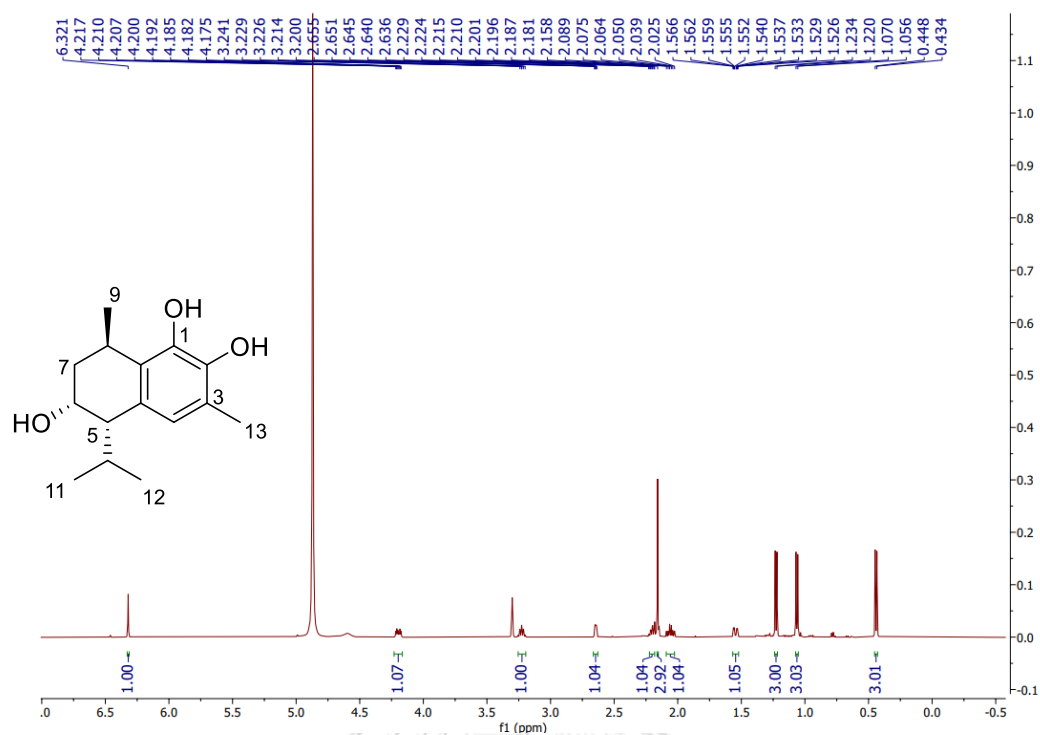


Figure A44. ^1H NMR spectrum (500 MHz, methanol- d_4) of compound **18**

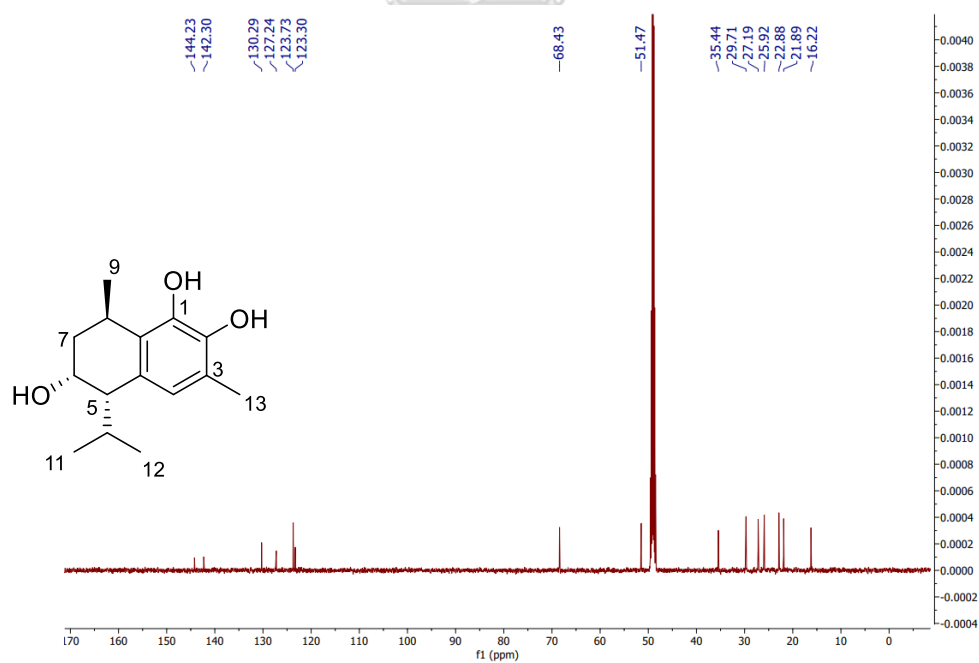
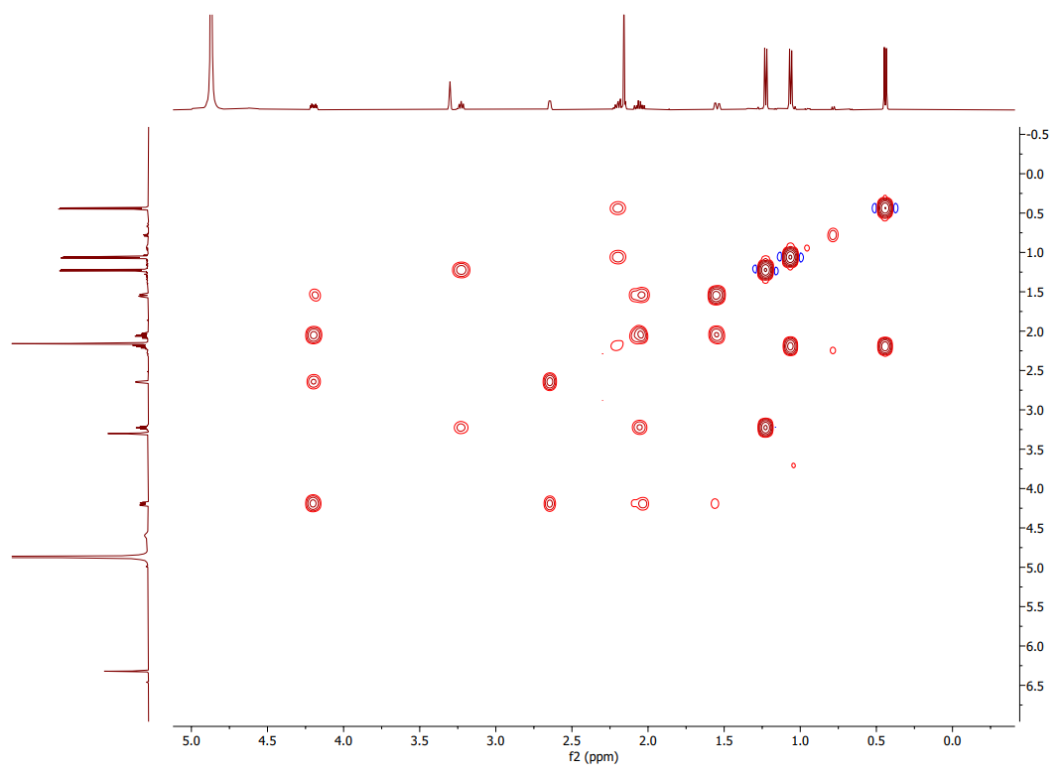
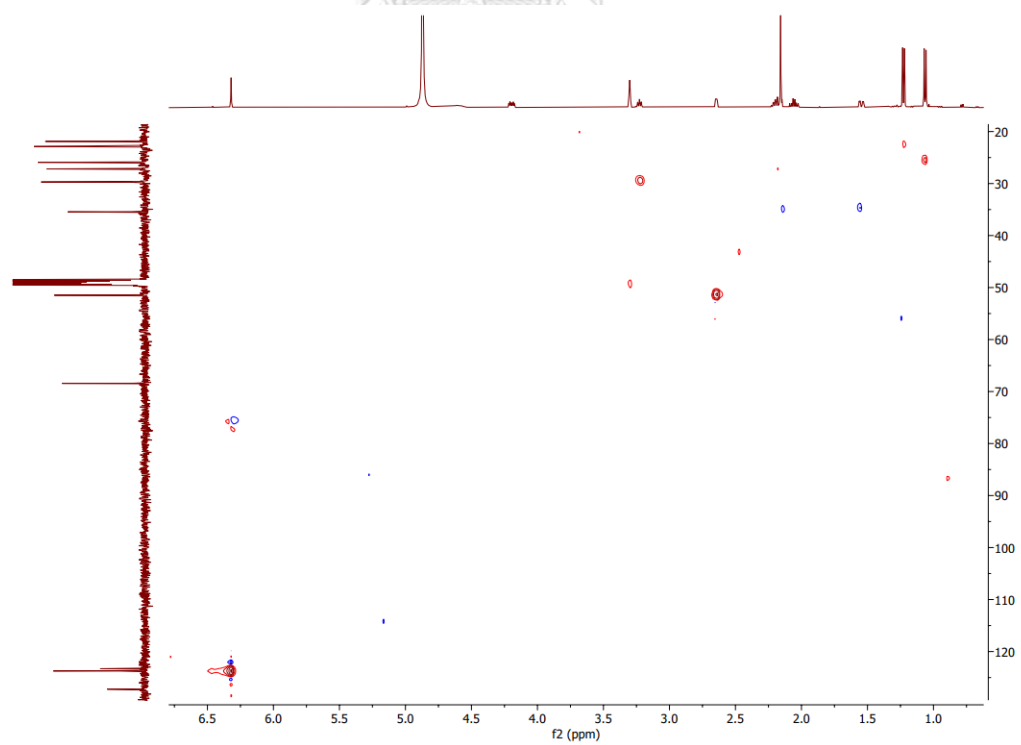
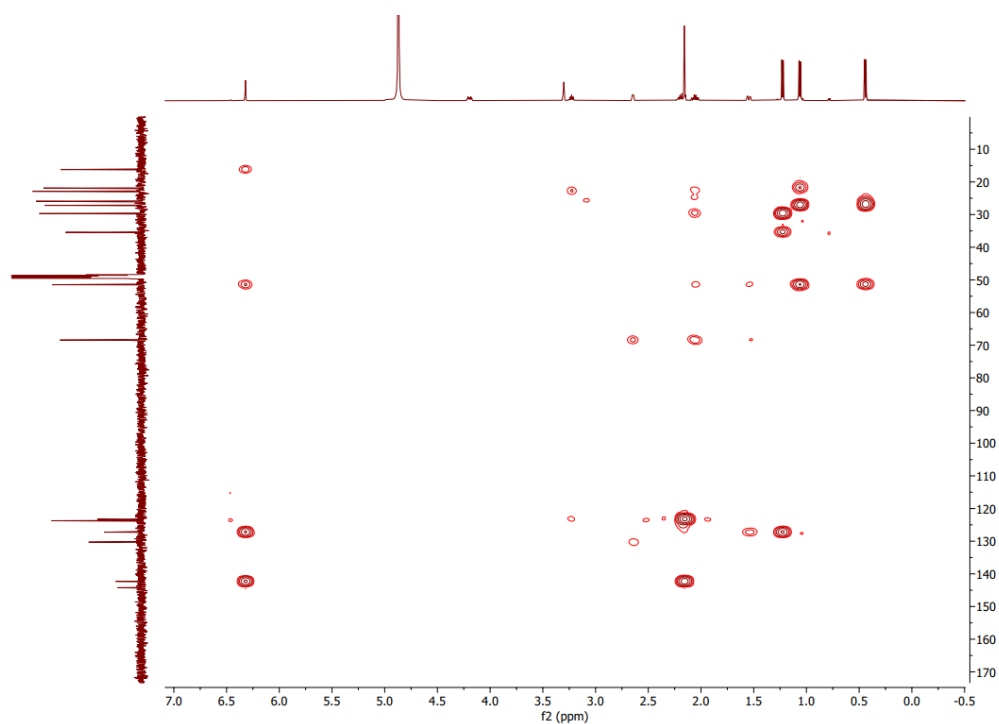
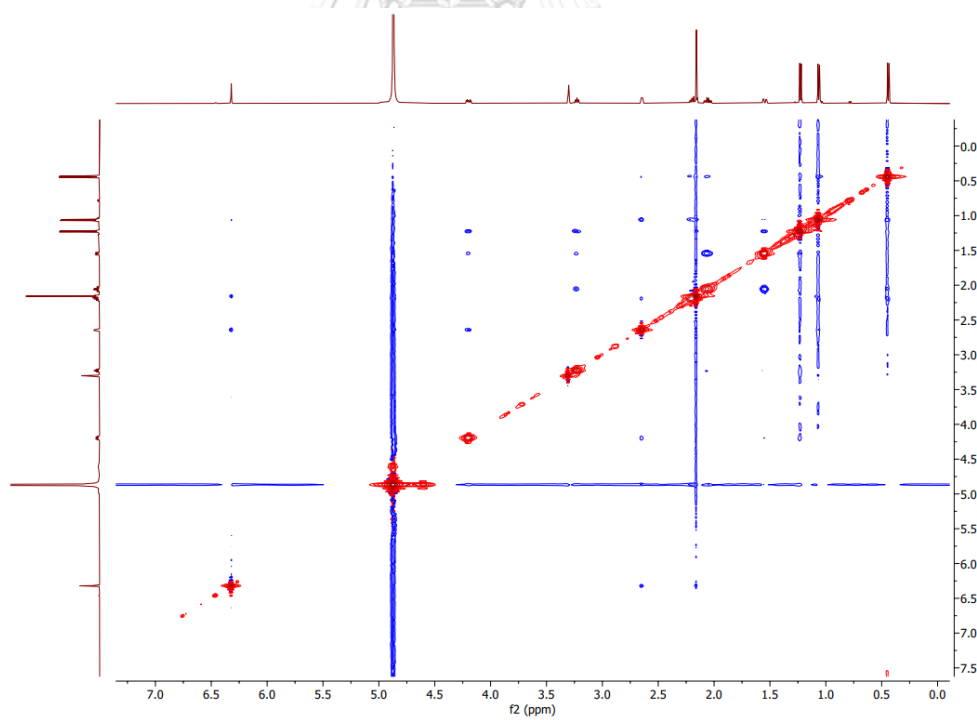


Figure A45. ^{13}C NMR spectrum (125 MHz, methanol- d_4) of compound **18**

Figure A46. ^1H - ^1H COSY spectrum of compound **18**Figure A47. HSQC spectrum of compound **18**

Figure A48. HMBC spectrum of compound **18**Figure A49. NOESY spectrum of compound **18**

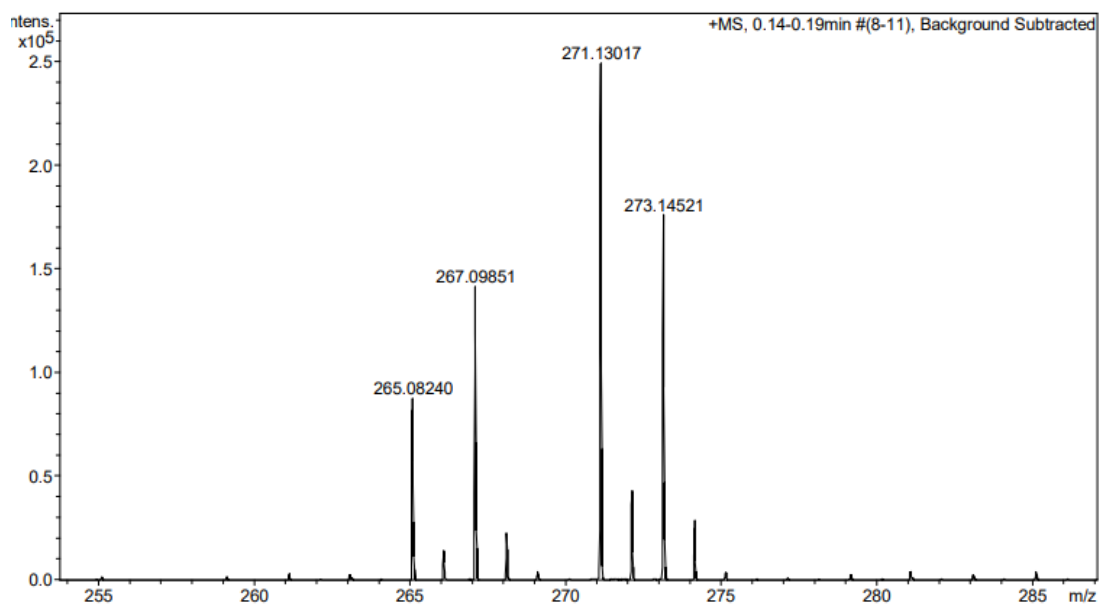
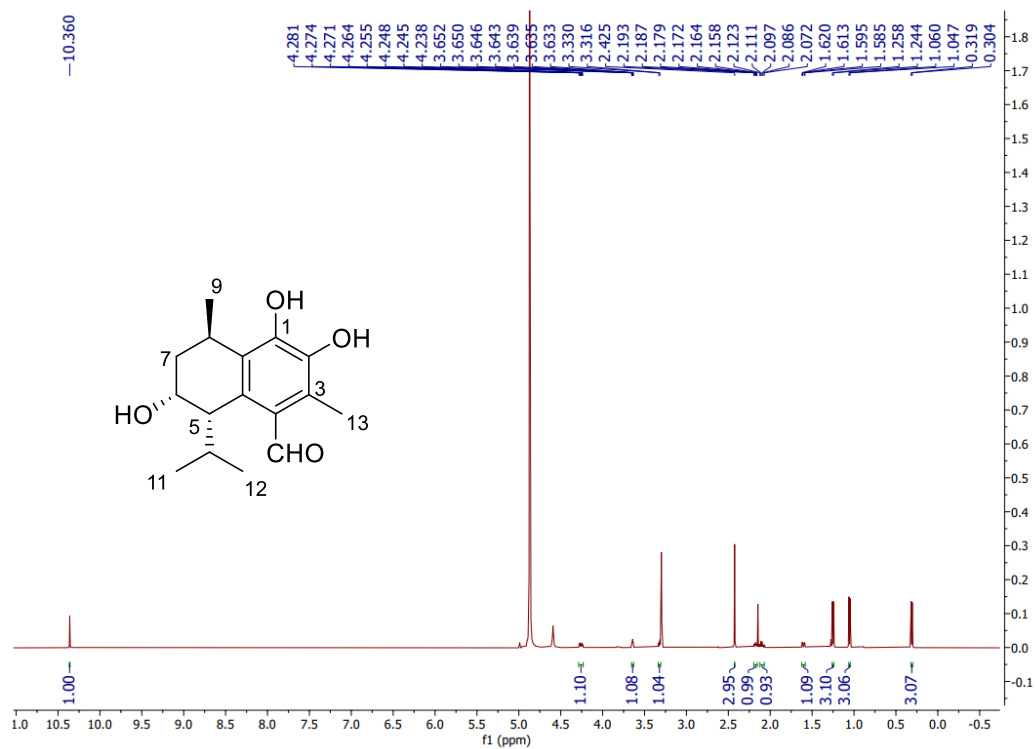
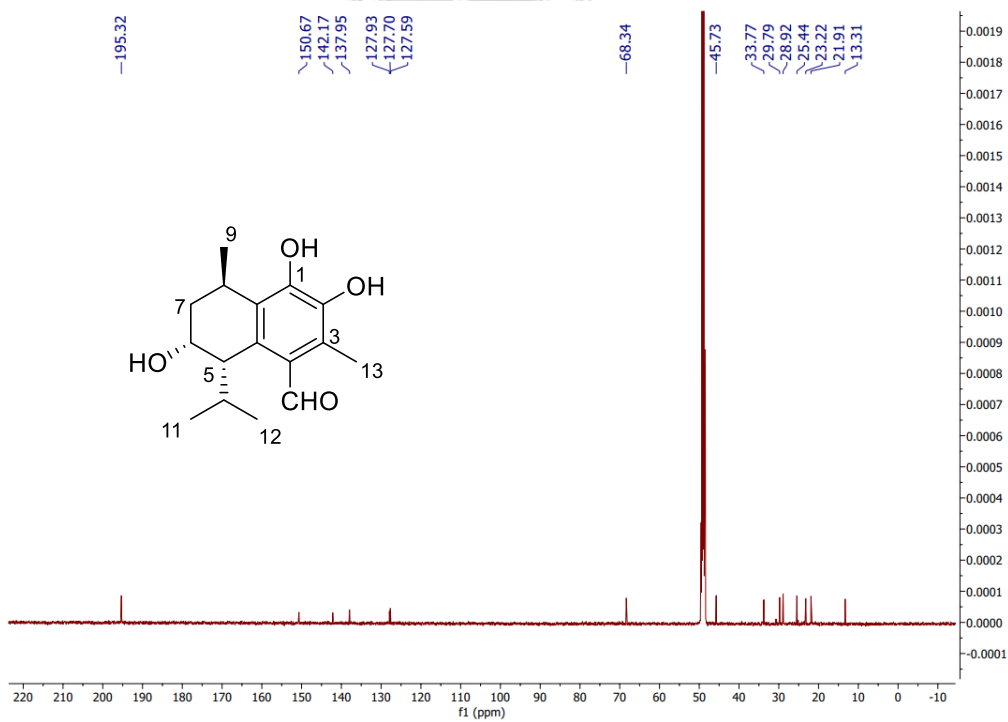


Figure A50. HRESIMS spectrum of compound **18**



Figure A51. ^1H NMR spectrum (500 MHz, methanol- d_4) of compound **19**Figure A52. ^{13}C NMR spectrum (125 MHz, methanol- d_4) of compound **19**

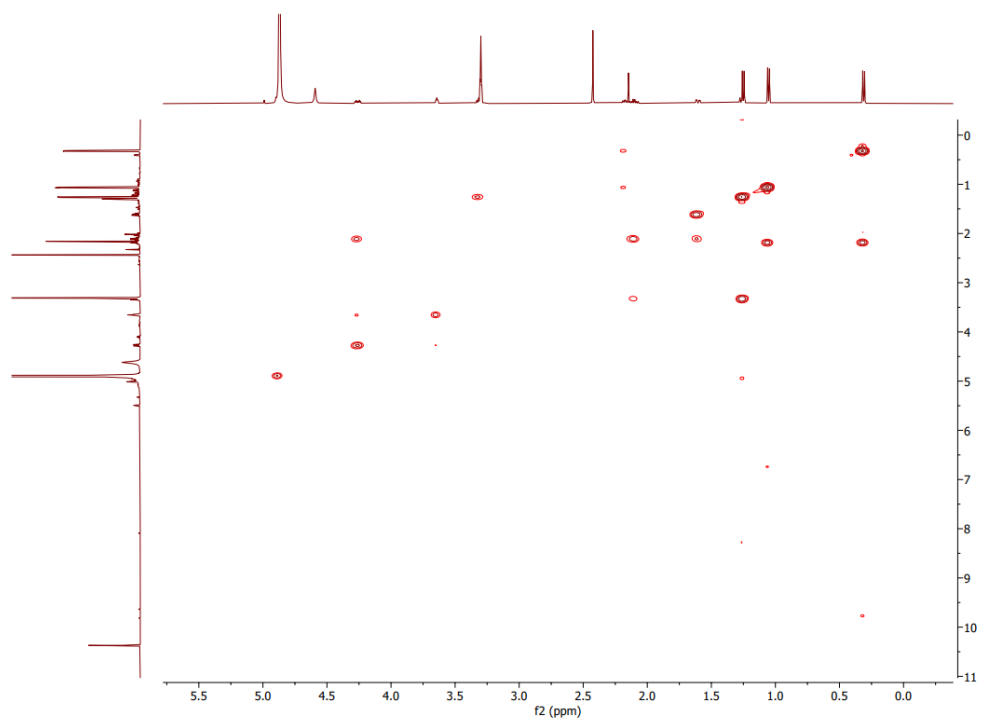
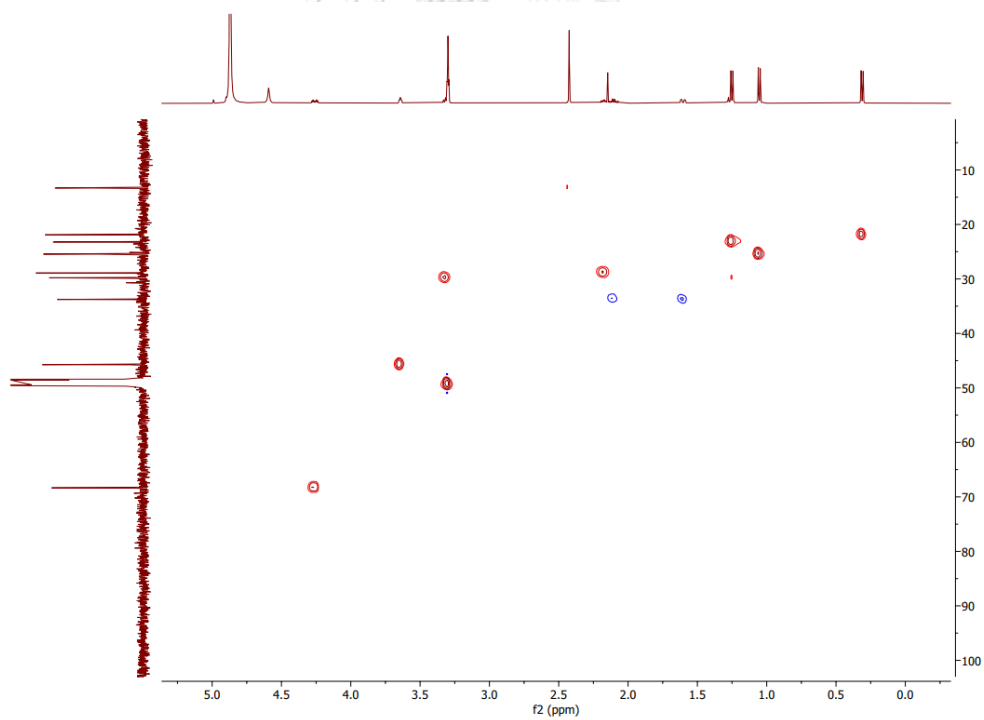
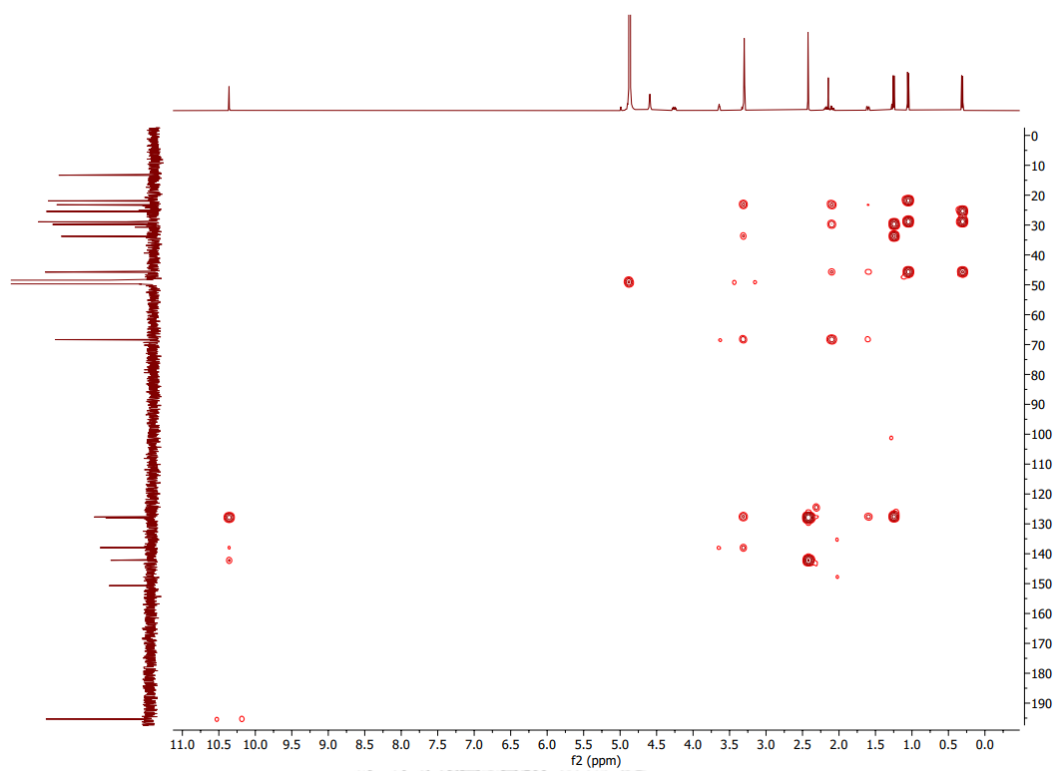
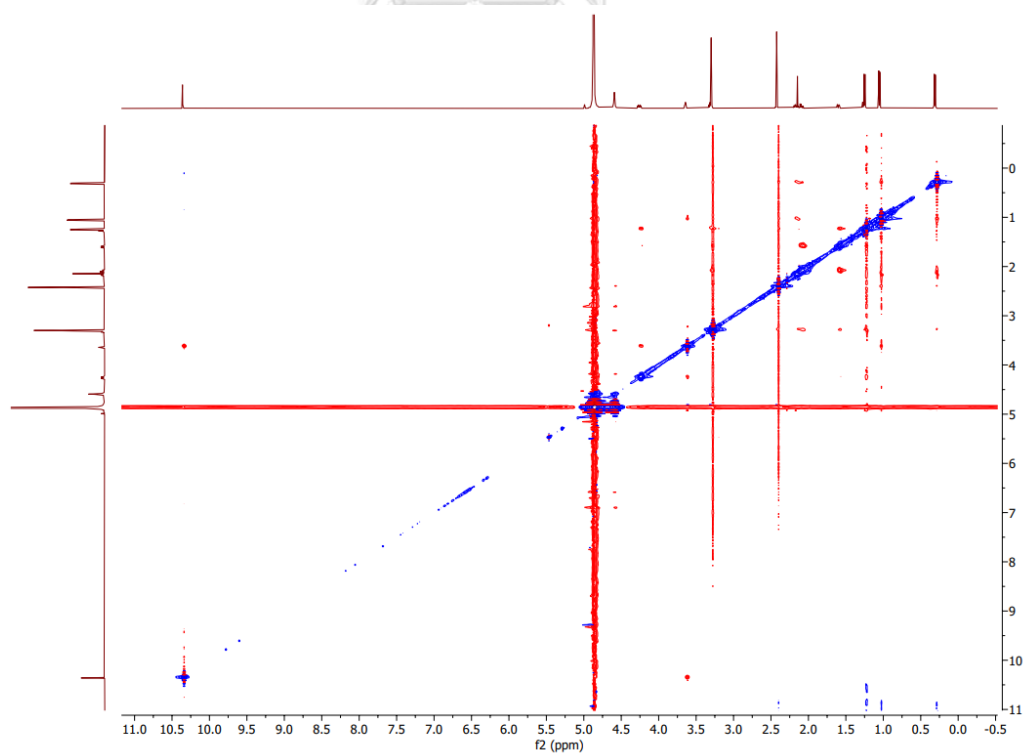
Figure A53. ^1H - ^1H COSY spectrum of compound 19

Figure A54. HSQC spectrum of compound 19

Figure A55. HMBC spectrum of compound **19**Figure A56. NOESY spectrum of compound **19**

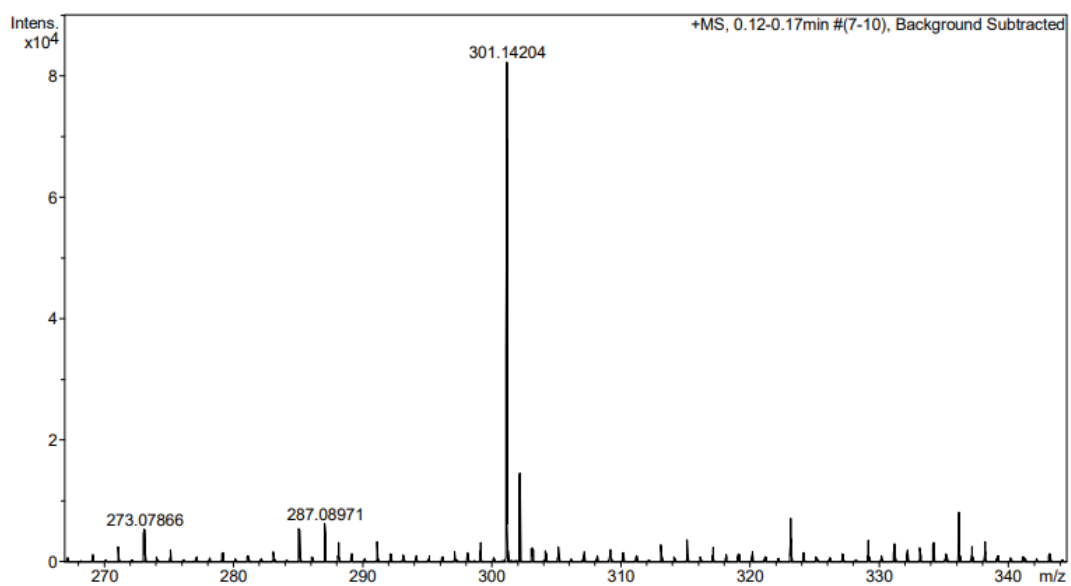
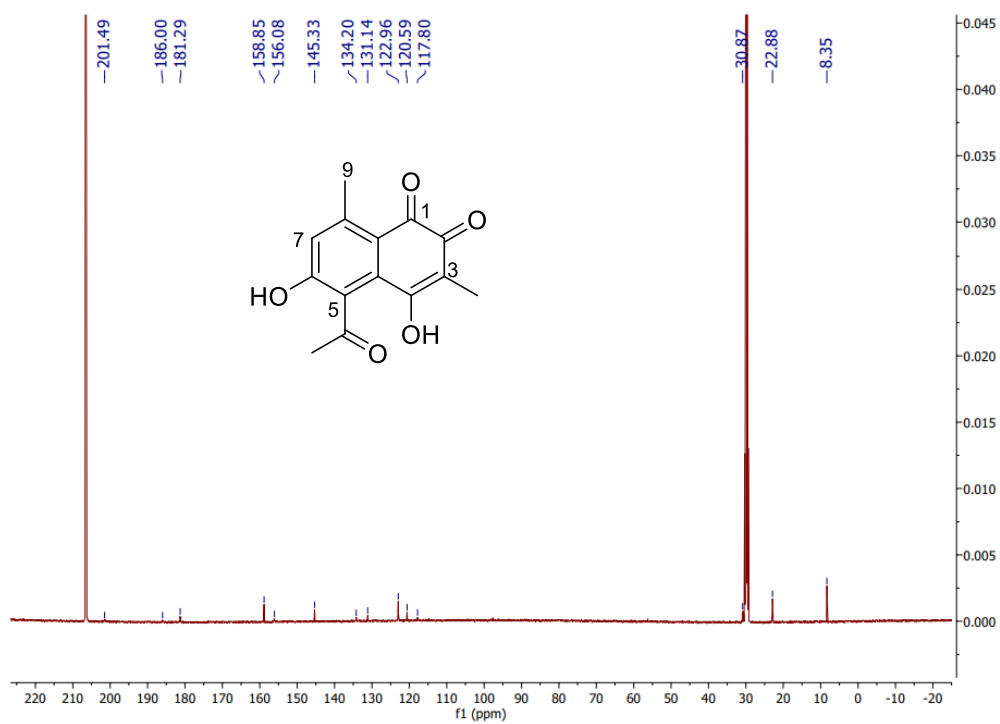
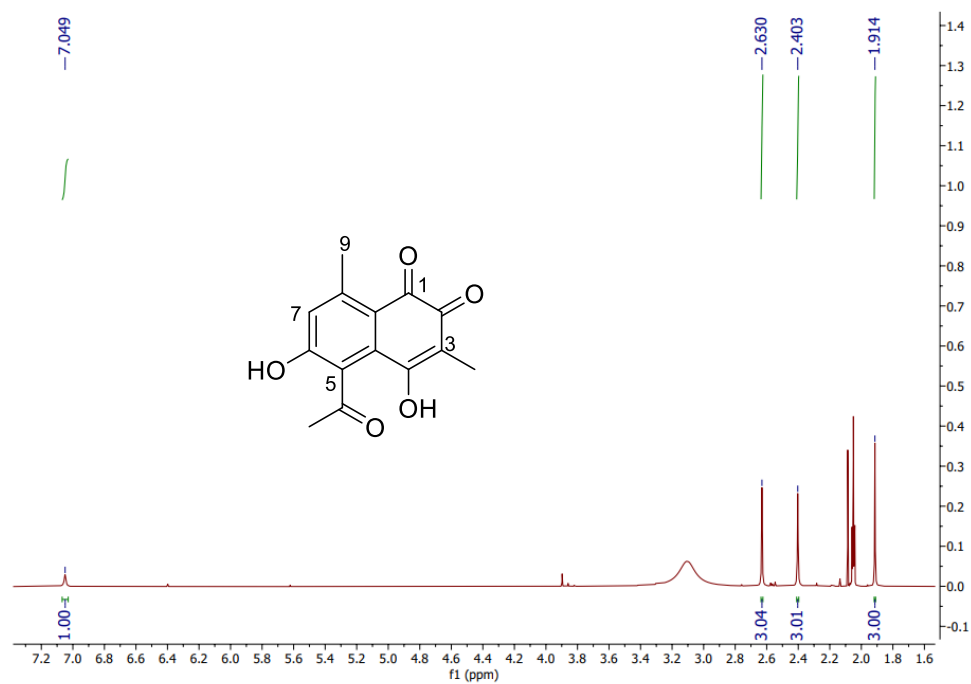


Figure A57. HRESIMS spectrum of compound **19**





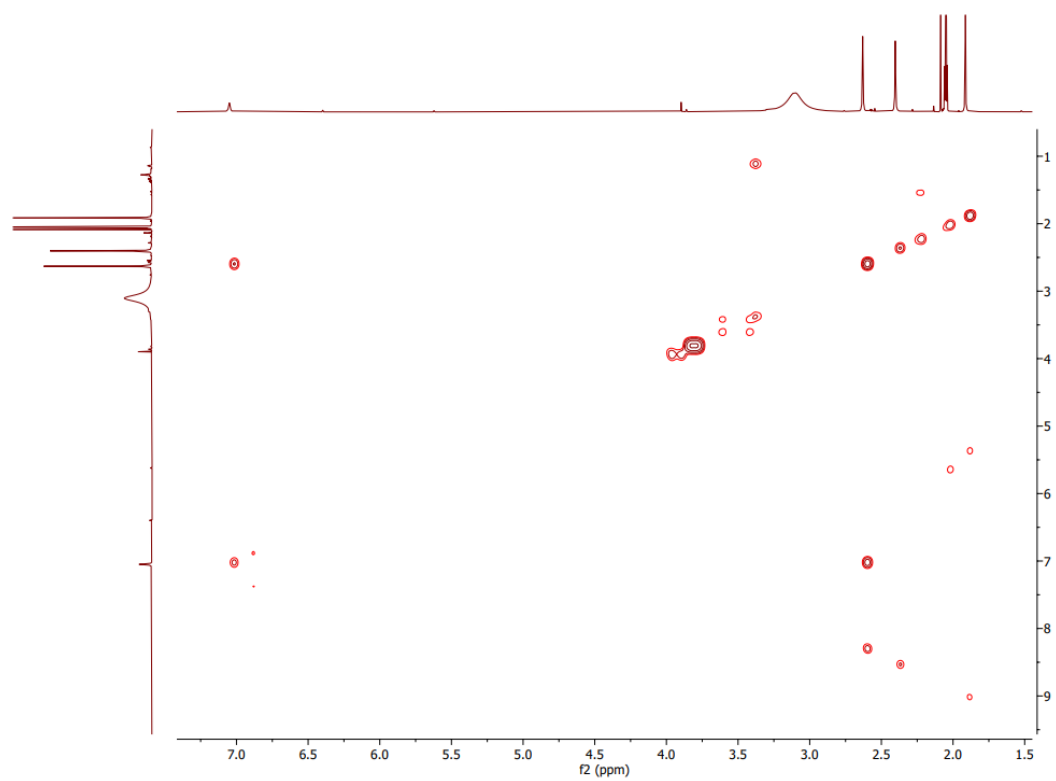
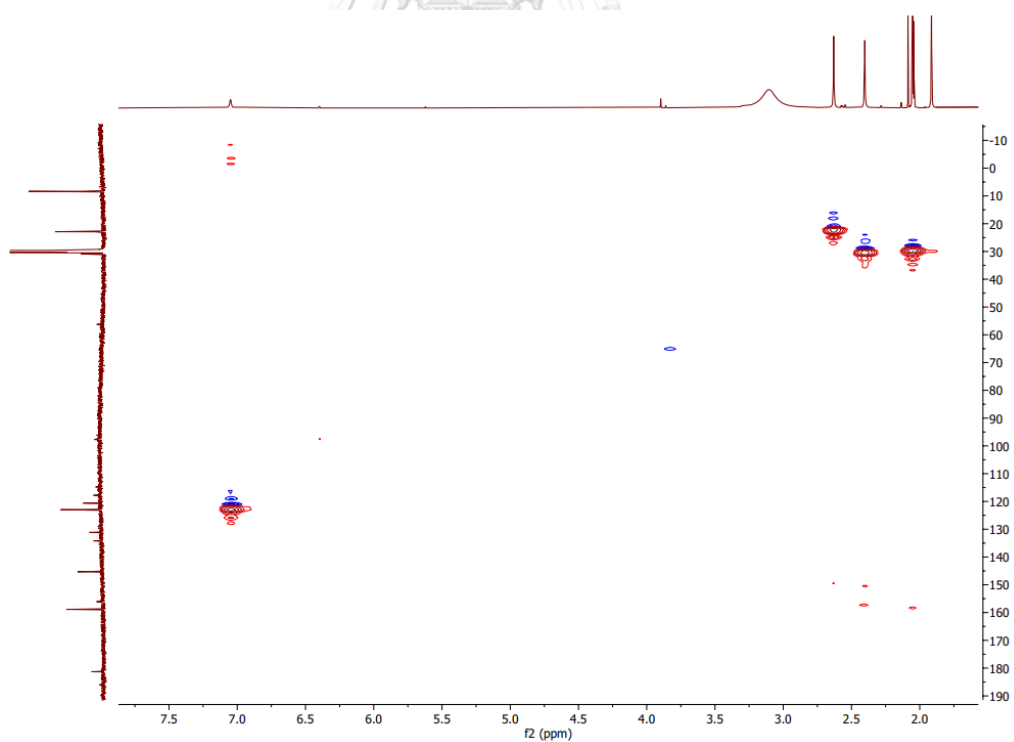
Figure A60. ^1H - ^1H COSY spectrum of compound 20

Figure A61. HSQC spectrum of compound 20

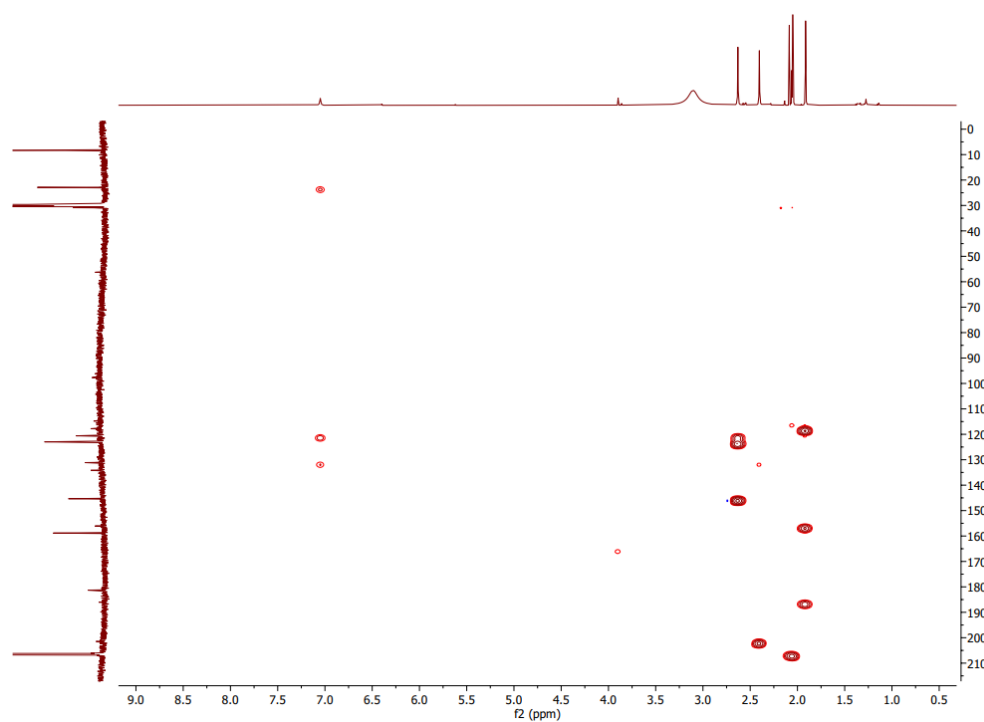


Figure A62. HMBC spectrum of compound 20

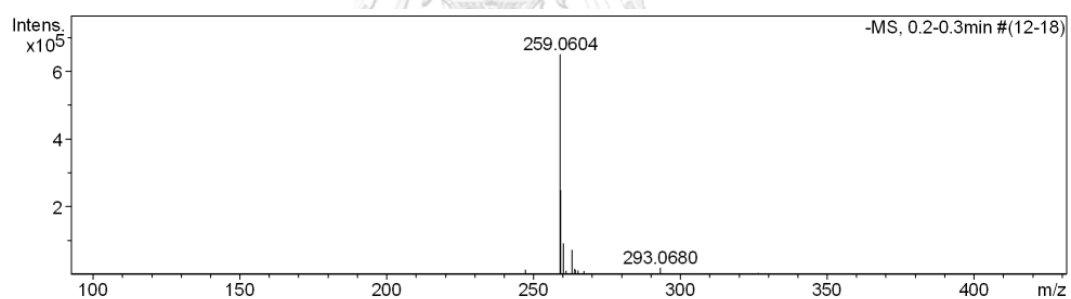
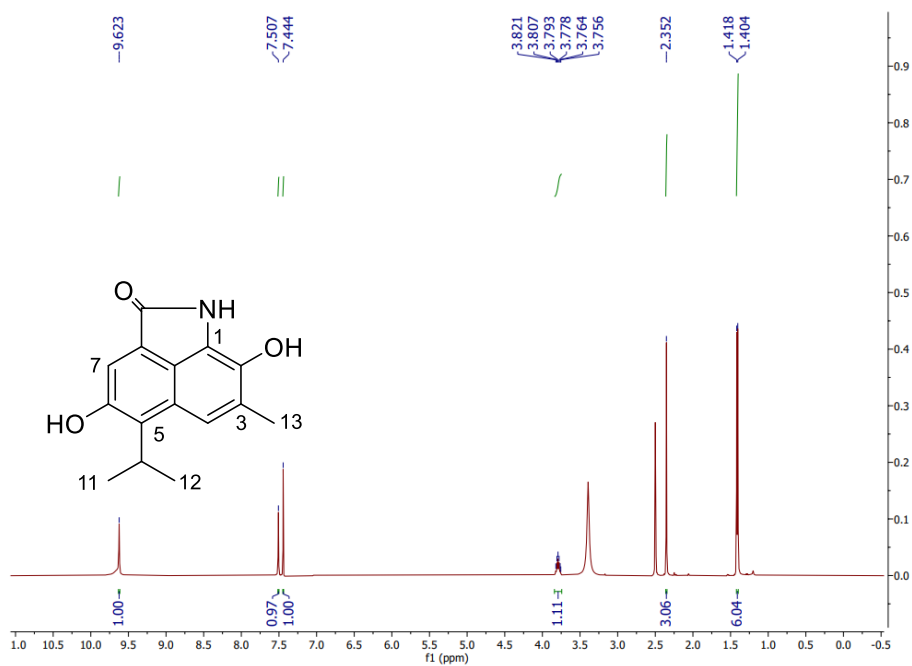
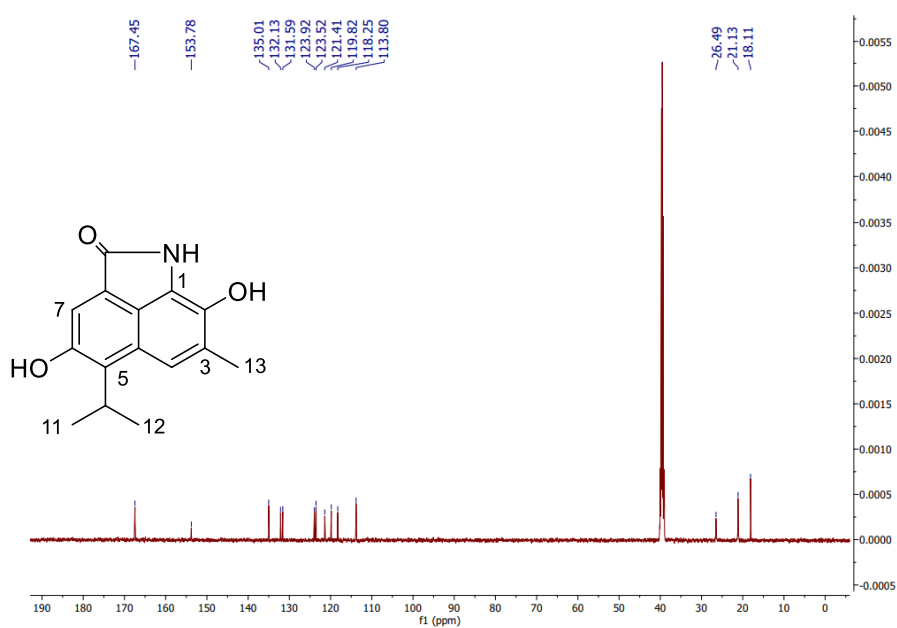
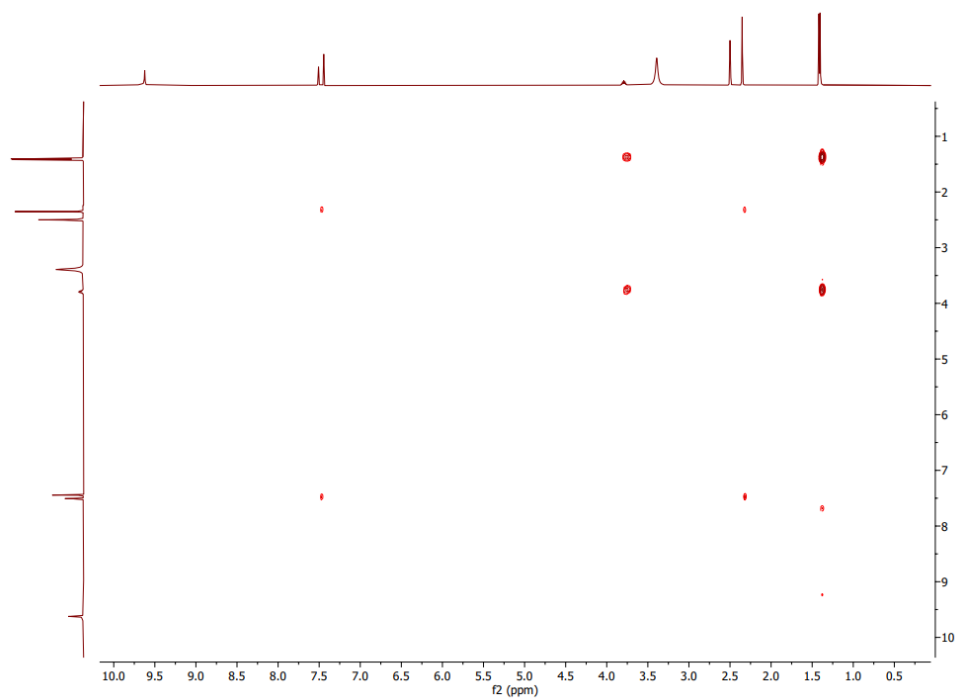
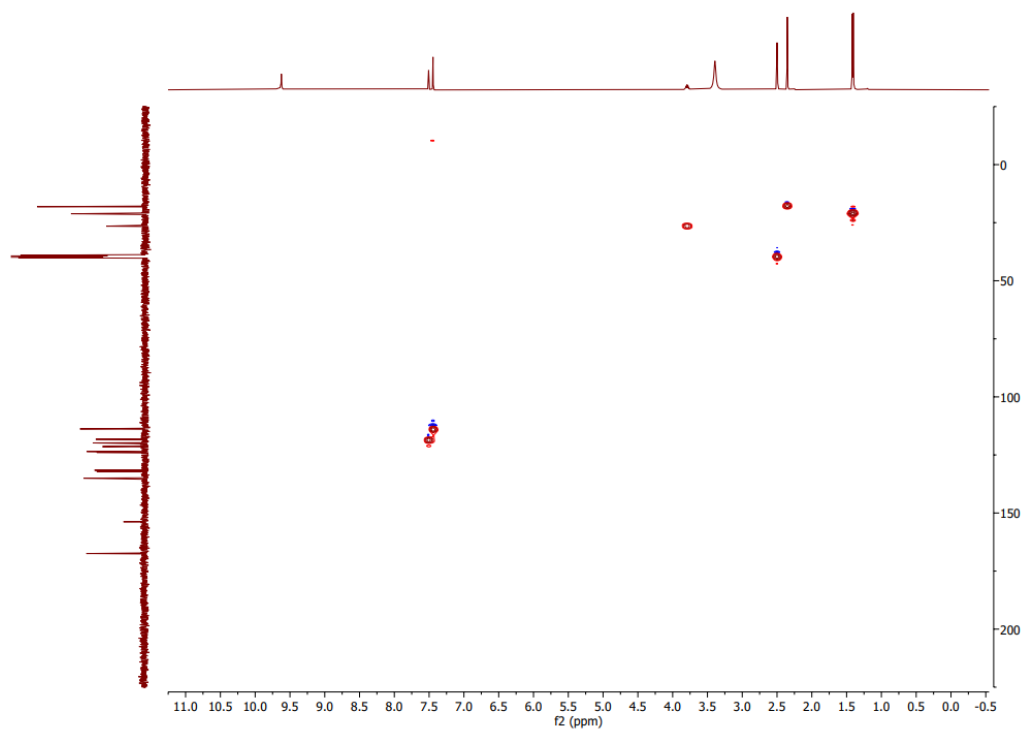
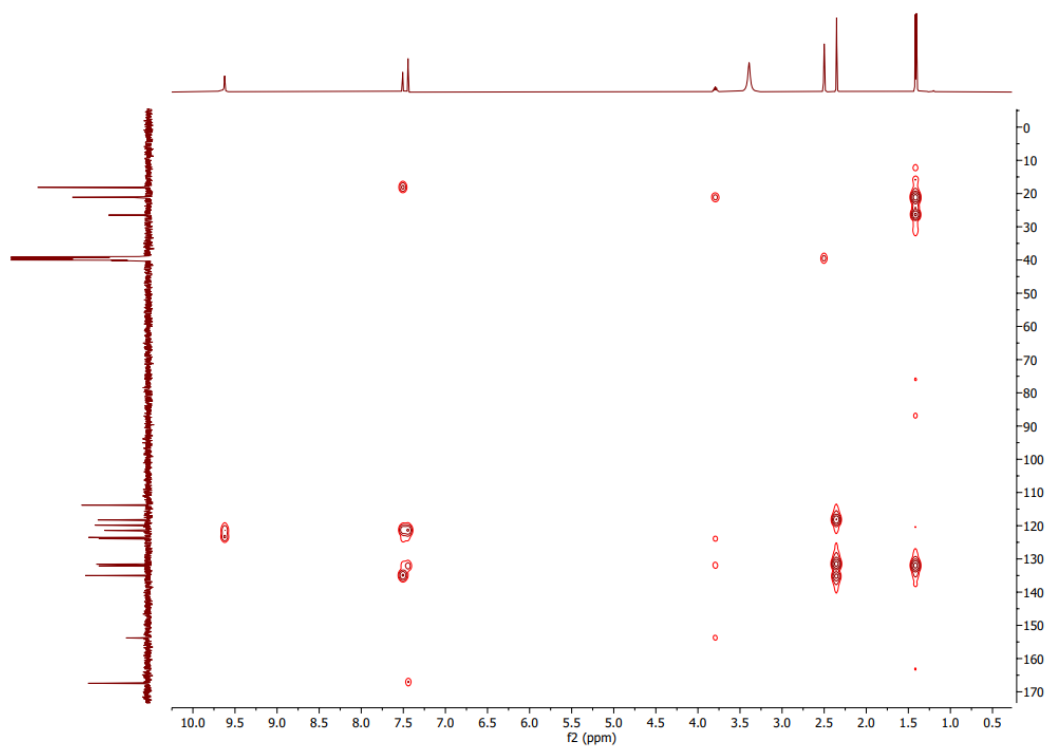
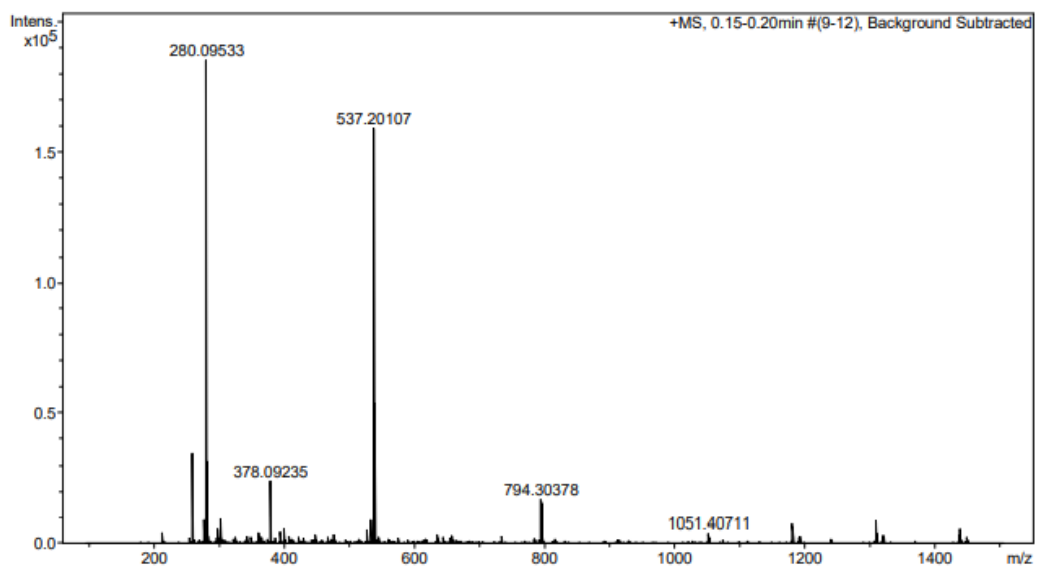
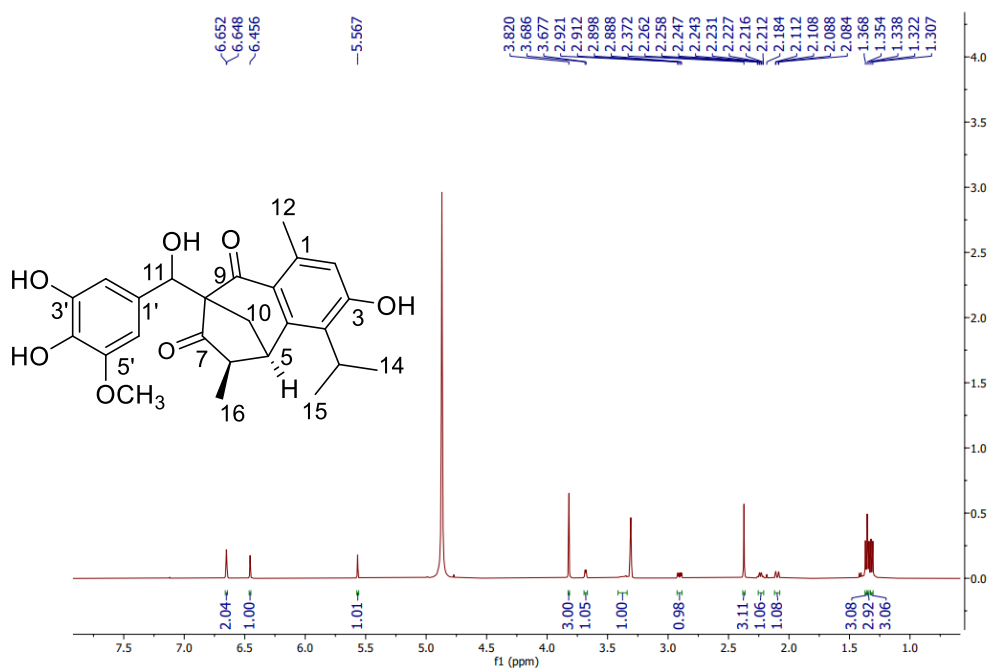
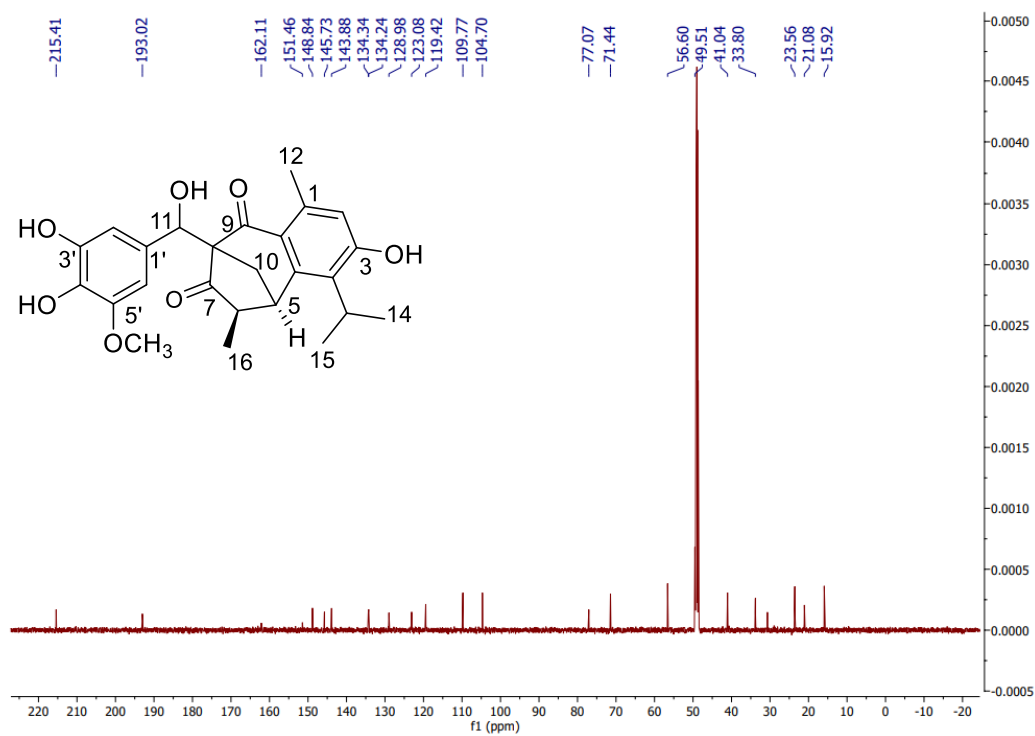


Figure A63. HRESIMS spectrum of compound 20

Figure A64. ^1H NMR spectrum (500 MHz, $\text{DMSO-}d_6$) of compound **21**Figure A65. ^{13}C NMR spectrum (125 MHz, $\text{DMSO-}d_6$) of compound **21**

Figure A66. ^1H - ^1H COSY spectrum of compound **21**Figure A67. HSQC spectrum of compound **21**

Figure A68. HMBC spectrum of compound **21**Figure A69. HRESIMS spectrum of compound **21**

Figure A70. ¹H NMR spectrum (500 MHz, methanol-*d*₄) of compound **22**Figure A71. ¹³C NMR spectrum (125 MHz, methanol-*d*₄) of compound **22**

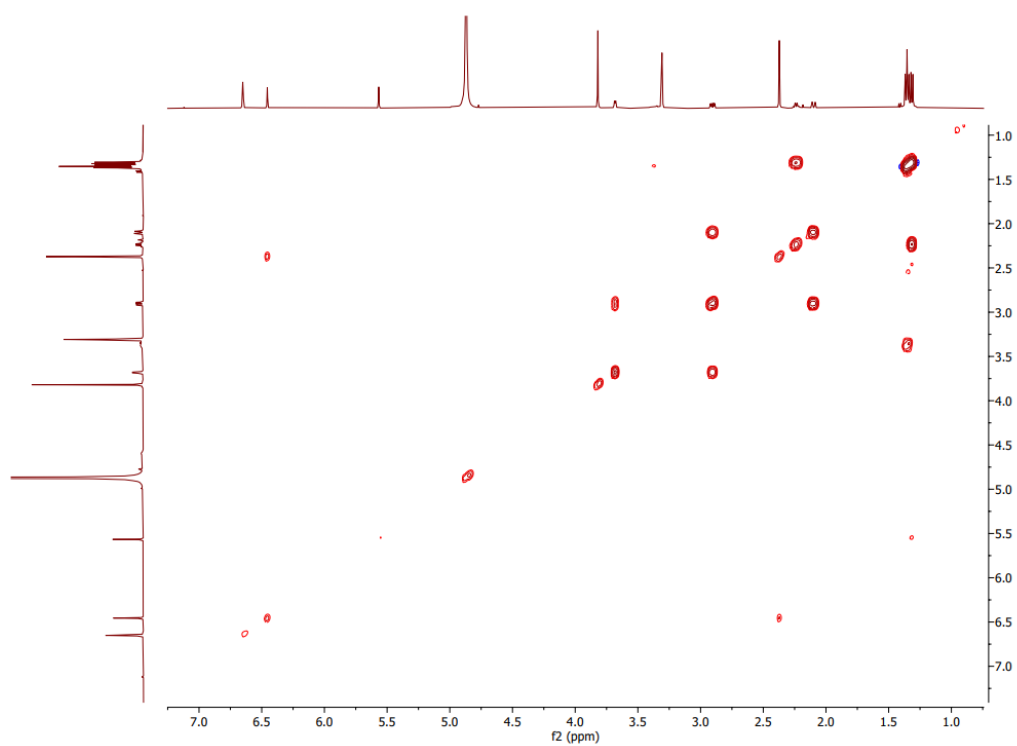
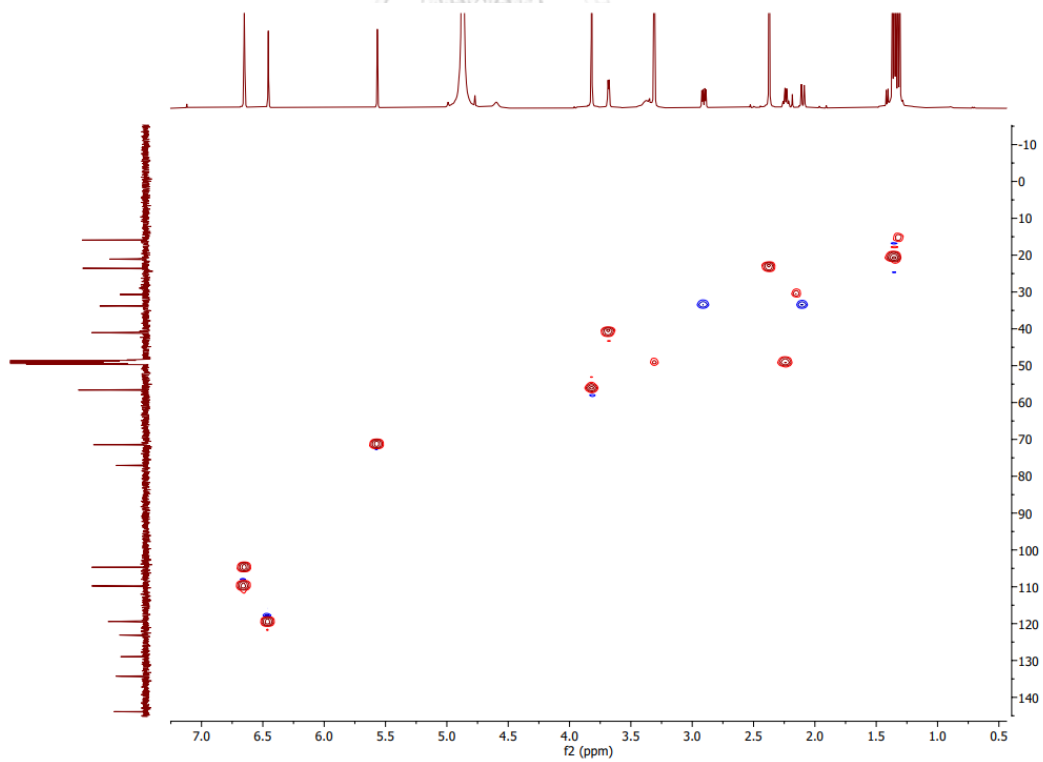
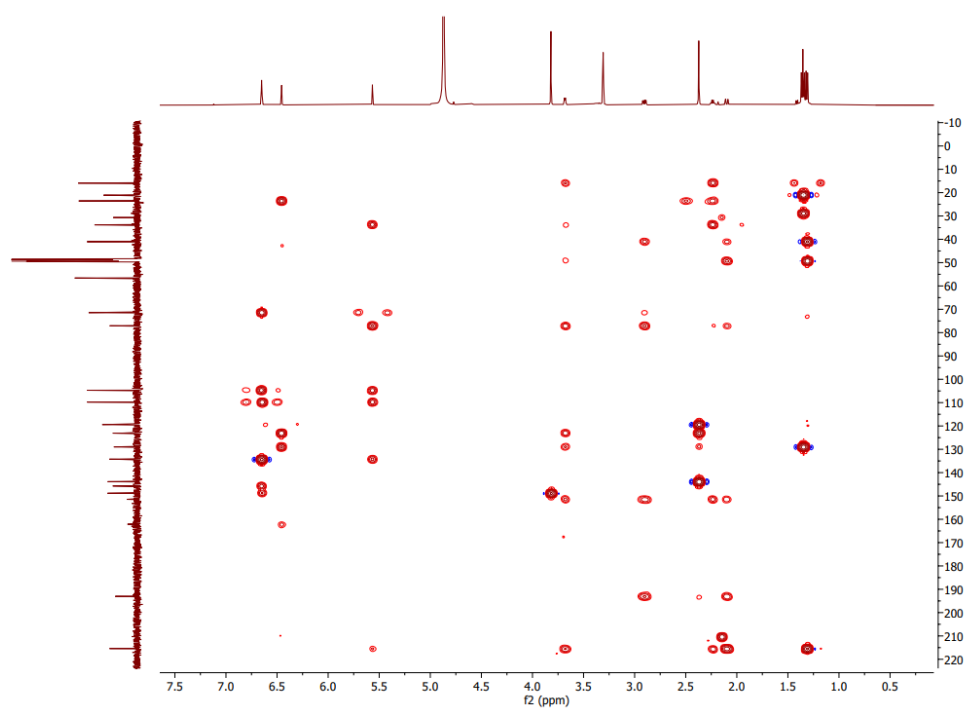
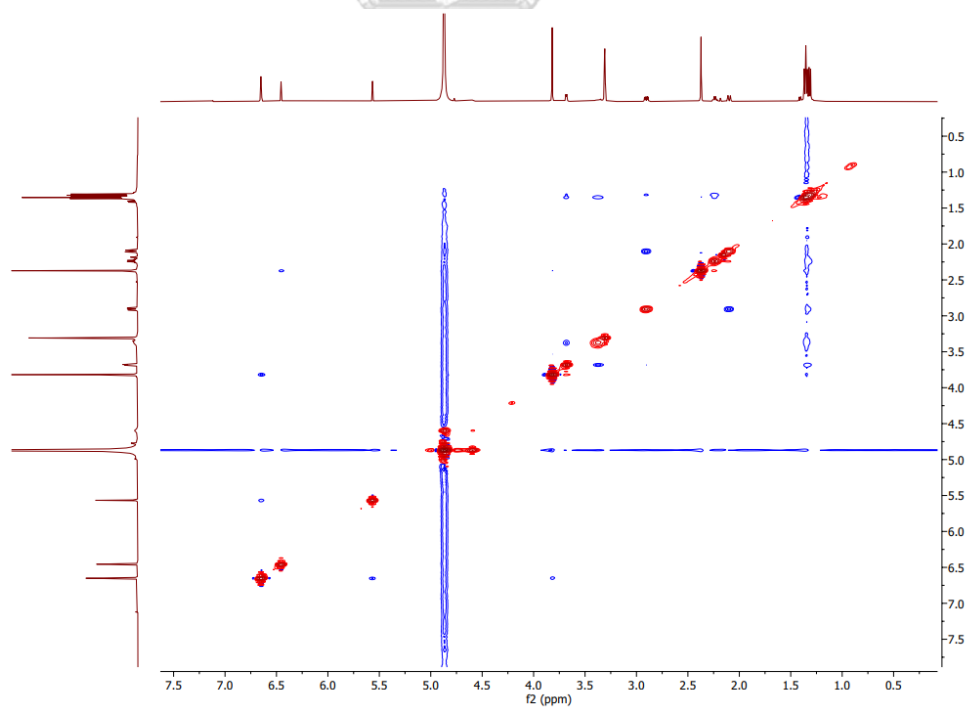
Figure A72. ^1H - ^1H COSY spectrum of compound 22

Figure A73. HSQC spectrum of compound 22

Figure A74. HMBC spectrum of compound **22**Figure A75. NOESY spectrum of compound **22**

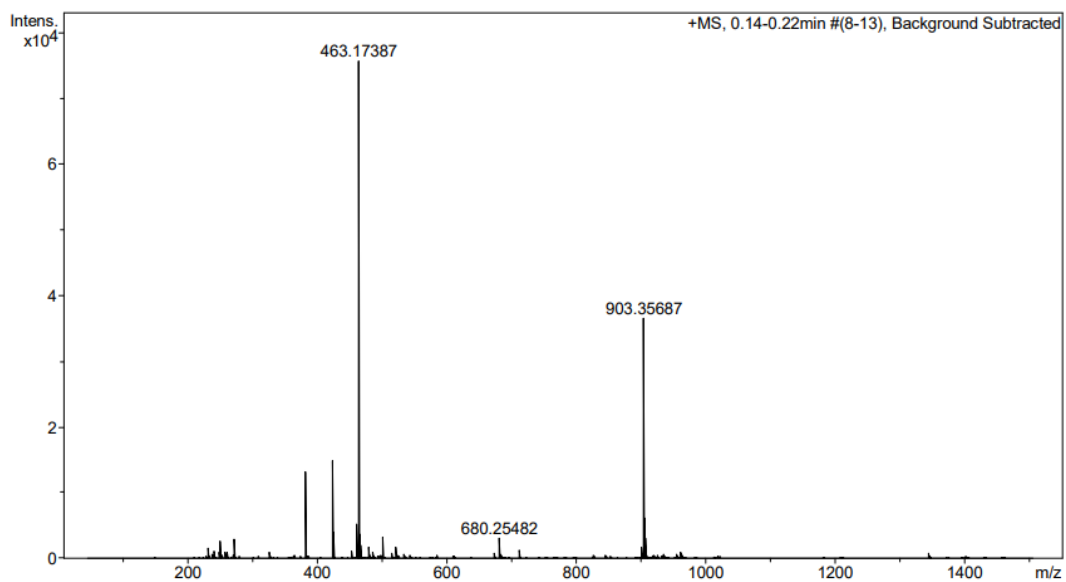
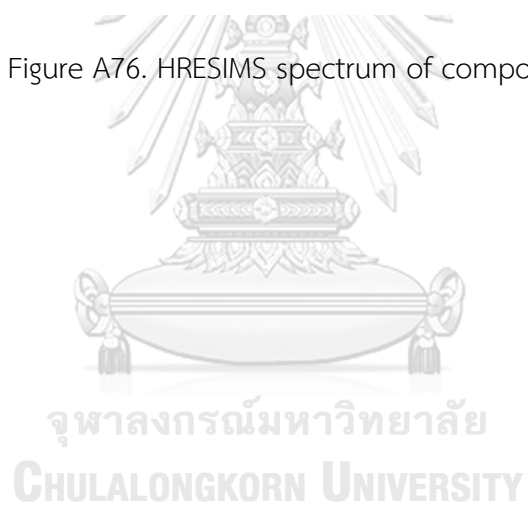


Figure A76. HRESIMS spectrum of compound 22



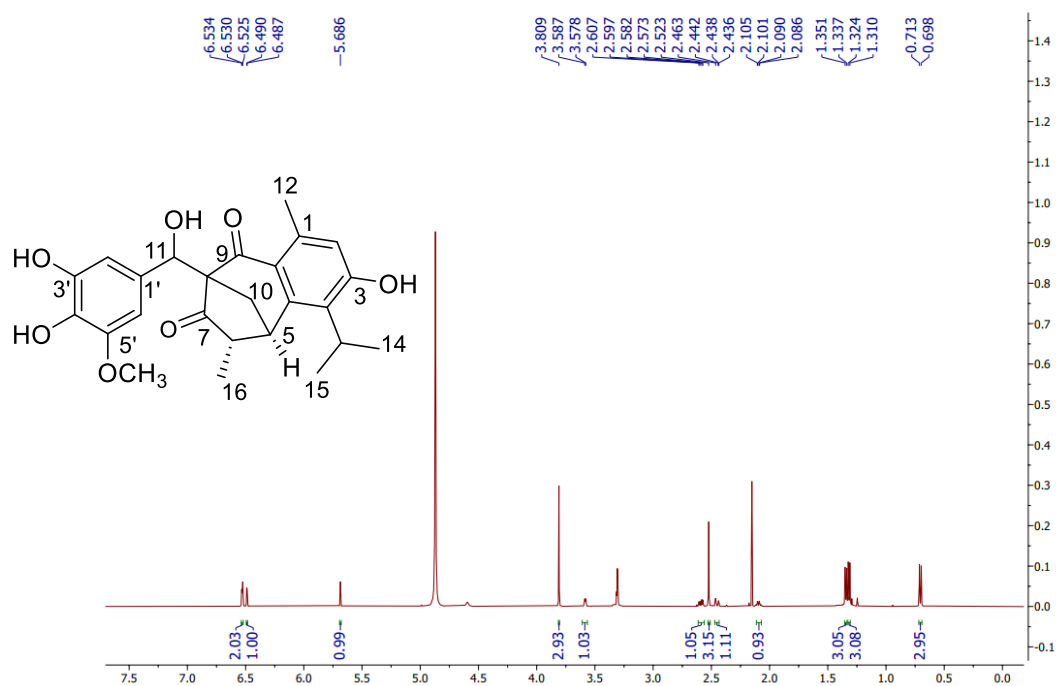


Figure A77. ^1H NMR spectrum (500 MHz, methanol- d_4) of compound **23**

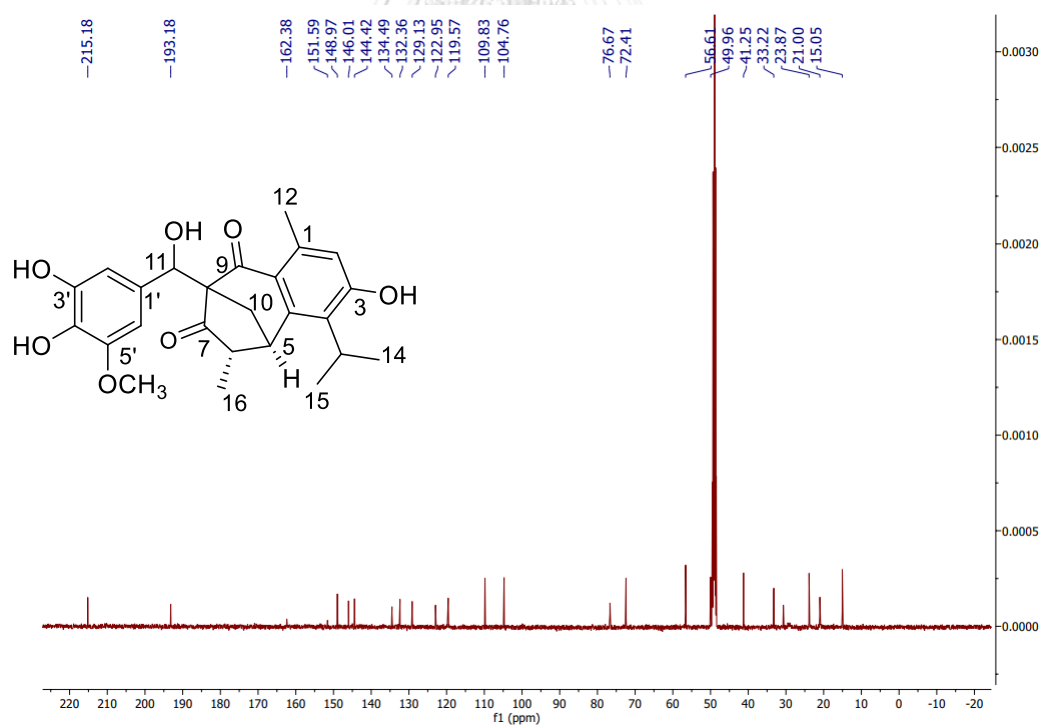
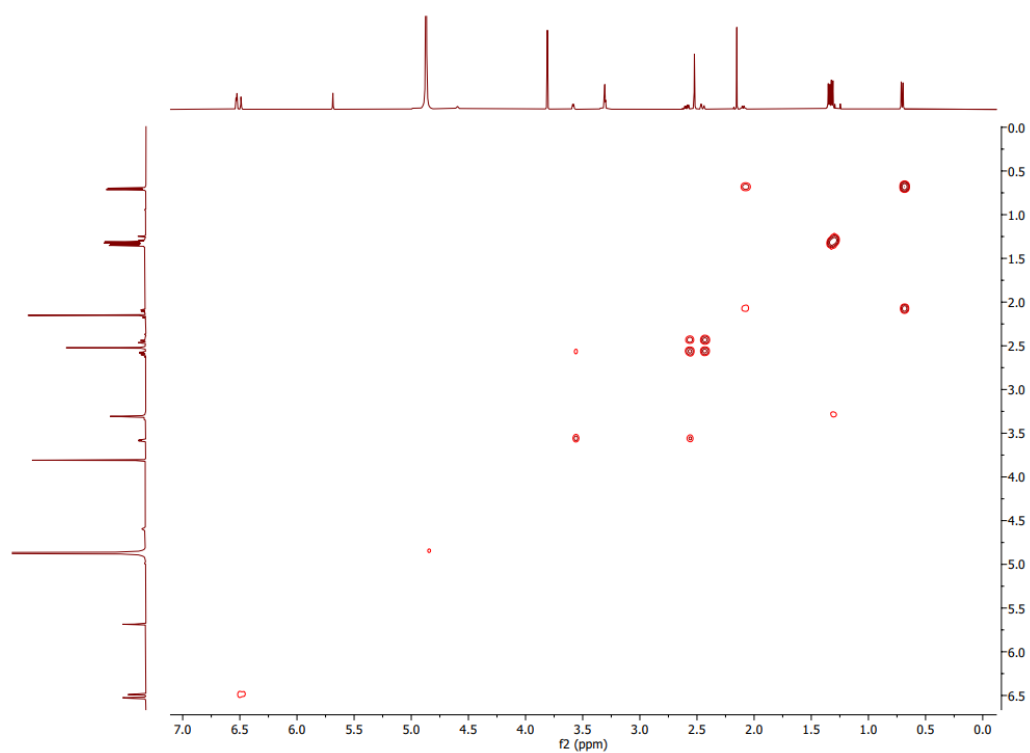
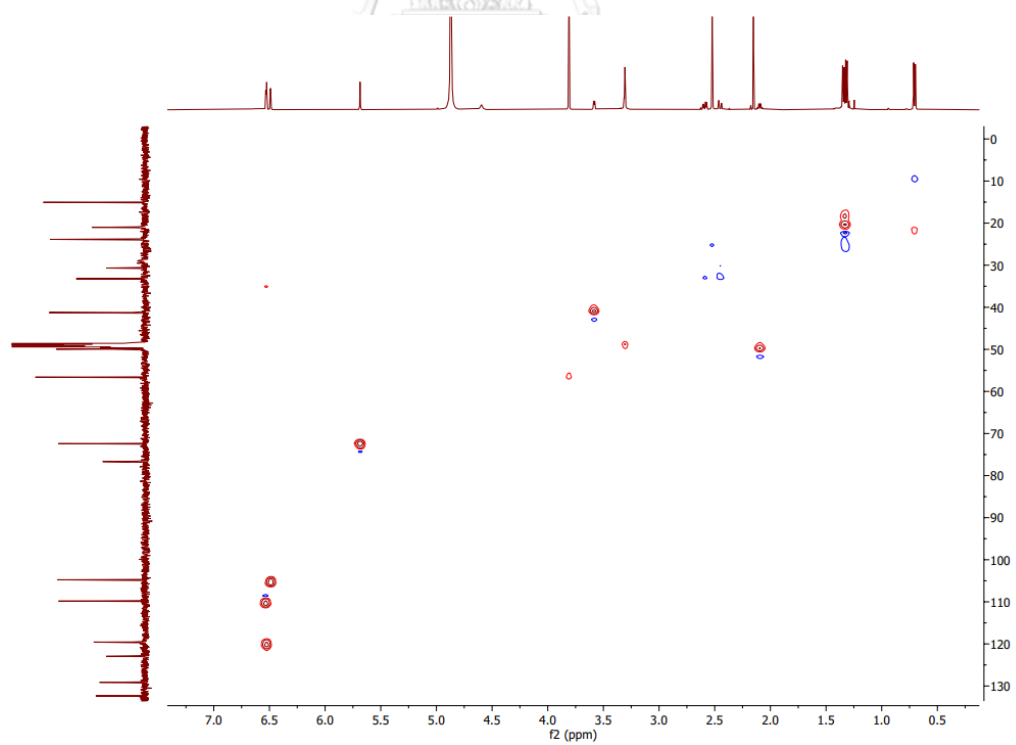
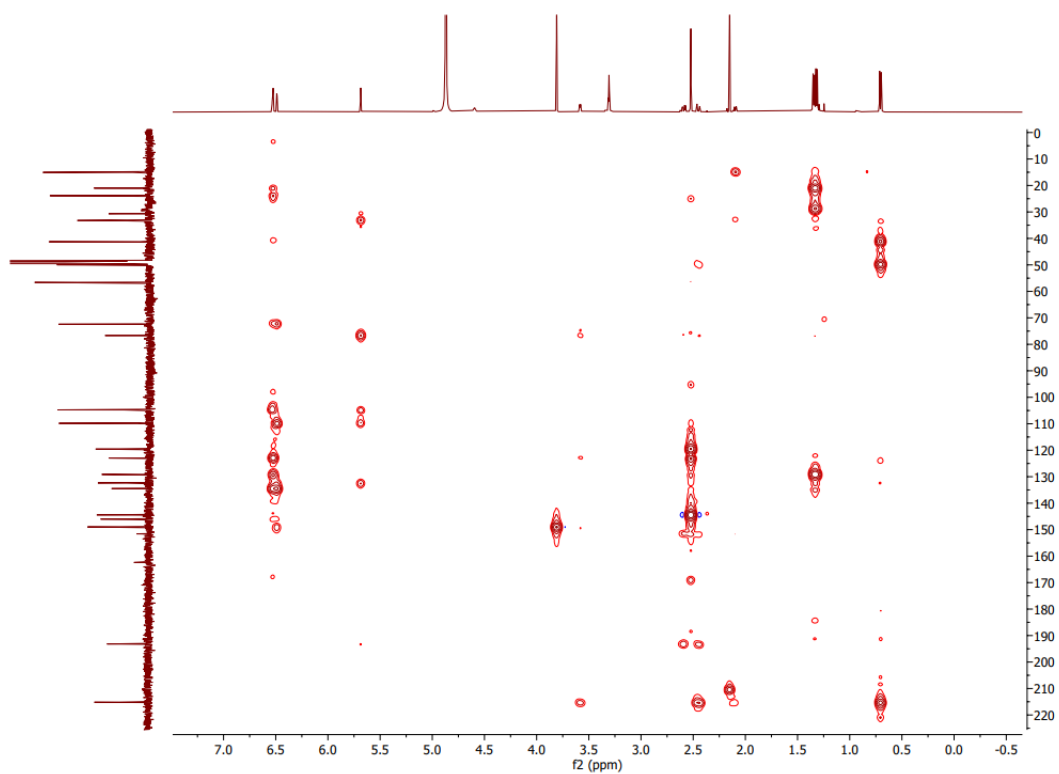
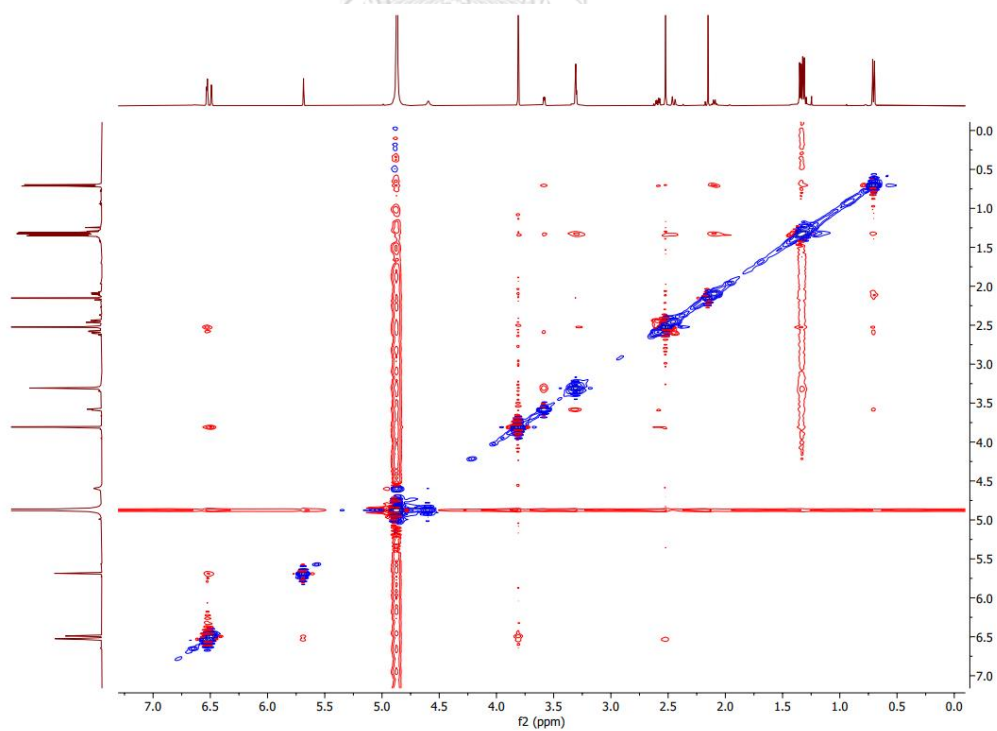


Figure A78. ^{13}C NMR spectrum (125 MHz, methanol- d_4) of compound **23**

Figure A79. ^1H - ^1H COSY spectrum of compound **23**Figure A80. HSQC spectrum of compound **23**

Figure A81. HMBC spectrum of compound **23**Figure A82. NOESY spectrum of compound **23**

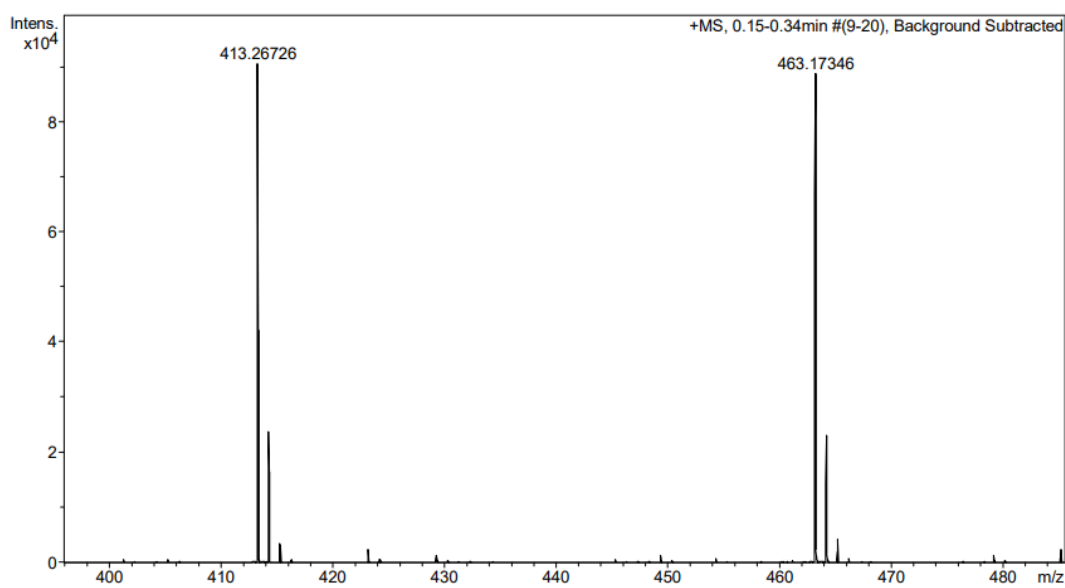


Figure A83. HRESIMS spectrum of compound 23



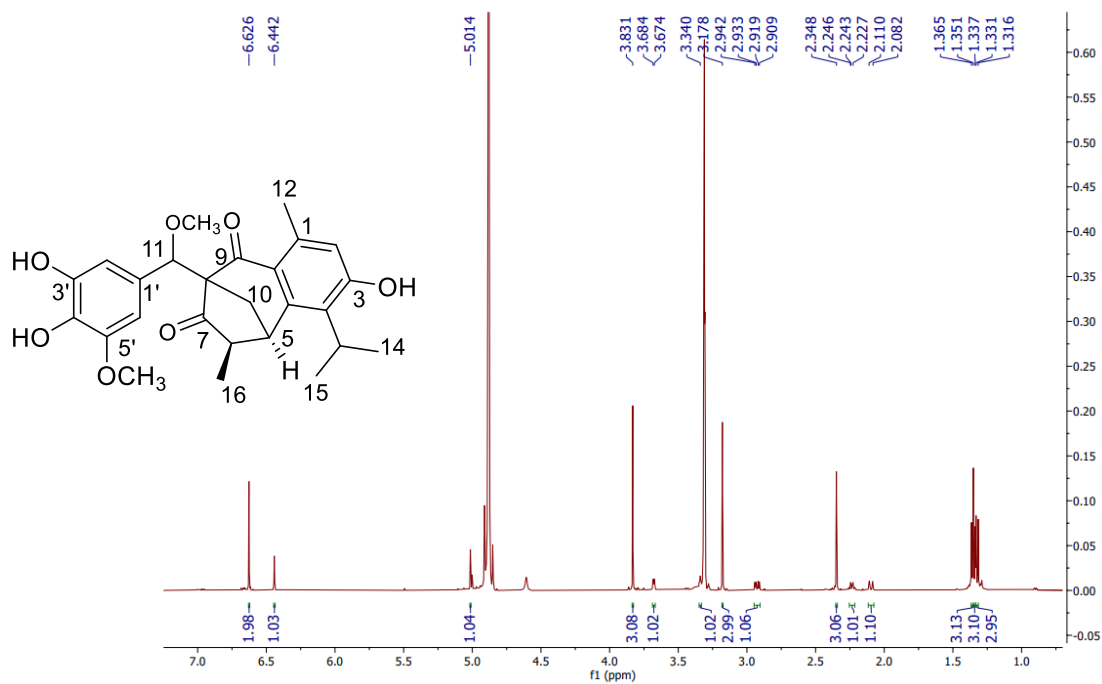


Figure A84. ^1H NMR spectrum (500 MHz, methanol- d_4) of compound **24**

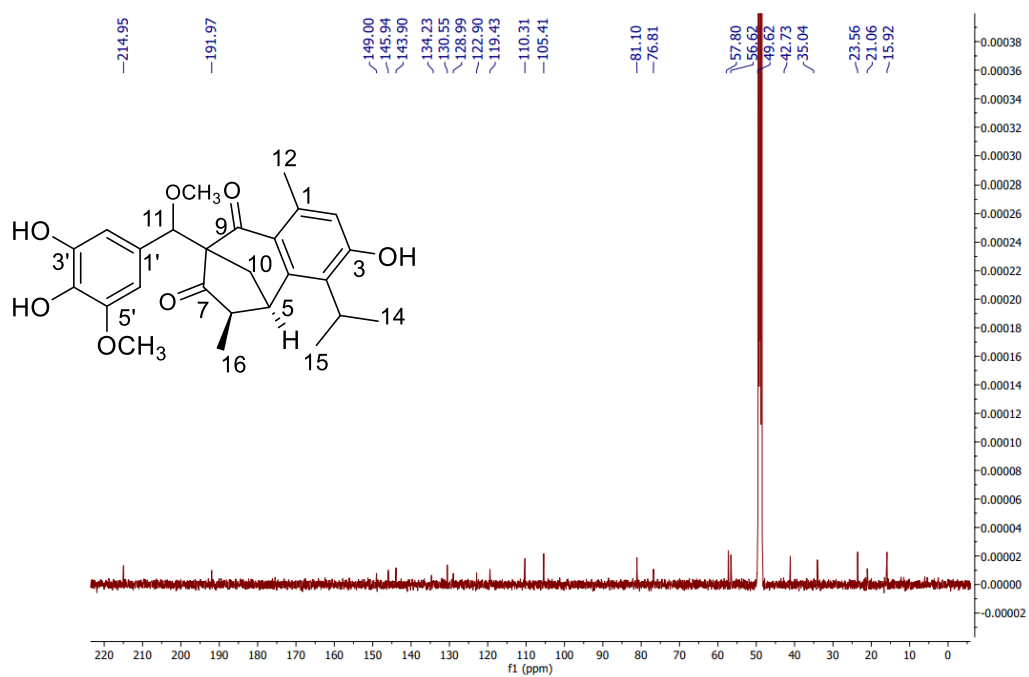
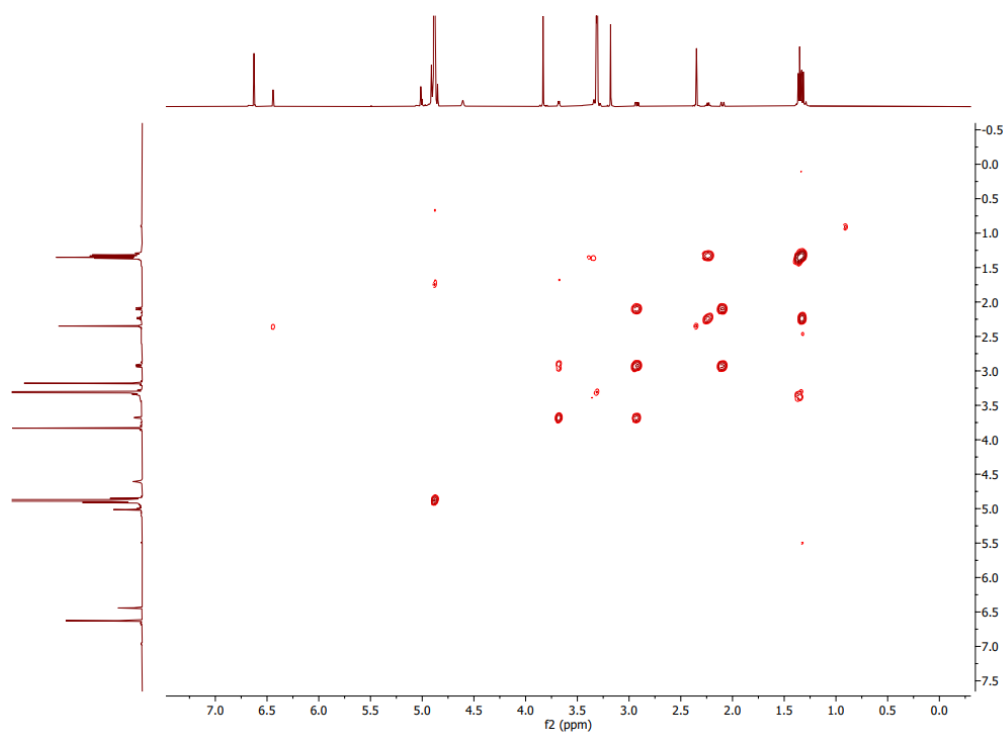
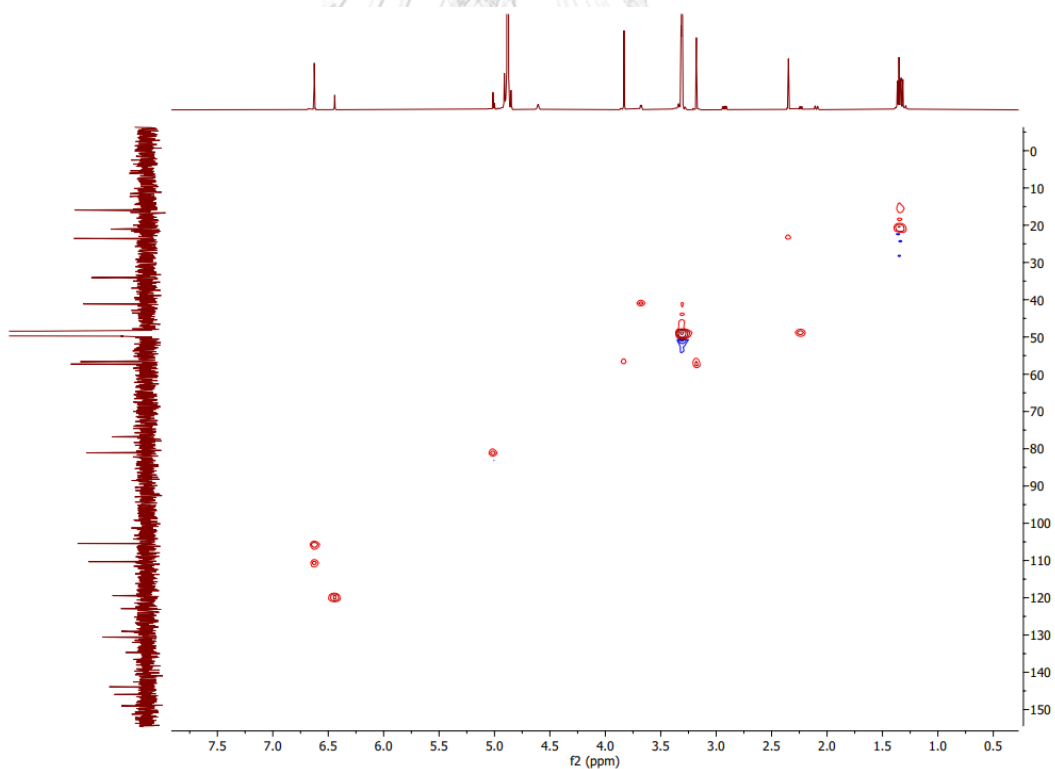


Figure A85. ^{13}C NMR spectrum (125 MHz, methanol- d_4) of compound **24**

Figure A86. ^1H - ^1H COSY spectrum of compound **24**Figure A87. HSQC spectrum of compound **24**

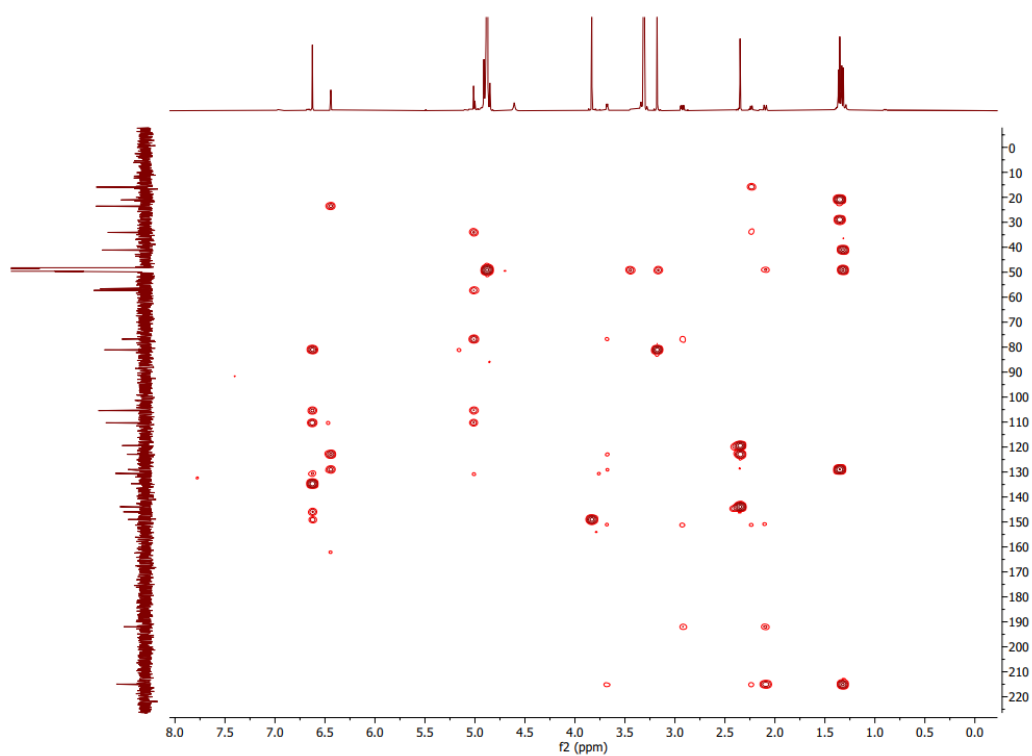


Figure A88. HMBC spectrum of compound 24

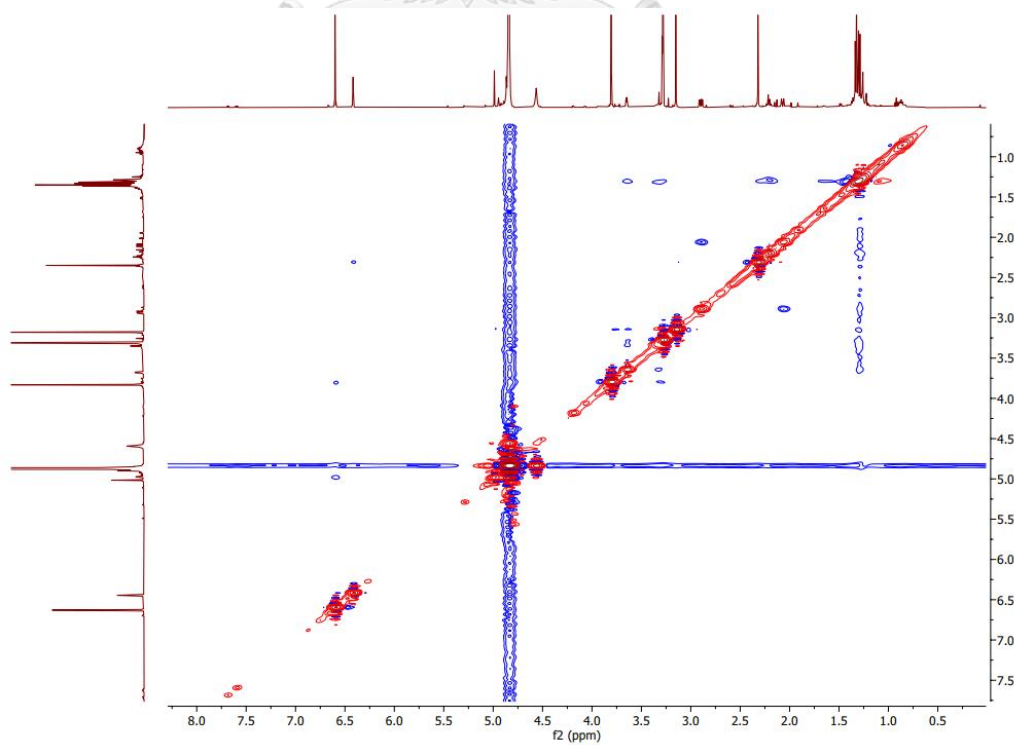


Figure A89. NOESY spectrum of compound 24

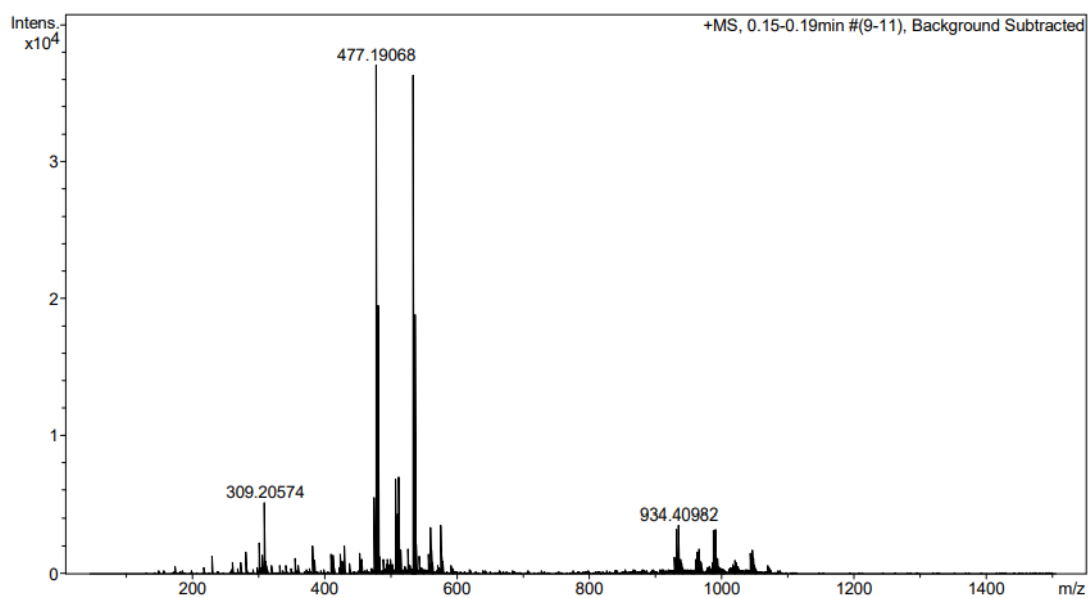


Figure A90. HRESIMS spectrum of compound 24



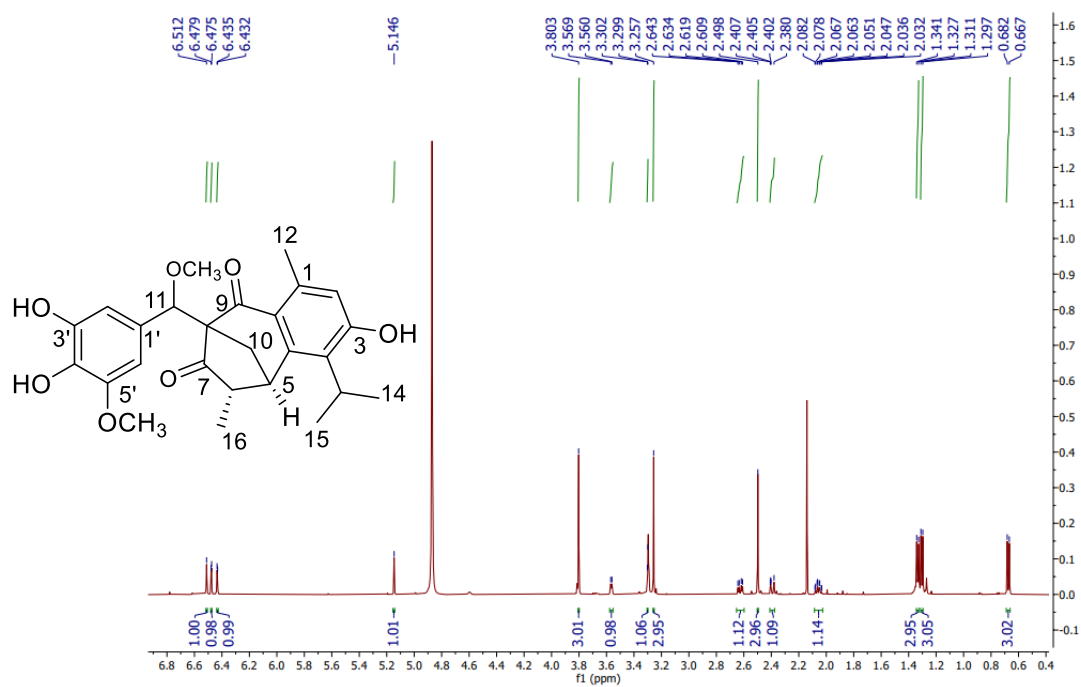


Figure A91. ^1H NMR spectrum (500 MHz, methanol- d_4) of compound 25

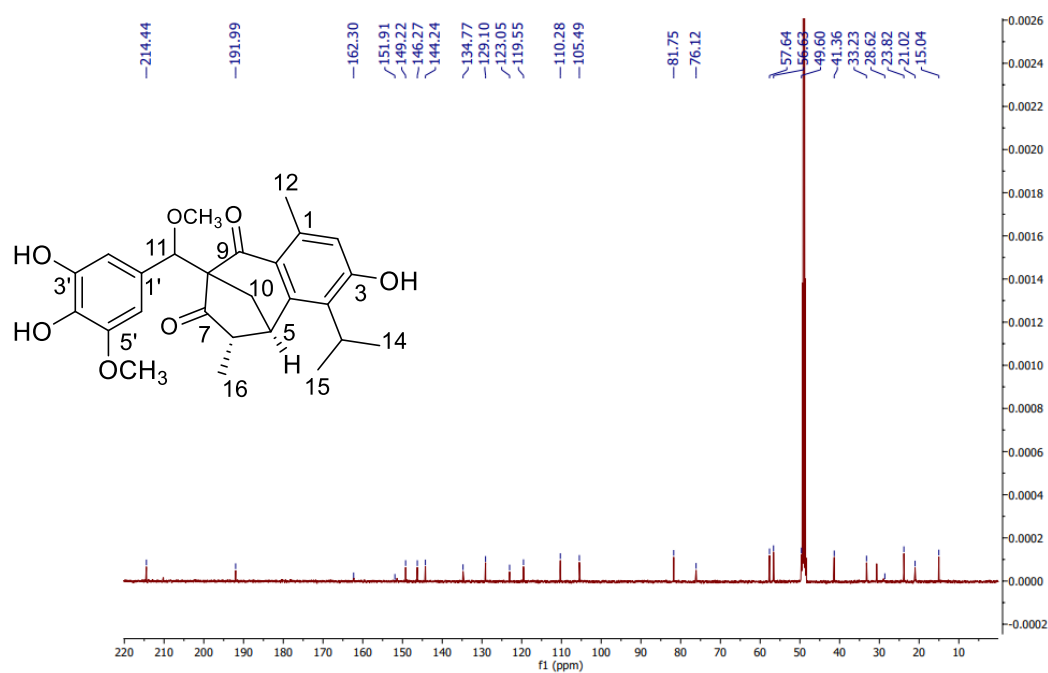


Figure A92. ^{13}C NMR spectrum (125 MHz, methanol- d_4) of compound 25

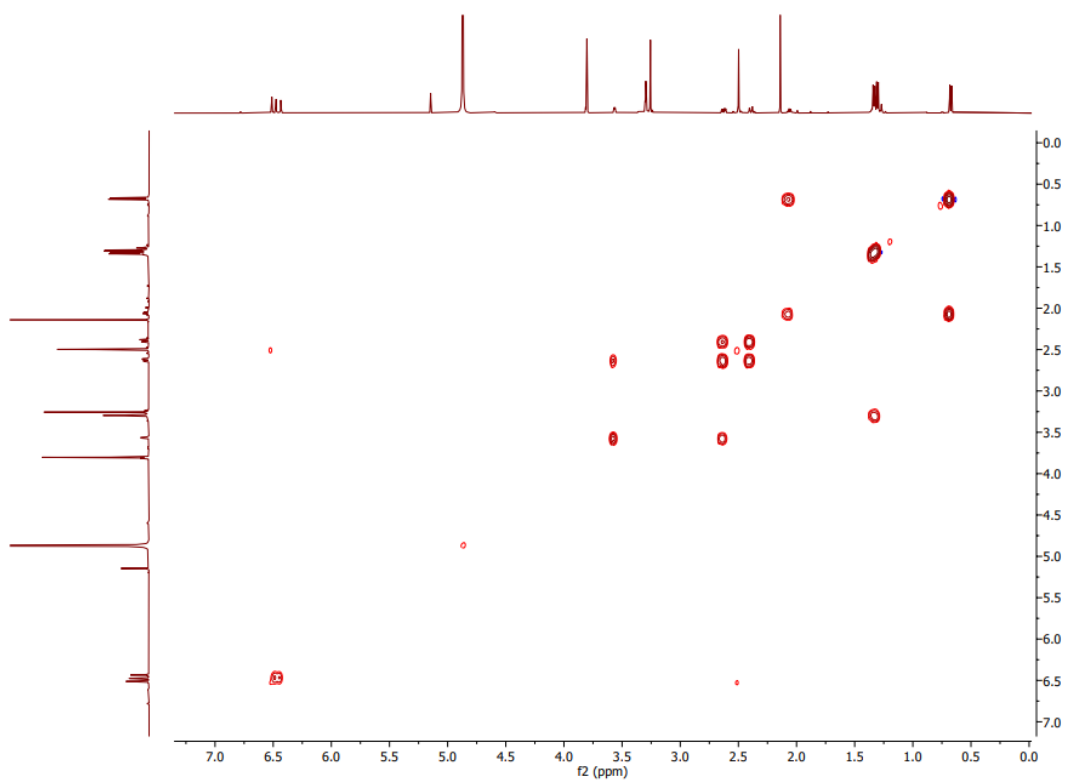
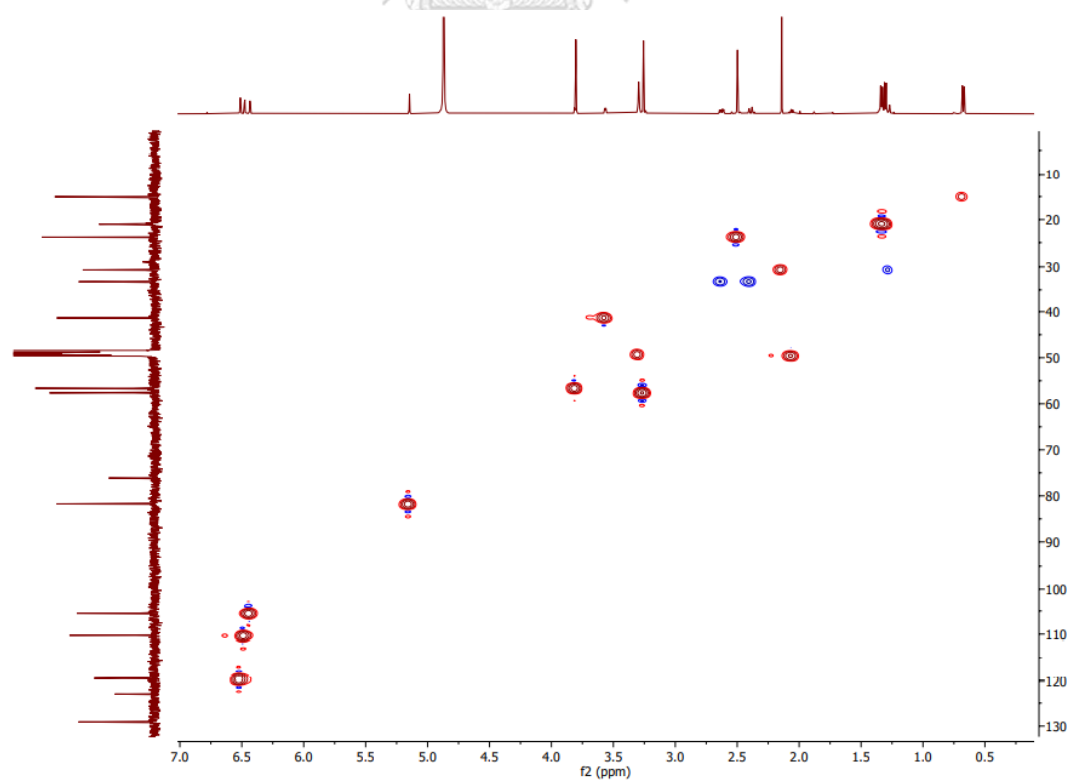
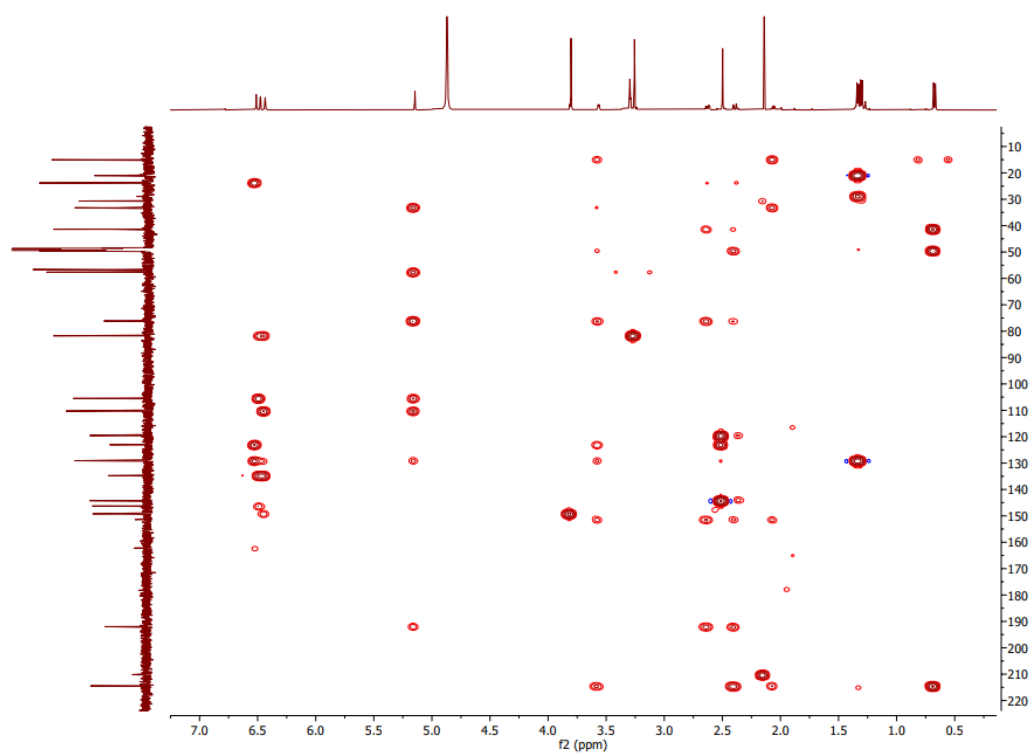
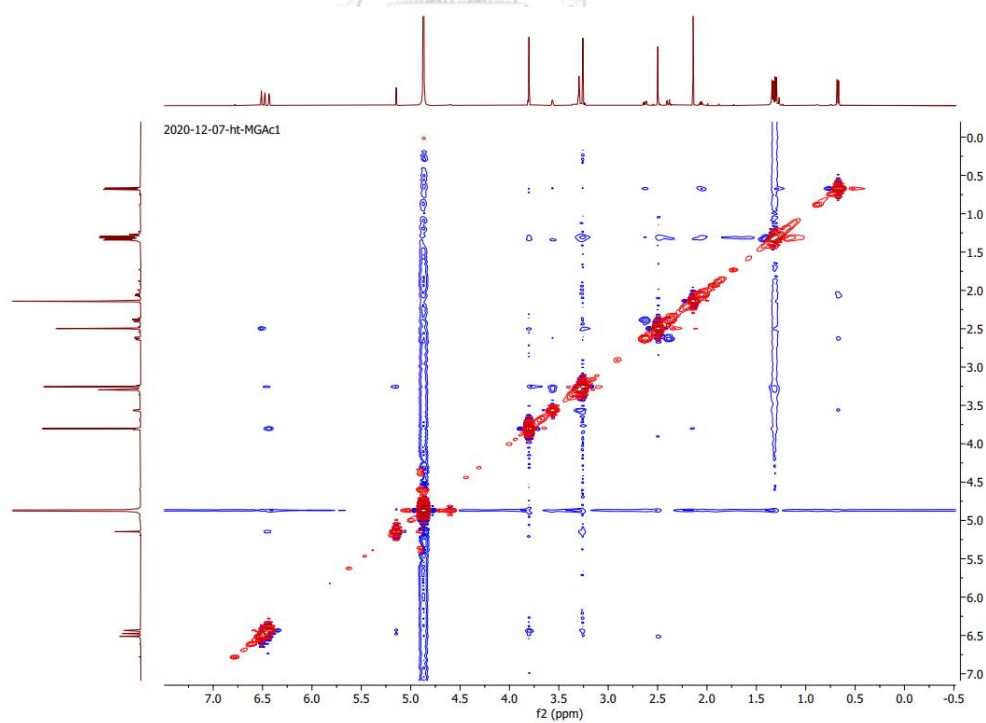
Figure A93. ¹H-¹H COSY spectrum of compound 25

Figure A94. HSQC spectrum of compound 25

Figure A95. HMBC spectrum of compound **25**Figure A96. NOESY spectrum of compound **25**

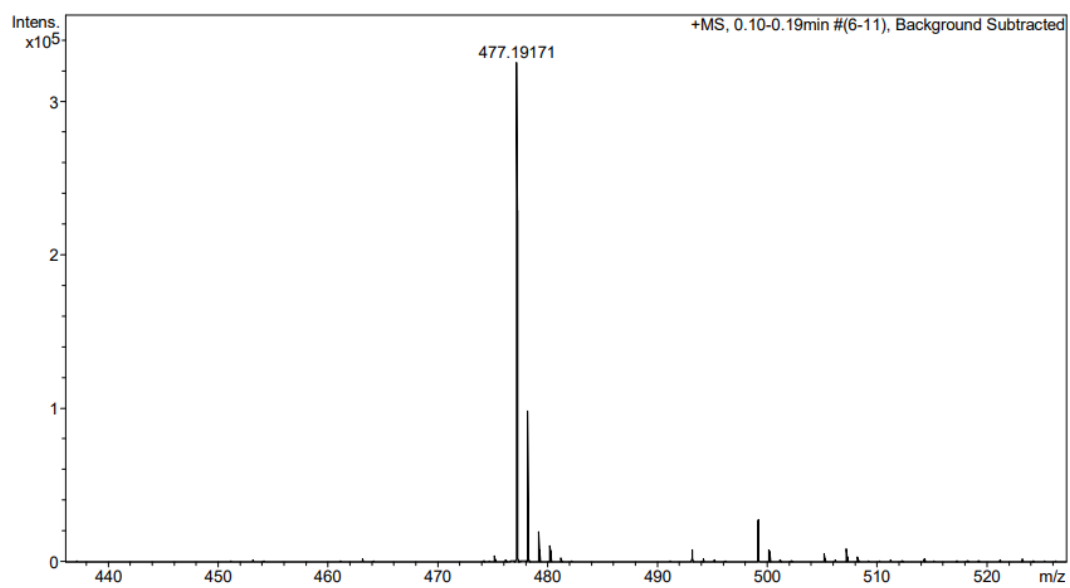
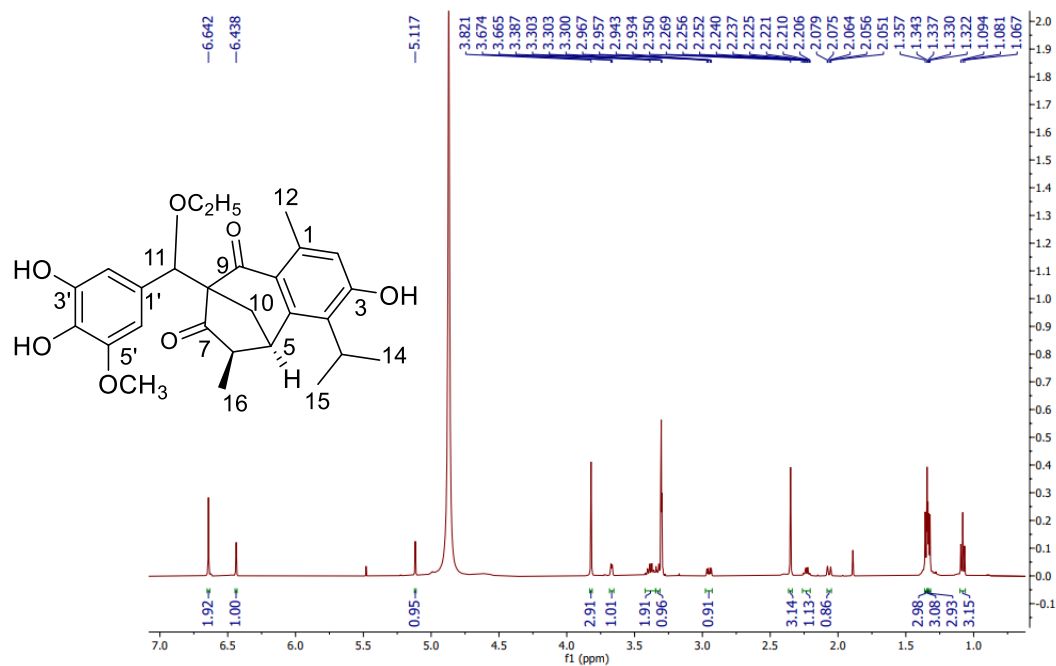
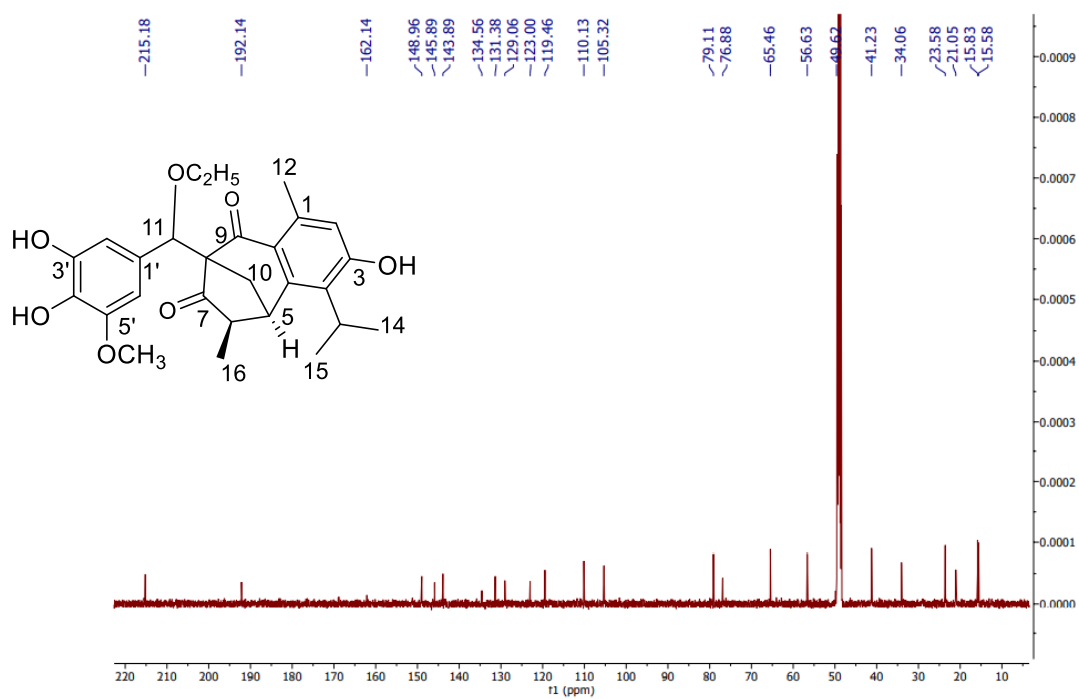


Figure A97. HRESIMS spectrum of compound **25**



Figure A98. ^1H NMR spectrum (500 MHz, methanol- d_4) of compound 26Figure A99. ^{13}C NMR spectrum (125 MHz, methanol- d_4) of compound 26

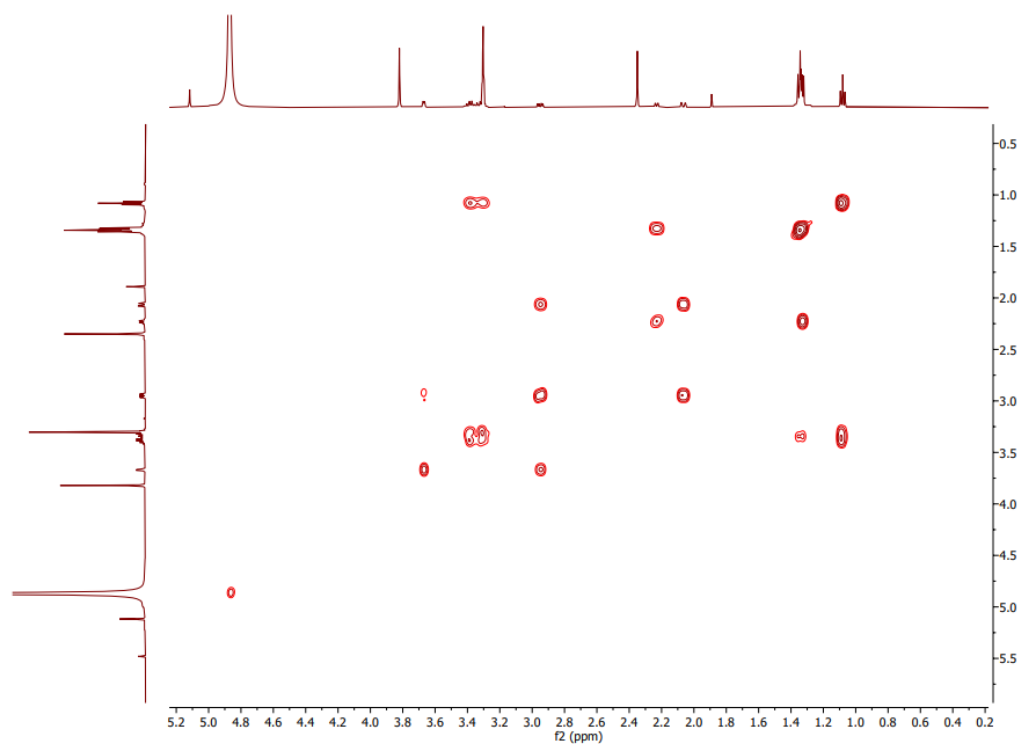
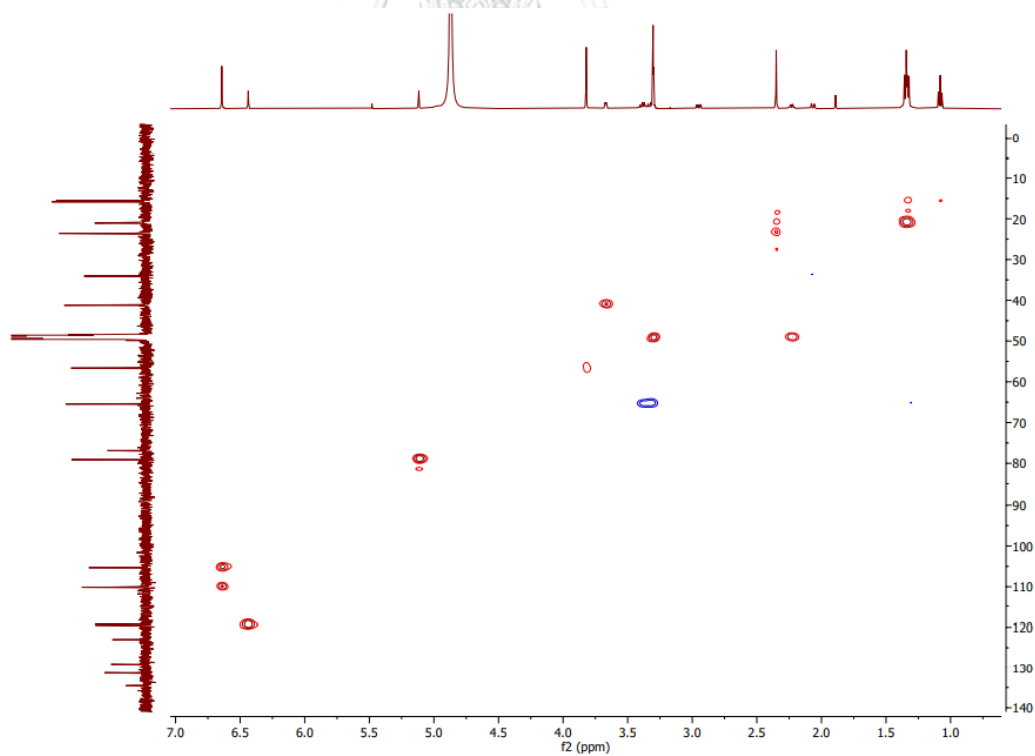
Figure A100. ^1H - ^1H COSY spectrum of compound 26

Figure A101. HSQC spectrum of compound 26

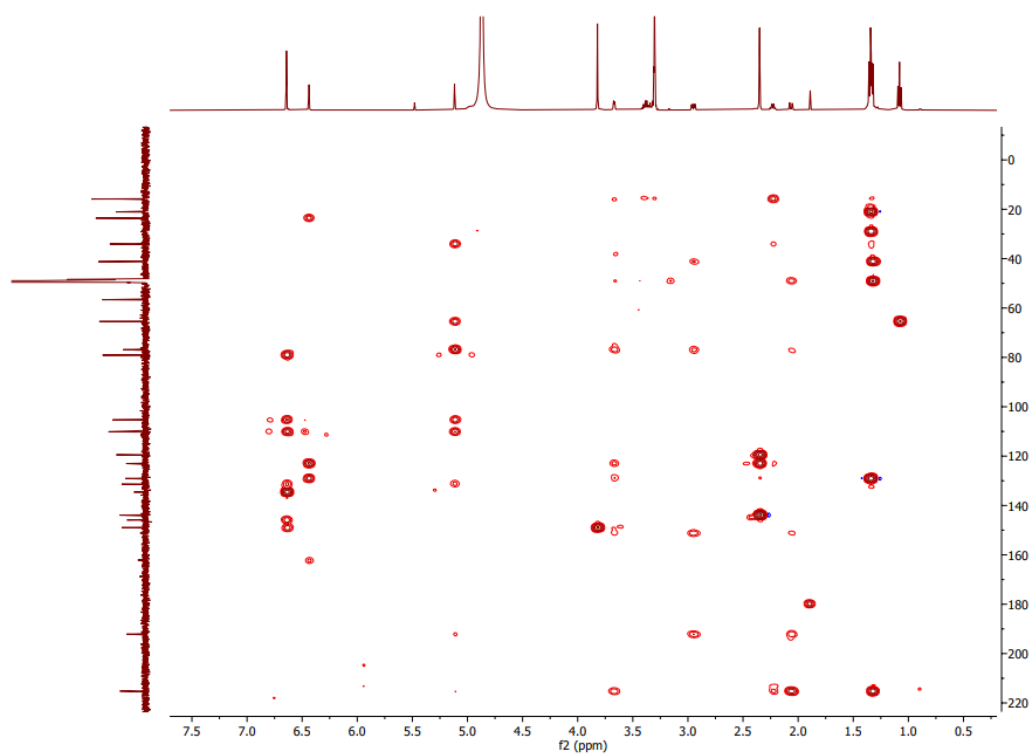


Figure A102. HMBC spectrum of compound 26

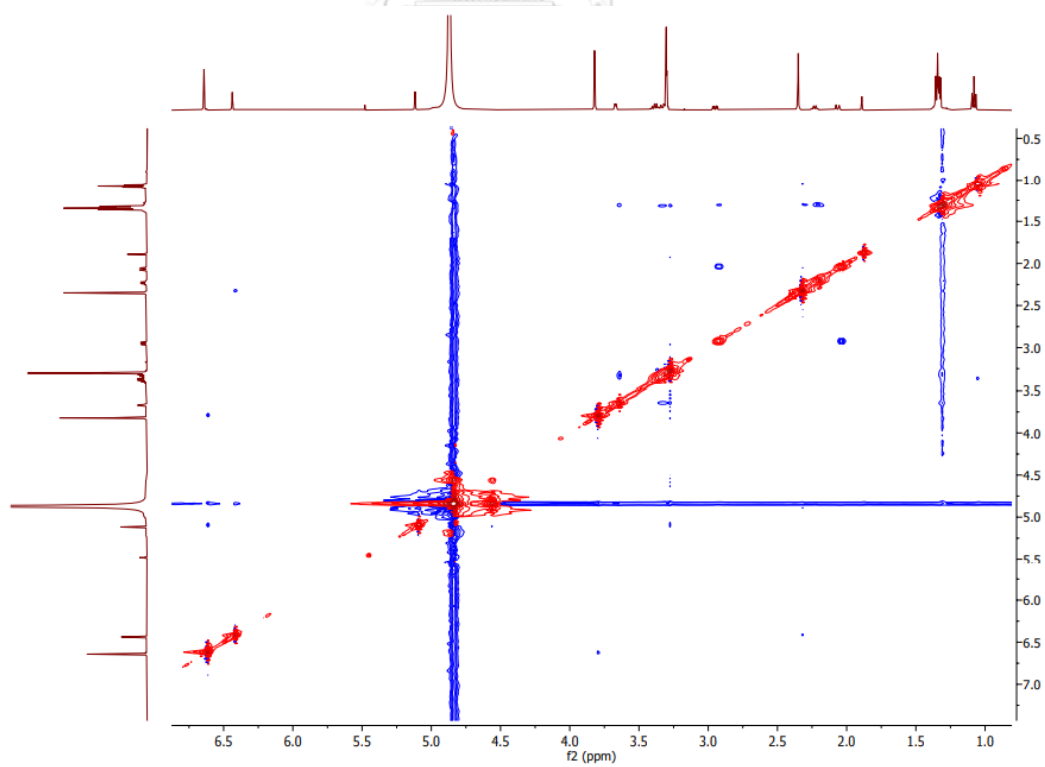


Figure A103. NOESY spectrum of compound 26

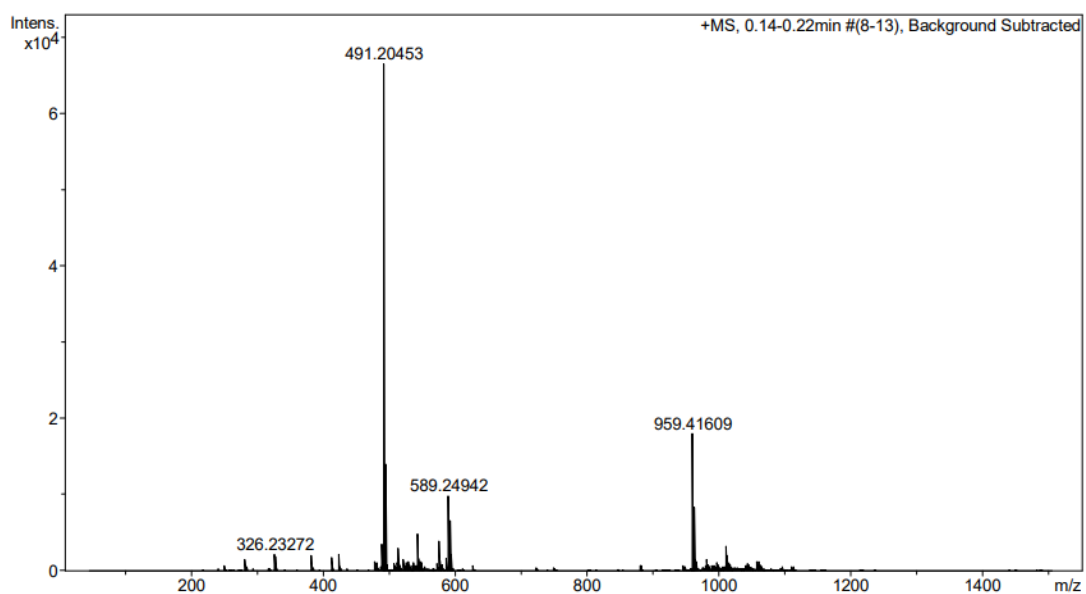
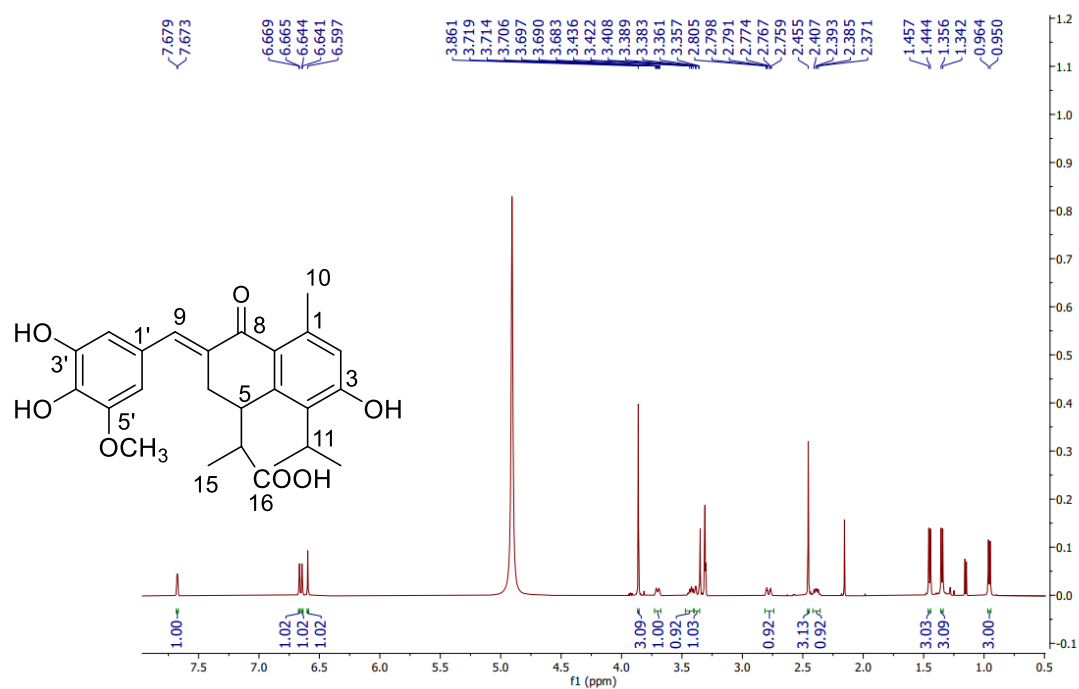
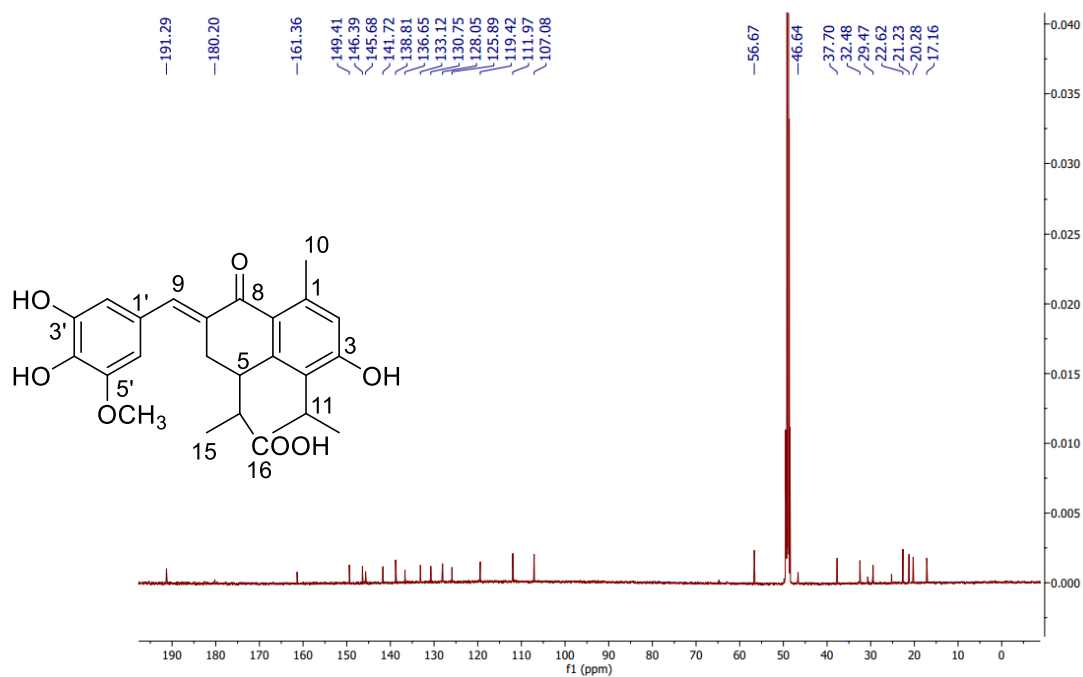
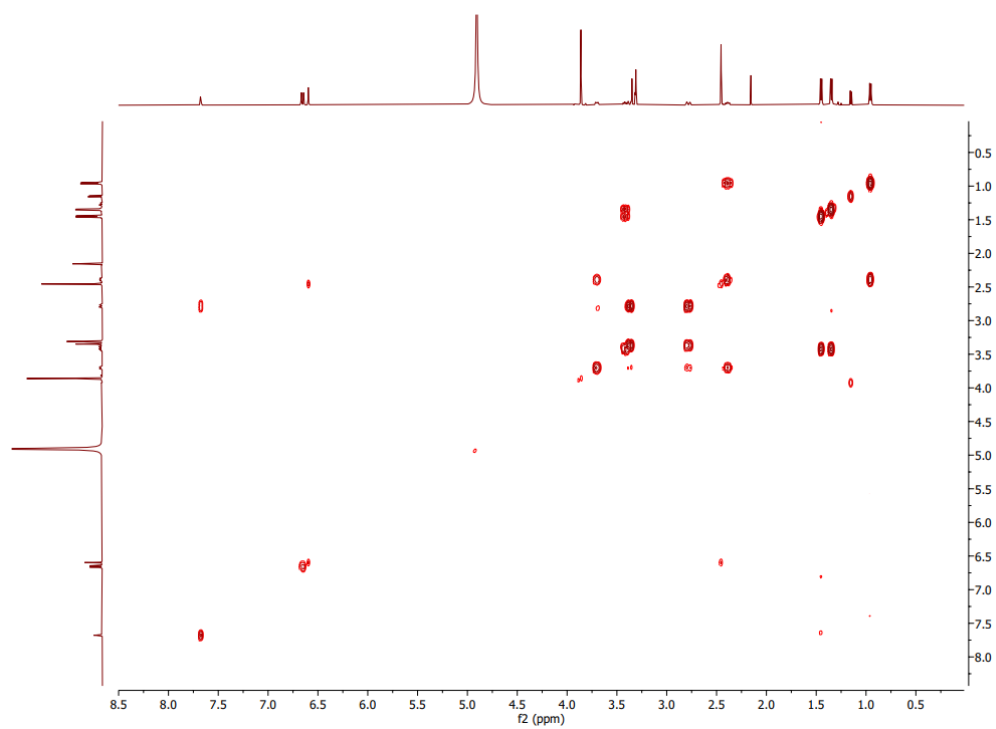
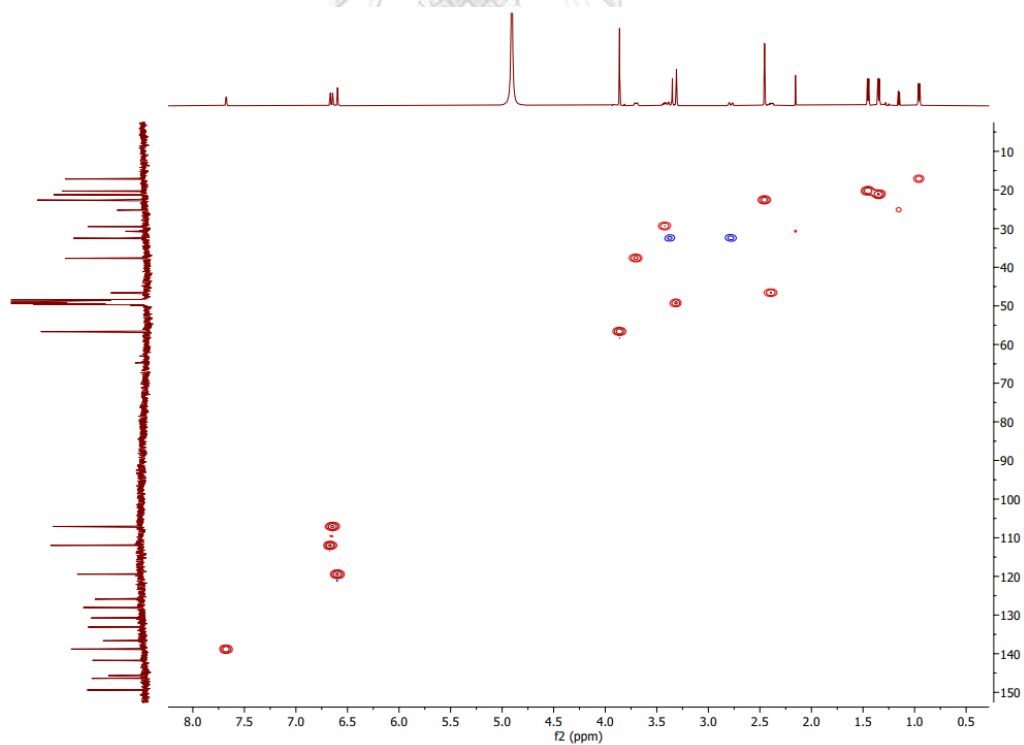


Figure A104. HRESIMS spectrum of compound **26**



Figure A105. ^1H NMR spectrum (500 MHz, methanol- d_4) of compound 27Figure A106. ^{13}C NMR spectrum (125 MHz, methanol- d_4) of compound 27

Figure A107. ^1H - ^1H COSY spectrum of compound **27**Figure A108. HSQC spectrum of compound **27**

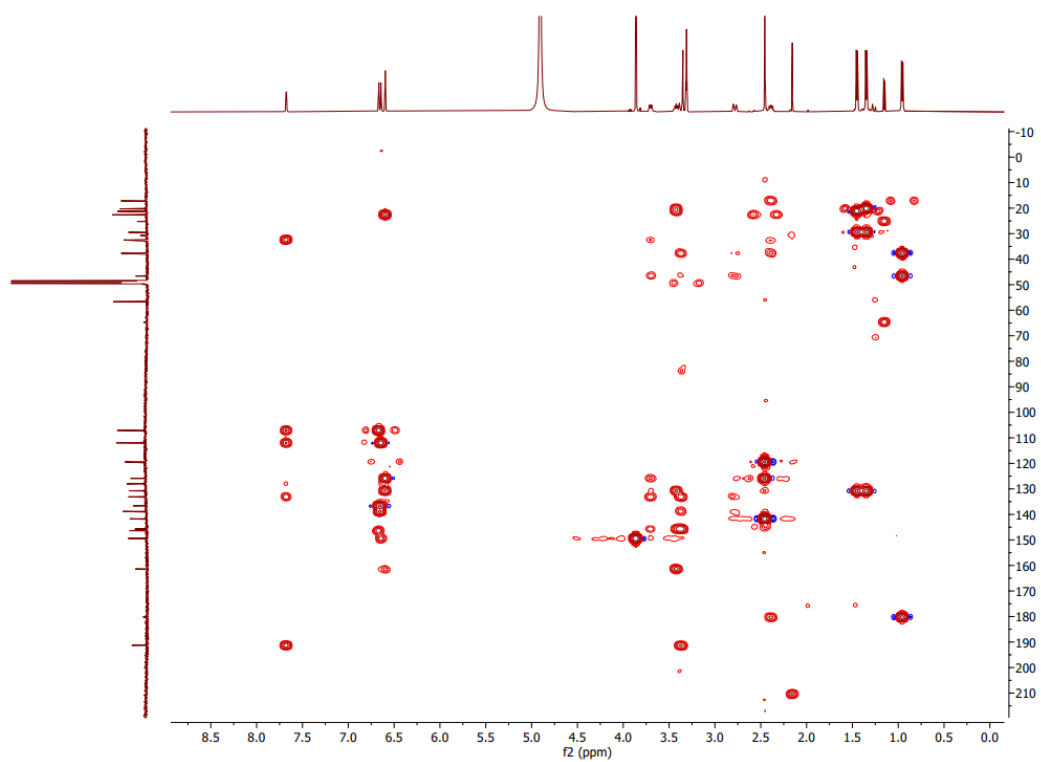


Figure A109. HMBC spectrum of compound 27

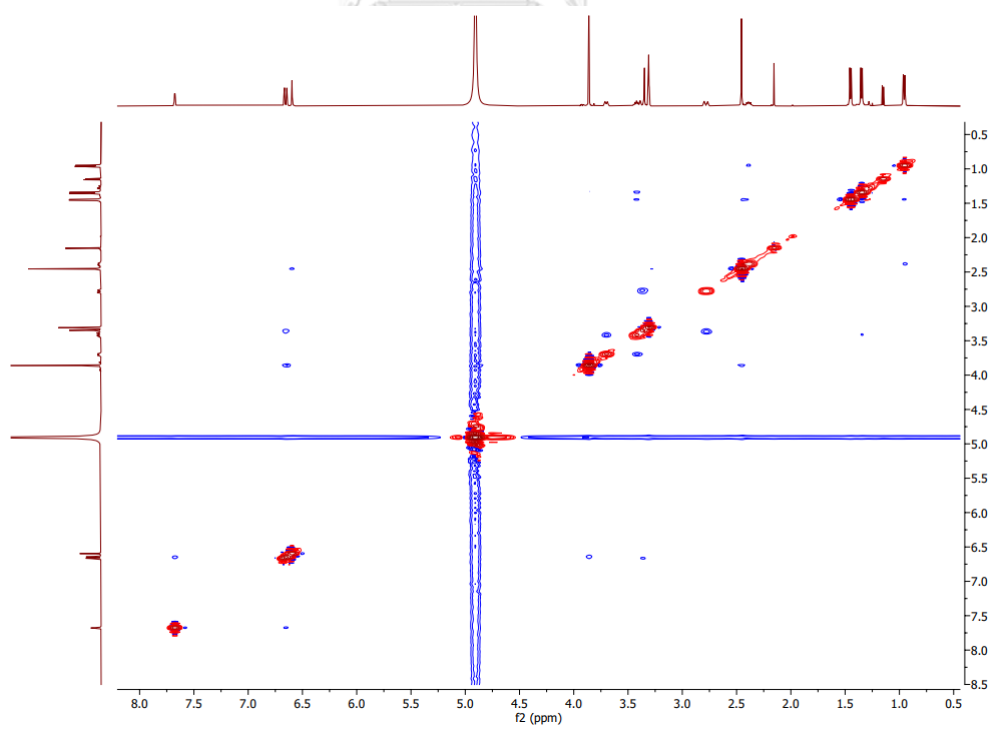


Figure A110. NOESY spectrum of compound 27

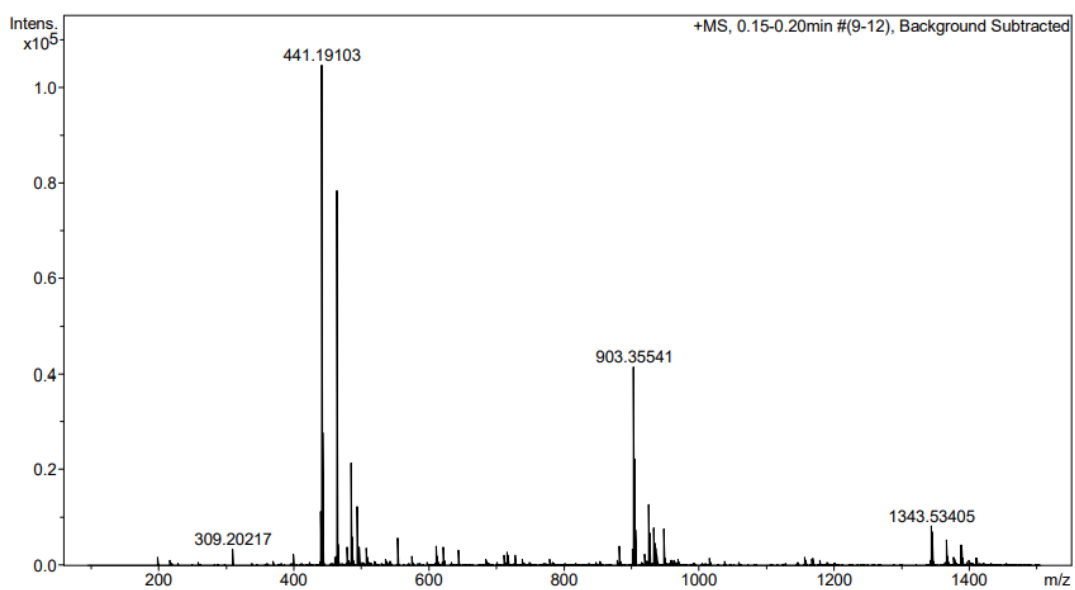


Figure A111. HRESIMS spectrum of compound 27



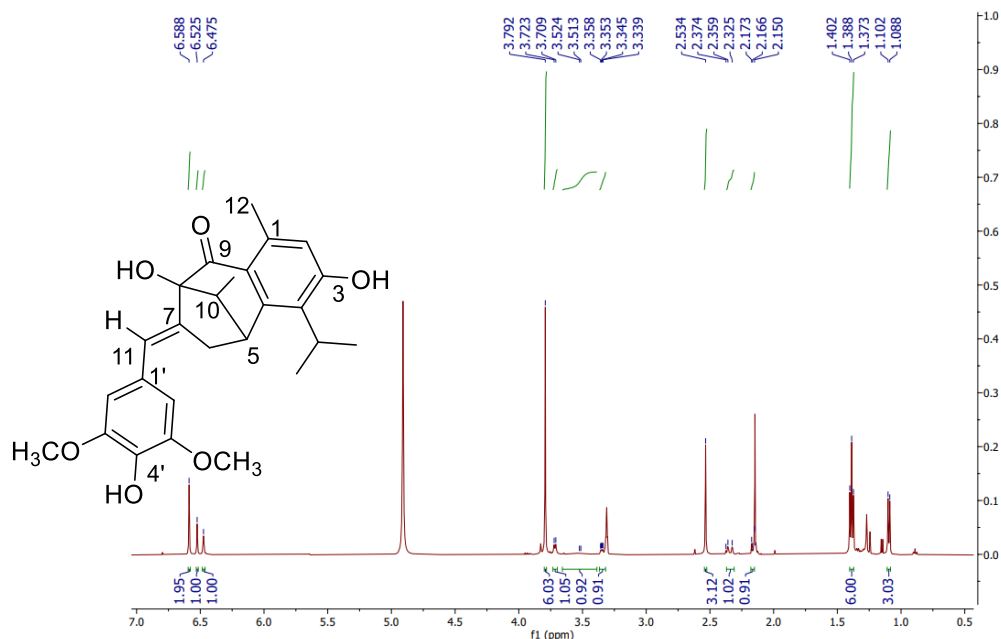


Figure A112. ^1H NMR spectrum (500 MHz, methanol- d_4) of compound **28**

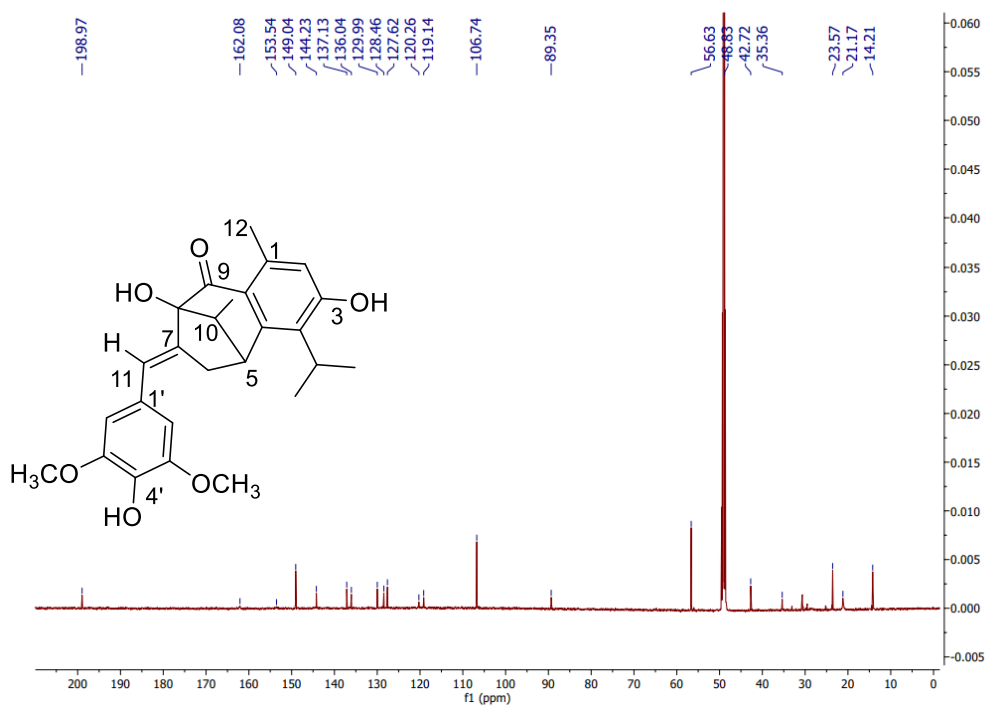
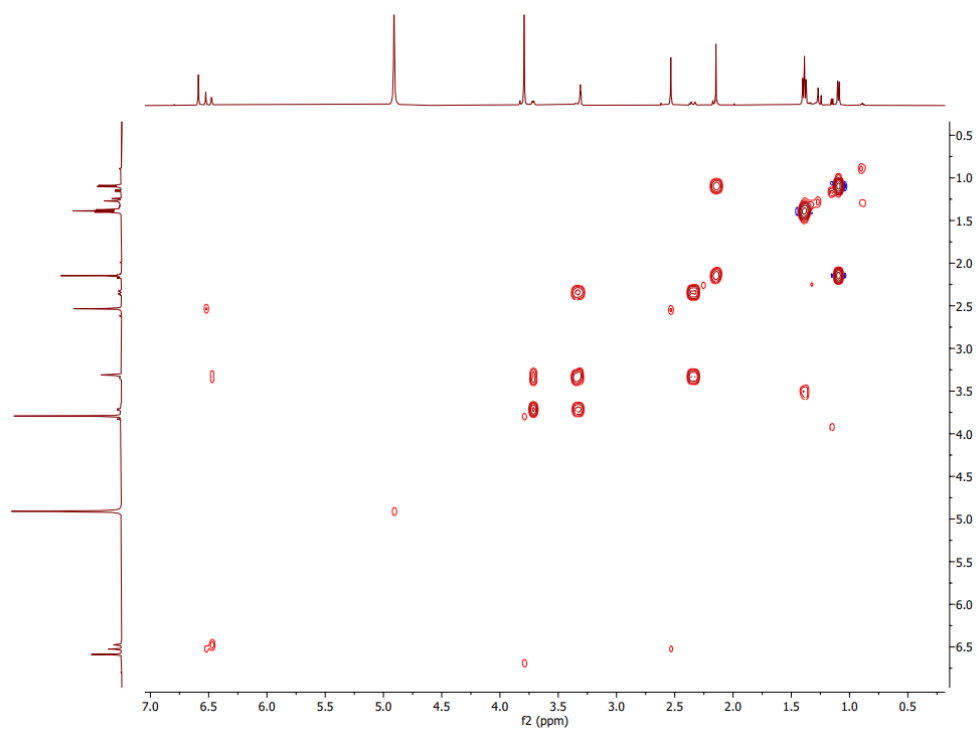
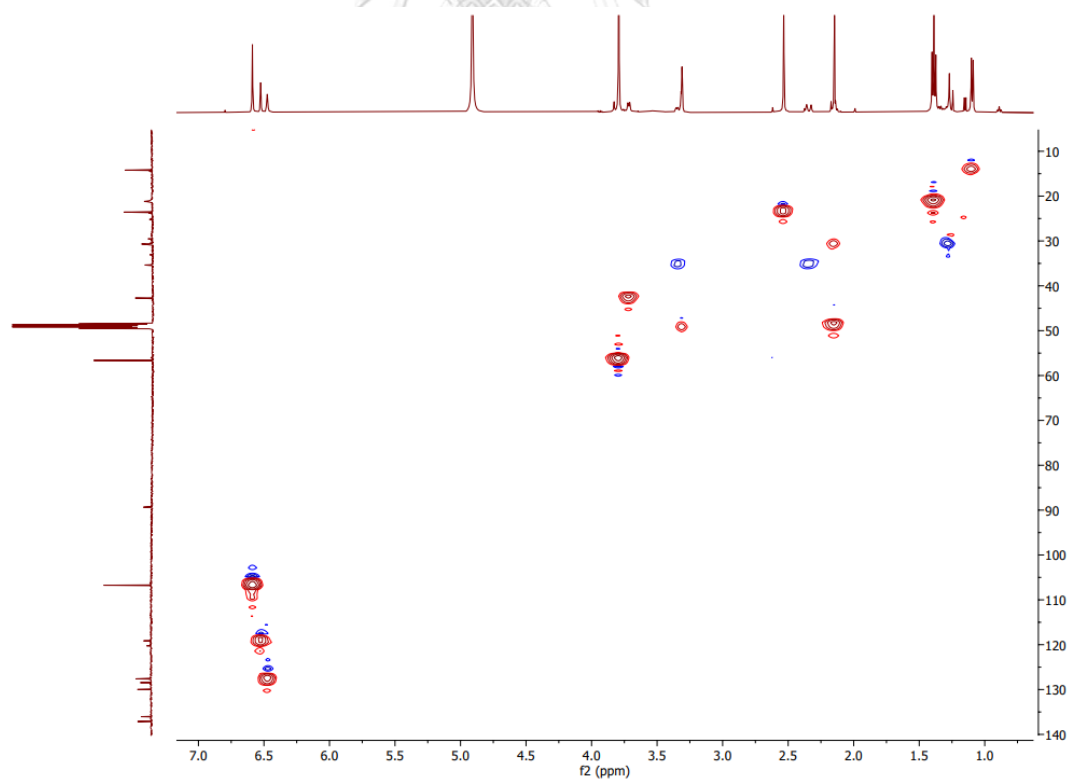
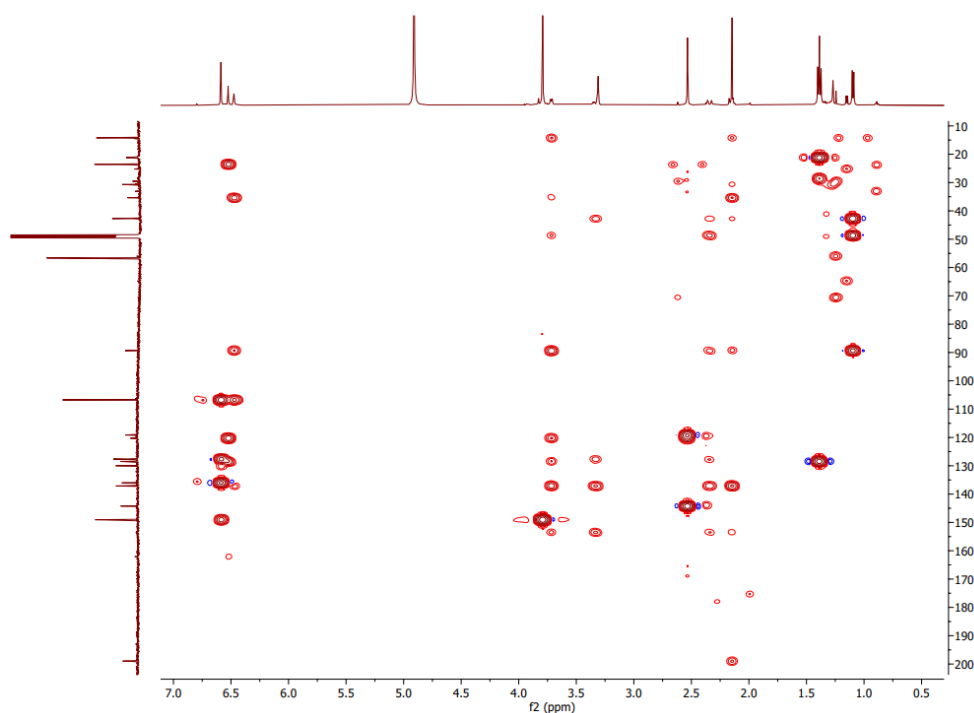
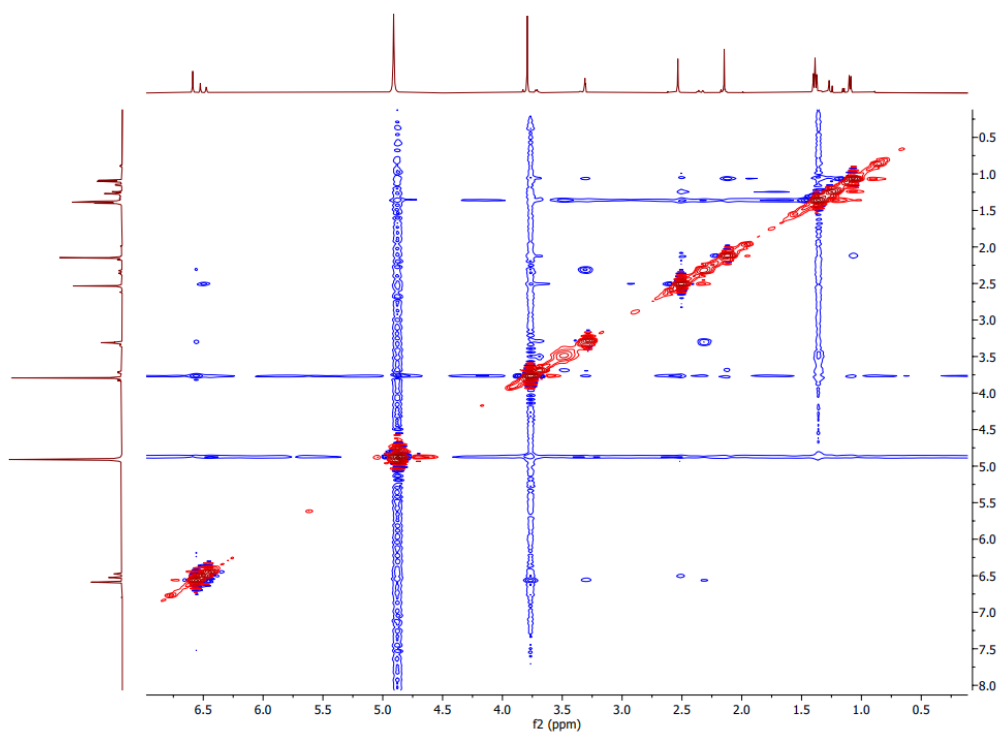


Figure A113. ^{13}C NMR spectrum (125 MHz, methanol- d_4) of compound **28**

Figure A114. ^1H - ^1H COSY spectrum of compound **28**Figure A115. HSQC spectrum of compound **28**

Figure A116. HMBC spectrum of compound **28**Figure A117. NOESY spectrum of compound **28**

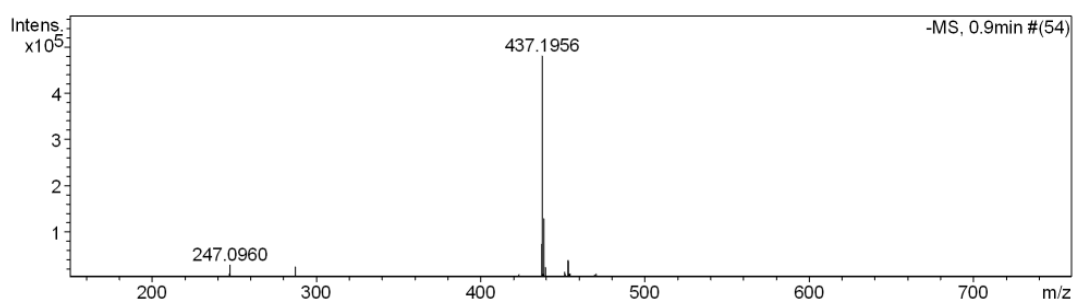


Figure A118. HRESIMS spectrum of compound **28**



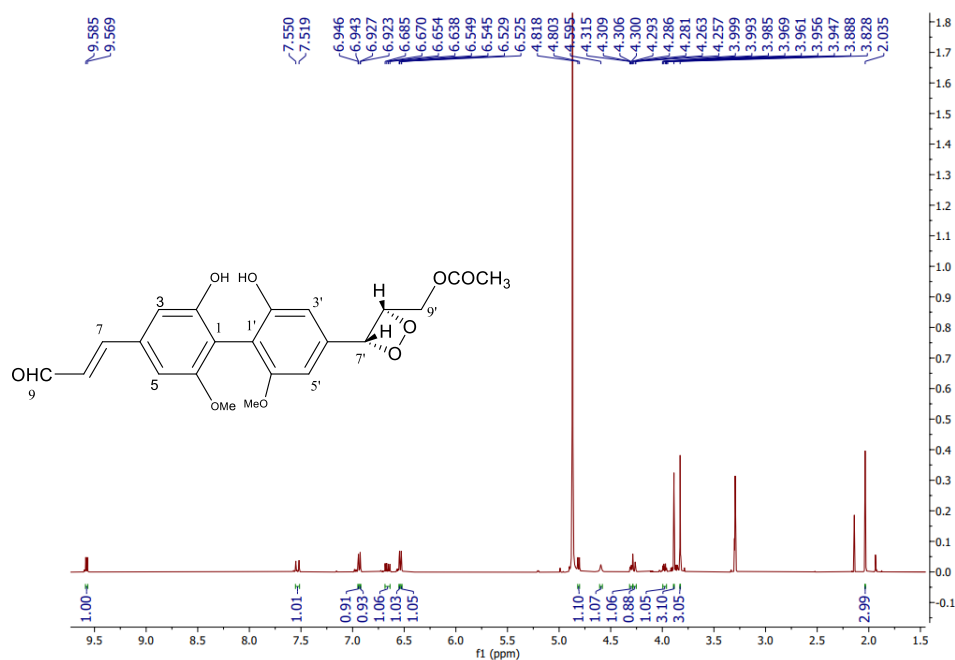


Figure A119. ¹H NMR spectrum (500 MHz, methanol-*d*₄) of compound 30

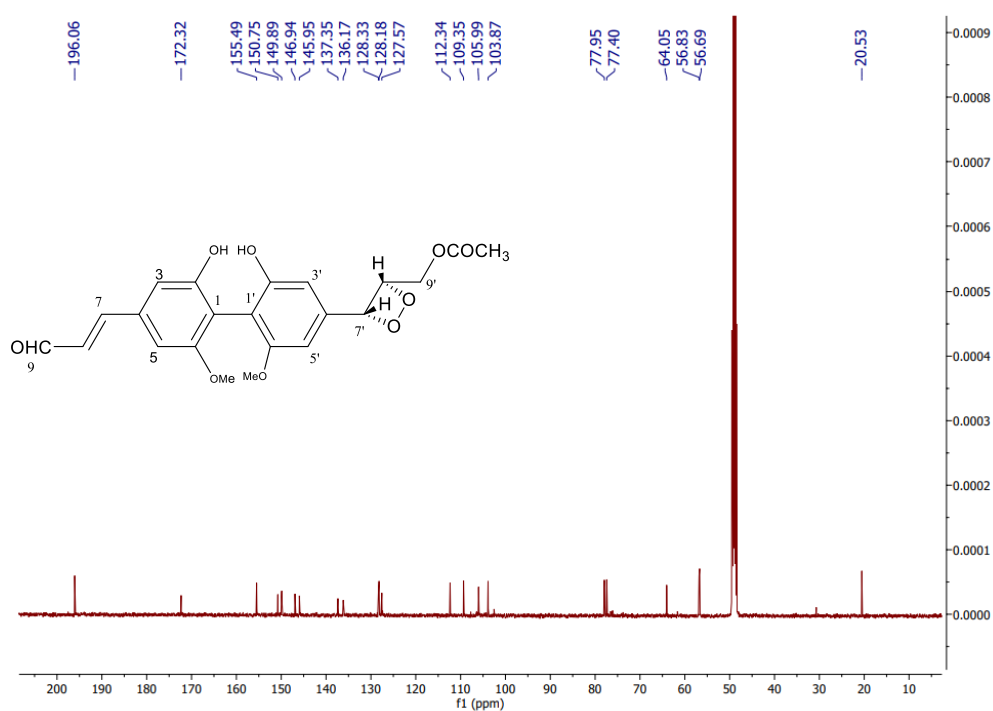
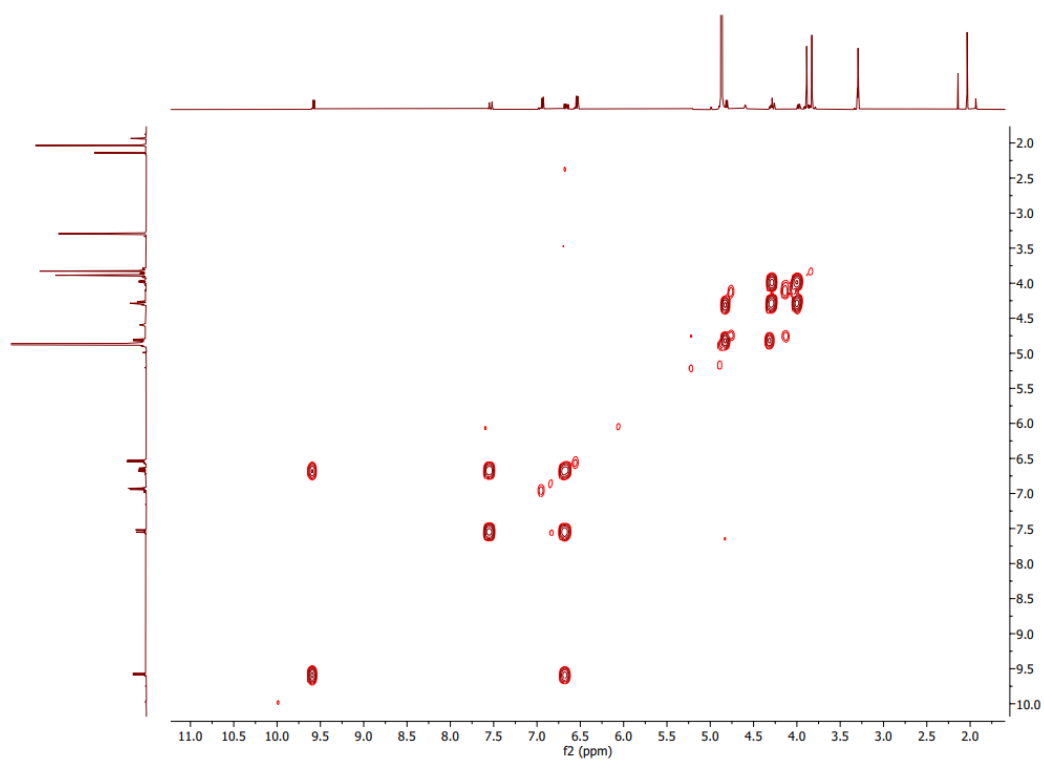
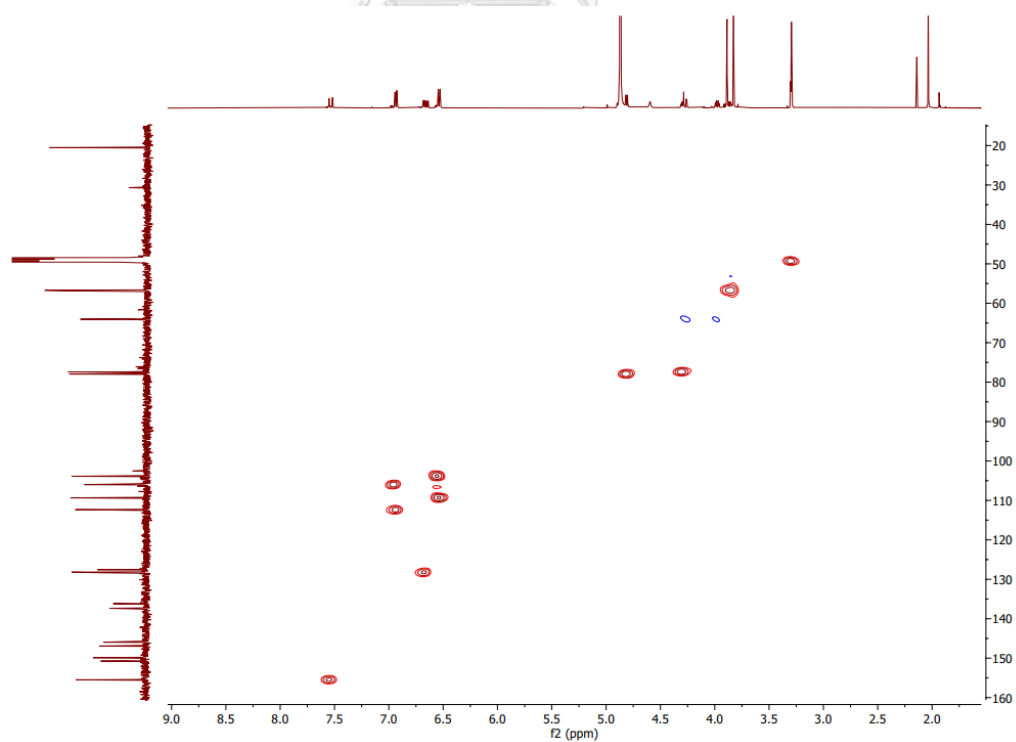


Figure A120. ¹³C NMR spectrum (125 MHz, methanol-*d*₄) of compound 30

Figure A121. ^1H - ^1H COSY spectrum of compound **30**Figure A122. HSQC spectrum of compound **30**

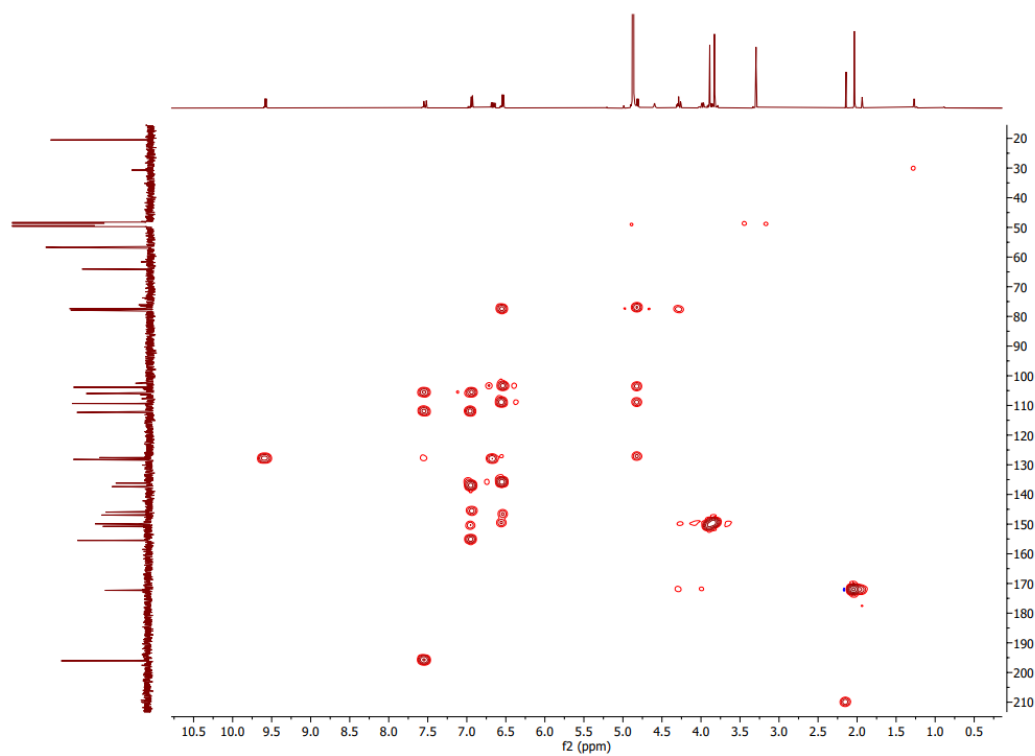


Figure A123. HMBC spectrum of compound 30

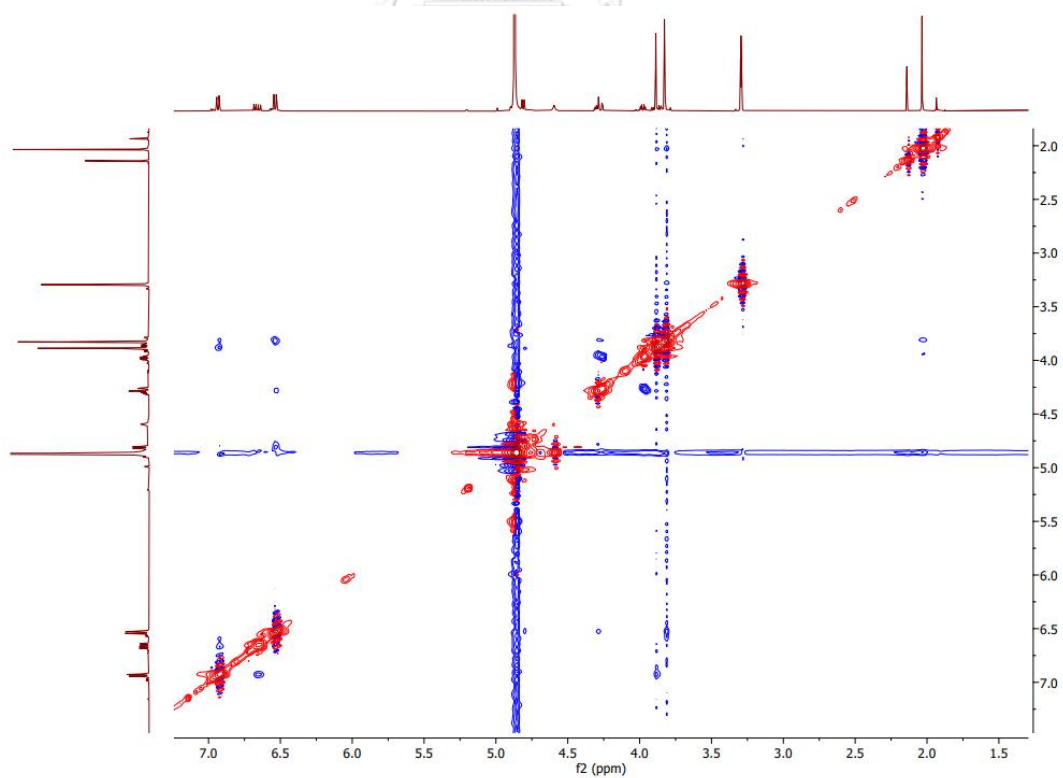


Figure A124. NOESY spectrum of compound 30

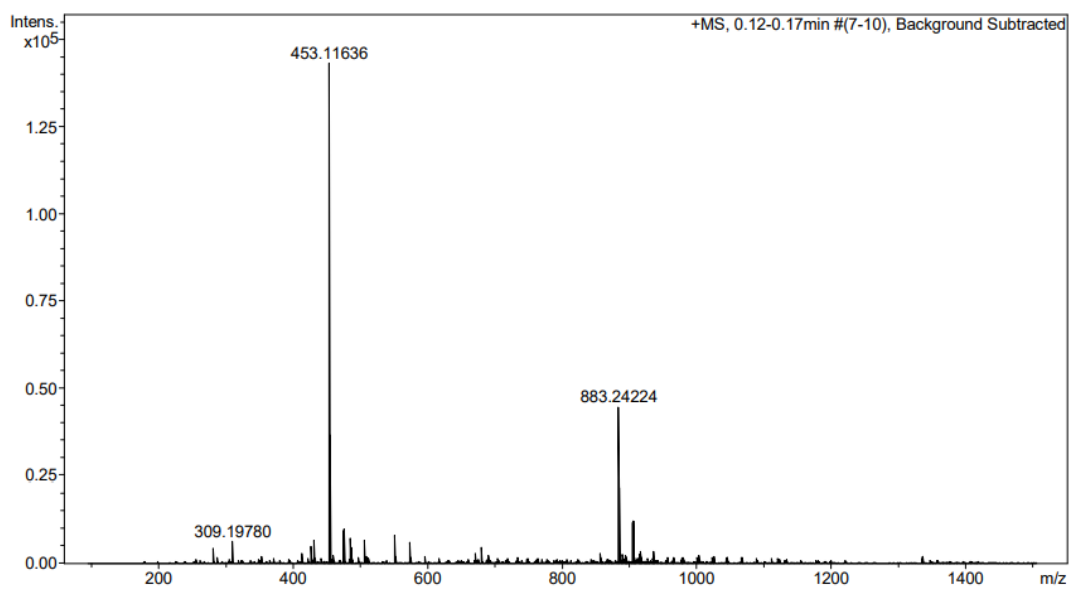


Figure A125. HRESIMS spectrum of compound 30



VITA

NAME	HUONG THI THU LE
DATE OF BIRTH	10 July 1980
PLACE OF BIRTH	Nghe An
INSTITUTIONS ATTENDED	Chemistry Department - Faculty of Science - Chulalongkorn University
HOME ADDRESS	Room 1613 CU Ihouse 268 Chulalongkorn Soi 9, Jaratmung Rd., Wangmai, Pathumwan, Bangkok 10330 Thailand.